Distributed Energy Systems with Wind Power and Energy Storage

Magnus Korpås

A thesis submitted to

Norwegian University of Science and Technology
Faculty of Information Technology, Mathematics and Electrical Engineering
Department of Electrical Power Engineering

in partial fulfillment of the requirements for the degree
Doktor ingeniør

Trondheim, 2004

PREFACE

The present work was carried out at the Department of Electrical Power Engineering at the Norwegian University of Science and Technology (NTNU) and started in November 1999. My first supervisor was the late Professor Øyvin Skarstein. After his most unfortunate and tragic death in 2000, Professor Arne T. Holen took over as my supervisor. Co-advisors during parts of the doctoral study have been Professor Georg Hagen at the Department of Materials Technology, NTNU and Ragne Hildrum at Statkraft SF.

The research was sponsored by Statkraft SF and the Research Council of Norway.

Acknowledgments

Most of all, my thanks goes to Professor Arne T. Holen for guiding me through the doctoral study, and for his optimistic and inspiring attitude. He has helped me in all aspects of the work, and he has made a great effort in keeping me focused in my research. Many thanks go to Statkraft for making this doctoral study possible. Especially I want to mention Dr. Ragne Hildrum, who contributed a lot to this work. Our collaboration has been very useful and inspiring for me. My thanks also go to Professor Georg Hagen at NTNU and Dr. Steffen Møller-Holst and Sintef Energy Research for their advice and important contributions, especially during the first part of the study.

My colleagues and friends Audun Botterud, Klaus Vogstad and Ingunn Ettestøl at the Department of Electrical Power Engineering are acknowledged for their valuable support and cooperation throughout the doctoral study. I want to thank Kaare Gether at the Department of Energy and Process Engineering for providing essential inputs and ideas on energy

system analysis. Without his contributions, I have my doubts as to whether the thesis would have been published in March 2004. My thanks also go to the researchers at Sintef Energy Research who have given insightful comments and suggestions, as well as providing access to data and simulation codes. Special thanks to Dr. Edgardo Castronouvo at INESC in Porto for his hospitality and for fruitful discussions on modeling and optimization techniques.

The help from the Korpås family, Sivertsen family and Hurlen family is greatly appreciated. They have always been encouraging and interested in my work. I would like to thank my friends and NTNU-colleagues Randulf, Nina, Stian, Mick and Monika for accepting offers to take an academic coffee break at any time. Also, Mikael Åkerfeldt is acknowledged for creative inspiration and for helping me through heavy times of thesis writing.

Finally, I want to thank my girlfriend Guri for her kindness and love, and for being supportive and understanding when I am struggling with my computer code.

Magnus Korpås

Trondheim, March 2004

SUMMARY

The topic of this thesis is the study of energy storage systems operating with wind power plants. The motivation for applying energy storage in this context is that wind power generation is intermittent and generally difficult to predict, and that good wind energy resources are often found in areas with limited grid capacity. Moreover, energy storage in the form of hydrogen makes it possible to provide clean fuel for transportation. The aim of this work has been to evaluate how local energy storage systems should be designed and operated in order to increase the penetration and value of wind power in the power system. Optimization models and sequential and probabilistic simulation models have been developed for this purpose.

Chapter 3 presents a sequential simulation model of a general wind-hydrogen energy system. Electrolytic hydrogen is used either as a fuel for transportation or for power generation in a stationary fuel cell. The model is useful for evaluating how hydrogen storage can increase the penetration of wind power in areas with limited or no transmission capacity to the main grid. The simulation model is combined with a cost model in order to study how component sizing and choice of operation strategy influence the performance and economics of the wind-hydrogen system. If the stored hydrogen is not used as a separate product, but merely as electrical energy storage, it should be evaluated against other and more energy efficient storage options such as pumped hydro and redox flow cells. A probabilistic model of a grid-connected wind power plant with a general energy storage unit is presented in chapter 4. The energy storage unit is applied for smoothing wind power fluctuations by providing a firm power output to the grid over a specific period. The method described in the chapter is based on the statistical properties of the wind speed and a general representation of the wind energy conversion system and the energy storage unit. This method allows us to compare different storage solutions.

In chapter 5, energy storage is evaluated as an alternative for increasing the value of wind power in a market-based power system. A method for optimal

short-term scheduling of wind power with energy storage has been developed. The basic model employs a dynamic programming algorithm for the scheduling problem. Moreover, different variants of the scheduling problem based on linear programming are presented. During on-line operation, the energy storage is operated to minimize the deviation between the generation schedule and the actual power output of the wind-storage system. It is shown how stochastic dynamic programming can be applied for the on-line operation problem by explicitly taking into account wind forecast uncertainty. The model presented in chapter 6 extends and improves the linear programming model described in chapter 5. An operation strategy based on model predictive control is developed for effective management of uncertainties. The method is applied in a simulation model of a wind-hydrogen system that supplies the local demand for electricity and hydrogen. Utilization of fuel cell heat and electrolytic oxygen as by-products is also considered. Computer simulations show that the developed operation method is beneficial for grid-connected as well as for isolated systems. For isolated systems, the method makes it possible to minimize the usage of backup power and to ensure a secure supply of hydrogen fuel. For grid-connected wind-hydrogen systems, the method could be applied for maximizing the profit from operating in an electricity market.

Comprehensive simulation studies of different example systems have been carried out to obtain knowledge about the benefits and limitations of using energy storage in conjunction with wind power. In order to exploit the opportunities for energy storage in electricity markets, it is crucial that the electrical efficiency of the storage is as high as possible. Energy storage combined with wind power prediction tools makes it possible to take advantage of varying electricity prices as well as reduce imbalance costs. Simulation results show that the imbalance costs of wind power and the electricity price variations must be relatively high to justify the installation of a costly energy storage system. Energy storage is beneficial for wind power integration in power systems with high-cost regulating units, as well as in areas with weak grid connection.

Hydrogen can become an economically viable energy carrier and storage medium for wind energy if hydrogen is introduced into the transportation sector. It is emphasized that seasonal wind speed variations lead to high storage costs if compressed hydrogen tanks are used for long-term storage. Simulation results indicate that reductions in hydrogen storage costs are more important than obtaining low-cost and high-efficient fuel cells and electrolyzers. Furthermore, it will be important to make use of the flexibility

that the hydrogen alternative offers regarding sizing, operation and possibly the utilization of oxygen and heat as by-products.

The main scientific contributions from this thesis are the development of

- a simulation model for estimating the cost and energy efficiency of wind-hydrogen systems,

- a probabilistic model for predicting the performance of a grid-connected wind power plant with energy storage,

- optimization models for increasing the value of wind power in electricity markets by the use of hydrogen storage and other energy storage solutions

and the system knowledge about wind energy and energy storage that has been obtained by the use of these models.

CONTENTS

1 INTRODUCTION

1.1 Motivation

Renewable energy sources are fundamental for an environment-friendly energy supply. Today, the most important renewable energy sources are hydro power and bio energy. Moreover, the installed wind power capacity was over 30 GW worldwide by the end of 2002, and wind power is today the fastest growing electricity generation technology [1].

However, the intermittent nature of wind makes power system operation especially challenging. Rapid and flexible control of other generators is required to balance wind power generation with demand. In addition, the best wind resources are often found in rural areas far from existing high-capacity transmission lines.

Energy storage is a potential solution to the integration issues that are described above. Appropriate operation of energy storage could increase the value of wind power in the power system by ensuring a closer match between wind power generation and demand. In weak networks, storage of wind energy could also be used as a means for avoiding overloading of lines or undesirable voltage increase in periods with high wind speed. Storage of wind energy in the form of hydrogen has received especial attention. Hydrogen produced from electrolysis of water is the link between wind energy and a "hydrogen economy"[1]. Hydrogen is a flexible fuel that can be used for stationary energy supply and as a fuel for transportation. There also exists a range of other energy storage solutions that could be applied for energy management in connection with wind power, such as secondary batteries, pumped hydro, redox flow cells and compressed air storage.

[1] A vision for a future hydrogen economy is outlined in [2], which describes how imported fossil fuels could be replaced by hydroelectric hydrogen in Iceland.

This thesis proposes different applications of energy storage for wind power plants. The aims of the work have been to evaluate how energy storage systems should be sized and operated to match a highly variable wind power generation with different energy demands within different market conditions and grid restrictions. Several modeling approaches have been applied for this purpose.

1.2 Contributions

The idea of using hydrogen storage and other storage solutions to balance wind power fluctuations is not new. Although the field has received increasing attention as the share of wind power in power systems increases and as the development of storage technologies continues, published studies on energy management of such systems are few. The main contributions of this work are the development of new methods for evaluating three principal opportunities for energy storage and hydrogen in connection with wind power:

- Wind is intermittent and difficult to predict. Energy storage could be valuable for balancing wind power generation with demand and for reducing generation uncertainty. It is shown that energy storage systems with relatively low power rating and storage capacity provides substantial operational benefits for wind power in electricity markets with moderate to high price variations and imbalance costs. Optimization of generation scheduling and on-line operation by the use of wind power forecasts is crucial to obtain these benefits.

- Good wind sites are often located in remote areas. Storage of wind energy could defer grid upgrades in weak grids and reduce the dependency of fossil fuels in isolated power systems. However, this will prove to be a costly alternative if seasonal storage of wind energy is necessary. In the case of hydrogen, reduction of hydrogen storage costs would be more important than obtaining low-cost and high-efficient fuel cells and electrolyzers.

- Hydrogen as a storage medium for wind energy could provide clean fuel for transportation. Operation strategies for electrolytic hydrogen production as a flexible load for wind energy have been developed. Through simulations, it is shown how the electrolyzer can be operated to exploit excess wind energy and to take advantage of electricity price variations. Moreover, considerable cost savings could be obtained by using the same hydrogen storage system for providing energy for stationary use and for transportation.

The simulation models that have been built as a part of this work are:

- A general probabilistic model for predicting the performance of a grid-connected wind-storage system. The model is based on a methodology for calculating the expected firm power output of the combined plant. The model takes into account how limited power capacity influences the smoothing ability of the storage system.

- A time sequential model for evaluating the cost and energy efficiency of wind-hydrogen systems. The model includes control strategies for a range of different applications. A method for calculating the cost of delivered electricity and hydrogen has been implemented as a part of the model.

- A time sequential model of a general wind-storage system which includes algorithms for optimization of short-term generation scheduling. The control strategy for on-line operation is based on minimization of deviations from the generation schedule. The scheduling problem is implemented as a deterministic dynamic programming problem and as a linear programming problem.

- An extension of the above-mentioned model by implementing a stochastic dynamic programming algorithm for the on-line operation problem. The model takes into account the uncertainties in predictions of future wind speed.

- A time sequential model of a wind-hydrogen system, which includes generation scheduling and optimal operation based on principles of model predictive control. The possibilities of using oxygen and fuel cell heat as by-products are taken into account. Generation scheduling and on-line operation are implemented as linear programming problems.

1.3 Outline of the thesis

This chapter has presented the motivation for the work and the main contributions to the field. The rest of the thesis is organized as follows:

Chapter 2 gives a more detailed background for the work and places it in a broader context. The chapter discusses integration issues of wind power and gives an overview of different energy storage systems.

Chapter 3 presents an evaluation of different wind-hydrogen alternatives by the use of computer simulations and a cost model. Three types of wind-

hydrogen systems are studied, and several control strategies are proposed for the different integration alternatives.

Chapter 4 describes a probabilistic model for predicting the performance of energy storage as a way of smoothing wind power fluctuations. A comparison of different storage systems is carried out by the use of this model.

Chapter 5 introduces a method for short-term generation scheduling of a general wind-storage system and for how the system should be controlled to minimize deviations from the generation schedule during on-line operation. The method is implemented in a simulation model, which is used for evaluating different storage sizing alternatives and for evaluating the impact of storage efficiency and wind prediction accuracy. The chapter also presents an extension of the method by the use of stochastic dynamic programming.

Chapter 6 presents a method for generation scheduling and optimal operation of wind-hydrogen systems. Results from three different simulation case studies are presented: A thermal-based power system, a hydro-based power system and an isolated power system with a backup plant.

Chapter 7 starts with a discussion of the different systems that have been evaluated. The chapter also includes a discussion of the developed methods and simulation models. The last part of the chapter concludes the thesis and gives suggestions for further work.

Appendix A provides a list of symbols and abbreviations used in the thesis.

Appendix B consists of reprints of three papers written as a part of this work in the period 2001-2003.

2 PERSPECTIVES

This chapter gives an overview of the background and motivation for the topics that have been addressed in the doctoral study. Issues of integrating wind power in the power system are discussed in section 2.1 . Application of energy storage is one of several methods for increasing the penetration and value of wind. Section 2.2 and 2.3 gives an overview of different energy storage options. Hydrogen storage is given especial attention in this thesis and is considered as a future alternative since it is still in its relatively early development stage. Therefore, section 2.4 presents some relevant demonstration projects on wind-hydrogen and solar-hydrogen systems.

2.1 Wind integration

2.1.1 Network issues

Many electricity grids have been constructed for supplying dispersed loads with power generated at large, centralized plants. Power losses from source to end-use can be high at both transmission level and distribution level, depending on the grid layout and the distance between the power plants and load centers. In the Nordic power system for example, there is a considerable net power export from the northern parts with large hydro power plants to the much denser populated areas in the south. Furthermore, in the sparsely populated parts of Norway, the distribution grids consist of long, radial feeders. These feeders often have an R/X-ratio (resistance/reactance) that gives rise to high grid losses. Thus, installation of small, distributed generating units near the loads will reduce power flow from the central plants and thus reduces losses. In fact, a study of a 6 kV rural network in New Zealand has shown that dispersed and properly sized wind turbines will not only have a positive effect on losses, but could also improve voltage quality [3]. Simulations of regional grids at 66 kV level at Vikna in Mid-Norway and 132 kV level in Italy have also concluded that distributed wind power plants reduce losses [4, 5]. The Italian case study also showed how wind power could defer grid upgrades due to expected

increase in the electricity demand. However, since wind is a highly intermittent energy source, it is claimed that any such benefit is likely to be small and will be site-specific [6]. Installation of energy storage could enhance the wind farm performance and thus delay or even avoid grid upgrades. A study by the Oak Ridge National Laboratory on a 25 kV distribution network near Eastsound, USA showed that an MW-scale wind farm with battery storage could be an economic viable alternative to upgrading distribution facilities [7]. Another example is the remote island Røst in the northern part of Norway. The island is today connected to the mainland via a sea cable that should be replaced by 2008 to maintain a secure power supply [8]. The municipal and the local energy company have evaluated different alternatives to a new cable, including a MW-sized wind-hydrogen system.

Local and regional voltage rise problems are likely to occur as more wind power is integrated in the grid, [9, 10]. It is now common to build large wind farms, which give high concentration of wind power at a regional level. For instance, the wind power potential is especially good along the coastline in the northern part of Norway, which has led to a large interest for development of wind farms. Figure 1 shows a map of wind farms that are considered to be built in the area. Studies have shown that it is not possible to realize all the wind farm projects east of Balsfjord (near Kvaløya shown in the map), without reinforcements of the existing 132 kV grid [11]. Upgrading to a new 420 kV line will make it possible to install up to 900 MW. However, the potential is probably far larger than the capacity of the proposed new line. Since the study concluded that the wind power integration is limited by voltage stability and not the thermal limit of the new line, it is not possible to increase the wind penetration by further upgrade of the grid inside the area. It would then be necessary to build another strong connection out of the area, for instance southwards to Finland [11].

This example is characteristic for wind power integration in weak grids, namely that problems associated with voltage rise and voltage stability occurs before the thermal limits of the lines are reached [12, 13]. Traditional grid planning procedures would in this case recommend upgrading of existing lines or building of new lines, either locally or regionally, or both. However, the relatively low utilization factor of wind power may give lower utilization of the grid capacity than desirable for expensive grid investments. Furthermore, geographical and environmental constraints obstacle grid upgrades in some areas. However, there are other alternatives that can overcome voltage-quality constraints [13-15]:

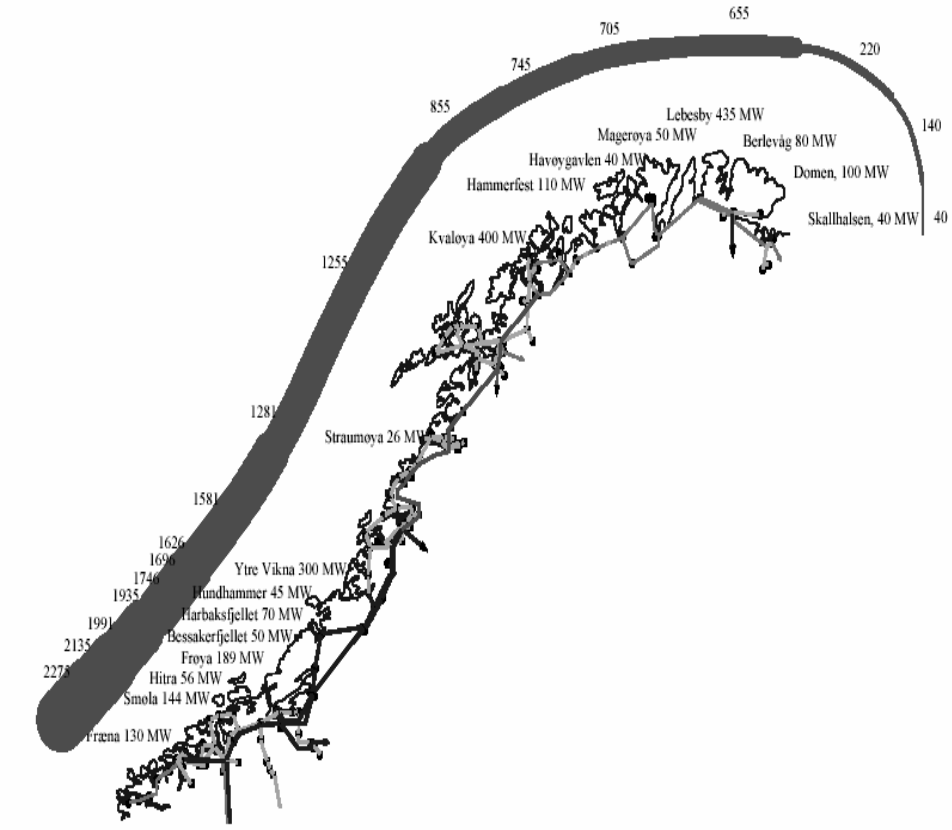

Figure 1. Geographical overview of wind farms that are considered in northern Norway. The thick line displays the increasing transmission requirement. Source: Statnett [11].

- Dissipation of wind energy
- Reactive power regulation
- Control of tap changing transformers
- Load management
- Application of energy storage

These alternatives can be defined as *active* control actions in contrast to the grid upgrade alternative, which is *passive* in the sense that wind turbines are regarded as uncontrollable power generating units.

Dissipation of wind energy can be carried out by shutting down individual turbines, by blade pitching or by controlling a dump load, e.g. in the form of an electrical heater. Such operating principles have for example been used for wind farm connections in USA and in Denmark [15, 16]. The reduction in delivered energy implies a loss of revenue for the wind farm operator. However, since dissipation of wind power due to voltage increase is most

likely to occur in low load periods, such as summer nights in northern Europe, the economic impact may not be crucial for the investment decision if the price for wind power follows the system price. On the other hand, if the installed wind power capacity is high relative to the load, it may be necessary to reduce wind power output even in periods with high electricity consumption. Dissipation of excess wind power has recently gained interest in connection with large-scale integration of wind power in the Irish electricity network [16].

The voltage level can be controlled by the use of reactive power support such as mechanically switched shunt capacitors, Static Var Compensators (SVCs) or power electronics integrated in the electrical system of the wind turbines. A review of new developments in power electronic technology for wind turbines is given in [17]. HVDC-transmission and IGBT-converters make it possible to control the reactive power in the power system on the island of Gotland in Sweden, which has a high level of wind penetration [17]. The benefits of SVCs are exemplified in [12], which presents an analysis on connecting a 200 MW wind farm to the transmission grid via a long, existing 132 kV radial. Dynamic simulations show that it is technically possible to exploit the existing line up to the thermal limit by reactive power compensation. With no compensation, the voltage stability limit is reached at active power generation equal to 40% of the thermal capacity. The dynamic simulation model did not include regulators for tap changing transformers, since the reaction time is normally in the range of minutes. However, control of tap changing transformers is an interesting and presumably a cost-efficient solution in cases where steady-state voltage rise limits the acceptable wind power output [10, 13].

Scott [18] defines load management as “the control of consumer’s electrical appliances by a party other than the consumer”. The paper investigates methods for increasing demand in weak grids when wind generation is creating too high voltage. Similar control schemes can be applied to battery energy storage and pumped hydro stations, which make it possible to avoid unacceptable voltage rise by storing excess wind energy. The energy can be released later when the grid voltage is lower [19]. Such control strategies have for instance been applied in a simulation study of a wind farm and pumped storage connected to a 10 kV feeder in County Donegal, Ireland [9].

A hydrogen storage system can be designed and operated for load management and/or electricity storage purposes, depending on the inclusion of a power-generating unit such as a fuel cell. The first option has been proposed for large-scale wind power integration in Ireland [20]. The paper

describes a hypothetical case study of 100 MW wind power capacity in the region of Cork, where water electrolysis can be used to prevent dissipation of wind energy due to transmission constraints. In yet another Irish case study, a fuel cell is considered to enhance the flexibility of the hydrogen storage system [21]. The case study is of Achill Island, which took part in the Alterner project "100% Renewable Islands". The electrical infrastructure consists of a weak 10 kV distribution network with limited export possibilities, and the study included scenarios for near 100% renewable energy supply to the island.

Hydrogen storage could also be applied in windy areas with no electrical infrastructure. Wind power will in that case be used exclusively for hydrogen production, which requires special solutions for the electrical connection between the generator and the electrolyzer. In addition, the electrolyzer must be able to handle fluctuating operating condition with minimal electrochemical degradation. Because of the low volumetric density, the hydrogen gas must be compressed or liquefied and then transported to load centers by pipelines, trucks, ships, or railway. As an example, hydrogen has been proposed as an alternative to new HVDC lines for transmitting 4,000 MW of new wind power from the Great Plains in North Dakota to Chicago [22]. Similar ideas have been reported for exploiting the wind resources in rural areas of Argentina [23]. Moreover, hydrogen has received attention as a possible carrier for offshore wind energy, as an alternative to new electrical infrastructure [24-26].

2.1.2 Matching supply and demand

Today, there is large diversities in the mechanisms that determine the price for wind power. Even within a single transmission operator's area, there are different remuneration schemes for wind energy. In western Denmark, for example, wind turbines that have been grid-connected for more than 10 years receive an electricity price that varies with the spot price, while newer wind turbines receive a fixed feed-in tariff [27]. Other power systems, such as the Portuguese, have varying tariffs so that the price for wind generation is highest in peak hours [28]. The varying tariff reflects that the marginal cost of generation increases with demand. In electricity markets, the hourly price variations will typically follow the demand, but the relative variations in price depend heavily on the available generators. This is exemplified in Figure 2, which shows samples of the spot price in a market dominated by hydropower (Nordpool – The Nordic Power Exchange) and a market dominated by thermal power (EEX – The European Energy Exchange). It is clear that the flexibility of hydropower results in small price differences during the day, while the operating cost of peaking units in a thermal system give rise to large variations.

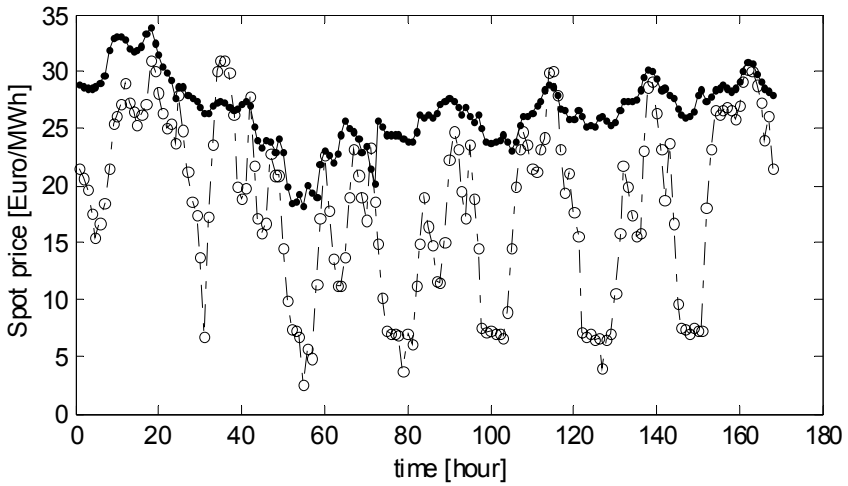

Figure 2. Samples of the spot price of electricity for Nordpool (-.-) and EEX (-o-) from 23.12.2003 to 29.12.2003.

Energy storage makes it possible for wind farm owners to take advantage of price variations by shifting generation from periods with low demand to peak periods. Several authors have assessed the value of applying energy storage for this purpose. Amos [29] examined the possibility of storing off-peak wind power using a hydrogen bromide (HBr) reversible electrolyzer/fuel cell system. The electricity cost model was based on data for the New England Power Pool. The objectives of the control logic of the storage system were, in brief, to sell as much power as possible during peak periods (6:00 am to 10:00 am, Mon-Fri except holidays) and sell no power during off-peak periods. Transmission constraints during peak periods were also considered. The control logic was based on a decision tree methodology with different triggers for when to charge and discharge the storage. Castronuovo and Pecas Lopes [28] also used a price model which distinguished between peak and off-peak, but this price model was based on the Portuguese wind energy remuneration tariffs. In [28], an operation-planning model of a wind-pumped hydro system was presented. The objective of the model was to maximize the profit over a 24-hour period by optimal operation of the pumping unit and the hydro generator. Cruden and Dudgeon [30] have also used an optimization approach to determine how energy storage, in this case a hydrogen storage system, can be used for maximizing wind farm revenue. This study was motivated by the new electricity trading arrangements (NETA) within the UK. The problem for stochastic generators within NETA is their inability to guarantee a specified energy delivery, which give rise to financial penalties [31].

Wind fluctuations do not only make it difficult to obtain a high selling price in the spot market, but the fluctuations also imply imbalance costs. This is

because the actual wind power generation seldom matches the expected generation. An example of how energy storage can be used for "firming" of wind power (i.e. reduce fluctuations) was presented in [30]. Another study based on the market conditions of NETA is presented in [32]. The paper describes an optimization model for the combined dispatch of wind and energy storage, taking into account both spot price variations and imbalance costs due to wind forecasting errors. In this model, wind power is contracted by its forecasted value. The optimal operation policy of the energy storage is determined by weighting the benefit of reducing imbalance costs of wind against the income from trading in the spot market.

At low penetration levels, uncertainties in wind power generation will not have significant impacts on power system operation because wind power in this case can be regarded as a negative load. However, as the share of wind power in the system increases, the system operator needs more spinning reserves and dispatchable capacity to handle the fluctuations. The present situation in the power system of western Denmark is a typical example. The energy mix of the region consists of about 3,100 MW centralized thermal stations, 1,600 MW dispersed combined heat and power plants and 2,300 MW wind power (1. January 2003) [27]. The massive development of wind farms in the area has resulted in a situation where the system operator Eltra often is forced to sell exported wind power for a low price. Moreover, it also happens that unexpected low wind speed causes a power deficit in the area, which must be covered by imports. Therefore, Eltra has started to consider the possibility of storing excess wind energy in the form of hydrogen [33].

The idea of introducing hydrogen storage in the Danish power system is not new. Ambitious governmental plans for renewable energy in Denmark[2] initiated a comprehensive system analysis project on using hydrogen storage to handle the stochastic nature of wind energy and solar energy [34]. In the study, hydrogen was proposed as storage medium where the hydrogen could be used both for electricity regeneration and as a fuel for vehicles. The objective of the hydrogen storage in this study was not to increase the value of individual wind farms, but to ensure power balance at a regional scale. Both large-scale hydrogen storage systems in underground caverns and decentralized small-scale hydrogen storage systems were considered.

[2] Renewables should cover more than 50% of the *energy* demand in 2030.

2.2 Hydrogen energy technology

2.2.1 Water electrolysis

Water is split to hydrogen and oxygen in an electrolysis cell by supply of direct current to the electrodes. Although the electrolysis process has been known since before the 19th century, only 0.5% of the hydrogen production today comes from electrolysis. It is at present significantly cheaper to produce hydrogen from hydrocarbons. However, this situation is expected to change in the future, both due to limitations of fossil resources and due to CO_2-emissions [35]. The net reaction for splitting of water is:

$$H_2O \rightarrow H_2 + \frac{1}{2}O_2 \tag{2.1}$$

The voltaic efficiency of the electrolysis process is defined as the relation between the reversible cell voltage U_{rev} and the actual cell voltage U_{cell}:

$$\eta_U = \frac{U_{rev}}{U_{cell}} \tag{2.2}$$

where U_{rev} = 1.23 V at room temperature and atmospheric pressure. An example of how the cell voltage depends on the operating conditions is presented in Figure 3, which shows the polarization curve of an electrolysis cell. The difference between U_{rev} and U_{cell} is due to irreversibilities, referred to as overvoltage, overpotential or polarization. The overvoltage originates primarily from electrical resistance (R) and kinetic overvoltage at the electrodes:

$$U_{cell} = U_{rev} + U_{cat} + U_{an} + IR \tag{2.3}$$

where U_{cat} and U_{an} are the kinetic losses at the cathode respectively the anode. I is the cell current. The kinetic overvoltage comprises activation and concentration potential. Activation potential is the result of electronic barriers that have to be overcome prior to current and ion flow, and concentration potential is due to gas transport losses especially at high currents.

Faraday's law gives that the amount of produced hydrogen is directly proportional to the cell current. The current efficiency of the electrolysis cell can be stated as:

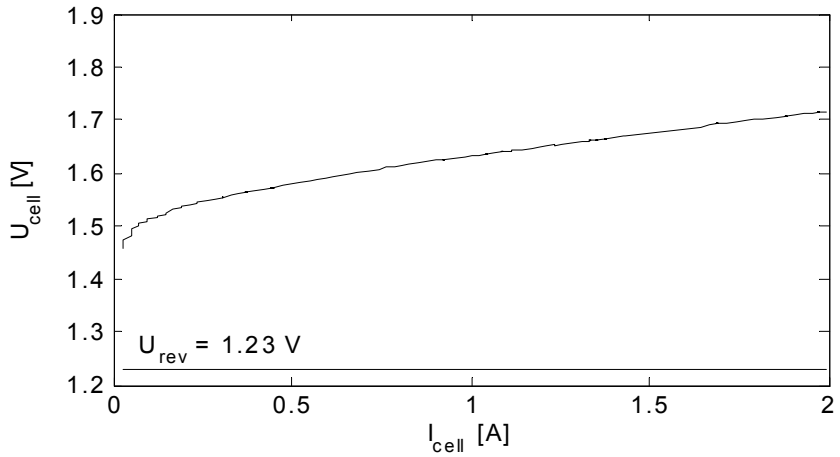

Figure 3. Polarization curve of an electrolysis cell with solid polymer electrolyte. (The author's own measurements[3]). The active cell area is 5 cm^2.

$$\eta_I = \frac{nF \cdot \dot{n}_H}{I} \tag{2.4}$$

where F is Faradays number (96,485 As/mol), $\dot{n}_H$ is the molar production rate of hydrogen, and I is the cell current (A). The number of electrons (n) involved in the reaction is 2 for water splitting. The current efficiency is close to 100% for electrolyzers with proton exchange membrane [36]. Industrial electrolyzers consist of many cells, which are connected in series and/or parallel. Thus, as seen in Figure 3, the voltaic efficiency can be improved by installing more cells and operating the electrolyzer at low current densities. However, the efficiency gain must be weighted against increased investment cost.

Normally, the electrolyzer capacity is expressed by the volumetric hydrogen production rate (Nm^3/h):

$$\dot{V}_{He} = \frac{3600}{1000} \cdot \frac{M_r}{\rho \cdot nF} \cdot \eta_I I \tag{2.5}$$

where M_r is the relative molecular mass (2.016 g/mol) and ρ is the density of hydrogen gas (0.08988 kg/Nm^3). The unit Nm^3 refers to "Normal cubic meters" at 20 °C and 1.01 bars. In the thesis, the electrical efficiency of the electrolyzer is defined as the specific power consumption (kWh/Nm^3):

[3] The measurements were carried out in collaboration with Harald Miland at Dept. of Materials Technology, NTNU, spring 2002.

$$\eta_e = \frac{P_e}{\dot{V}_{He}} = \frac{1}{3600} \cdot \frac{\rho_H nF \cdot U_{rev}}{\eta_I \eta_U M_r} \tag{2.6}$$

In Figure 4, the hydrogen production rate and the efficiency are plotted as a function of power consumption by using the polarization curve in Figure 3. The graphs are based on the assumptions that the current efficiency is 100% and that the maximum cell current is 2 A.

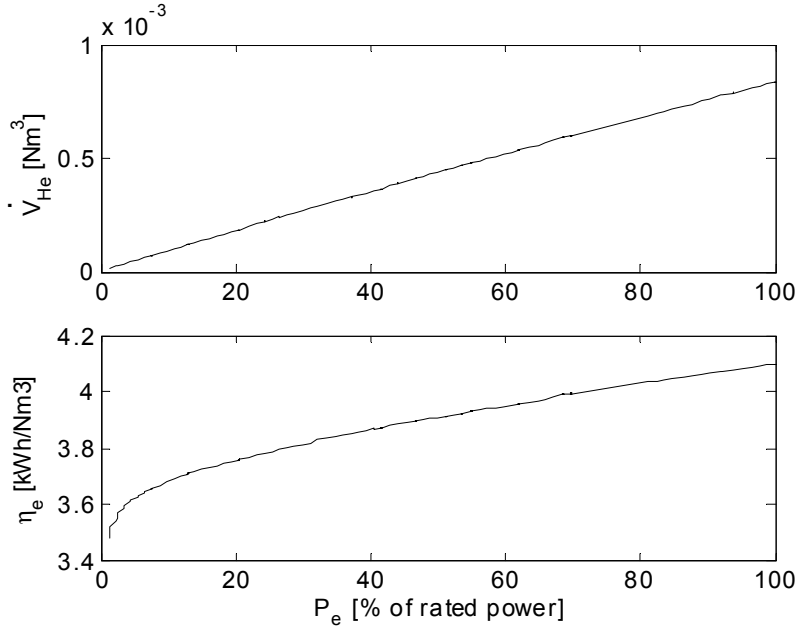

Figure 4. Hydrogen production rate (top graph) and efficiency (bottom graph) of an electrolysis cell plotted as a function of power consumption.

Electrolysis plants with alkaline electrolytes are commercially available both for large-scale and small-scale hydrogen production. The electrolyte is aqueous, usually with ~30% KOH of weight, and the basic reactions are:

$$\text{Cathode:} \quad 2H_2O_{(l)} + 2e^- \rightleftarrows H_{2(g)} + 2OH^- \tag{2.7}$$

$$\text{Anode:} \quad 2OH^- \rightleftarrows \frac{1}{2}O_{2(g)} + H_2O_{(l)} + 2e^- \tag{2.8}$$

In addition to the electrolysis cells, an alkaline electrolysis plant consists of additional equipment for the following functions [37]:

- direct-current supply
- feed-water supply
- electrolyte circulation

- gas separation and purification
- cooling
- inert gas supply
- process control
- power supply to auxiliary equipment

A flow sheet of a typical electrolysis plant is shown in Figure 5. Traditionally, alkaline electrolyzers have been designed for constant hydrogen production rates. In conjunction with wind power on the other hand, the electrolyzer must be able to follow sudden changes of operating conditions because of the variation of the wind. The electrochemical reactions are fast enough to follow load changes within seconds. A 100 kW pressurized GHW-electrolyzer was reported to react to a jump between 20% and 100% in less than 3 seconds [38]. Most of the delay was due to non-optimized controller characteristics of the rectifier. Furthermore, laboratory test of a pressurized 10 kW HYSOLAR electrolyzer showed that power fluctuations had no significant effect on the electrical stability [39].

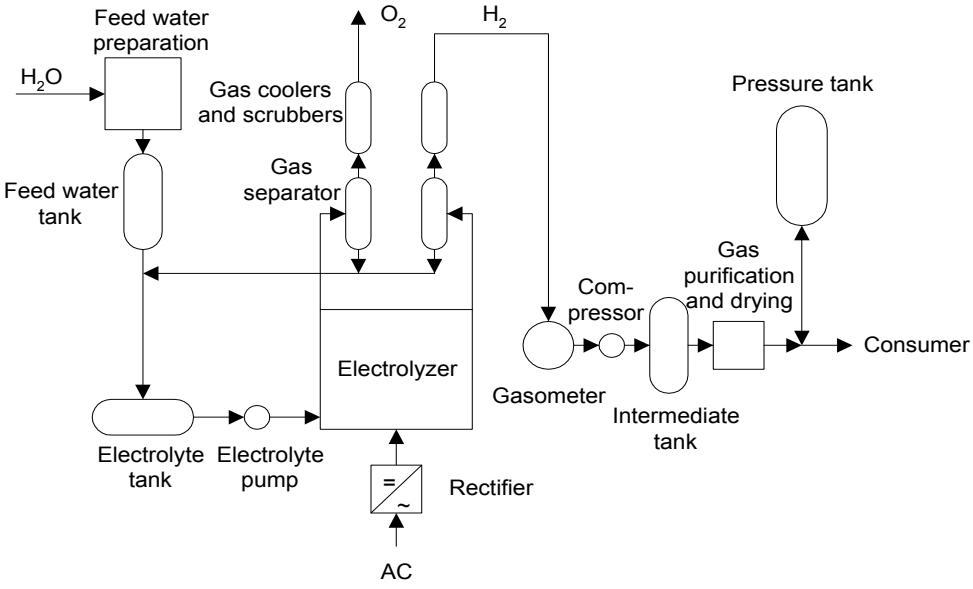

Figure 5. Illustration of a conventional alkaline electrolyzer plant. Based on [37].

Intermittent operation may cause impurity of hydrogen in oxygen and vice versa [37]. The reason is that sudden changes in gas production affect the circulation balance of the electrolyte, and pressure differences between the anode side and the cathode side may arise. Consequently, gas from one of the electrodes can diffuse through the diaphragm[4] (gas separator) to the wrong side. Hydrogen in oxygen is a safety risk regarding explosion, while

[4] The diaphragm separates individual cells that are stacked in parallel.

oxygen in hydrogen lowers the quality and thus the value of hydrogen. Moreover, fast power fluctuations can lead to incomplete separation of the gases from the electrolyte so that hydrogen and oxygen are mixed in the electrolyte [40]. It is important to ensure as equal pressure levels as possible on the cathode side and the anode side to prevent gas impurities. Pressurized electrolyzers use controlled expansion valves for this purpose. In the tests of the 10 kW HYSOLAR electrolyzer referred to above, the pressure control system was designed to minimize the difference between constant and intermittent power operation. It was concluded that fast dynamics of the power input did not significantly affect the gas impurity level.

Another issue with wind-electrolyzer systems is how to operate the electrolyzer in periods of low wind speed. Since the alkaline electrolyte is very corrosive, the electrode will corrode if the production is stopped. The electrodes should be polarized as long as they are in contact with the electrolyte to prevent corrosion. A polarization current must be provided from an external power source. For long periods with no hydrogen production, one can alternatively remove the electrolyte from the system. However, such shutdown procedures will increase the power consumption during start-up [40].

Electrolyzers with solid polymer electrolyte (SPE), also denoted proton exchange membrane (PEM), have simpler process layout, since there is no circulating liquid electrolyte. Thus, the PEM electrolyzer is easier to operate and provides fast start-up. Other advantages are high power density and energy efficiency. A comparison of the performance of selected electrolyzers is given in Figure 6. The basic electrode reactions are:

$$\text{Cathode:} \quad 2H^+ + 2e^- \rightleftarrows H_{2(g)} \tag{2.9}$$

$$\text{Anode:} \quad H_2O_{(l)} \rightleftarrows 2H^+ + \frac{1}{2}O_{2(g)} + 2e^- \tag{2.10}$$

PEM electrolyzers have not yet been competitive with alkaline electrolyzers mainly because of high costs for noble metal catalysts and polymer membrane [41]. However, the massive research effort in bringing down the amount of noble metals in PEM fuel cells would also bring down the cost of PEM electrolyzers.

To the author's knowledge, there are few studies of intermediate operation of PEM electrolyzers. However, an interesting effect was observed by Rasten while working with different metal oxide catalysts that were polarized anodically [41]. An aging effect gave rise to a slow increase in the

overvoltage over a 1-30 minute period. The interesting result was that sudden changes in the cell current counteract this effect. Thus, it was reported that it could be advantageous with respect to efficiency if the power input is fluctuating, as is the case for wind power.

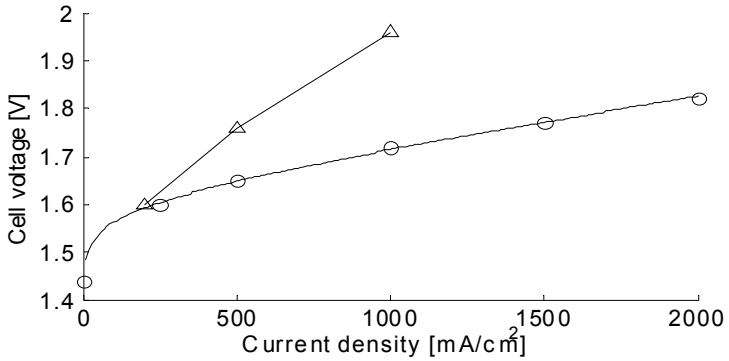

Figure 6. Selected polarization curves of electrolyzers. (Δ) represents a pressurized alkaline electrolyzer (graph adapted from [38]*). (o) represents a PEM electrolyzer (graph adapted from* [41]*).*

2.2.2 Hydrogen storage

Hydrogen can be stored as compressed gas, as cryogenic liquid, in solids (metal hydrides, carbon materials) and in liquid hydrogen carriers (methanol, ammonia). In the thesis, it is focused on large-scale stationary storage systems, which makes compressed gas storage most relevant. Compression of hydrogen is normally obtained by the use of piston compressors or centrifugal compressors. Several stages of compression are required because of the low density of hydrogen. The theoretical work for isothermal compression of ideal gas from pressure p_1 to p_2 is given by [42]:

$$W_{1,2} = p_1 V_1 \ln\left(p_2 / p_1\right) \tag{2.11}$$

where V_1 is the volume of the gas at pressure p_1. Because of the logarithmic relationship, the electricity consumption of the compressor is highest in the low-pressure range. It is therefore interesting to consider high-pressure electrolyzers that can reduce or even eliminate the electricity consumption related to hydrogen compression.

Conventional methods of above-ground hydrogen storage range from small high-pressure gas cylinders (>200 bar) to large low-pressure 12-16 bar spherical gas containers [43]. For large-scale storage of hydrogen, underground storage is expected to be two orders of magnitude cheaper [43, 44]. However, this option requires hydrogen storage in for example salt caverns or depleted natural gas reservoirs, which limits the potential usage.

2.2.3 Fuel cells

In a fuel cell powered by hydrogen, the reverse reaction of water electrolysis takes place:

$$H_2 + \frac{1}{2}O_2 \rightarrow H_2O \tag{2.12}$$

The chemical energy content of hydrogen is directly converted to electrical energy in the fuel cell. Therefore, a fuel cell can theoretically obtain higher electrical efficiency than thermal engines that are limited by the efficiency of the Carnot-cycle. However, kinetic overvoltages at the electrodes and electrical resistance cause relatively high losses in practical systems. An example of a polarization curve is shown in Figure 7. For this particular cell, the cell voltage is about 50% of the reversible cell voltage when the current density is 850 mA/cm^2.

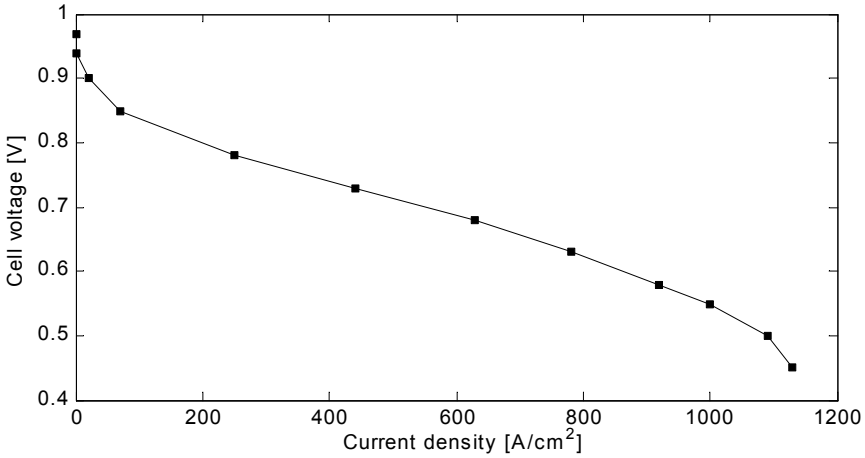

Figure 7. Polarization curve of PEM fuel cell, adapted from [45].

As for electrolyzers, fuel cells can be of alkaline type (AFC) and proton exchange membrane type (PEMFC), which are classified as low-temperature fuel cells with operating temperature of 70-90 °C. In addition, higher-temperature fuel cells with phosphoric acid electrolyte (150-210 °C), molten carbonate electrolyte (550-650 °C) and solid oxide electrolyte (750-1100 °C) have been developed [46]. In wind-hydrogen systems, the low-temperature cells are considered as most interesting because of their operating flexibility regarding startup and shutdown procedures as well as intermittent operation.

The power consumption of auxiliary equipment such as air blower and de-ionized water pump reduces the performance of a fuel cell system. In Figure 8, the net efficiency curve of a PEM fuel cell system is plotted. It clearly deviates from the polarization curve in the low power range. This shows

that it is important not only to develop energy efficient cells, but also to optimize the plant design. One way of achieving higher efficiencies is to make use of the heat produced in the stack. Testing of a Ballard PEM fuel cell has showed that heat could be recuperated from the water cooling system in the range 50-100% of full power [47]. The dynamic properties of this fuel cell system have also been reported. In power systems dominated by wind power, it is important that the fuel cell can respond fast to sudden load changes. It was concluded that the Ballard fuel cell responded to load commutations faster than 0.15 s.

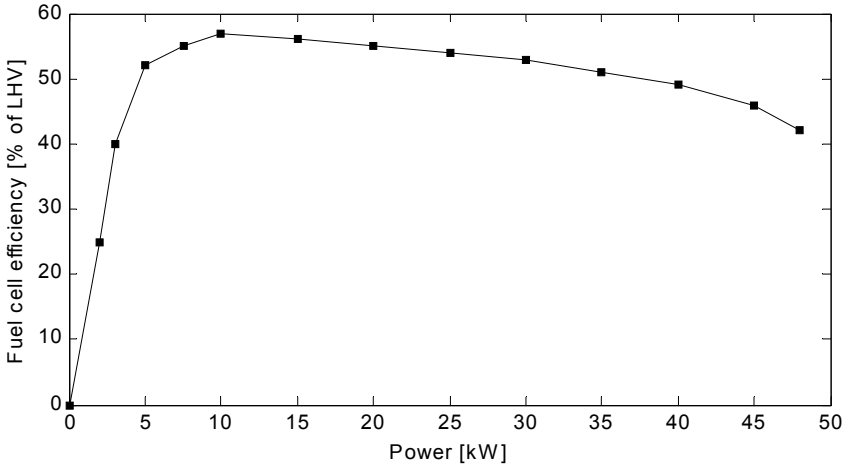

Figure 8. Part-load characteristics of PEM fuel cell, based on [48]. *The efficiency is measured in percentage of the lower heating value (LHV) of hydrogen.*

Reversible fuel cells are design to operate in either water electrolysis mode or power generation mode. For a wind-hydrogen system that stores hydrogen energy for later conversion back to electricity, reversible fuel cells may offer cost benefits compared to separate units for hydrogen production and power generation. For other applications, such as portable devices and spacecraft, reversible fuel cells are attractive because of low weight and volume. Reversing the electrochemical reaction within the same cell is challenging because of the technical problems of optimizing the electrode structure and composition. According to Militsky et al. [49] reversible PEM fuel cells with appropriate catalysts have been demonstrated to have high cycle life and equally good performance as individual electrolyzers and fuel cells. By storing the oxygen produced in electrolysis mode and by using the pure oxygen in fuel cell mode, the performance is significantly improved compared to using air. However, this benefit must be weighted against the added cost and complexity of including oxygen storage tanks in the system.

The electrical round-trip efficiency of reversible PEM fuel cells has been demonstrated to reach 40-46% at 500 mA/cm^2 current density [49, 50],

which is satisfactory compared to the present performance of individual electrolyzers and fuel cells. Losses are higher in fuel cell mode than in electrolyzer mode. Common for both operation modes is that the oxygen reaction contributes most to the losses because of activation overpotential at the electrode. Hydrogen evolution and reduction cause low overvoltages in comparison [51]. It is therefore interesting from a system performance point of view to evaluate alternatives to oxygen. For example, there have been some research-activities on reversible hydrogen-chlorine cells:

$$2\,HCl_{(l)} \underset{\text{discharge}}{\overset{\text{charge}}{\rightleftharpoons}} H_{2(g)} + Cl_{2(g)} \qquad (2.13)$$

The demonstrated overpotential of the Cl_2/Cl^- redox couple is significantly lower than for the corresponding O_2/OH^- redox couple [52]. An electrical round-trip efficiency of 75% has been achieved at 300 mA/cm^2 current density which is a promising result [53]. Similarly high efficiencies are possible for reversible fuel cells with the hydrogen-bromine couple [54]. The interest in H_2-Cl_2 has been low compared to H_2-O_2 systems, but H_2-Cl_2 systems have recently regained attention in fuel cell research at the Norwegian University of Science and Technology [55].

2.2.4 Electrical integration

Electrolyzers and fuel cells are DC-current devices. Thus, DC/AC conversion is required in order to connect the devices to the utility. Moreover, a wind turbine normally drives a three-phase AC generator, which means that AC/DC conversion is necessary to connect the wind power plant to an electrolyzer. In addition to controlling the active power flow, power converters could also be designed for providing reactive power support. Power converters based on thyristors require that the AC-grid is available. Thus, these so-called grid-commuted converters are not suitable for stand-alone operation [56]. Another type of power converters is based on semiconductor power devices known as "controllable switches" like GTO[5]-thyristors and IGBT[6] [57]. These devices can be controlled independently of the grid [56].

The choice of solution for electrical integration of wind-hydrogen systems is dependent on geographical conditions and the layout of the nearby grid. In cases where the wind-hydrogen system is considered to be connected to a strong grid, simple and low-cost solutions would be preferable. If the wind-hydrogen system should be connected to a weak or isolated grid, the ability

[5] GTO: Gate-Turn-Off
[6] IGBT: Insulated Gate Bipolar Transistors

to provide reactive power support and the ability of improving power quality, such as reducing flickering and harmonic currents, may be crucial. In both cases, there exist many different integration alternatives. Figure 9 and Figure 10 illustrate two possibilities for weak-grid integration, partly based on [56]. The first drawing shows an alternative where the different components are connected individually to the local grid, while the second drawing shows how the components can be connected to the grid by a common DC-link.

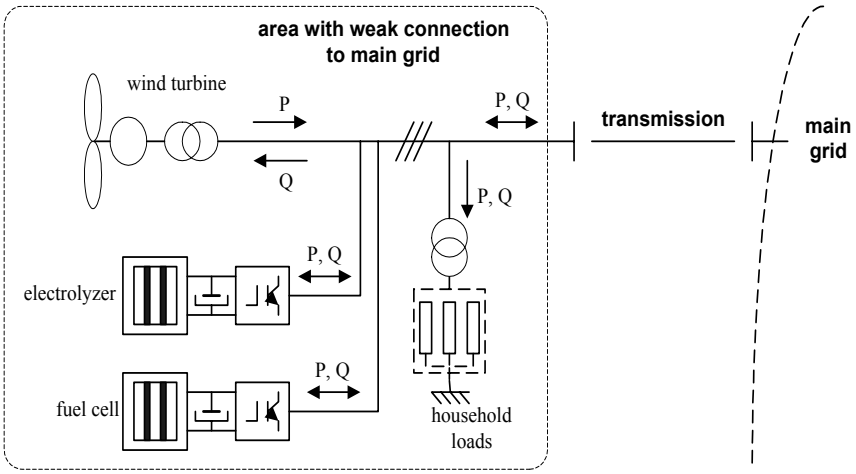

Figure 9. Wind-hydrogen system with individual integration of the different components, partly based on [56]. *P is active power and Q is reactive power.*

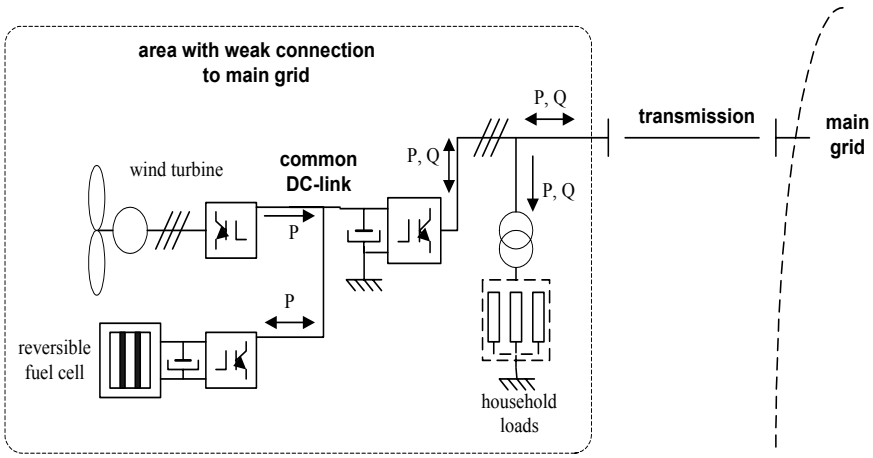

Figure 10. Wind-hydrogen system with integration through a common DC-link, partly based on [56]. *P is active power and Q is reactive power.*

2.3 Other energy storage solutions

In this section, only energy storage technologies which are suitable for storing energy for more than several hours are considered. Short-term energy storage technologies like superconducting magnetic energy storage, ultra capacitors and flywheels could also play an important role in conjunction to intermittent energy sources like wind, since they are able to smooth wind power fluctuations with response time from 0.1 s to 0.01 s [58]. These technologies seem to be suitable for storing energy in the range of seconds to minutes, but not for hours or more. The short-term storage alternatives is not considered further in the thesis, since the focus is on units that are suitable for storing energy for several hours or more. Systematic overviews of different energy storage systems and their applications can be found in [58-61].

2.3.1 Pumped hydro

Pumped hydro is a well-developed and reliable storage option. Energy is stored by pumping water from a low reservoir to a high reservoir and is released by passing the stored water through a hydro turbine back to the low reservoir. Thus, a pumped hydro plant requires two lakes separated by a vertical distance of at least 100 m [58]. This puts a substantial geographical limit on the number of suitable sites. Nonetheless, about 73 GW of pumped hydro capacity was operating worldwide in 1990 [56]. Furthermore, pumped hydro is cost-effective and efficient, with a round-trip efficiency of around 70% [61] and a reverse time of about 10 s [58].

2.3.2 Compressed air

In compressed air energy storage (CAES), air is compressed and stored in an underground cavern. Electricity generation is done by heating and then expanding the stored air through a high-pressure turbine. The air is then mixed with fuel (normally natural gas) and combusted. The exhaust is extracted through a low-pressure gas turbine [62]. Hydrogen has also been considered as a fuel in the combustion process [58]. Like pumped hydro, the distribution of CAES is limited by geographical conditions, since an airtight underground cavern is required for storage. Large-scale CAES systems have been successfully installed in Germany and USA [63]. The round-trip efficiency is about 70-75% [62, 63].

2.3.3 Secondary batteries

Secondary batteries are rechargeable batteries where electrochemical energy is stored in the electrode materials. Thus, the energy capacity is coupled to the power capacity, in contrast to fuel cell systems. This puts a practical limit to the energy capacity of the battery if high power capacity is required,

since the battery then tends to be large and expensive. Nevertheless, multi-MW battery storage systems with energy storage capacity in the MWh-range have been successfully demonstrated in several places [59, 64]. The most common battery is the lead-acid battery, which has frequently been installed in isolated power systems together with solar panels and wind turbines. Moreover, emerging battery technologies like the sodium-sulphur battery show promising performance [64]. Secondary batteries like the lead-acid battery are typically very efficient, with round-trip efficiencies of 75-90%, but have drawbacks with respect to operating life and power and energy density [65].

2.3.4 Redox flow cells

Redox flow system, also called flow batteries, can be regarded as hybrids of secondary batteries and fuel cells. External tanks contain reactive electrolyte chemicals that are pumped through an electrode stack where the electrochemical reactions take place. Thus, the energy capacity is independent of the power capacity, such as in hydrogen storage systems. Several emerging technologies have proven to be efficient for large-scale storage of energy, including the vanadium battery, the zinc-bromide battery and the sodium bromide-sodium polysulfide battery [61, 66, 67]. Apart from the ability of storing power in the multi-MW range for at least several hours, the advantage of flow batteries is that they obtain a round-trip efficiency of about 75% [63].

2.4 Renewable hydrogen demonstration projects

In this section, some relevant experimental studies and demonstration projects on the coupling of intermittent renewable energies and hydrogen storage are presented. Experimental studies on solar-hydrogen systems have received more attention in the past than wind-hydrogen systems. Gained experience in the design and operation of solar-hydrogen test systems is in many aspects valuable to wind-hydrogen systems, since solar energy also is an intermittent energy source.

One of the most successful small-scale demonstration projects has been carried out at the University of Helsinki, where an experimental 1 kW system consisting of a PEM electrolyzer and a PEM fuel cell was tested [68]. In an earlier project, the research group tested a system consisting of an alkaline electrolyzer, a pressure vessel for hydrogen storage and a phosphoric acid fuel cell [69]. This system had a poor operating efficiency, mainly because of problems with the fuel cell. A feature of the newer system is that the hydrogen is bound in metal hydrides instead of stored in a pressure tank. Depending on the temperature and operating current, the

round-trip efficiency of hydrogen varied between 24% and 32%. The paper concludes that the technical feasibility is good enough for small-scale seasonal storage and an overall efficiency close to 40% may be achieved by using state-of-the-art components. Another solar-hydrogen power plant that has shown promising results is located at the HSU Telonicher Marine Laboratory in California [70]. According to the reported operating experience, the electrolyzer had an excellent safety and performance record, but also here it has been difficult to provide a well working fuel cell unit.

Germany has been one of the most active countries in the field of renewable hydrogen energy research. During the nineties, several extensive projects were initiated, of which the three most important are the German-Saudi HYSOLAR Program [71], the Neunburg vorm Wald solar hydrogen demonstration project [72] and the Phoebus-Jülich demonstration plant project [73]. The major objective of the Phoebus-Jülich project was to test an autonomous solar electric energy supply system for a large building, in order to achieve high operational reliability and efficiency. The project concluded that the economics and operational reliability must be significantly improved and that the auxiliary energy requirement (compressors, power converters and controllers) is relatively high compared to the available solar energy. Nevertheless, the electrolyzer and the fuel cell showed relatively good performance. In the Neunburg vorm Wald project, a more comprehensive study of hydrogen energy systems has been carried out [72]. The demonstration plant consists of 135 kW solar generators, three different electrolyzers, hydrogen and oxygen gas systems, two different fuel cell plants, heating boilers and an automated liquid hydrogen filling station for test vehicles. Results from the test programs indicate that the integration of components into a meaningful overall plant concept is often more difficult and complex than commonly believed.

Hydrogen production from wind is more challenging than from solar since the power fluctuations are faster and more irregular. A prototype wind-hydrogen system has been installed at the ENEA Casaccia Research Centre in Italy as a part of an EC-funded project [39, 74]. The demonstration plant consisted of a 5.2 kW wind turbine, a 330 Ah battery, a 2.25 kW electrolyzer and a connection to the grid for electricity supply to auxiliary equipment. Intermittent operation did not present any major stability problems or general operational problems for the electrolyzer. Hydrogen and oxygen qualities were reported to be satisfactory. However, the electrolyzer suffered from reduced performance when operated at low power levels. A similar wind-hydrogen plant has been installed at the University of Applied Sciences in Stralsund, Germany. This system comprises a 100 kW windmill, a 20 kW alkaline electrolyzer and a 200 Nm^3

pressure tank [75]. Investigations of the electrolyzer behavior gave also here satisfactory results with respect to irregular power fluctuations.

A small, but comprehensive renewable energy system has been set up in Canada at Université du Québec à Trois-Rivières [76, 77]. A 10 kW wind turbine and a 1 kW solar panel provide the energy input to a DC bus controller. A 5 kW Stuart electrolyzer and a 5 kW Ballard fuel cell stack are connected to the DC bus. The DC bus also connects to batteries for voltage stability and to a dc-ac inverter that delivers a constant 60 Hz 115 V output to an electrical load. The hydrogen is stored at 10 bars. It was reported that the system showed reliable and safe long-term performance. However, the overall storage losses are high. Energy losses in hydrogen production and compression were reported to be 40%, while energy losses in the fuel cell were 55%. At Folkecenter of Renewable Energy in Denmark, a complete pilot hydrogen supply chain including a 75 kW windmill, a 20 kW electrolysis plant, a hydrogen storage tank and a filling station with dispenser for hydrogen-fueled cars have been set up [78]. Through advanced electronic control, it is possible to operate the electrolyzer in the full range of 0-100% of rated power and thus obtain optimal utilization of fluctuating wind power. The hydrogen fuels a Ford Focus with compressed hydrogen storage and a 2.0-liter modified petrol engine.

Some interesting large-scale wind-hydrogen projects have recently been initiated. At Australia's Antarctic Mawson Station, a 900 kW wind turbine is installed to supply 80% of the station's energy needs. By 2007, it is expected that the excess wind energy will be used for hydrogen production, so that fuel cells can replace the existing diesel generators at the station [79, 80]. In North Ayrshire, Scotland, installation of a 3 MW electrolysis plant is planned for production of hydrogen in response to the power output of a 25 MW wind power plant and in response to local balancing requirements. The stored hydrogen would be combusted in a hydrogen gas engine with maximum output of 10 MW [81].

There are also several ongoing renewable hydrogen demonstration projects in Norway. At Institute for Energy Technology (IFE), a hydrogen storage laboratory has been build, which includes a 1 kW PEM electrolyzer, a 1 kW PEM fuel cell, metal hydride, secondary batteries, electrical load, DC power supply and power controller [82]. Furthermore, a renewable energy system has been installed at the Agder University College, which comprises a thermal system and an electrical system. The electrical system includes two 10 kW solar panel, a 50 kW, 15 bar alkaline electrolyzer and a 2.5 kW fuel cell stack. The hydrogen is stored at 15 bars [83].

A large-scale wind-hydrogen project is coordinated by Norsk Hydro ASA for the small island Utsira at the west coast of Norway. The energy plant is planned to be finished in 2004. It will comprise a 600 kW wind turbine, a 5 kWh flywheel, a 50 kW alkaline electrolyzer, a 3 kW compressor, 2000 Nm^3 pressurized hydrogen storage and hydrogen engines and fuel cells with 60 kW total capacity [84, 85]. Another interesting wind-hydrogen project has recently been established between Statkraft, Stuart Energy Systems and Corporación Energía Hidroeléctricia de Navarra S.A. (EHN). The objective of the collaboration is the evaluation, demonstration and development of solutions based on hydrogen generated from renewable energy sources. A part of this project is to install a 5 kW electrolyzer in the Universidad Pública de Navarra, Spain and to operate the electrolyzer with simulated wind power as input. Moreover, a hydrogen station will be build for fueling three city buses in Pamplona, Spain. A hydrogen demonstration facility will also be installed in Norway [86].

3 EVALUATION OF WIND-HYDROGEN SYSTEMS USING A TIME SEQUENTIAL SIMULATION MODEL

3.1 Introduction

The purpose of this chapter is to describe different possibilities for hydrogen storage in connection with wind power and to give a techno-economical evaluation of the integration alternatives. The focus is on how to use hydrogen storage to increase the penetration of wind power in areas with limited transmission capacity to the main grid. In order to perform this study, a computer model for time sequential simulation of wind-hydrogen systems has been developed. The evaluation is based on the levelised cost of supplied electricity and the levelised cost of supplied hydrogen. In order to limit the scope of the work, the analysis of the different wind-hydrogen systems is based on one representative case study. Three wind-hydrogen alternatives are analyzed. In Type A, hydrogen from water electrolysis is used as a fuel for transportation. In Type B, hydrogen is converted back to electricity for stationary energy use. Type C combines the two other types by using hydrogen both for stationary energy supply and as a fuel for transportation. Figure 11 shows schematic drawings of the three different types.

The chapter is divided into three main sections. In section 3.2 , the analysis method is presented. The section describes the plant model, the operating strategies and the cost model. Section 3.3 describes the case study. Sections 3.4 - 3.8 present the simulation results and give a thorough discussion and evaluation of the different integration alternatives.

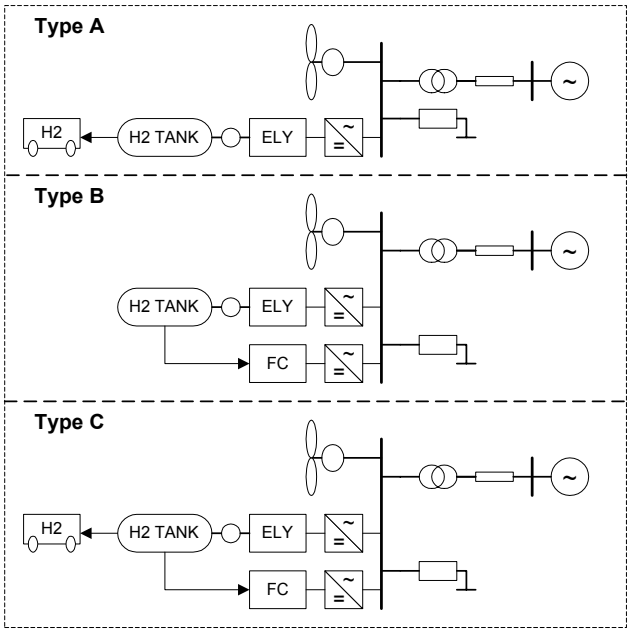

Figure 11. Different types of wind-hydrogen systems. ELY: electrolyzer, FC: fuel cell.

3.2 Method

3.2.1 Plant model

In the wind-hydrogen system defined as Type C, hydrogen can be used both for transportation and to power a stationary fuel cell for electricity production. Since Type C comprises all components that are present in the other two types, the energy equations described below are based on Type C. The equations are applicable to Type A and Type B by omitting the fuel cell respectively the hydrogen load. Figure 12 shows the wind-hydrogen system with variable names for all components.

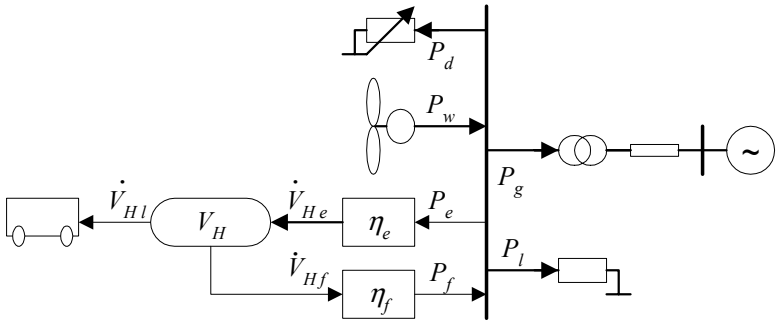

Figure 12. Variable names in the wind-hydrogen plant model.

Power exported to the main grid P_g can take both positive values (export) and negative values (import). The power balance is given by

$$P_e(t) + P_d(t) + P_g(t) - P_f(t) = P_w(t) - P_l(t) \tag{3.1}$$

where the plant variables are on the left hand side of the equality sign and the external inputs are on the right hand side. Power export and import are constrained by

$$-P_g^{max} \le P_g(t) \le P_g^{max} \tag{3.2}$$

where P_g^{max} is the maximum allowable transmission of power to the main grid. For simplicity, P_g^{max} is set to a constant value, and the import capacity is set equal to the export capacity. In periods when the local power surplus exceeds the grid capacity, wind power has to be dissipated. This is represented as a controllable dump load P_d in Figure 12. Alternatively, reduction of wind power output can be obtained by a wind power controller, which reduces the wind power output to P_w–P_d. The model does not distinguish between these control mechanisms.

The relations between power and hydrogen flow rate in the electrolyzer and the fuel cell are given by

$$P_e(t) = \eta_e \dot{V}_{He}(t) \tag{3.3}$$

$$P_f(t) = \eta_f \dot{V}_{Hf}(t) \tag{3.4}$$

where η_e is the specific power consumption of the electrolyzer, including rectifier losses and consumption of power for hydrogen compression. Similarly, η_f is the specific power output of the fuel cell, taking into account inverter losses. Electrolyzer and fuel cell operation are limited by the following restrictions:

$$P_e^{min} \le P_e(t) \le P_e^{max} \quad \text{or} \quad P_e(t) = 0 \tag{3.5}$$

$$P_f^{min} \le P_f(t) \le P_f^{max} \quad \text{or} \quad P_f(t) = 0 \tag{3.6}$$

where P_e^{max} and P_f^{max} are the maximum power capacities of the components, which is also referred to as rated power in the text. A feature of the model is the specification of a minimum electrolyzer power P_e^{min} and minimum fuel cell power. In normal operation mode, the electrolyzer must either be operated at $P_e \ge P_e^{min}$ or be switched off. Thus, values of P_e in the range $<0, P_e^{min}>$ are not allowed. Analogously, the fuel cell cannot be operated in the range $<0, P_f^{min}>$. With present technology, electrolyzers have a minimum operating point ranging from 10% to 50% of nominal

power depending on the manufacturer. The efficiency of actual electrolyzer plants and fuel cell plants approaches zero for low operating points because of the power consumption of auxiliary equipment. In addition, alkaline electrolyzers must maintain a minimum protection current [87]. The procedure of on/off switching is important if the electrolyzer is used for wind power smoothing. It could be better to maintain hydrogen production, even when the wind power generation drops to zero, because of mechanical wear and possibly electrochemical degradation related to frequent on/off switching. These issues are component specific and are not considered further here.

The hydrogen storage balance is expressed as

$$V_H(t+1) - \frac{P_e(t)}{\eta_e}\Delta t + \frac{P_f(t)}{\eta_f}\Delta t = V_H(t) - \dot{V}_{Hl}(t)\Delta t \tag{3.7}$$

where the hydrogen load $\dot{V}_{Hl}$ is an external input with a fixed value for each time step. The amount of hydrogen that can be stored is constrained by

$$0 \le V_H(t) \le V_H^{max} \tag{3.8}$$

where V_H^{max} is the maximum storage capacity.

To evaluate the performance of the wind-hydrogen system over a period of time, it is necessary to calculate the net electricity production, consumption and export as well as hydrogen production and consumption in the different parts of the system. For all components, the net electrical energy production or consumption is

$$E = \sum_{t=1}^{T} P(t)\Delta t \tag{3.9}$$

Similarly, total hydrogen demand is given by

$$V_{Hl} = \sum_{t=1}^{T} \dot{V}_{Hl}(t)\Delta t \tag{3.10}$$

where T is the final time step and Δt is the time resolution in hours. The net power export to the grid P_g was introduced in (3.1). By the use of equation (3.9), it is possible to calculate the net energy export to the grid over the simulation period. It is also valuable to distinguish between the power export and power import, which is achieved by the following expressions:

$$
\begin{aligned}
&\text{if } P_g(t) \le 0 \\
&\quad P_{imp}(t) = -P_g(t) \\
&\quad P_{exp}(t) = 0 \\
&\text{else} \\
&\quad P_{imp}(t) = 0 \\
&\quad P_{exp}(t) = P_g(t)
\end{aligned}
$$

where P_{exp} and P_{imp} are power export and power import, respectively. The total amount of exported and imported energy can then be calculated from (3.9). Moreover, the power import used for hydrogen production is found by introducing the expression

$$
\begin{aligned}
&\text{if } P_{imp}(t) \le P_l(t) \\
&\quad P_{imp,e}(t) = 0 \\
&\text{else} \\
&\quad P_{imp,e}(t) = P_{imp}(t) - P_l(t)
\end{aligned}
$$

where $P_{imp,e}$ is the imported power used for electrolytic hydrogen production.

The utilization factors of the wind power plant, electrolyzer and fuel cell are calculated from

$$UF = \frac{\sum_{t=1}^{T} P(t)\Delta t}{\sum_{t=1}^{T} P^{max}\Delta t} = \frac{1}{P^{max}} \cdot \frac{E}{T\Delta t} = \frac{\overline{P}}{P^{max}} \tag{3.11}$$

while the utilization factor of the cable which connects the local system to the main grid is calculated by taking the absolute value of P_g:

$$UF_g = \frac{\sum_{t=1}^{T} \left| P_g(t) \right| \Delta t}{\sum_{t=1}^{T} P_g^{max}\Delta t} \tag{3.12}$$

3.2.2 Control strategies for Type A: Hydrogen used as a transportation fuel

Maximum utilization of grid capacity

This control strategy is developed for using the electrolyzer as a controllable load for wind power plants in grids with transmission constraints. The objectives of the control strategy are to minimize dissipation of wind energy and to provide sufficient amounts of hydrogen to the filling station. The electrolyzer is operated if the wind power exceeds the sum of the local load and the grid capacity or if the hydrogen storage drops below a specified supply security limit V_H*. The latter operation condition is important in order to ensure that there is sufficient hydrogen in the storage tank for filling of vehicles. The control strategy is defined by the logical expression

$$
\begin{aligned}
&\text{if } V_H(t) < V_H^* \\
&\quad P_e(t) = P_e^{max} \\
&\text{elseif } P_w(t) > P_l(t) + P_g^{max} \\
&\quad \min_{P_e(t)} \{P_d(t)\} \\
&\text{else} \\
&\quad P_e(t) = 0
\end{aligned}
$$

The notation in line four expresses that the electrolyzer power P_e is the control variable which is used for minimizing wind power dissipation P_d. The system constraints are given by the plant equations (3.1)-(3.8) with $P_f^{max} = 0$ and $P_f^{min} = 0$ in (3.6). During normal operation, P_d is zero. However, some operating conditions lead to dissipation of wind power. Such cases occur if the hydrogen storage level has reached the maximum limit or if the local power surplus exceeds the electrolyzer rating.

Using local energy surplus for hydrogen production

Hydrogen is produced for two purposes in the operation strategy described in the previous section; either because the grid limit is exceeded, or because the hydrogen storage level drops below a minimum supply security limit. Another approach is to produce hydrogen from wind energy whenever there is a local power surplus. In this case, hydrogen production has a higher priority than export of wind power. Such an operating strategy could be beneficial if there are high grid losses or the market price of power export is low. It is necessary to make a slight modification of the previous logical expression to define this operating strategy:

$$
\begin{aligned}
&\text{if } V_H(t) < V_H^* \\
&\quad P_e(t) = P_e^{max} \\
&\text{elseif } P_w(t) > P_l(t) \\
&\quad \min_{P_e(t)} \left\{ P_{exp}(t) \right\} \\
&\text{else} \\
&\quad P_e(t) = 0
\end{aligned}
$$

which states that the electrolyzer is operated if there is a local surplus of power or if the hydrogen level reaches the specified low level limit V_H*. The system constraints are given by the plant equations (3.1)-(3.8) with $P_f^{max} = 0$ and $P_f^{min} = 0$ in (3.6).

Using wind energy primarily for hydrogen production

With this control strategy, wind energy is used primarily for hydrogen production, and excess energy is consumed by the local load or exported to the main grid. Thus, the hydrogen load has a higher priority than the electrical load. This operating strategy is relevant for the cases where wind-derived hydrogen has a higher market value than wind power, or if we want to simulate a stand-alone wind-electrolyzer plant. The control strategy for the electrolyzer power is

$$
\begin{aligned}
&\text{if } V_H(t) < V_H^* \\
&\quad P_e(t) = P_e^{max} \\
&\text{else} \\
&\quad \min_{P_e(t)} \left\{ P_w(t) - P_e(t) \right\}
\end{aligned}
$$

which states that the electrolyzer power primarily follows the wind power generation, but it also draws power from the grid if needed for supplying the hydrogen load in periods with little or no wind. The system constraints are given by the plant equations (3.1)-(3.8) with $P_f^{max} = 0$ and $P_f^{min} = 0$ in (3.6).

3.2.3 Control strategies for Type B: Hydrogen used as electrical energy storage

Maximum utilization of grid capacity

The objective of this control strategy is to minimize wind power dissipation. Therefore, the hydrogen storage is restricted to be used for storing excess wind energy that would otherwise have been dissipated due to grid constraints. When the wind power generation is less than the sum of local

consumption and grid capacity, the stored hydrogen is sent to the fuel cell for power generation. The control strategy is expressed as

$$\begin{aligned}
&\text{if } P_w(t) > P_l(t) + P_g^{max} \\
&\quad \min_{P_e(t)} \{P_d(t)\} \\
&\quad P_f(t) = 0 \\
&\text{else} \\
&\quad \max_{P_f(t)} \{P_g(t)\} \\
&\quad P_e(t) = 0
\end{aligned}$$

The system constraints are given by the plant equations (3.1)-(3.8) with $\dot{V}_{Hl}(t) = 0$ in (3.7). The control variable for minimizing wind power dissipation is electrolyzer power. The fuel cell also acts as a control variable for this purpose, by releasing as much of the stored hydrogen as possible whenever the local surplus is below the grid limit. In this way, it will be possible to store more hydrogen at a later stage when the wind power generation is high.

Matching local generation and consumption

Here, hydrogen storage is applied for matching fluctuating generation with fluctuating load. Thus, the objective of the control strategy is to minimize the import *and* export of power. If the value of exported wind energy is zero, this control strategy represents the operation of a stand-alone power system based on wind-hydrogen with a backup plant. The electrolyzer is operated when wind generation exceeds the local consumption, and the fuel cell is operated in the opposite case. The system constraints are given by the plant equations (3.1)-(3.8) with $\dot{V}_{Hl}(t) = 0$ in (3.7), and the control logic becomes

$$\begin{aligned}
&\text{if } P_w(t) > P_l(t) \\
&\quad \min_{P_e(t)} \{P_{exp}(t)\} \\
&\quad P_f(t) = 0 \\
&\text{else} \\
&\quad \min_{P_f(t)} \{P_{imp}(t)\} \\
&\quad P_e(t) = 0
\end{aligned}$$

which states that the electrolyzer is operated for minimizing power export and the fuel cell is operated for minimizing power import.

3.2.4 Control strategies for Type C: Hydrogen used as fuel for transportation and for stationary energy supply

Matching local generation and consumption

The Type C system comprises both a hydrogen filling station and a stationary fuel cell. Hence, wind energy and electrolytic hydrogen can cover the total local energy demand, including energy for transportation. The control strategy is to try to match local power generation and consumption by active operation of electrolyzer and fuel cell. In addition, hydrogen is withdrawn from the compressed storage tanks to be used by vehicles. Therefore, it must be ensured that the hydrogen level is above a supply security limit V_H* as for the Type A system. The control variables are also here electrolyzer power and fuel cell power, and the control strategy is given below:

$$
\begin{aligned}
&\text{if } V_H(t) < V_H^* \\
&\quad P_e(t) = P_e^{max} \\
&\quad P_f(t) = 0 \\
&\text{elseif } P_w(t) > P_l(t) \\
&\quad \min_{P_e(t)} \left\{ P_{exp}(t) \right\} \\
&\quad P_f(t) = 0 \\
&\text{else} \\
&\quad \min_{P_f(t)} \left\{ P_{imp}(t) \right\} \\
&\quad P_e(t) = 0
\end{aligned}
$$

The system constraints are given by the plant equations (3.1)-(3.8). It is decided that the hydrogen load has higher priority than the electrical load, as stated by the first if-sentence in the control strategy. When $V_H(t) > V_H^*$, the control strategy of Type C is identical to Type B for balancing the local electricity generation and consumption.

3.2.5 Cost model

In order to estimate the production cost of hydrogen and electricity from the wind-hydrogen plant, an economic model based on the principles of the "levelised production cost" method has been developed. In [88], a method for calculating the levelised prodution cost of wind energy is explained. Here, the method is extended for the combined supply of hydrogen and electricity from wind.

The discounted present value of the total cost for component *j* is

$$TC_j = IC_j + \sum_{y=1}^{Y} OM_j(y) \cdot (1+r)^{-y} + RI_j \cdot (1+r)^{-(L+1)} - SV_j \cdot (1+r)^{-Y} \quad (3.13)$$

where IC_j is the initial investment cost, $OM_j(y)$ is the operation and maintenance cost during year y, RI_j is reinvestment cost, and SV_j is the salvage value of the component. The analysis period is Y years and the economic lifetime of the component is L years. It is assumed that OM_j is constant for all years, which gives

$$\sum_{y=1}^{Y} OM_j(y) \cdot (1+r)^{-y} = OM_j \sum_{y=1}^{Y} (1+r)^{-y} = \frac{OM_j}{a_{r,Y}} \quad (3.14)$$

where $a_{r,Y}$ is the annuity factor for discount rate r and Y years.

If the lifetime of the component exceeds the length of the analysis period, the salvage value (rest value) is calculated from

$$SV_j = IC_j \cdot \frac{a_{r,L}}{a_{r,L-Y}} \quad (3.15)$$

On the contrary, some components have shorter lifetime than the analysis period, which makes it necessary to reinvest. For simplicity, it is assumed that the reinvestment cost RI_j is equal to the initial investment cost IC_j, although for instance the cost of fuel cells is expected to decrease. After the end of the analysis period, the reinvested component will have a salvage value

$$SV_j = RI_j \cdot \frac{a_{r,L}}{a_{r,R}} \quad (3.16)$$

where R is the rest period, i.e. the number of years after the analysis period that the reinvested component has left of its lifetime.

For wind power plants with no hydrogen storage, the levelised production cost of electricity is calculated from

$$LPC_{el} = \frac{a_{r,Y} \cdot TC_w}{E_w - E_d} \quad (3.17)$$

where E_w is the potential energy output of the wind power plant and E_d is dissipated energy due to grid constraints. If a hydrogen storage system is included, we get

$$LPC_{el} = a_{r,Y} \cdot \frac{\sum_{j} TC_j}{E_w + E_f - E_e - E_d} \tag{3.18}$$

where the denominator is the annual energy delivered by the wind-hydrogen system. The *j* components comprise wind turbines, power conversion system, electrolyzer, compressor, storage tank and fuel cell.

A special case occurs when the generated wind power is used both for supplying an electrical load and a hydrogen load via water electrolysis. It must be decided what part of the total cost that should be associated with hydrogen supply and electricity supply. This is relevant for the Type A and Type C systems defined in Figure 11. The procedure of calculating electricity and hydrogen production cost is different for the two types.

Type A

Since wind energy is utilized for both supply of electricity and production of hydrogen, a method that divides the total cost between electricity cost and hydrogen cost is developed. The electricity production cost is calculated from a reference system with no hydrogen storage and the same amount of wind energy delivered to the grid:

$$LPC_{el} = \frac{a_{r,Y} \cdot TC_w^{ref}}{E_w - E_d - E_e} \tag{3.19}$$

where the denominator is the net energy delivered to the grid, and TC_w^{ref} is the total cost of a wind power plant with net energy output equal to E_w - E_d - E_e. The hydrogen production cost is found by subtracting the total cost of the reference systems from the total cost of the wind-hydrogen system

$$LPC_{H2} = a_{r,Y} \frac{\sum_{m} TC_m - TC_w^{ref}}{V_{Hl}} \tag{3.20}$$

where V_{Hl} is the annual volume of delivered hydrogen (Nm^3) and the *m* components comprises wind turbines, power conversion system, electrolyzer, compressor and compressed storage tanks.

Type C

Hydrogen is used both as a source of transportation fuel and stationary energy in Type C. The choice of method for finding the cost of supplied hydrogen and electricity depends on the primary usage of the hydrogen. In

this context, it is decided that hydrogen is used primarily for stationary energy, so that hydrogen delivered to the filling station is a by-product. The electricity cost is calculated from a reference system with no hydrogen filling station, which delivers the same amount of wind energy to the grid:

$$LPC_{el} = a_{r,Y} \cdot \frac{\sum_j TC_j^{ref}}{E_w + E_f - E_e - E_d} \tag{3.21}$$

where the denominator is the annual net energy delivered to the grid. TC_w^{ref} is the total cost of a wind-hydrogen system with no filling station with annual energy output equal to $E_w+E_f-E_e-E_d$. The hydrogen production cost is found by subtracting the total cost of the reference system from the total cost of the wind-hydrogen system

$$LPC_{H2} = a_{r,Y} \cdot \frac{\sum_j TC_j - \sum_j TC_j^{ref}}{V_{Hl}} \tag{3.22}$$

where V_{Hl} is the annual volume of delivered hydrogen.

3.2.6 Computer implementation

A computer model has been developed in Matlab for simulations of wind-hydrogen systems based on the proposed control strategies. Time series for wind, electricity load and hydrogen load are inputs to the model. The time stepsize in the simulations is chosen to be one hour. Energy balances and hydrogen flow balances are calculated for each time step based on the plant model and the specified control strategy. Calculation of the hydrogen storage level at the beginning of time step t+1 requires the storage level of the previous time step t as input, according to equation (3.7). After the final time step, the simulation data is used for calculation of main results, which comprises net electrical energy production and consumption, net hydrogen production and consumption, utilization factors and energy efficiencies. Finally, the program calls a function that calculates the levelised production cost of electricity and hydrogen. Figure 13 displays a flowchart of the simulation model.

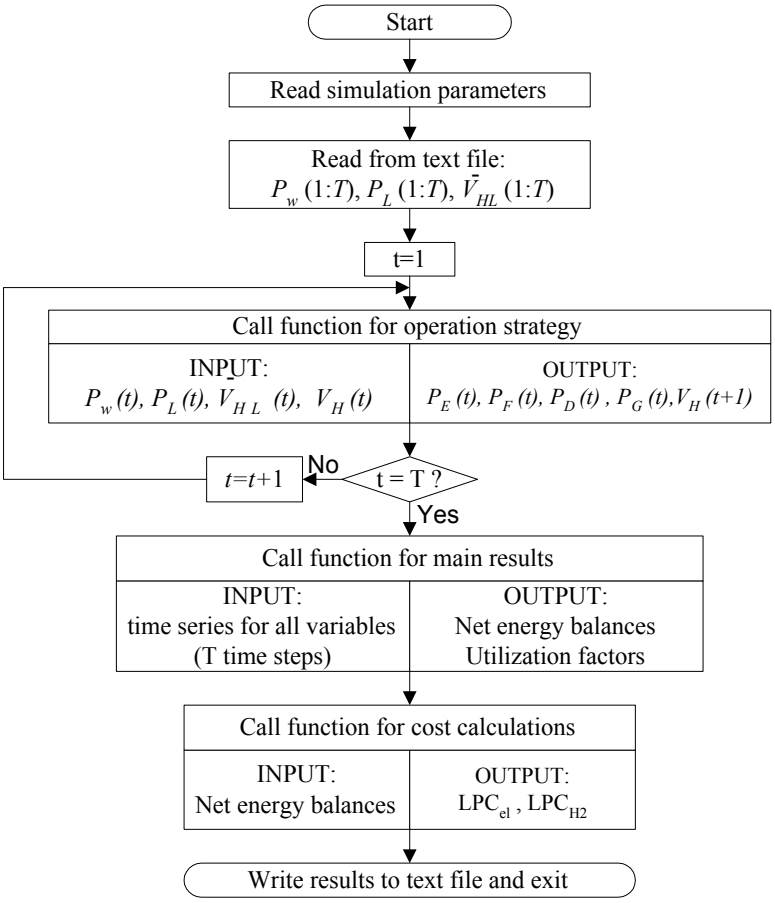

Figure 13. General flowchart of the Matlab-model.

3.3 Case study

3.3.1 Example system and simulated electrical load

A representative example system has been constructed to be used in a case study. The system is constructed in the sense that it is not a representation of an actual system, but rather a system that has similarities to real systems. Figure 14 illustrates the example system. The hypothetical location is chosen to be an island with good wind resources but with limited possibilities of exporting wind power due to grid constraints. There is a demand for electricity at the island, with an average load of 1,250 kW. The electricity load follows a typical Norwegian pattern, with high demand at winter and low demand at summer. The minimum and maximum loads are set to 700 kW and 1,900 kW, respectively. Figure 15 shows how the load varies over the day and the year. The load series is originally made by Sintef

Energy Research for the simulation tool WDLTOOLS [101]. A sea cable with a maximum capacity of 5,000 kW connects the island to the main grid. With no wind power installed and no electrolytic hydrogen production, the utilization factor of the cable is 25%. In addition to electricity, there is also an energy demand for transportation, which for instance could be cars, buses, ships and fishing boats.

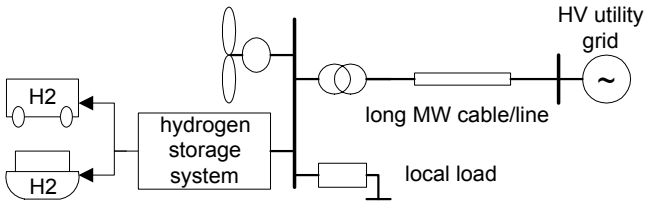

Figure 14. Example system.

Even if the chosen location is a relative small island, the analysis carried out here is transferable to larger areas. For instance, there is a large wind power potential in Finnmark in northern Norway. However, as explained in chapter 2.1, full exploitation of the resources demand grid reinforcements of a relatively weak 132 kV connection east of Balsford [11]. Other relevant areas are parts of Ireland, Scotland, Denmark, Germany and Spain with high wind energy penetration. A further increase of wind energy in these areas can be difficult both because of grid limitations and because wind fluctuations demand extensive regulating capacity.

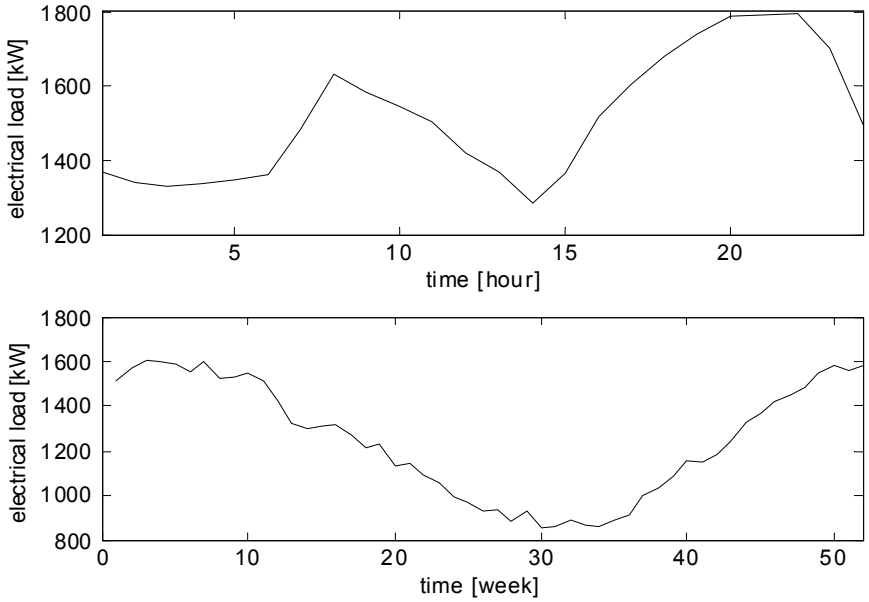

Figure 15. Daily and seasonal electrical load pattern.

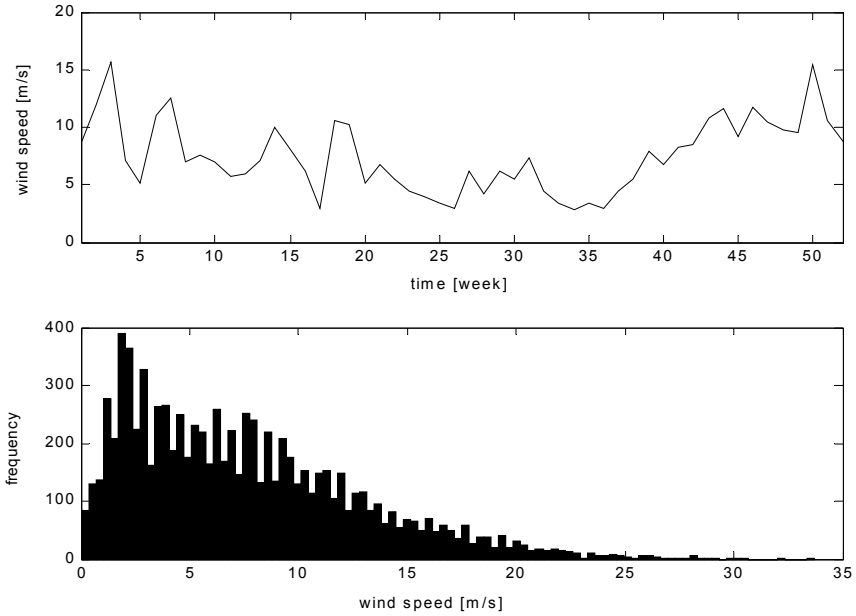

Figure 16. The wind data used in the simulations. The upper graph shows weekly average values of wind speed over the year, while the lower graph is a histogram of the 8760 wind speed values.

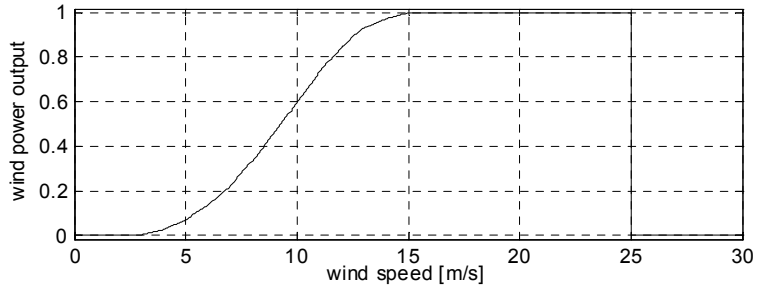

Figure 17. Normalized wind power curve.

3.3.2 Simulated wind power output

The wind data are from Torsvåg in northern Norway. The average wind speed for the chosen wind data is 5.8 m/s. However, wind measurements are taken at relatively low height, typically 10 meter above the ground, while modern wind turbines have a hub height of 60-90 meters. The wind speed increases with height, and the relation between the wind speed at height h_2 and h_1 can be approximated by:

$$v_2 = v_1 \cdot \frac{\ln(h_2 / r)}{\ln(h_1 / r)} \tag{3.23}$$

where the roughness factor r is assumed to be 0.01 m, which is typical for flat terrain [89]. Taking h_1 = 10 m and h_2 = 80 m, we obtain a correction factor equal to 1.301 for the original wind data. The average yearly wind speed then becomes 7.5 m/s. It should be mentioned that this is a relatively low value compared to what we find in other places in Norway.

A sequential plot and a histogram of the wind speed are shown in Figure 16. We see that the wind speed follows a seasonal pattern, with high values in winter and low values in summer, which is typical for many locations in Norway, as reported by Tande and Vogstad [90]. This could have a positive effect on the energy balance since the electricity demand variations follows a similar pattern. The wind power curve is shown in Figure 17, which is similar to the Danish BONUS turbines. The utilization factor UF_w of the wind power plant is defined in equation (3.11), and for the chosen wind data and wind power curve, UF_w is equal to 0.34.

3.3.3 Simulated hydrogen demand

For the scenarios where hydrogen is used as a fuel for transportation, one must establish a time series for the hydrogen demand. As for electricity demand, the demand of transportation fuel in an area will vary both on a daily and seasonal basis. Moreover, the demand pattern will be different for e.g. cars, buses and boats. However, for this study it is assumed that a simplified representation of the hydrogen demand is sufficient. A filling station for hydrogen is directly connected to the compressed hydrogen storage tanks in the wind-hydrogen system. Filling of hydrogen vehicles (or boats) occurs in the period 2:00-6:00 each night. The basic filling pattern is repeated each day of the year, and the same amount of hydrogen is withdrawn from the storage tanks every day. The filling period is chosen to be at night because electricity price normally is low at that time. Moreover, a filling period of four hours is chosen instead of for example one hour, in order not to simulate a system with oversized capacity of the filling equipment.

Four different hydrogen-filling scenarios have been defined in Table 1. With respect to the lower heating value (LHV) of hydrogen, the hydrogen load corresponds 12.5%, 25%, 50% and 100% of the average electrical load, respectively. The lower heating value of hydrogen is 2.995 kWh/Nm^3.

Table 1. The four different scenarios for hydrogen demand.

H_2-load scenario	1	2	3	4
Daily H_2-load [Nm^3]	1,250	2,500	5,000	10,000
Daily H_2-load [% of $\overline{P}_l$]	12.5	25	50	100

If hydrogen produced electrolytically from wind was one of several sources of transportation fuel, it would be beneficial to let the wind-hydrogen contribution follow the wind variations to reduce the required hydrogen storage capacity. A seasonal hydrogen delivery pattern that follows the wind variations is shown in Figure 18. The total amount of hydrogen delivered over the year is equal to the original case with constant demand.

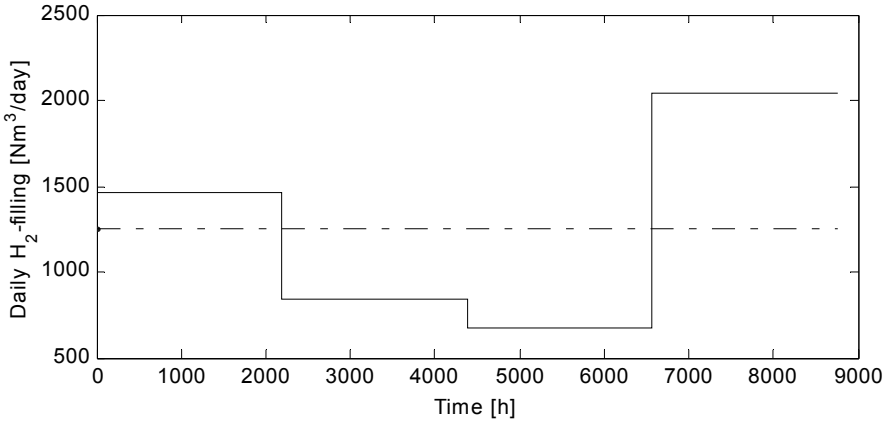

Figure 18. Daily hydrogen demand over the year for hydrogen load scenario 1. The solid line shows a filling pattern with seasonal variations. The dotted line shows a constant filling pattern with the same total amount of hydrogen.

Table 2. Data for the different technologies. The O&M costs are given as percentage of investment per year.

Component	Investment	O&M [%]	Efficiency	Lifetime [yr]
Wind power plant	\$800/kW	2		20
Power conversion	\$150/kW	2	95%	20
Alkaline electrolyzer	\$450/kW	4	4.0 kWh/Nm^3	15
Compressor	\$1,000/kW	4	0.2 kWh/ Nm^3	10
Storage tanks	Variable[a]	2		30
Fuel cell	\$1,000/kW	4	2.0 kWh/Nm^3	15

[a] Inv. Cost=\$95*2,500*(V_H^{max}/2,500)$^{0.75}$ taking into account economics of scale, which is well documented for compressed hydrogen storage. Based on [44].

3.3.4 Cost and efficiency data

It is difficult to choose proper investment cost data and operation cost data for the different sub-components in a wind-hydrogen system. Even for mature technology, such as wind power plants and compressed hydrogen storage, the differences in reported investment costs vary significantly. Since important components such as fuel cells and advanced electrolyzers

with variable load operation are not fully commercial available today (or at least not cost competitive), near-future estimates (~ year 2010) are used. The chosen for investment costs, operational & management costs, average efficiencies and lifetime are given in Table 2.

3.4 Integration with no storage

First, the possibilities of utilizing wind resources without local energy storage are studied. Since the grid capacity is 5,000 kW and the minimum simulated load is 700 kW, it is possible to install at least 5,700 kW of wind power without curtailing the power generation. If the installed wind power capacity is above 5,700 kW, wind power must be dissipated during the periods when the power generation exceeds the demand and cable capacity. This is illustrated in Figure 19, where the average energy flow is plotted for different wind power capacities. We clearly see that the average dissipated power P_d increases significantly for high penetration levels. The utilization factor of the wind power plant is reduced analogously, as seen from Figure 20. Moreover, dissipation of wind energy affects the production cost of wind energy, as shown in Figure 21. For wind power installations above 6,000 kW, the production cost grows approximately linearly as a function of wind power capacity. An increase in wind power capacity of from 8,000 kW to 14,000 kW (75% increase) leads to 40% increase in the production cost.

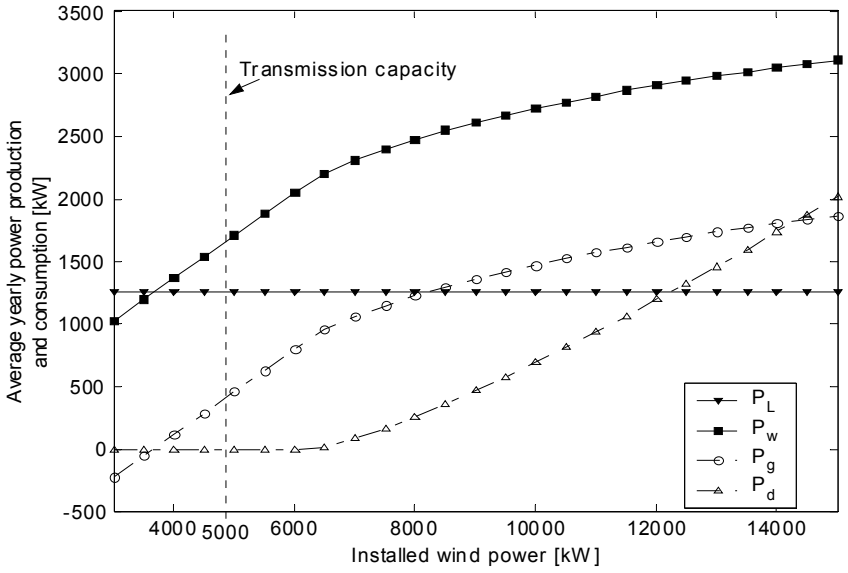

Figure 19. Grid integration of wind power with dissipation of excess energy. P_l is electrical load, P_w is wind power, P_g is power export to the grid and P_d is dump load.

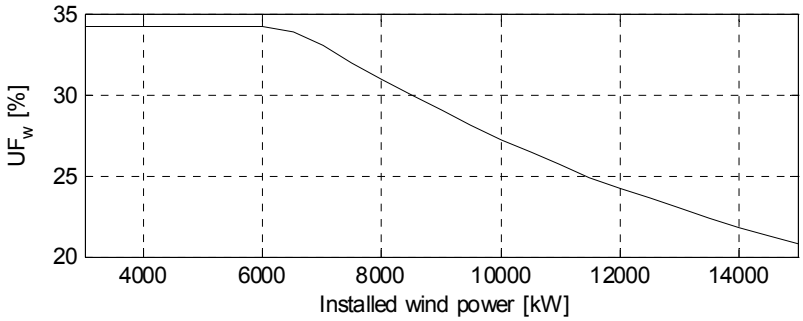

Figure 20. Utilization factor of wind power for increasing capacity.

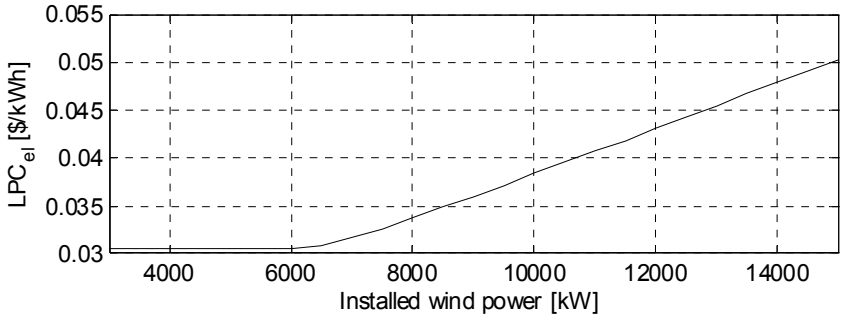

Figure 21. Levelised production cost of wind energy for increasing capacity.

Table 3. Imported energy, exported energy and dissipated energy for different wind installations.

P_w^{max} [kW]	E_{imp}/ E_l [%]	E_{exp} / E_w [%]	E_d / E_w [%]
1,000	73	0.4	0
4,000	44	50	0
7,000	38	64	4
10,000	35	56	20

In the simulation model, the characteristics of the external power system are not specified, except that the capacity of the cable is limited to 5,000 kW. Grid losses and production costs of other generators are not specified. In actual systems, it may be beneficial to obtain a close match between local generation and consumption in order to reduce grid losses and avoid undesirable prices for export and import of electricity. In Table 3, the relative amounts of exported energy, imported energy and dumped energy are displayed for selected wind farm sizes. Even though the seasonal variations of wind power generation and electricity demand follows a relatively similar pattern, the flexibility of the external power system is often used for balancing local generation and consumption. For a wind

power capacity of 4,000 kW, the annual wind power generation is approximately equal to the annual load. However, as much as 50% of the wind energy is exported to the grid in this case. Consequently, about 50% of the load is covered by energy import. For the other wind power capacities shown in Table 3, the imbalance is even more evident.

3.5 Type A: Hydrogen used as a transportation fuel

In this section, hydrogen production by electrolysis is investigated as a possibility for increasing the wind integration. Hydrogen is used a transportation fuel but not for local power generation. Consequently, from a power system point of view, the electrolysis plant is operated as a dispatchable load and not as electrical energy storage.

3.5.1 Constant electrolyzer power

First, we study the effects of operating the electrolyzer at constant power, which is common practice for conventional electrolysis plants. For simplicity, the electrolyzer rating is decided to be equal to

$$P_e^{max} = P_w^{max} - P_g^{max} - \min\{P_l(t)\} \tag{3.24}$$

such that the dissipation of wind power is always zero. The last term is the lowest value of electricity demand in the time series. The daily hydrogen production is set equal to the daily hydrogen consumption. Since filling of hydrogen vehicles takes place from 2:00 to 6:00 at night, the filling rate must satisfy

$$\sum_{i=3}^{6} \dot{V}_l(i) = \sum_{j=1}^{24} \dot{V}_e(j) \tag{3.25}$$

where i and j represents hour of the day. The period 0:00 to 1:00 corresponds to i=1. The filling rate then becomes

$$\dot{V}_l(i) = \begin{cases} 6 \cdot \dfrac{P_e^{max}}{\eta_e} & \text{for } i = [3,6] \\ 0 & \text{for } i \neq [3,6] \end{cases} \tag{3.26}$$

The hydrogen storage capacity is minimized by setting

$$V_H^{max} = 20 \cdot \frac{P_e^{max}}{\eta_e} \tag{3.27}$$

which allows the hydrogen storage to exactly reach its upper limit before the first filling hour. After the last filling hour, the hydrogen storage becomes completely empty.

The power balance for different levels of wind integration is shown in Figure 22. Because the rating of the electrolyzer is proportional to the wind power rating, and it is operated at full power in all hours, the power consumption of the electrolyzer becomes very high as the wind power capacity increases. Consequently, the average power exported to the grid decreases and reaches zero at approximately P_w = 6,700 kW. Furthermore, it is not possible to increase the wind power capacity beyond approximately 8,800 kW, because the power consumption of the electrolyzer becomes so high that the restriction on power import is violated in periods with high electrical load.

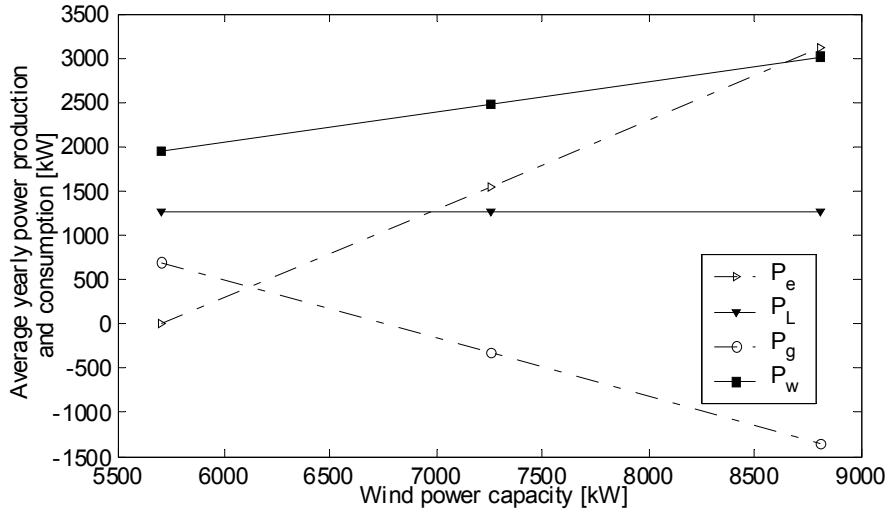

Figure 22. Grid integration of wind power with electrolyzer operating at constant production rate. P_e is electrolyzer power, P_w is wind power, P_l is electrical load and P_g is power exported to the grid.

As long as the annual energy consumed by the electrolyzer is less than or equal to the annual wind power generation, one can say that hydrogen in average is produced from wind energy, although grid power is used in periods of low wind speed. Hydrogen production cost is therefore chosen to be calculated based on wind power cost and not the price of electricity from the grid. By this approach, the levelised production cost of hydrogen LPC_{H2} is found to be 0.20 \$/Nm^3 (0.066 \$/kWh LHV) for the wind-hydrogen system with constant electrolyzer power. It should be emphasized that the simulation model also allows us to define a market price for export and import of electricity, either constant or time varying. The market simplification made here makes it possible to estimate the hydrogen production cost in a power system where the electricity price is equal to the cost of wind power. More detailed electricity market models are used in chapter 5 and 6.

Table 4 shows the main results for the different hydrogen load scenarios. The wind power capacity for each scenario is the maximum possible with no dissipation of wind power. The storage capacity is low, since the required hydrogen for the filling station is produced at a constant rate each day. Consequently, the hydrogen production cost is minimized. The drawback of constant electrolyzer power is evident when we look at the relative amount of hydrogen that is produced from grid power. Between 32% and 45% of the hydrogen is produced by electricity imported from the main grid. Unless the imported electricity is generated from non-fossil sources like hydro and wind, electrolytic hydrogen production should be avoided from an environmental and energy-efficiency point of view. If the energy mix for instance contains of a significant amount of natural gas, it would be less polluting and cheaper to use that resource directly for hydrogen production by reforming [81]. In order to produce hydrogen directly derived from wind power, it is necessary to operate the electrolyzer in variable power mode.

We see from Figure 22 that it should be possible to increase wind integration considerably since the average power export to the grid is mostly below zero. This can be accomplished by installing a larger hydrogen storage and by operating the electrolyzer on varying power. The question is how such a strategy will influence the cost of hydrogen, which is the subject of the next section.

Table 4. Results for the different hydrogen load scenarios with constant hydrogen production rate.

H_2-load scenario	P_w^{max} [kW]	P_e^{max} [kW]	V_H^{max} [Nm^3]	E_{imp}/E_l [%]	$E_{imp,e}/E_e$ [%]	E_{exp}/E_w [%]	LPC_{H2} [$/Nm3]
1	6,000	300	1,200	44	32	58	0.20
2	6,200	500	2,270	47	35	55	0.20
3	6,700	1,000	4,560	51	40	49	0.20
4	7,700	2,000	9,440	56	45	40	0.20

3.5.2 Maximum utilization of the existing grid capacity

Using the electrolyzer as a flexible load for storing wind energy that otherwise would have been dissipated is beneficial in relation to energy efficiency. As can be seen from Figure 20, the utilization factor of the wind farm drops to about 25% for 11,500 kW installed wind energy in the no-storage case. In comparison, the utilization factor is 34% if the grid constraint is not violated. This means that 27%, or 10 GWh, of the total yearly wind energy potential is dissipated. If all the excess energy could be

used for hydrogen production, we could theoretically obtain a daily hydrogen supply of 6,200 Nm^3.

This section demonstrates how it is possible to exploit the wind resources by operating the electrolyzer in variable power mode. First, simulation results are presented using the hydrogen load pattern with no seasonal variations. Then we present the results for seasonal hydrogen load. As will be shown, major economic benefits could be obtained if the hydrogen load followed the seasonal wind speed pattern.

Constant daily hydrogen load

As a first approach, the electrolyzer and the hydrogen storage tanks are sized so that no wind energy is dissipated, and the hydrogen load is always supplied. The electrolyzer rating is then given by equation (3.24), while the hydrogen storage tanks are sized according to the following criterion

$$0 < V_H(t) < V_H^{max} \qquad \text{for } t = 1...N \tag{3.28}$$

so that the hydrogen storage does not reach the lower and upper limits during the simulation period.

For each of the hydrogen-load scenarios, simulations have been run for different wind power capacities. In Figure 23, the required hydrogen storage capacity for the different hydrogen-filling scenarios and wind power capacities have been plotted. We see that for each scenario, there is a non-linear relationship between the required hydrogen storage and the installed wind power. We also notice that for a fixed wind power capacity, a lower hydrogen-filling rate leads to larger hydrogen storage. This can be explained by recalling that with normal operating conditions, only excess wind power is used for hydrogen production. If the hydrogen-filling rate is low, it takes longer time to reduce the hydrogen content in the storage tanks. Thus, a higher storage capacity is necessary to prevent that the upper limit is reached. Figure 24 shows the production cost of hydrogen as a function of wind power capacity for the different hydrogen-filling scenarios. The hydrogen production cost increases rapidly, because of the extra investment in electrolyzer and especially hydrogen storage tanks needed to prevent dissipation of wind energy. All the curves reach a point where the increase in cost changes significantly. This point is chosen as the maximum preferable wind power capacity for the corresponding scenario. Hydrogen production cost increases approximately linearly with wind power capacity below this point.

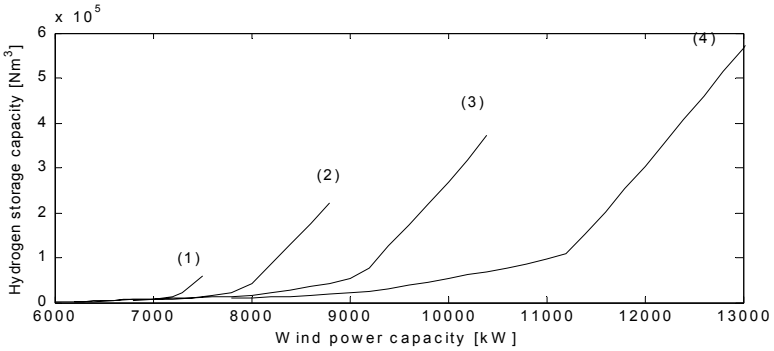

Figure 23. Required hydrogen storage capacity for the different hydrogen-filling scenarios. Hydrogen-load scenario 1 is denoted (1), scenario 2 is denoted (2) etc.

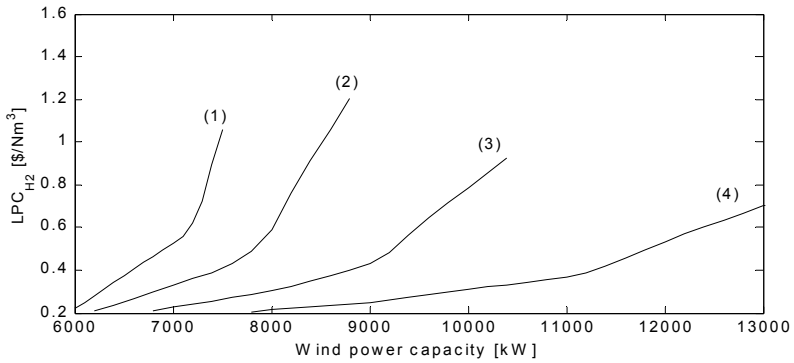

Figure 24. Levelised production cost of hydrogen for the different hydrogen-filling scenarios. Hydrogen-load scenario 1 is denoted (1), scenario 2 is denoted (2) etc.

In Table 5, the main results for the preferred wind power capacity in the different hydrogen-load scenarios are displayed. The installed wind power is 16-43% higher than for the case with constant electrolyzer power (See Table 4). However, the gained energy utilization has its price. As we see by comparing the two tables, the extra installation of hydrogen storage equipment causes a great increase in hydrogen production cost. When increasing the wind power capacity, it is also necessary to increase the electrolyzer rating and the storage volume to avoid wind power dissipation. Samples of the duration curves for the electrolyzer, hydrogen storage and the sea-cable that connects the local system to the main grid are shown in Figure 25. It can be seen that the cable capacity in this case is fully utilized for about 23% of the year. During the rest of the year, the hydrogen production is low, and this leads to a low utilization factor of the electrolyzer. Furthermore, the electrolyzer is almost never operated at full power. The criterion for electrolyzer sizing is given by equation (3.24), which seems to be too strict in this case. By reducing the electrolyzer rating

by 20%, the hydrogen production cost is reduced by 7%. The reduced electrolyzer capacity caused a negligible increase in dissipated wind energy.

Table 5. Results for the different hydrogen load scenarios. Hydrogen is primarily produced from excess wind power that otherwise would be dissipated due to grid constraints.

H_2-load scenario	P_w^{max} [kW]	P_e^{max} [kW]	V_H^{max} [Nm^3]	E_{imp}/E_l [%]	$E_{imp,e}/E_e$ [%]	E_{exp}/E_w [%]	LPC_{H2} [$/Nm3]
1	7,000	1,300	8,290	40	32	62	0.53
2	7,500	1,800	12,270	41	35	60	0.41
3	9,000	3,300	52,500	40	34	56	0.43
4	11,000	5,300	97,100	41	36	49	0.37

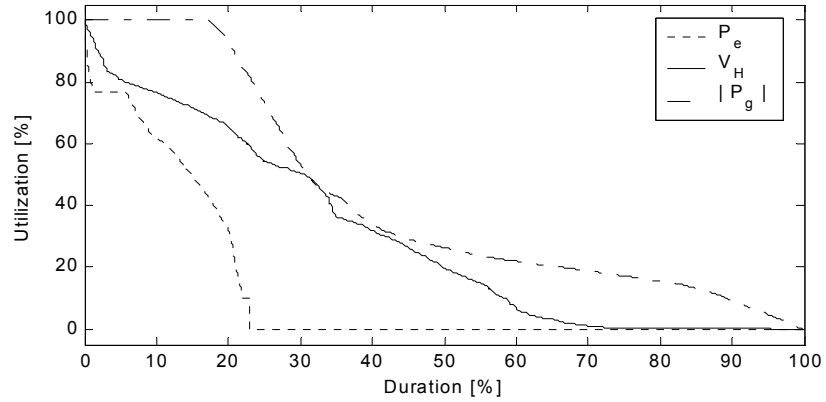

Figure 25. Duration curves for hydrogen storage, electrolyzer and grid capacity. The values are calculated relative to the maximum capacity. Hydrogen-filling scenario 1 with 7,500 kW installed wind power is used in the simulation.

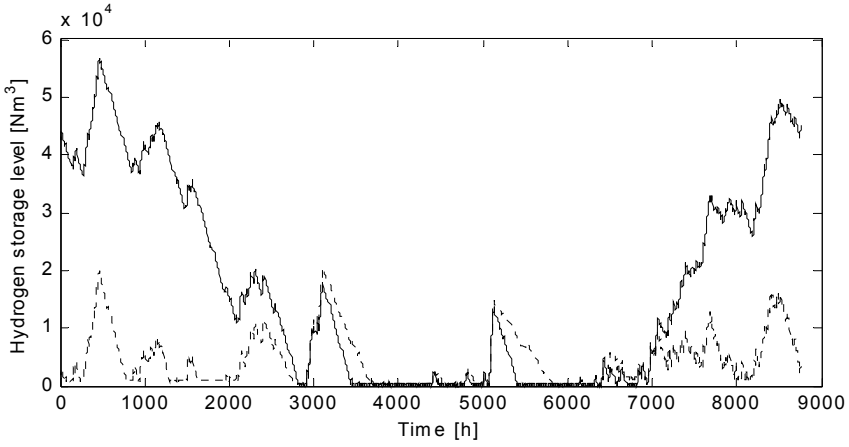

Figure 26. Hydrogen storage level for scenario 1 with P_w^{max}=7,500 kW. (-): Constant hydrogen demand. (- -): Seasonal hydrogen demand.

Another important result is that the hydrogen storage capacity must be large because of the seasonal wind pattern. Figure 26 shows how the storage level varies over the year in this case. The seasonal effect of high average winter wind speed is evident, as the hydrogen storage fills up in winter and gets empty in summer.

Seasonal varying hydrogen load

If the daily hydrogen demand followed the seasonal wind variations instead of being constant throughout the year, the storage requirements could be significantly reduced. Since hydrogen is thought of being used as a fuel for transportation, the required energy must then show the same seasonal variations as the wind. This might not be the case, which means that hydrogen must be provided from other sources during the low-wind season. Figure 26 clearly illustrates how the required storage capacity can be reduced if the filling pattern of hydrogen follows the seasonal wind variations. Furthermore, Figure 27 and Figure 28 show how the storage capacity and hydrogen production cost varies for all four hydrogen-demand scenarios. The impact of the new filling pattern can be understood by comparing these graphs with the corresponding graphs for constant daily hydrogen demand (Figure 23 and Figure 24). The sudden increase in hydrogen storage capacity, and consequently hydrogen production cost, is no longer evident. This means that the benefits of a seasonal hydrogen load pattern are distinct for high wind penetration levels. The difference is smaller for lower wind penetration levels, since the investment cost of the electrolyzer then dominates the hydrogen production cost.

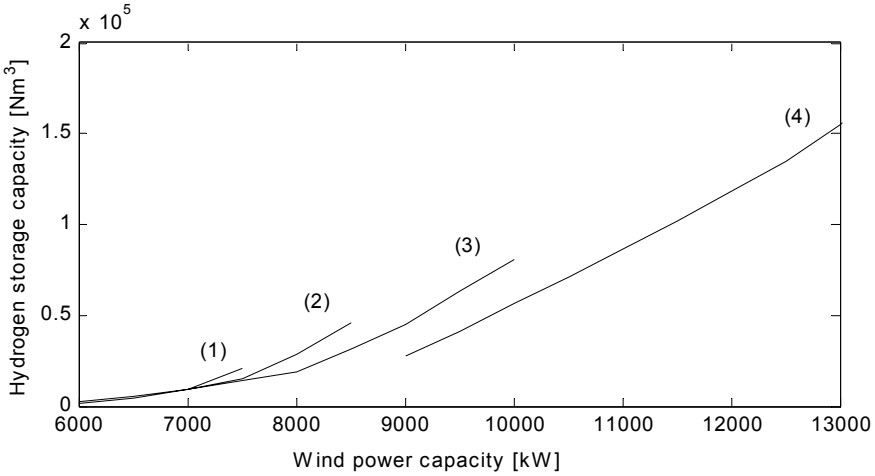

Figure 27. Required hydrogen storage capacity for the different hydrogen-filling scenarios with seasonal variations. Hydrogen-load scenario 1 is denoted (1), scenario 2 is denoted (2) etc.

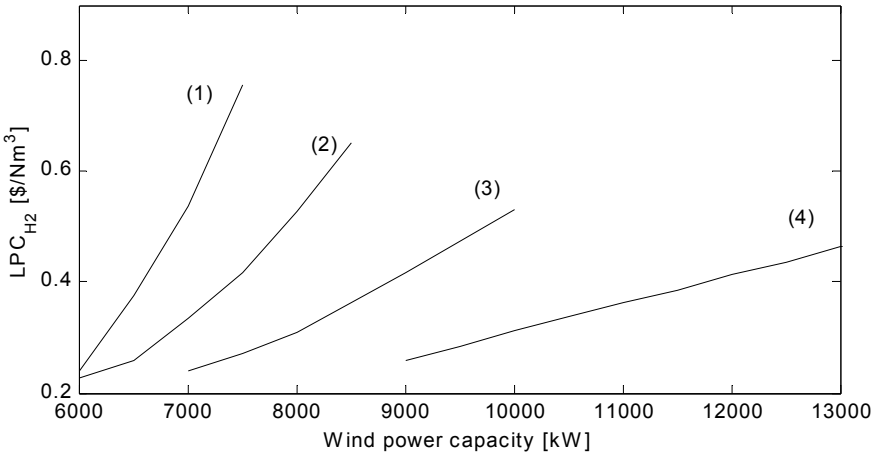

Figure 28. Levelised production cost of hydrogen for the different hydrogen-filling scenarios with seasonal variations. Hydrogen-load scenario 1 is denoted (1), scenario 2 is denoted (2) etc.

In section 3.5.1 , it was argued that variable electrolyzer power could reduce the amount of hydrogen that is produced from imported electricity in the cases that this is important. Table 5 showed that the imported power is still above 30% of the total power consumption of the electrolyzer. The reason is that hydrogen is only produced directly from wind energy when the local power surplus exceeds the grid restrictions. Hydrogen is produced by the use of power from the grid when the hydrogen storage level drops below the supply security limit, which happens relatively often during the summer as shown in Figure 26.

The benefits of seasonal hydrogen load have been discussed earlier, but it is also interesting to investigate the possibilities for hydrogen load variations at a shorter time scale. It is emphasized that this requires other sources of hydrogen to balance the actual demand and the demand that can be supplied by wind-derived hydrogen. In Figure 29, the average grid import for different hydrogen load patterns are shown for P_w^{max} = 7,000 kW and hydrogen-filling scenario 1. It is evident that if the hydrogen load follows the daily wind variations, it would be possible to reduce the grid import considerably. Even seasonal variations have a significant positive effect. Another possibility of increasing the amount of hydrogen produced directly from wind power is to operate the electrolyzer whenever the local wind power generation exceeds the local electrical load. This is covered in the next section.

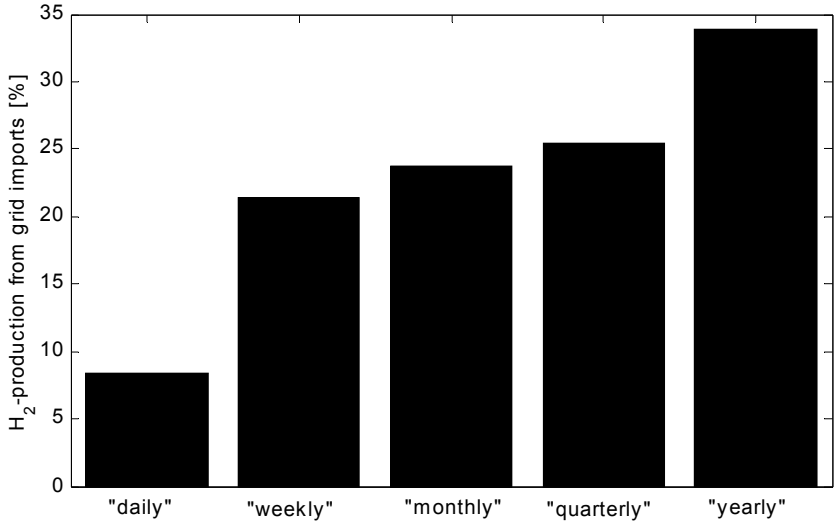

Figure 29. Relative amount of hydrogen produced from power import for scenario 1 with P_w^{max}=7,000 kW. The term "daily" represents daily hydrogen load variations, "weekly" represents weekly hydrogen load variations etc.

3.5.3 Using excess wind energy for hydrogen production

Hydrogen is produced for two purposes in the operation strategy described in the previous section; either because the local power surplus exceeds the grid capacity, or because the hydrogen storage level drops below the minimum supply security limit. Another approach is to produce hydrogen from wind energy when there is a local power surplus so that the export of wind power to the main grid is minimized. A characteristic of this operation strategy is that there will be no power import for hydrogen production if the wind-hydrogen storage system is properly sized.

The hydrogen storage volume is found by requiring that hydrogen should only be produced from wind power. To obtain a yearly energy balance, the simulations are re-run with different wind power capacities until the hydrogen storage level at the end of the simulation period is approximately equal to the initial storage level. For the simulation results shown in Table 6, the size of the electrolyzer is determined by equation (3.24), as earlier. This is the lowest possible electrolyzer size that gives no wind energy dissipation. Figure 30 shows the duration curve of electrolyzer power (P_e) and the local power surplus (P_w - P_l). We see that no hydrogen is produced when there is a local power deficit and that the electrolyzer is mostly run on rated power when there is a local power surplus.

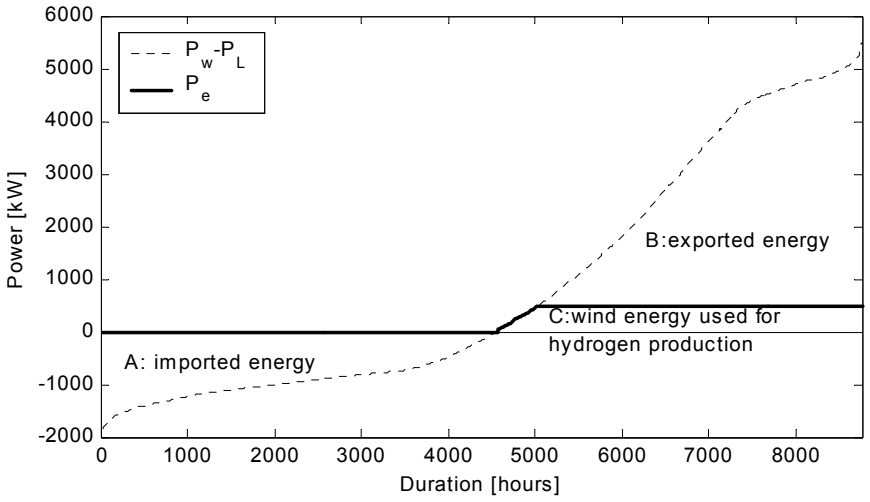

Figure 30. Duration curve of electrolyzer power (thick line) and the difference between wind power and electrical load (dotted line) for hydrogen filling scenario 1 with P_w^{max} = 6,200 kW and P_e^{max} = 500 kW.

Table 6. Results for the different hydrogen load scenarios with constant daily hydrogen load over the year. Hydrogen is primarily produced from excess wind power that otherwise would be exported to the main grid.

H_2-load scenario	P_w^{max} [kW]	P_e^{max} [kW]	V_H^{max} [Nm^3]	E_{imp}/E_l [%]	E_{exp}/E_w [%]	LPC_{H2} [$/$Nm^3$]
1	6,200	500	82,500	40	54	0.95
2	6,750	1,050	162,000	39	47	0.84
3	7,900	2,200	335,000	37	37	0.76
4	10,300	4,550	729,000	36	25	0.71

Table 7. Results for the different hydrogen load scenarios with seasonal hydrogen load. Hydrogen is primarily produced from excess wind power that otherwise would be exported to the main grid.

H_2-load scenario	P_w^{max} [kW]	P_e^{max} [kW]	V_H^{max} [Nm^3]	E_{imp}/E_l [%]	E_{exp}/E_w [%]	LPC_{H2} [$/$Nm^3$]
1	6,200	500	25,700	40	54	0.53
2	6,750	1,050	54,500	39	47	0.51
3	7,900	2,200	109,000	37	37	0.47
4	10,300	4,550	219,000	36	25	0.40

The hydrogen production cost in Table 6 is in some of the scenarios almost twice as high as in Table 5, and the wind power export is significantly

reduced due to the new operating strategy. It is evident from the table that the seasonal wind variations require high storage volume for a constant daily hydrogen load. By introducing a seasonal varying hydrogen load in the model, the hydrogen volume is reduced to about 30% of the original value. Hence, the hydrogen production cost will also be significantly reduced. Table 7 summarizes the main results for seasonal varying hydrogen load.

3.5.4 Using wind energy primarily for hydrogen production

In this case, wind energy is used primarily for hydrogen production, and excess energy is consumed locally or exported to the main grid. This simulates a case where no electricity is imported for hydrogen production. The island would then be 100% self-supplied with electricity for hydrogen production, as would be required for a stand-alone wind-electrolysis plant. Moreover, if we set the value of excess wind power to zero, the hydrogen production cost is a rough estimate of the hydrogen production cost of an isolated system. The need for short-term storage (e.g. lead-acid batteries) in isolated systems is not taken into account here. This is discussed by Grimsmo, Korpås, Gjengedal and Møller-Holst in [91].

Minimizing excess wind energy

Here it is shown how the system can be sized to deliver the amount of hydrogen specified by the scenarios in Table 1. The electrolyzer rating is in the first place set equal to the wind power rating so that all available wind energy is used for hydrogen production (except when the wind power output is below the minimum electrolyzer power, which is 10% of the rated power). The results are given in Table 8, and we see that the component sizing follows the hydrogen demand given in Table 1, since the wind-hydrogen plant is sized exactly to cover the hydrogen demand over the year. The hydrogen production cost is not constant, which is due to the economics of scale for compressed hydrogen storage.

Table 8. Component sizing and hydrogen production cost for the different hydrogen-filling scenarios. The value of wind power not used for hydrogen production is set to zero.

H_2-load scenario	P_w^{max} [kW]	V_{H2}^{max} [Nm^3]	LPC_{H2} [\$/Nm^3]
1	700	96,700	1.09
2	1,400	193,000	0.96
3	2,800	387,000	0.85
4	5,600	773,000	0.76

Table 9. The impact of minimum electrolyzer power on sizing, energy balance and hydrogen production cost for scenario 1.

P_e^{min} / P_e^{max} [%]	P_w^{max} [kW]	V_H^{max} [Nm^3]	E_e / E_w [%]	LPC_{H2} [\$/Nm^3]
0	680	95,800	100	1.08
10	700	96,700	98.1	1.09
20	720	102,100	94.6	1.13

In real systems, the minimum electrolyzer power will depend on the type of electrolyzer and the design of the control system. With increased P_e^{min}, it is necessary to install a larger wind turbine and hydrogen storage, since the amount of wind energy not used for hydrogen production increases. The default value in the simulations is set to 10% of the rated power. The impact of this value on the system sizing and economics is shown in Table 9. We see that the differences in performance between 0% ("theoretical best"), 10% and 20% are relatively small.

Minimizing hydrogen production cost

As mentioned above, the results were obtained by setting the electrolyzer rating equal to the wind power rating and thus minimizing the amount of wind energy that is not used for hydrogen production. Furthermore, the value of excess wind energy was set to zero, since we wanted to find an estimate for the cost of hydrogen as a primarily product of wind power. But even though the value of excess wind power is zero, the electrolyzer rating should be lower than the wind power rating if the objective is to minimize the cost of hydrogen. By oversizing the wind turbine and reducing the size of the electrolyzer and the hydrogen storage, it is possible to find an optimum sizing combination for a specified hydrogen demand. Simulation runs for different sizing combinations are shown in Table 10 for scenario 1. The electrolyzer rating in the table varies between 100% and 20% of the wind power capacity. The lowest cost is obtained when rated wind power is twice as high as the electrolyzer rating. In this case, one third of the annual wind energy is not used for hydrogen production. This is illustrated in Figure 31, which shows the duration curve for wind power and electrolyzer power.

The optimum sizing combination for all scenarios is shown in Table 11. It is emphasized that the chosen investment cost of the electrolyzer is low compared to the wind power plant. The investment cost of the electrolyzer is based on an optimistic estimate (\$450/kW), and it might be that electrolyzers that manage to follow a varying power input are going to be

more expensive. In that case, it would probably be beneficial to reduce the rating of the electrolyzer even further.

As for the previous systems, the constant daily filling rate of hydrogen vehicles requires a large storage volume to compensate for the seasonal wind variations. It was found that the hydrogen production cost for scenario 1 was reduced from \$1.03/Nm^3 to \$0.54/Nm^3 by simulating the system with seasonal variations of the hydrogen load.

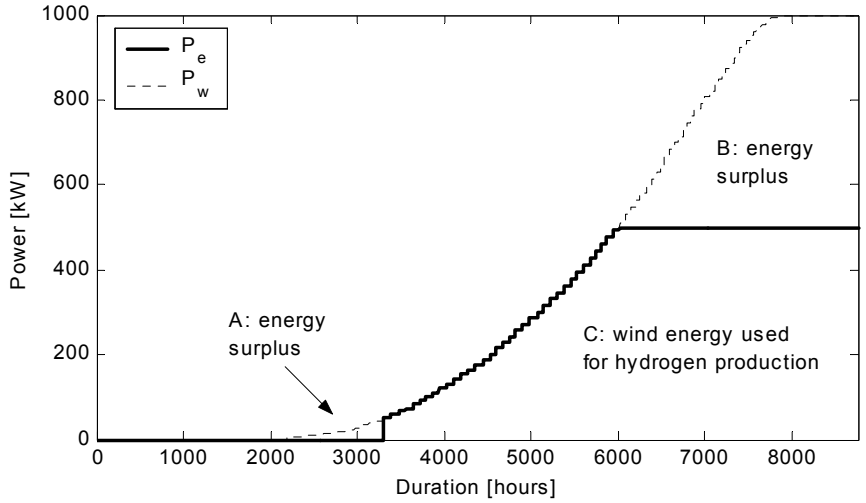

Figure 31. Duration curve of wind power (dotted line) and electrolyzer power (thick line) for hydrogen filling scenario 1 with P_w^{max}=1,000 kW and P_e^{max} = 500 kW.

Table 10. The impact of electrolyzer rating on the wind power capacity, hydrogen storage capacity, energy balance and hydrogen production cost. The results are for hydrogen filling scenario 1.

P_e^{max}/P_w^{max} [%]	P_w^{max} [kW]	V_H^{max} [Nm^3]	E_e/E_w [%]	LPC_{H2} [\$/Nm^3]
100	700	96,700	98.1	1.092
90	715	96,200	94.3	1.088
80	750	95,800	89.2	1.076
70	800	93,800	83.0	1.066
60	900	86,000	75.7	1.032
50	**1,000**	**83,500**	**67.4**	**1.027**
40	1,175	79,700	57.6	1.031
30	1,450	76,000	46.5	1.055
20	2,000	71,600	33.5	1.128

Table 11. Optimum component sizing and hydrogen production cost for the different hydrogen-filling scenarios. The value of wind power not used for hydrogen production is set to zero.

H_2-load scenario	P_w^{max} [kW]	P_e^{max} [kW]	LPC_{H2} [\$/Nm^3]
1	1,000	500	1.03
2	2,000	1,000	0.91
3	4,000	2,000	0.81
4	8,000	4,000	0.73

3.6 Type B: Hydrogen used as electrical energy storage

The possibility of storing hydrogen for later use in a fuel cell for stationary power generation is studied here. Two different operation strategies are employed, and the possibility of using a reversible fuel cell is compared with separated electrolyzer and fuel cell.

3.6.1 Maximum utilization of the existing grid capacity

In this analysis, hydrogen storage is restricted to be used for storing excess wind energy that would otherwise have been dissipated due to grid constraints. It is important to remember that the hydrogen storage could also be used for other valuable purposes, such as optimizing the power output with respect to a varying electricity price. Such operation strategies are investigated in other parts of the thesis and are not studied in this chapter. The operation strategy used here is straightforward, namely to only produce hydrogen when the local power surplus exceeds the capacity of the cable that connects the island to the mainland. When wind power generation is less, hydrogen is sent to the fuel cell for power generation. Hence, the hydrogen storage should be empty as soon as possible to give space for more hydrogen when the wind picks up again. It is clear that the size of the storage is determined by the seasonal wind pattern, which therefore has a major influence on the electricity cost.

Reversible fuel cell

The system has been simulated with a reversible fuel cell as a first approach. The capacity of the reversible fuel cell is derived from equation (3.24), as for the Type A system, while the hydrogen storage capacity is chosen to be the highest simulated value of the hydrogen storage level. Figure 32 shows the required storage capacity as a function of installed wind power. The installed storage capacity increases linearly up to

approximately 15 MW, followed by a rapid increase after this value. This affects in its turn the cost of electricity, which follows a similar pattern. It is clear that the cost of electricity is remarkably high when comparing with the corresponding cost of wind electricity using no storage (see Figure 21). On the other hand, for high wind penetration levels, hydrogen storage gives a significant better utilization of the wind energy compared to the option of dissipating excess energy, despite the high storage losses. For P_w^{max} = 15 MW, the average power export to the grid is about 1,800 kW with no storage, while the grid export is about 2,700 kW if hydrogen storage is used.

Since the electrolyzer is only operated when wind power generation exceed the sum of the electrical load and the grid capacity, most of the wind energy is directly consumed by the local load or exported to the grid. Therefore, the average efficiency of the combined wind-hydrogen plant is relatively high, although the hydrogen storage efficiency is below 50%. The system efficiency of the wind-hydrogen system is defined as

$$\eta_{sys} = \frac{E_w - E_d - E_e + E_f}{E_w} \tag{3.29}$$

which takes into account hydrogen storage losses and dissipation of wind energy. The system efficiency is plotted as a function of wind power capacity in Figure 33 and drops to about 70% at P_w^{max} = 20,000 kW.

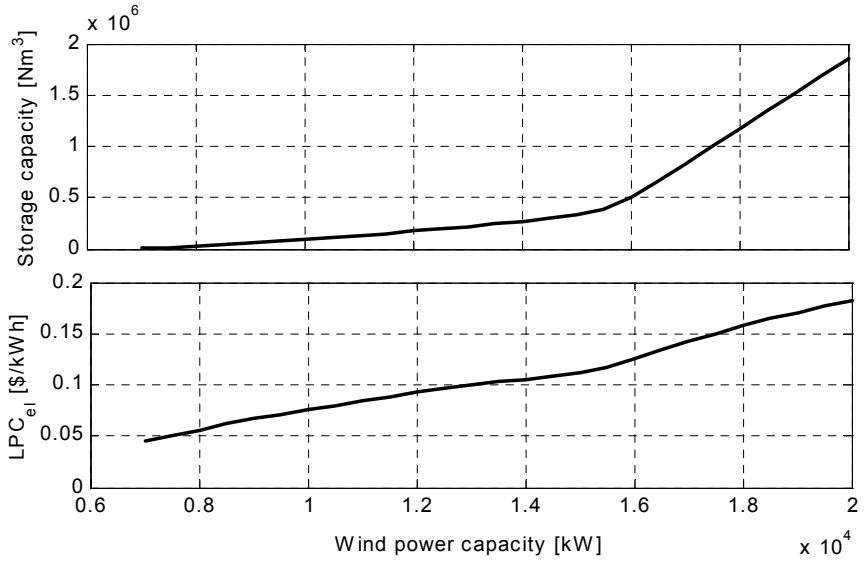

Figure 32. Implications for storage capacity and electricity production cost when increasing the wind power capacity above the transmission limit.

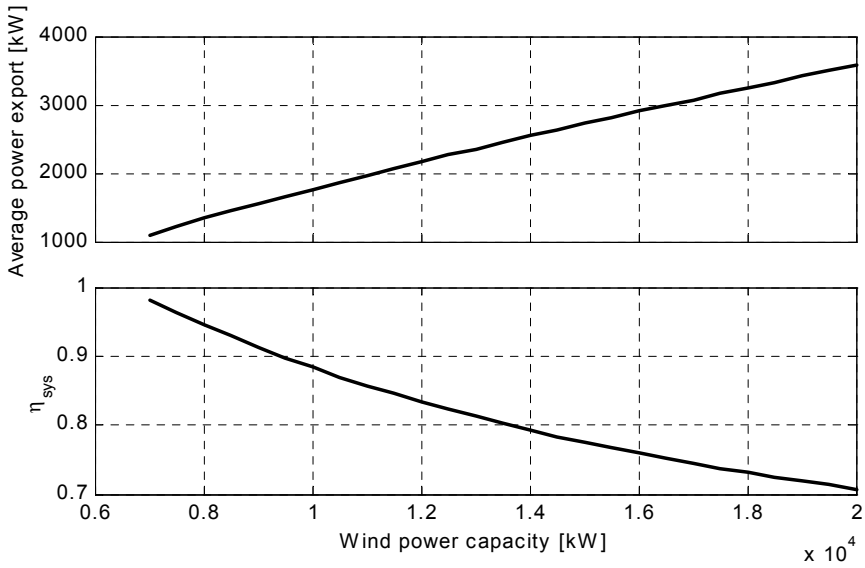

Figure 33. Implications for yearly average power export and system efficiency when increasing the wind power capacity above the transmission limit.

Separated electrolyzer and fuel cell

If separated devices for electrochemical hydrogen production and combustion are chosen instead of a reversible fuel cell, the size of the fuel cell that minimizes total cost should be chosen. The sizing of the electrolyzer is calculated from equation (3.24) in order to avoid dissipation of wind energy in periods with high wind speed and low load. Figure 34 shows how the electricity production cost varies as a function of fuel cell capacity for P_w^{max} = 12,000 kW. We see that the optimum is approximately P_f^{max} = 2,300 kW, which is the same order as the maximum local load. Moreover, for the chosen component costs, a storage system with separate electrolyzer and fuel cell gives approximately the same electricity cost as a storage system with reversible fuel cell.

The storage tanks contribute most to the total cost of the hydrogen storage system, as shown in Figure 35. At the same time, it can be seen from Figure 36 that the utilization of the installed storage capacity is unsatisfactory low. This is because the hydrogen storage is designed to ensure that no wind energy is dissipated, or in other words, that the storage level never reaches the maximum value. If we allow a small amount of wind energy dissipation over the year, it is possible to reduce the storage capacity. Figure 37 shows that a significant reduction in electricity production cost is possible by allowing some wind energy dissipation.

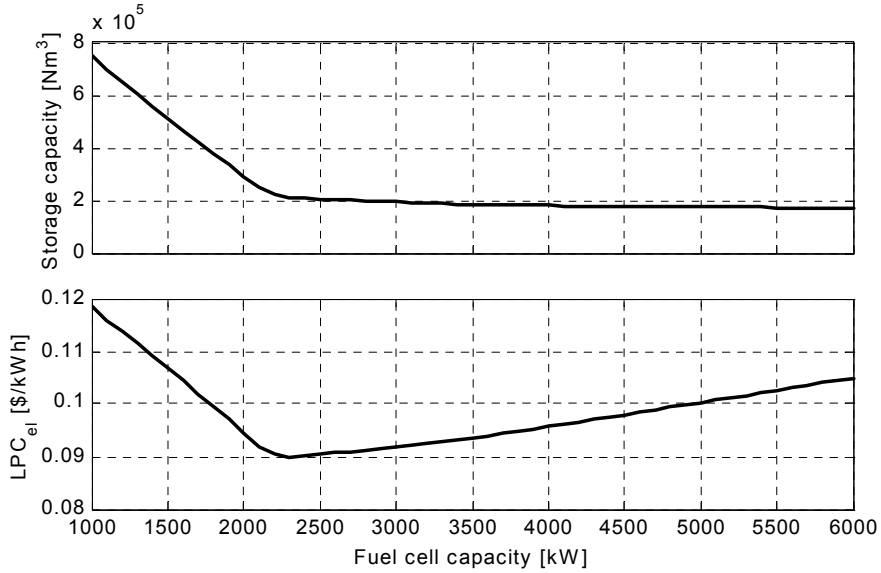

Figure 34. Storage capacity and electricity production cost as a function of fuel cell capacity for P_w^{max} = 12 MW.

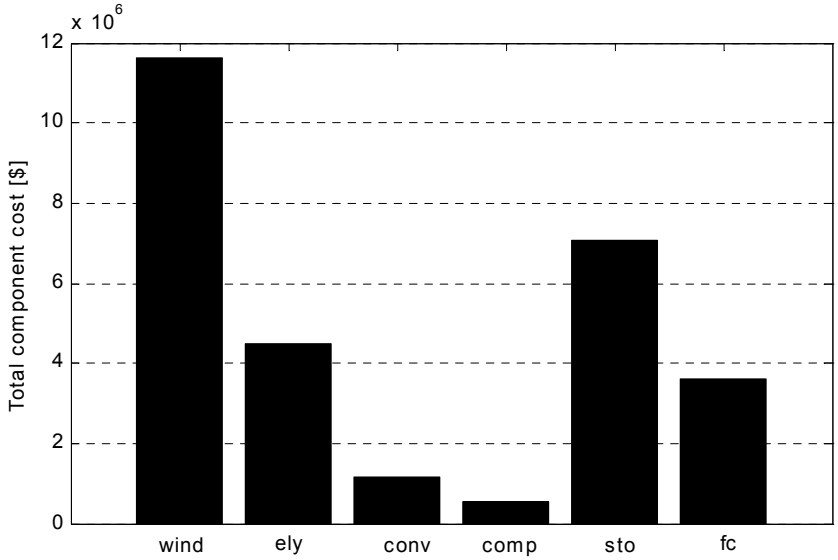

Figure 35. Contribution to total cost (discounted present value) for the different components for P_w^{max} = 12 MW. "wind": wind power plant, "ely": electrolyzer, "conv": power conversion units, "comp": hydrogen gas compressor, "stor": hydrogen storage tanks, "fc": fuel cell.

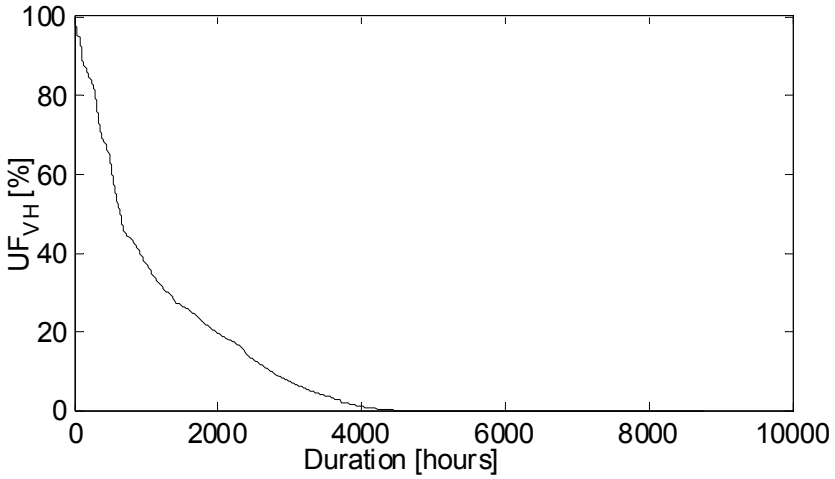

Figure 36. Utilization factor of the compressed hydrogen storage for P_w^{max} = 12 MW and no dissipation of wind energy.

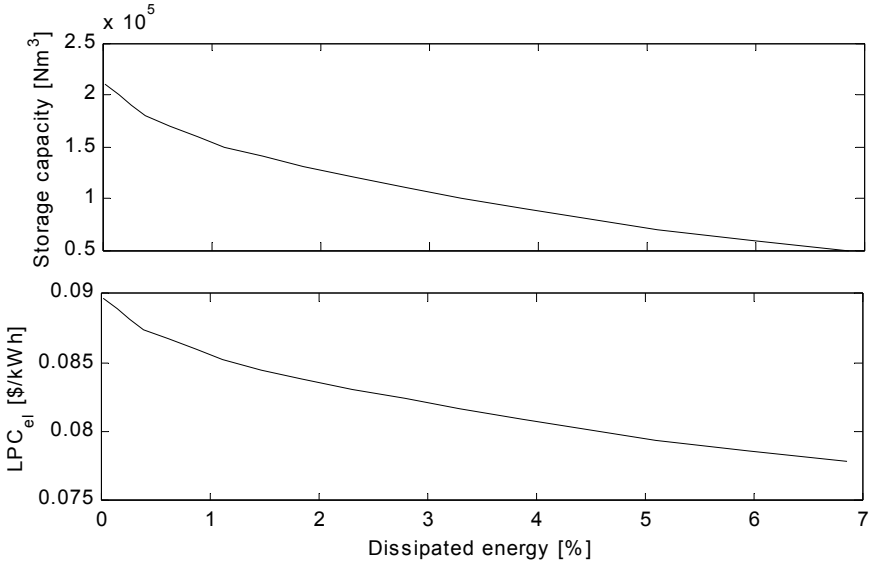

Figure 37. Storage capacity and electricity production cost allowing a small amount of dissipated wind energy for P_w^{max} = 12 MW.

3.6.2 Matching local generation and consumption

In the previous section, the motivation for installing hydrogen storage was to maximize the integration of wind power behind a bottleneck in the grid. Therefore, energy was only stored when the local power surplus exceeded the export limit. In this section, hydrogen storage is applied for matching fluctuating generation with fluctuating load. The main operation strategy is

to operate the electrolyzer when wind generation exceeds the local consumption and to operate the fuel cell in the opposite case. The cable that connects the island to the main grid is therefore only used as backup and for exporting excess wind power. If the value of exported wind energy is set to zero, the model can be regarded a simplified representation of a stand-alone power system based on wind-hydrogen with a backup plant.

Results for 100% self-supply of electricity

An important issue is component sizing. As a first approach, the wind-hydrogen system is designed for exactly matching the annual wind power generation with the consumption. This implies that no import of electricity is required, so that the island is 100% self-supplied with electricity. The capacity of the electrolyzer and the fuel cell is decided by the following equations

$$P_e^{max} = P_w^{max} - \min\{P_l(t)\} \tag{3.30}$$

$$P_f^{max} = \max\{P_l(t)\} \tag{3.31}$$

while the sizing criterion for the hydrogen storage capacity is that the maximum and minimum limits are not reached. The capacity of the wind power plant is found by requiring that the hydrogen storage level at the end of the year is equal to the initial value.

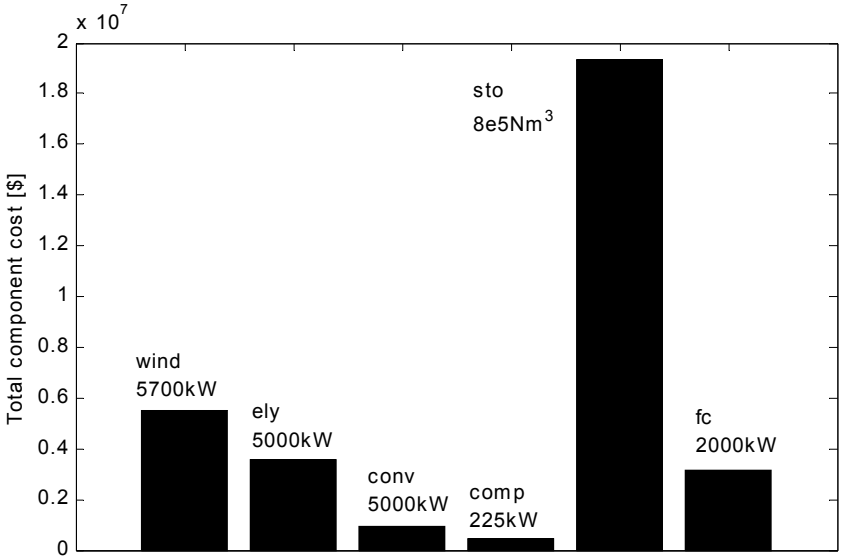

Figure 38. Cost and capacity of the components that comprises the wind-hydrogen system.

By applying these sizing rules, we obtain LPC_{el} = 0.28 \$/kWh, with corresponding component capacities and total discounted costs shown in Figure 38. It is obvious that the dominating cost factor is the hydrogen

storage tanks, because of the need to store excess wind energy at winter for later use in summer. The wind energy and the load follow somewhat similar seasonal patterns, but the relative seasonal difference is higher for wind than load for the time series used here. This leads us to the idea that it may be convenient to oversize the wind power plant in order to reduce the storage capacity and thus reduce costs. In a stand-alone system, this will lead to a lower degree of energy utilization, since more electrical energy will be available than needed. For the system studied here, on the other hand, oversizing of the wind power plant leads to more export of energy to the main grid. Even if the value of exported energy is set to zero, oversizing of the wind turbine will result in economic gains, as for the wind-electrolyzer system in section 3.5.4 . When increasing the wind power capacity in the model, it is at the same time necessary to reduce the electrolyzer rating so that there is balance between the start level and end level of the hydrogen storage. In the original simulation with 5,700 kW installed wind power, the electrolyzer rating was set to 5,000 kW so that all wind power was consumed either by the local load or by the electrolyzer. Simulation results for other combinations of electrolyzer capacity and wind power capacity are shown in Table 12.

The optimum combination is found to be P_w^{max} = 7,200 kW and P_e^{max} = 3,000 kW, which requires a significantly lower hydrogen storage volume than in the original case. Almost 25% of the wind energy is exported to the main grid, and the value of the exported electricity is set to zero. The production cost of electricity is \$0.267/kWh, which is 6% lower than in the original case. The economic gain is relatively low due to the economics of scale for compressed hydrogen storage. By comparison, it was found that the optimum size of a reversible fuel cell is 3,000 kW, which resulted in LPC_{el} = \$0.264/kWh. This is slightly lower than for separate electrolyzer and fuel cell.

Table 12. The impact of electrolyzer rating on the wind power capacity, hydrogen storage capacity, energy balance and electricity production cost.

P_e^{max} [kW]	P_w^{max} [kW]	V_H^{max} [Nm3]	E_{exp} / E_w [%]	LPC_{el} [\$/kWh]
5,000	5,700	811,000	0.9	0.284
4,500	5,700	813,200	0.9	0.280
4,000	5,800	819,900	3.3	0.278
3,500	6,200	800,100	10.5	0.274
3,000	**7,200**	**732,000**	**23.0**	**0.267**
2,500	8,500	705,600	36.4	0.270
2,000	12,000	635,900	40.0	0.283

Reduced level of self-supply

Another important factor for hydrogen storage sizing is the level of self-supply. The cost values obtained in Figure 38 are obtained by setting the level of self-supply to 100%, which means that no electricity is imported to the island. By reducing the level of self-supply, it is also possible to reduce the capacity of the hydrogen storage. This is illustrated in Figure 39, which shows that the level of self-supply and the electricity production cost are approximately linear functions of storage capacity.

Motivated by the need to reduce storage costs, we now look at different design alternatives that exist for a specified level of self-supply. Figure 40 shows several combinations of wind power capacity and storage capacity that gives 99% self-supply. It is evident that an economic improvement is obtained by oversizing the wind power plant. The value of exporting excess power to the main grid is set to zero, as would be the case for a stand-alone system.

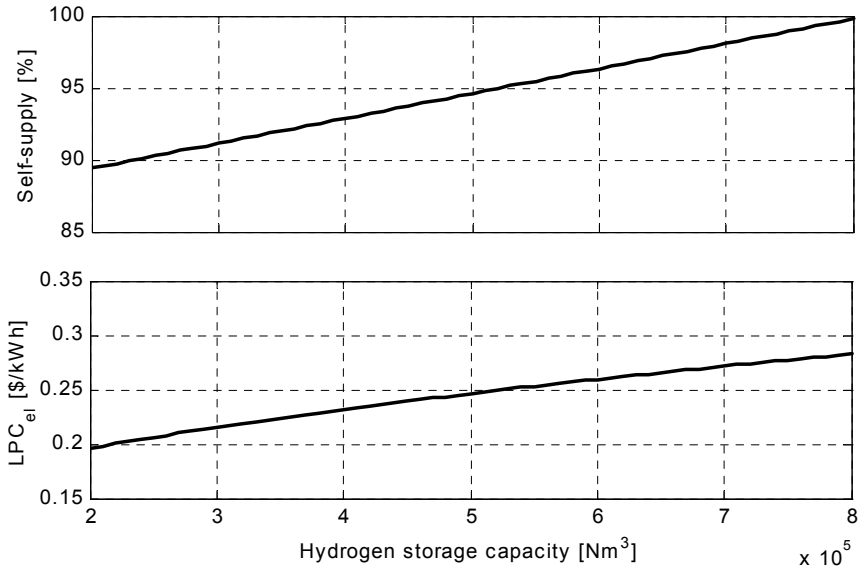

Figure 39. Self-supply and electricity cost as a function of hydrogen storage capacity.

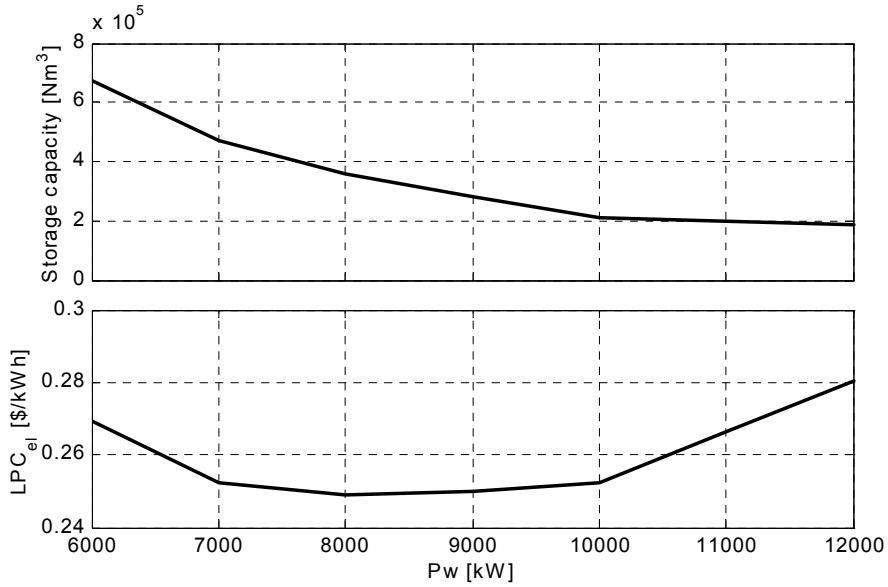

Figure 40. The top graph displays different combinations of wind power capacity and hydrogen storage capacity that gives 99% self-supply of the local load. The bottom graph displays the corresponding electricity production cost.

3.7 Type C: Hydrogen used as fuel for transportation and for stationary energy supply

The final system to be presented combines the two previous systems to form a complete wind-hydrogen system for distributed energy supply. The system comprises both a hydrogen filling station and a stationary fuel cell, such that wind energy and hydrogen can cover the total energy demand at the island, as well as export excess electricity and hydrogen to the mainland. The approach is to ensure that the island is self-supplied with both hydrogen and electricity, as would be the case for a stand-alone wind-hydrogen energy system. The operation strategy is therefore to try to match local power generation and consumption by active operation of the electrolyzer and the fuel cell. In addition, hydrogen is withdrawn from the compressed storage tanks to be used by hydrogen-fuelled vehicles and/or boats.

To be able to calculate electricity production cost and hydrogen production cost, an equivalent system with no filling station is chosen as reference system. This system is described in section 3.6.2 , where it was found that the electricity cost is $0.27/kWh for 100% self-supply of the local electrical load. The hydrogen production cost is therefore associated with the extra investments needed for supplying hydrogen to the filling station, which is calculated from equation (3.22).

Results for the different hydrogen-filling scenarios are given in Table 13. The sizing of the electrolyzer is given by equation (3.30), which maximizes the local usage of wind energy. Results for economic optimum electrolyzer capacity are given in Table 14, which shows a significant reduction of hydrogen production cost compared to Table 13.

Table 13. Main results for the different hydrogen-filling scenarios. The component sizing maximizes local usage of wind energy.

H_2-load scenario	P_w^{max} [kW]	P_e^{max} [kW]	V_H^{max} [Nm^3]	LPC_{el} [\$/kWh]	LPC_{H2} [\$/Nm^3]
1	6,300	5,400	912,100	0.27	1.01
2	7,000	6,300	988,000	0.27	0.78
3	8,200	7,500	1,198,400	0.27	0.69
4	11,000	10,300	1,532,900	0.27	0.62

Table 14. Main results for the different hydrogen-filling scenarios. The component sizing minimizes hydrogen production cost.

H_2-load scenario	P_w^{max} [kW]	P_e^{max} [kW]	V_H^{max} [Nm^3]	LPC_{el} [\$/kWh]	LPC_{H2} [\$/Nm^3]	E_{exp}/E_w [%]
1	8,650	3,250	813,500	0.27	0.55	22.9
2	9,500	3,750	867,000	0.27	0.55	28.7
3	11,250	4,700	1,024,200	0.27	0.55	27.8
4	14,000	7,000	1,388,400	0.27	0.55	22.3

It is interesting to find the reduction in hydrogen production cost that is obtained by using hydrogen storage for supplying hydrogen both to a stationary fuel cell and to the filling station, compared to filling station only (see Table 11). The cost savings are \$0.18-0.48/Nm^3 (25-46%) depending on the hydrogen load scenario. The reason for the high economic gain is that production of hydrogen for two different purposes increases the utilization factor of the electrolyzer. However, as the hydrogen load increases, a less share of the electrolyzer capacity is used to produce hydrogen for the fuel cell. Thus, the hydrogen cost approaches the hydrogen cost for the system with no fuel cell. This leads to a lower economic gain for the scenarios with high hydrogen load.

3.8 Conclusions

Three types of grid-connected wind-hydrogen systems have been studied by using a time sequential simulation model:

Type A: Hydrogen used a fuel for transportation

In Type A, hydrogen is produced by electrolysis to be used at a filling station. If the electrolyzer is operated at constant power, independently of the wind power output, the required hydrogen storage capacity is low. It is therefore possible to obtain a low cost for hydrogen, assuming that the price of electricity from the grid is equal to the cost of electricity generated by wind. However, the benefits of combining wind and hydrogen are very limited with this approach.

To maximize the penetration of wind power, it is proposed that hydrogen is produced from wind energy that would otherwise have been dissipated due to grid constraints. This integration alternative tends to be expensive because of the large hydrogen storage capacity that is needed. In addition, it is necessary to import power for hydrogen production in periods with low and average wind speed. Instead, it may be more convenient to operate the electrolyzer whenever there is a local energy surplus. By properly sizing of the hydrogen storage system, it is possible to reduce the power import for hydrogen production to zero with this operating strategy. The electrolyzer is operated more frequently, which results in a higher required hydrogen storage capacity. Furthermore, it was shown that a seasonal hydrogen load, which follows the variations in the wind, reduced the hydrogen production cost by 40% compared to a constant daily hydrogen load.

Another option for the electrolyzer operation is to follow the wind power generation directly, so that excess wind power is consumed by the local load or exported to the main grid. With this operating strategy, it was found that the optimal electrolyzer rating is 50% of the rated wind power. This reduced the hydrogen production cost by 6% compared to identical rating of the two components.

Type B: Hydrogen as electrical energy storage

In Type B, hydrogen is used as a stationary storage for wind energy by installing a fuel cell in addition to the electrolyzer and the compressed storage tanks. There is no hydrogen load in this case. In the first operation strategy, hydrogen is produced whenever the local power surplus exceeds the grid capacity. The stored hydrogen is used for power generation when the wind power output is lower. Because of the seasonal wind variations, the required storage capacity tends to be high. Consequently, storage of

wind energy resulted in twice as high power generation cost than the alternative with wind power dissipation. On the other hand, the total losses were reduced by 45% in one case, even though more than half of the stored energy is lost in the electrolyzer and fuel cell processes. If we allow a small amount of wind energy dissipation over the year for the wind-hydrogen system, it is possible to reduce the storage capacity. This leads to significant lower electricity production cost than the case with no wind energy dissipation.

Hydrogen storage can also be installed to ensure that the local electricity consumers are self-supplied by energy from wind. However, the energy cost is high, mostly due to the high cost of compressed hydrogen tanks. By reducing the level of self-supply from 100% to 95%, the required hydrogen storage capacity is reduced by as much as 40%. The corresponding electricity cost reduction is 10%. With the cost estimates used here, it was found that a reversible fuel cell gives somewhat lower electricity cost than a system with separate electrolyzer and fuel cell.

Type C: Multi-purpose hydrogen storage

In Type C, hydrogen is used both for stationary energy supply and as a fuel for vehicles. This causes a synergy effect with respect to the utilization of the hydrogen storage system, which gives an economically positive result. The cost savings of Type C is 25-50% compared to the sum of Type A and Type B for the same amount of delivered electricity and hydrogen. This result shows that multi-usage of hydrogen is beneficial from an economic point of view, and it is this flexibility that makes hydrogen an interesting carrier of wind energy.

4 A PROBABILISTIC MODEL OF ELECTRICAL ENERGY STORAGE APPLIED TO WIND POWER SMOOTHING

4.1 Introduction

This chapter describes a probabilistic model for predicting the performance of a grid-connected wind farm with energy storage. A method is employed for finding an estimate of the average firm power output of the combined wind-storage plant based on the stochastic properties of wind, a wind power curve and a general representation of an energy storage unit. Firming (smoothing) of wind power could be valuable in power systems with high wind penetration or costly balancing rules for intermittent generators. In addition, as described in the chapter, the calculated firm power level is also a measure of the minimum required transmission capacity. Thus, energy storage is considered both for increasing the value of wind power in the power system and for reducing the amount of dissipated wind power due to grid constraints.

The model is well suited for studying how efficiency and sizing of the charging and discharging device influence the overall system performance. A simple criterion is applied for estimating the required energy capacity of the storage system. The disadvantage of the model compared to a chronological simulation model such as presented in the previous chapter, is that it gives no information about how the storage level changes with time. It is not a simulation model for the on-line operation of the system, but a planning model that tells us about what we could expect of the system performance *if* a proper operation strategy were applied. The probabilistic model does only require the stochastic properties of the wind, and not detailed time-series. It is easy to apply the model for different locations and

different wind conditions, since background data for estimating the probability density function for wind speed are normally easy to obtain. On the contrary, wind series with hourly resolution, which is required for chronological simulation models, could be difficult to find for many locations. Although not important here, it should also be mentioned that the computational effort showed to be considerably less for the probabilistic model than for the chronological model. Both models are implemented in Matlab. The possibilities of using the methodological principles derived here in a chronological simulation model are discussed in chapter 7.2.

The model described in the chapter is a modified version of the model from the paper "Hydrogen Energy Storage for Grid-connected Wind Farms" which was presented at the 6th IASTED Power and Energy Systems Conference, Rhodes, Greece, 2001. The paper is reprinted in Appendix B.

4.2 Model of wind energy converter system

Probabilistic modeling of wind energy converter systems (WECS) is not a new subject. The implemented WECS-model is based on [92, 93], in addition to general statictics theory [94].

The wind speed is assumed to have a Weibull probability density function (pdf) given by:

$$f_v(v) = \frac{k}{c}\left(\frac{v}{c}\right)^{k-1} \exp\left[-\left(\frac{v}{c}\right)^{k}\right] \tag{4.1}$$

where v is the wind speed, k is the shape parameter, and c is the scale parameter defined as:

$$c = \mathrm{E}(v) / \Gamma(1 + k^{-1}) \tag{4.2}$$

where Γ is the gamma function[7] and $\mathrm{E}(v)$ is the expectation value of the wind speed. The cumulative distribution function (cdf) of the wind speed $F_v(v^*)$ is defined as the probability that v is less than or equal to v^*:

$$F_v(v^*) = \Pr(v \le v^*) \tag{4.3}$$

[7] $\Gamma(x) = \int_0^\infty e^{-t} t^{x-1} dt \qquad (\mathrm{Re}\, x > 0)$

Mathematically, the Weibull cdf can be expressed as

$$F_v(v^*) = \int_{-\infty}^{v^*} f_v(v)dv = \int_0^{v^*} f_v(v)dv = 1 - \exp\left[-\left(\frac{v^*}{c}\right)^k\right] \tag{4.4}$$

Figure 41 illustrates the Weibull pdf and cdf with expectation value E(v) = 8.5 m/s and shape parameter k = 2. A Weibull distribution with k = 2 is called a Rayleigh distribution and is typical for the wind conditions in Northern Europe [89].

The wind power output is given by the power curve, which is expressed as

$$P_w(v) = \begin{cases} 0 & \text{for } v \le v_i \text{ , } v > v_o \\ \Phi(v) & \text{for } v_i < v \le v_r \\ P_w^{max} & \text{for } v_r < v \le v_o \end{cases} \tag{4.5}$$

where v_i, v_r and v_o are the cut-in, rated and cut-out wind speed respectively. The function $\Phi(v)$ describes the shape of the wind power curve between cut-in wind speed and rated wind speed. The cdf of wind power $F_P(P_w)$ is found by combining (4.4) and (4.5):

$$F_P(P_w) = \begin{cases} F_v(v_i) + (1 - F_v(v_o)) & \text{for } P_w = 0 \\ F_v(v(P_w)) + (1 - F_v(v_o)) & \text{for } 0 < P_w < P_w^{max} \\ 1 & \text{for } P_w = P_w^{max} \end{cases} \tag{4.6}$$

where $v(P_w)$ is given by

$$v(P_w) = \Phi^{-1}(P_w) \tag{4.7}$$

Figure 42 shows the cdf of wind power, using a stepwise linear wind power curve. The expectation values of wind speed and wind power are calculated from the following equations:

$$\mathrm{E}(v) = \int_0^{\infty} v \cdot f(v)dv \tag{4.8}$$

$$\mathrm{E}(P_w) = \int_0^{\infty} P_w(v) \cdot f(v)dv \tag{4.9}$$

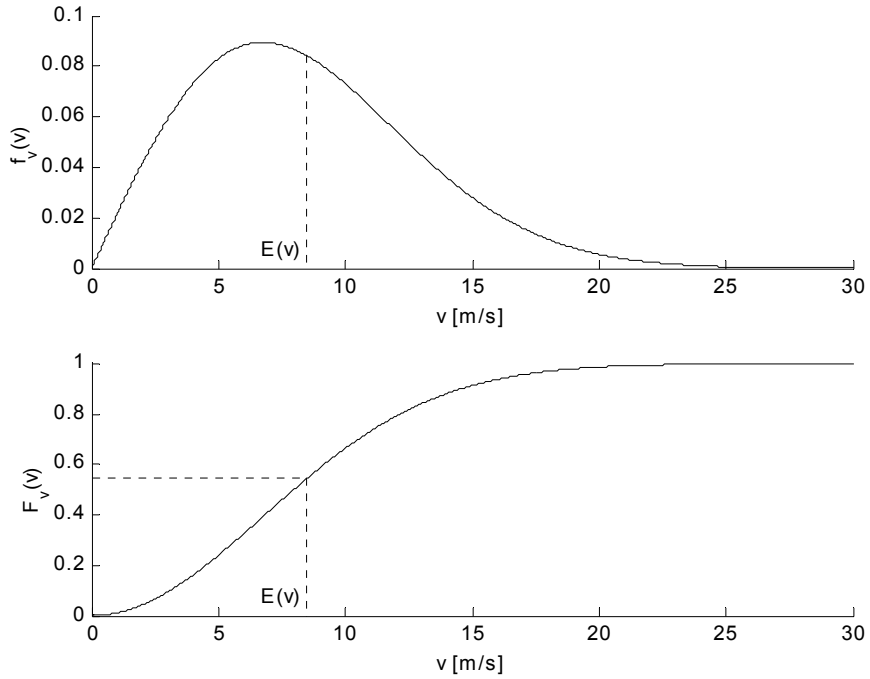

Figure 41. The pdf (upper) and the cdf (lower) of wind speed.

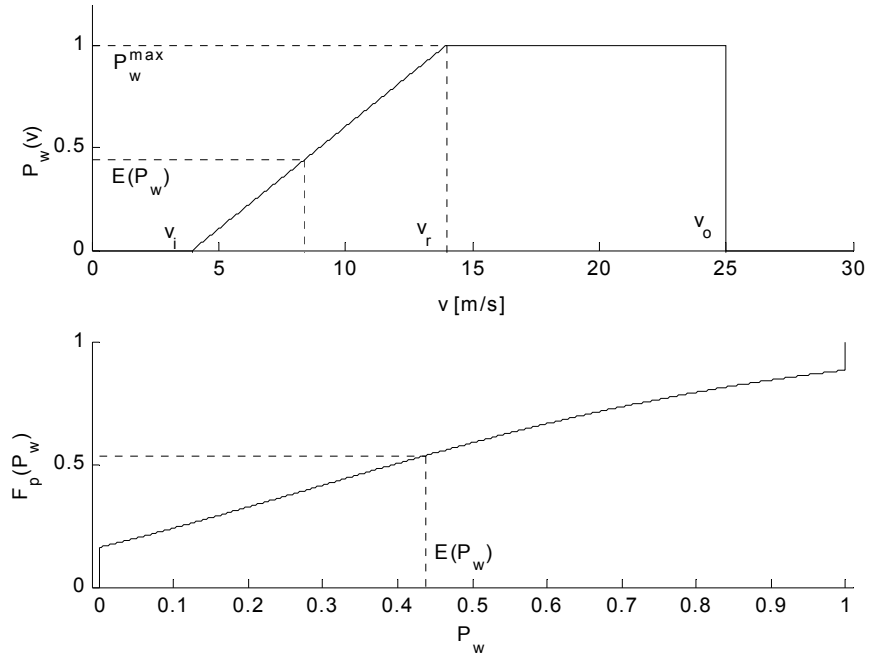

Figure 42. Wind power curve (upper) and cdf of wind power (lower).

4.3 Model of wind-storage system

4.3.1 Base model

An energy storage device is now introduced in the model. The energy storage device is in the first place only characterized by its charging efficiency (η_{ch}) and its discharging efficiency (η_{dch}) in the base model:

$$\dot{S}_{ch} = \eta_{ch}(P_{ch}) \cdot P_{ch} \tag{4.10}$$

$$\dot{S}_{dch} = \frac{P_{dch}}{\eta_{dch}(P_{dch})} \tag{4.11}$$

where $\dot{S}_{ch}$ is the energy flow into the storage during charging, and $\dot{S}_{dch}$ is the energy flow out of the storage during discharging. The efficiency is represented as a function of the operating point of the storage device. For simplicity, η_{ch} and η_{dch} are chosen to be constants in the rest of the chapter. This does not put any limitations on the usage of the method, since it also holds for general, non-linear efficiency functions.

The purpose of the energy storage is to smooth the stochastic wind variations in order to obtain a firm power output to the grid P_{fp} for the combined plant. If the wind power output exceeds the desired level P_{fp}, the excess power P_w - P_{fp} is used for charging of the storage. Stored energy is converted back to electricity (discharging) when the wind power output is less than P_{fp}. Thus, the charging and discharging power is calculated from

$$P_{ch}(v) = \begin{cases} P_w(v) - P_{fp} & \text{for } P_w(v) > P_{fp} \\ 0 & \text{for } P_w(v) \le P_{fp} \end{cases} \tag{4.12}$$

$$P_{dch}(v) = \begin{cases} P_{fp} - P_w(v) & \text{for } P_w(v) \le P_{fp} \\ 0 & \text{for } P_w(v) > P_{fp} \end{cases} \tag{4.13}$$

The probability of discharging is calculated from the cdf of wind power:

$$\Pr(P_w \le P_{fp}) = F_P(P_{fp}) \tag{4.14}$$

where F_p is given by (4.6). Thus, the probability of charging is given by

$$\Pr(P_w > P_{fp}) = 1 - \Pr(P_w \le P_{fp}) = 1 - F_P(P_{fp}) \tag{4.15}$$

since the probability that P_w is either equal to or below P_{fp} or above P_{fp} is always 1. Moreover, P_{fp} can never be zero, because there is always a probability that $v_i < v < v_o$. Likewise, P_{fp} can never be equal to P_w^{max}. By using (4.6) we get the following expression for the probability of discharging:

$$\Pr(P_w \le P_{fp}) = F_v(v(P_{fp})) + (1 - F_v(v_0)) \tag{4.16}$$

where $v(P_{fp})$ is given by (4.7). A graphical illustration of the principles for charging and discharging is shown in Figure 43. Also shown is the duration curve of wind power, defined as [92]:

$$H_P(P_w) = 1 - F_P(P_w) \tag{4.17}$$

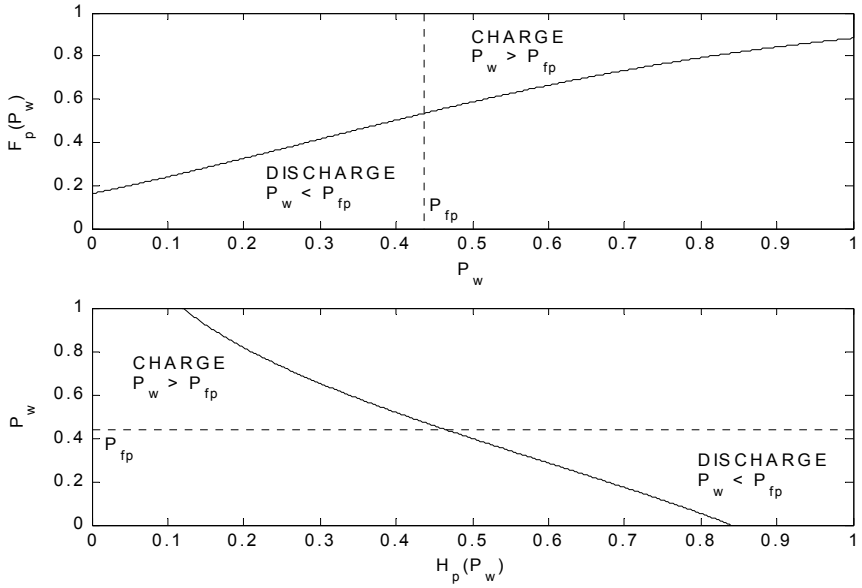

Figure 43. The principles for charging and discharging represented by the cdf of wind power (upper graph) and the duration curve of wind power (lower curve). The areas denoted "CHARGE" and "DISCHARGE" are the total shares of electrical energy that corresponds to charging and discharging, respectively.

The criterion for setting the firm power level P_{fp} is that "the expected increase in storage level during charging must be equal to the expected decrease in storage level during discharging":

$$\mathrm{E}(\dot{S}_{ch}) = \mathrm{E}(\dot{S}_{dch}) \tag{4.18}$$

By using this criterion, we ensure that there is a balance between stored and released energy, so that the system will not move towards sustained energy

deficit or surplus. The following deduction of the energy equations for the storage is based on the assumption that *the maximum and minimum storage levels are not reached*. In a case study presented later, it is shown how it is possible to make a reasonable estimate for the required storage capacity.

First, we find an expression for the expected energy flow $\mathrm{E}(\dot{S}_{ch})$ into the storage. Since $\mathrm{E}(\dot{S}_{ch})$ is a function of the random variable *v*, the expectation value is

$$\mathrm{E}(\dot{S}_{ch}) = \int_0^{\infty} \dot{S}_{ch}(v) \cdot f(v) dv \tag{4.19}$$

But charging of the storage does only take place when $P_w > P_{fp}$, so the integration interval is reduced:

$$\mathrm{E}(\dot{S}_{ch}) = \int_{v(P_{fp})}^{v_o} \dot{S}_{ch}(v) \cdot f(v) dv = \int_{v(P_{fp})}^{v_o} \eta_{ch} \cdot (P_w(v) - P_{fp}) \cdot f(v) dv \tag{4.20}$$

The expression for the expected energy flow out of the storage $\mathrm{E}(\dot{S}_{dch})$ is derived in a similar manner:

$$\begin{aligned} \mathrm{E}(\dot{S}_{dch}) &= \int_0^{\infty} \dot{S}_{dch}(v) \cdot f(v) dv = \int_0^{\infty} \eta_{dch}^{-1} \cdot (P_{fp} - P_w(v)) \cdot f(v) dv \\ &= \eta_{dch}^{-1} \cdot P_{fp} \cdot \left(F_v(v_i) + (1 - F_v(v_o)) \right) + \ldots \\ &\ldots + \int_{v_i}^{v(P_{fp})} \eta_{dch}^{-1} \cdot (P_{fp} - P_w(v)) \cdot f(v) dv \end{aligned} \tag{4.21}$$

The three equations (4.18), (4.20) and (4.21) form a set of non-linear equations that must be solved for P_{fp}, $\mathrm{E}(\dot{S}_{ch})$ and $\mathrm{E}(\dot{S}_{dch})$. This is carried out by an iterative procedure in the implemented computer model.

A special case occurs when the round-trip efficiency of energy storage is 100%. Since it is assumed that there are no capacity limitations, all the excess wind energy is stored and released later. With 100% charging and discharging efficiency, the firm grid power becomes equal to the mean wind power output. For efficiencies lower than 100%, the firm grid power will be lower than the mean wind power because of energy losses during charging and discharging. Sample results for different efficiencies are shown in Figure 44. The round-trip efficiency of storage is defined as

$$\eta_{rt} = \eta_{ch} \cdot \eta_{dch} \tag{4.22}$$

Constant values for the charging and discharging efficiencies have been used in Figure 44. We see from the figure that the energy input to the storage decreases for increasing η_{rt}.

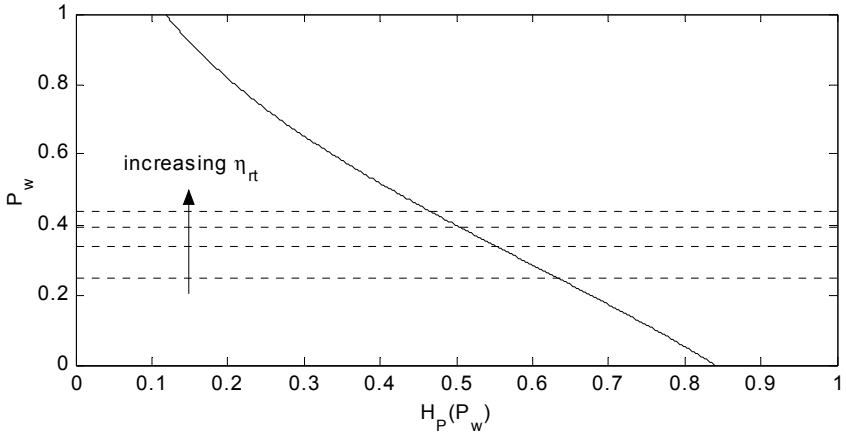

Figure 44. The impact of storage efficiency on the firm power output P_{fp} (dotted lines). The four lines represent η_{rt} = 25%, 50%, 75% and 100%. The solid line is the duration curve for wind power.

4.3.2 Power ratings of the storage device

It will now be described how limited power ratings of the storage device are modeled. We distinguish between charging capacity and discharging capacity, although they would be the same for instance in a reversible fuel cell. With limited power ratings, the expressions for charging and discharging are modified to

$$P_{ch}(v) = \begin{cases} \min\left[P_w(v) - P_{fp}, P_{ch}^{max} \right] & \text{for } P_w(v) > P_{fp} \\ 0 & \text{for } P_w(v) \le P_{fp} \end{cases} \tag{4.23}$$

$$P_{dch}(v) = \begin{cases} \min\left[P_{fp} - P_w(v), P_{dch}^{max} \right] & \text{for } P_w(v) < P_{fp} \\ 0 & \text{for } P_w(v) \ge P_{fp} \end{cases} \tag{4.24}$$

If there were no capacity limitations on charging power, it is possible to use all excess wind power for charging. This is expressed in (4.20), where the power curve $P_w(v)$ is used for integrating over the range of wind speed when charging occurs. However, if the charging capacity is lower than $P_w^{max} - P_{fp}$, it is not possible to use all the excess energy for charging. One way we can model this limitation is to introduce a modified power curve:

$$\tilde{P}_w(v) = \begin{cases} 0 & \text{for} \quad v \le v_i \ , v > v_o \\ \Phi(v) & \text{for} \quad v_i < v \le \tilde{v}_r \\ \min\left[P_w^{max}, P_{ch}^{max} + P_{fp} \right] & \text{for} \quad \tilde{v}_r < v \le v_o \end{cases} \tag{4.25}$$

where the modified rated wind speed is given by:

$$\tilde{v}_r = \begin{cases} v_r & \text{if} \quad P_w^{max} \le P_{ch}^{max} + P_{fp} \\ v(P_{ch}^{max} + P_{fp}) & \text{if} \quad P_w^{max} > P_{ch}^{max} + P_{fp} \end{cases} \tag{4.26}$$

Thus, $\tilde{v}_r$ is always less than or equal to v_r, and equations (4.25)-(4.26) also hold for unlimited charging capacity. The modified power curve is illustrated in Figure 45.

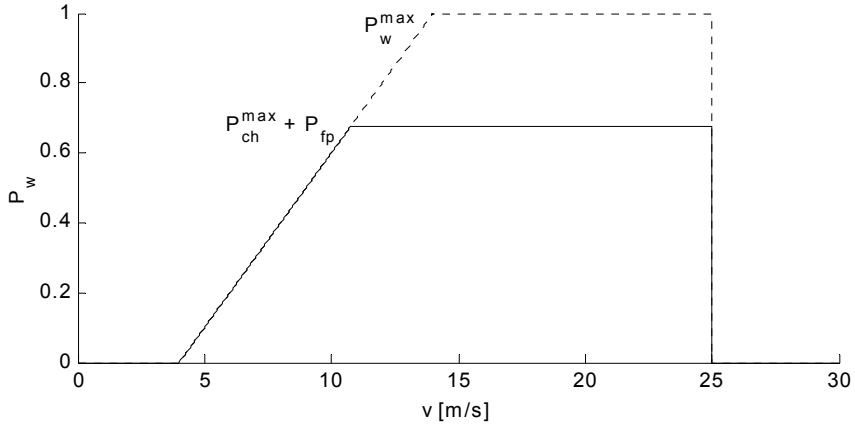

Figure 45. Plot of the modified power curve (solid line), which show the wind power available for charging when the charging capacity is lower than the wind turbine rating. The dotted line is the actual wind power curve.

The expected value of the energy flow into the storage is found by employing (4.20) with the modified power curve:

$$\mathrm{E}(\dot{S}_{ch}) = \int_{v(P_{fp})}^{v_o} \eta_{ch} \cdot (\tilde{P}_w(v) - P_{fp}) \cdot f(v) dv \tag{4.27}$$

To find the expected energy flow out of the storage, we use the new expression for discharging power given by (4.24):

$$\begin{aligned} \mathrm{E}(\dot{S}_{dch}) &= \int_0^{\infty} \dot{S}_{dch}(v) \cdot f(v) dv = \int_0^{\infty} \eta_{dch}^{-1} \cdot P_{dch}(v) \cdot f_v(v) dv \\ &= \eta_{dch}^{-1} \cdot \min\left[P_{fp}, P_{dch}^{max} \right] \cdot \left(F_v(v_i) + (1 - F_v(v_o)) \right) + \ldots \\ &\ldots + \int_{v_i}^{v(Pfp)} \eta_{dch}^{-1} \cdot P_{dch}(v) \cdot f_v(v) dv \end{aligned} \tag{4.28}$$

As for the base model, the three equations (4.18), (4.27) and (4.28) forms a set of non-linear equations that must be solved for P_{fp}, $\mathrm{E}(\dot{S}_{ch})$ and $\mathrm{E}(\dot{S}_{dch})$. The influence of limited charging and discharging capacities is illustrated in Figure 46. The "CHARGE" area is equal to the share of wind energy that is used for charging of the storage. When the excess wind power is higher than the charging capacity, there will be a "spillage" of electricity to the grid, so the actual net power output of the wind-storage system is higher than the desired firm power level. Similarly, there will be periods with energy deficit if the discharging capacity is lower than the firm power level. Figure 47 shows how the firm power level varies as a function of the charging and discharging capacities. It should be noticed that P_{fp} moves in opposite directions when changing P_{ch}^{max} and P_{dch}^{max}. This is due to the criterion that the energy flow into the storage must be equal to the energy flow out of the storage.

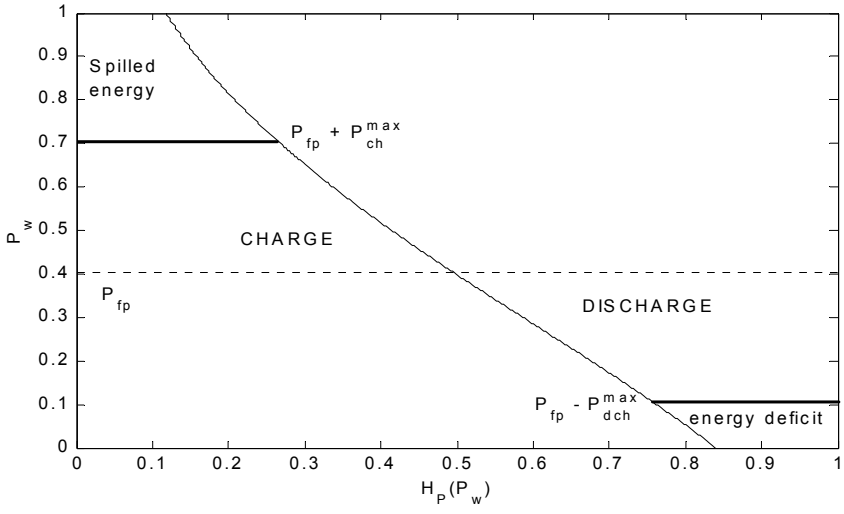

Figure 46. Illustration of limited charging and discharging capacity. Solid line is wind power duration curve. Dotted line is firm power level P_{fp}.

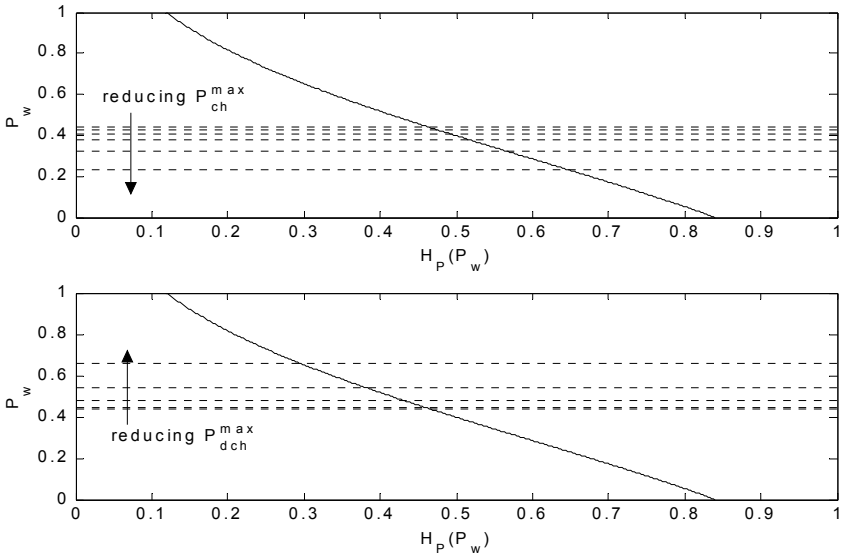

Figure 47. The effect of varying charging capacity (upper figure) and discharging capacity (lower figure) on the firm power output P_{fp} (dotted lines). The solid line is the duration curve for wind power.

4.3.3 Constant load

A constant electrical load can be included in the model with only minor modifications. The objective of the storage operation will now be to ensure a firm power balance with the grid:

$$P_{ch}(v) = \begin{cases} \min\left\{P_w(v) - (P_{fp} + P_l), P_{ch}^{max}\right\} & \text{for } P_w(v) > P_{fp} + P_l \\ 0 & \text{for } P_w(v) \le P_{fp} + P_l \end{cases} \quad (4.29)$$

$$P_{dch}(v) = \begin{cases} \min\left\{(P_{fp} + P_l) - P_w(v), P_{dch}^{max}\right\} & \text{for } P_w(v) \le P_{fp} + P_l \\ 0 & \text{for } P_w(v) > P_{fp} + P_l \end{cases} \quad (4.30)$$

where P_l is the electrical load. The variables P_{fp}, $\mathrm{E}(\dot{S}_{ch})$ and $\mathrm{E}(\dot{S}_{dch})$ are calculated in the same way as for the no-load case, by replacing P_{fp} with $P_{fp}+P_l$ in the equations in section 4.3.2 . The results presented in [95] are based on this model (see Appendix B).

4.4 Example

4.4.1 Assumptions

This section presents an application of the method on an example system consisting of a 1 MW wind turbine with energy storage. For simplicity, the piecewise linear power curve for the wind turbine shown in Figure 42 is used. The wind data is taken from the project reported in [89], where 30 years of daily wind speed for several locations in Norway were collected from the Norwegian Meteorological Institute (DNMI). In this example, the data for Helnes in northern Norway is employed to create average values of wind speed for each of the 52 weeks of the year. The mean wind speed for the 30-year period is 8.5 m/s, after converting the wind speed from 10 meters to 80 meters above ground. It is assumed that the wind speed follows a Rayleigh distribution during each week. The average weekly wind power output is calculated from equation (4.9) and the result is shown in Figure 48.

As explained in section 4.3.1 , the criterion for finding the firm power output is that the expected energy input to the storage is equal to the expected energy output of the storage. In this example, the criterion is used for each of the 52 weeks of the year to calculate the weekly firm power output of the wind-storage system. It is evident from Figure 48 that there is a strong seasonal effect on the average wind power output. If there were no particular seasonal variations, sufficient accuracy could be obtained by using a yearly wind speed distribution. However, in this case it is necessary to use for instance the weekly or monthly wind speed distribution so that the seasonal variations are taken into account.

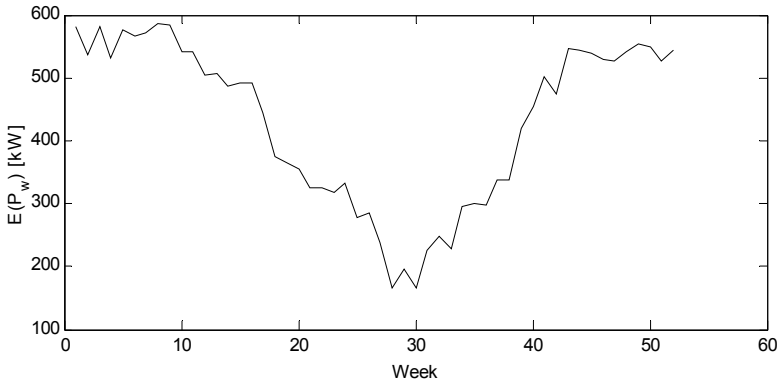

Figure 48. Seasonal variation of the expected wind power generation.

The ability of the energy storage system to provide a firm power output to the grid depends on the charging capacity and discharging capacity of the energy storage. It is of course possible to ensure a firm power output by setting the power capacity of the storage equal to the rated power of the

wind power. However, this leads to oversizing, since only the difference between the firm power level and the wind power output is balanced by the storage. The required power capacity of the storage is found after calculating the firm power level. For the example studied here, the equations for the necessary charging capacity and discharging capacities are as follows:

$$P_{ch}^{max} = \max\left[P_{w}^{max} - P_{fp}(t) \right] \quad \text{for} \quad t = 1...52 \tag{4.31}$$

$$P_{dch}^{max} = \max\left\{ P_{fp}(t) \right\} \quad \text{for} \quad t = 1...52 \tag{4.32}$$

where $P_{fp}(t)$ is the firm power level for week t.

It is possible to estimate the required storage capacity by defining a scenario where the wind speed is monotonous decreasing during the week. Hence, all charging of the energy storage occurs at the start of the week, and all discharging occurs at the end of the week. This gives us the maximum necessary storage capacity that will ensure a fixed weekly firm power output. Consequently, the maximum storage capacity is given by the week with highest wind power production. In our example, this is week 8, as observed from Figure 48. The equation for the energy storage capacity becomes:

$$S^{max} = \max\left\{ \mathrm{E}\left(\dot{S}_{ch}(t) \right) \cdot 24 \cdot 7 \right\} \quad \text{for} \quad t = 1..52 \tag{4.33}$$

where $\mathrm{E}\left(\dot{S}_{ch}(t) \right)$ is the average weekly energy flow into the storage given by equation (4.27). The energy flow (in kW) is multiplied by 24 (hours per day) and by 7 (days per week) to get the total energy amount in kWh.

It should be emphasized that the energy capacity equation (4.33) is based on assumptions that are found reasonable here, but this method of estimating the required storage capacity is a first approach. For example, if a "worst case" scenario was used, the storage capacity should be twice as high as given by equation (4.33), since the wind speed could be monotonically increasing as well as decreasing within a week. This would have resulted in an unreasonably high capacity compared to the utilization of the storage. A chronological simulation of a representative hourly wind series for a year is shown in Figure 49 to illustrate this. The figure displays a plot of the storage operation when the storage is used for providing a weekly firm power output. The storage efficiency is for simplicity set to 100% in the simulation. To provide 100% firm power output, it is necessary to have 43 MWh energy capacity. However, the full capacity is only used for a very short time period. By using the criterion given in (4.33) instead, the storage capacity becomes 28 MWh. This is illustrated with dotted lines in Figure 49. With 28 MWh energy capacity, deviations from the firm power output

occurs only 2.5% of the time. Further work will include improved methods of estimating the required storage capacity and the impact on the system performance.

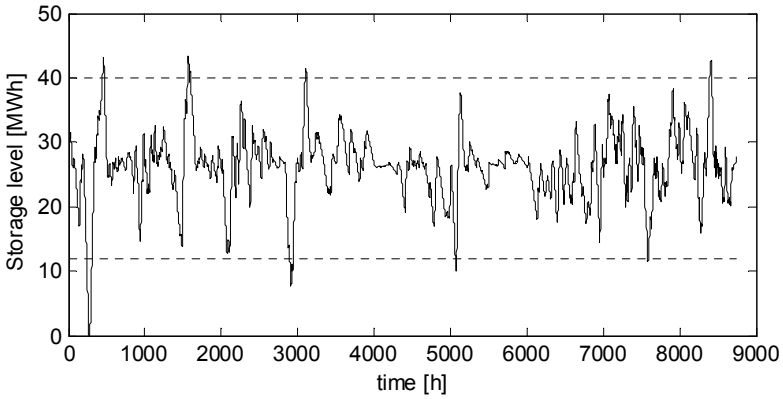

Figure 49. Chronological simulation of a wind-storage system with 100% round-trip efficiency. The dotted lines show an example of the upper and lower storage limits if equation (4.33) is employed for determining the energy capacity.

4.4.2 Main results

Table 15 shows the main results for four different values of the round-trip efficiency of energy storage. It is of course not possible to obtain 100% efficiency in actual systems, but this is used as an ideal reference case. The results for 75% efficiency can represent pumped-hydro storage and regenerative flow-cells. The cases with 25% and 50% efficiency roughly represent present and future performance of hydrogen energy storage systems. We see that the total amount of energy delivered to the grid E_g is clearly influenced by the storage efficiency. The system efficiency is calculated from:

$$\eta_{sys} = \frac{\sum_{t=1}^{52} \overline{P}_g(t)}{\sum_{t=1}^{52} \overline{P}_w(t)} = E_g / E_w \qquad (4.34)$$

where $\overline{P}_g(t)$ is the average power output to the grid in week t. In this case there is no spillage of energy or energy deficit. so that $\overline{P}_g(t)$ is equal to the firm power output $P_{fp}(t)$. Table 15 shows that the system efficiency is considerably higher than the storage efficiency. This is reasonable since only the difference between the firm power level and the wind power output is balanced by the storage. Most of the wind power is exported directly to the grid.

Table 15. Results for the example system with four different values for the round-trip efficiency of storage. Refer to the text or the symbol list in Appendix A for explanation of the variables.

η_{rt} [%]	100	75	50	25
E_w [MWh]	3,760	3,760	3,760	3,760
E_g [MWh]	3,760	3,400	2,910	2,140
η_{sys} [%]	100	91	78	57
P_{ch}^{max} [kW]	830	860	890	930
P_{dch}^{max} [kW]	590	540	470	360
max(P_{fp}) [kW]	590	540	470	360
S^{max} [MWh]	28	28	27	25
UF_{ch} [%]	17	19	22	27
UF_{dch} [%]	25	23	21	17
UF_{rfc} [%]	34	33	33	33

An additional feature of the firm power output is that it can be used for estimating the lowest allowable transmission capacity between the wind-storage system and the main grid. Table 15 shows the highest value of P_{fp} for the whole year. This value corresponds to the lowest possible transmission capacity that gives no dissipation of wind power during the year. If we have a wind turbine rated at 1 MW and an energy storage device with 75% efficiency, it will be theoretically possible to operate this system in a grid with 540 kW capacity without downregulating the output.

The maximum storage capacity S^{max} is approximately the same for all storage efficiencies and varies between 25 and 28 MWh. By dividing the storage capacity with the discharging capacity, we find that the output duration of the energy storage system varies between 47 hours and 70 hours, depending on the efficiency.

A remarkable result is that the required charging capacity is relatively close to the rated power of the wind turbine, which is 1 MW. This is due to the low wind speed in the summer, where the firm power output also is low. It is always a certain probability that the wind power output reaches the rated value, even for weeks with low expected wind speed. According to equation (4.31), the charging capacity is therefore set to a high value. This leads to low utilization of the charging device during the rest of the year, which is evident from the low utilization factor UF_{ch} of the charging device. Analogously, the utilization factor of the discharging device is also low, since the capacity is determined by the winter period with high wind speed. It is preferable to have a high utilization factor of the components, taking into account the investment costs. The utilization factor can be increased if it is possible to install a device that allows operation in reversible mode, for

instance a reversible fuel cell. The utilization factor UF_{rfc} of such a device is also shown in Table 15. The values of UF_{rfc} are calculated by setting the power capacity of the reversible fuel cell equal to the charging capacity shown in the table.

Another way of increasing the utilization factor is of course to reduce the power capacity. The drawback is that it will not always be possible to obtain a firm power output of the wind-storage system. However, the sizing criteria given in equation (4.31) and (4.32) are strict, and it is likely that at least a small reduction will not influence much the smoothing capabilities when we consider one year of system operation. Therefore, calculations were carried out for a range of charging and discharging capacities to investigate the impact on the system performance. The round-trip efficiency of energy storage is set to 75%. The results for different charging capacities are displayed in Figure 50. More wind energy is spilled when the capacity is reduced, according to Figure 46. However, Figure 50 shows that the spillage is insignificant for a charging capacity as low as 500 kW, which is half the rated power of the wind turbine. Thus, it is possible to use a much lower charging capacity than shown in Table 15 and still obtain close to optimal power smoothing capability. Furthermore, Figure 51 shows that it is possible to reduce the discharging capacity to at least 400 kW, without noticeable consequences for the performance. The corresponding value for the power capacity of a reversible charging/discharging device is approximately 500 kW, as seen from Figure 52.

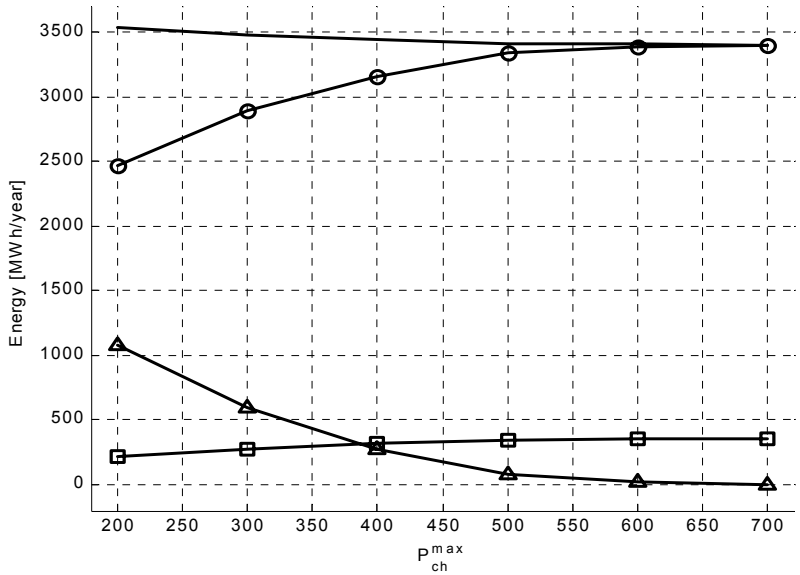

Figure 50. The effect of charging capacity on the performance of the wind-storage system. (-) is the yearly energy amount supplied to the grid, (o) is the sum of firm power for one year, (Δ) is yearly amount of spilled energy, (boxes) is yearly energy storage losses.

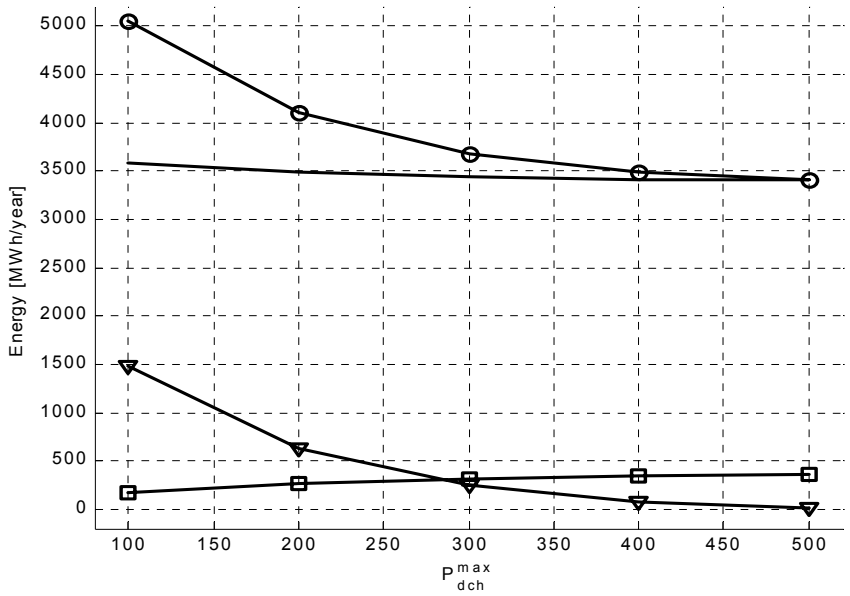

Figure 51. The effect of discharging capacity on the performance of the wind-storage systems. (-) is the yearly energy amount supplied to the grid, (o) is the sum of firm power for one year, (∇) is yearly energy deficit, (boxes) is yearly energy storage losses.

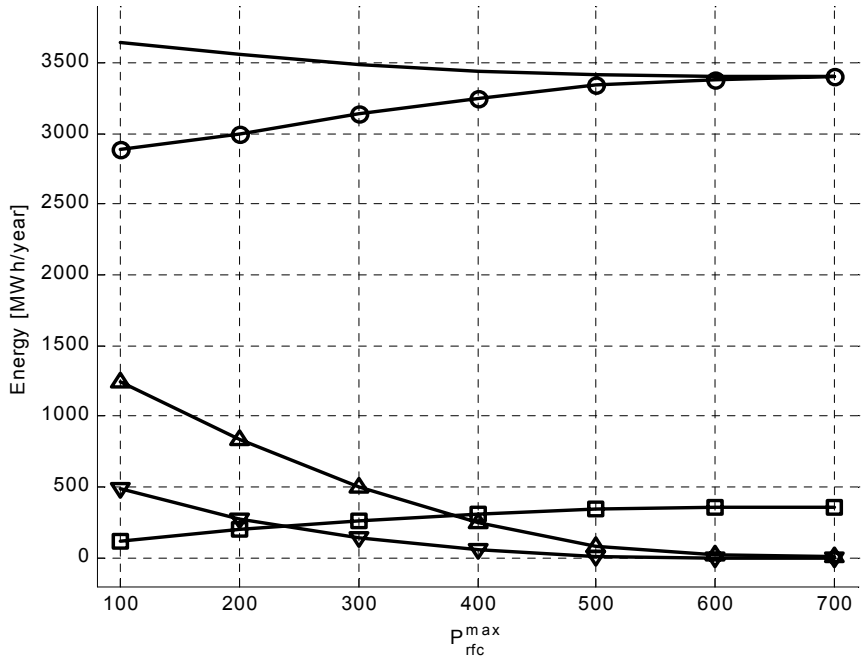

Figure 52. The effect of the power capacity of a regenerative fuel cell on the performance of the wind-storage system. (-) is the yearly energy amount supplied to the grid, (o) is is the sum of firm power for one year, (Δ) is yearly amount of spilled energy, (∇) is yearly energy deficit, (boxes) is yearly energy storage losses.

4.4.3 Comparison of storage alternatives

The type of energy storage has not yet been specified. It would be interesting to investigate how the capital costs and operating efficiencies of different storage applications influence on the cost of power smoothing. Therefore, a cost assessment of different wind-storage systems is presented based on results from the probabilistic model. Four different storage technologies have been chosen; pumped hydro, vanadium flow cell, hydrogen-bromine storage and hydrogen-oxygen storage. The chosen storage parameters are given in Table 16. It is important to notice that the rating of the wind turbine (1 MW) is arbitrarily chosen. In the case of pumped hydro, it would be more convenient to consider a larger wind farm. However, the results are scalable since economics of scale is neglected. The cost of electricity is calculated using the "levelised production cost" method, described in chapter 3.2.5. The discount rate is set to 7%, and the period of analysis is 20 years.

Table 16. Parameters for the different technologies. The O&M costs are given as percentage of investment per year.

Component		Investment	O&M [%]	Efficiency [%]	Lifetime [yr]
Wind power plant		$800/kW	2		20
Pumped hydro:	*Power*	$600/kW	1	75	30
	Energy	$15/kWh	0		30
Vanadium battery:	*Power*	$350/kW	4	75	20
	Energy	$30/kWh	4		20
H_2-Br reversible FC:	*Power*	$600/kW	6	75	15
	Energy	$15/kWh	2		30
H_2-O_2 reversible FC:	*Power*	$600/kW	4	40	15
	Energy	$15/kWh	2		30
H_2-O_2 ELY+FC:	*Power*	$2,000/kW	4	50	15
	Energy	$15/kWh	2		30

It is necessary to compare the electricity cost of the wind-storage system with the electricity cost of wind power alone, in order to evaluate the cost of applying energy storage for power smoothing. Two different cases have been studied for wind power with no storage. In the first case the grid can transmit all wind power production, while the other case includes a maximum transmission capacity lower than the wind turbine rating. Recalling that the maximum firm power output P_{fp} corresponds to the lowest possible transmission capacity for the wind-storage system, P_g^{max} is

set equal to 540 kW, as shown in Table 15 for 75% efficiency. Without energy storage, the transmission constraint causes 26% of the available wind energy to be dissipated over the year, mostly in winter. Furthermore, the electricity production cost increases by 38%; from \$24/MWh to \$33/MWh. The latter value is also the break-even cost of wind power if the grid is considered to be upgraded from 540 kW to 1 MW. The corresponding specific break-even cost of grid upgrades is \$640/kW, assuming 2% O&M cost and 20 years lifetime.

It is observed from Table 17 that the electricity cost of firm power for all the different wind-storage systems is significantly higher than the two no-storage cases. Pumped hydro gives lowest cost, and it is also the only alternative that is economic and technically mature today. It is important to remember that the availability of pumped hydro is dependent on the geographical conditions and therefore of limited use in conjunction with wind power, especially in weak grids. However, the results show that applying pumped hydro for smoothing of wind power is an economic very interesting alternative in those power systems where this is possible. In such cases, firm power output must be worth about twice as much as fluctuating power in the market in order to cover the extra investment costs and the reduced power output due to storage losses.

Table 17. Main results of the cost assessment. The power ratings of the wind turbine and energy storage system are 1 MW and 500 kW, respectively. The energy rating of the storage is 28 MWh. The alternative denoted wind only represents a grid-constrained case with grid capacity equal to 540 kW.*

Integration alternative	E_g [MWh/yr]	E_{sp} [MWh/yr]	E_{def} [MWh/yr]	η_{sys} [%]	LPC_{el} [\$/MWh]
wind only	3760	-	-	100	24
wind only*	2790	970	-	74	33
pumped hydro	3410	76	6	91	45
vanadium	3410	76	6	91	67
H_2-Br	3410	76	6	91	54
H_2-O_2 rev FC	2750	240	0	73	65
H_2-O_2 ELY+FC	2970	175	0	79	95

The other storage alternatives are expected to be more expensive, but they have the advantage of modularity and site-independence. These features are especially attractive in remote areas with low grid capacity. Hydrogen-oxygen storage with separated electrolyzer and fuel cell is clearly the least favorable option because of high investment costs. Hydrogen-bromine storage seems to be economic viable, but cost assumptions and

technological development are very uncertain. A somewhat surprising result is that H_2-O_2 with reversible fuel cell gives a slightly lower electricity cost than the vanadium battery, although the round-trip efficiency is only 40%. This result is actually a bit misleading, since the firmness of the power output is different for the two options. Table 17 shows that 9% of the wind energy is spilled in the H_2-O_2 case, while the corresponding value for the Vanadium battery is only 2%. It is necessary to raise the power rating of the H_2-O_2 system to 600 kW in order to obtain 2% energy spillage, which leads to an electricity cost of $70/MWh. Nevertheless, the result is still approximately the same as for the more efficient vanadium battery. The reason is the high specific *energy* cost of the vanadium battery compared to hydrogen storage, as illustrated in Figure 53.

The comparison of H_2-O_2 storage and vanadium battery showed that the cost of energy capacity is crucial for the cost of power smoothing. In the model, the energy capacity is found by a simple approach, see equation (4.33). It could be that it is possible to maintain a sufficient smoothing capability using even lower energy capacity, but it would be necessary to extend the model to verify this. In Figure 54, the economic impact of storage sizing is shown, and it is clear that the cost sensitivity is high for the vanadium battery compared with the other storage alternatives.

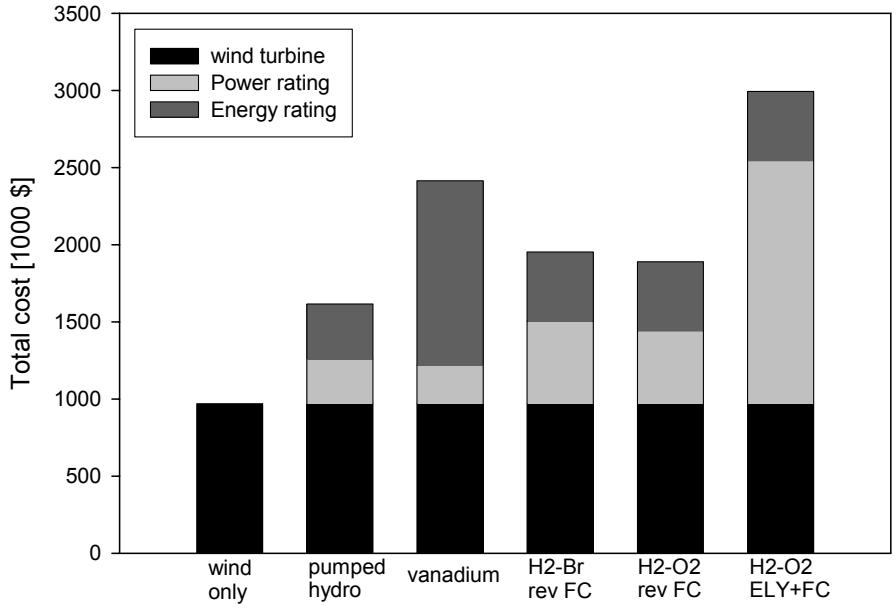

Figure 53. The discounted present value of the total cost for the different alternatives.

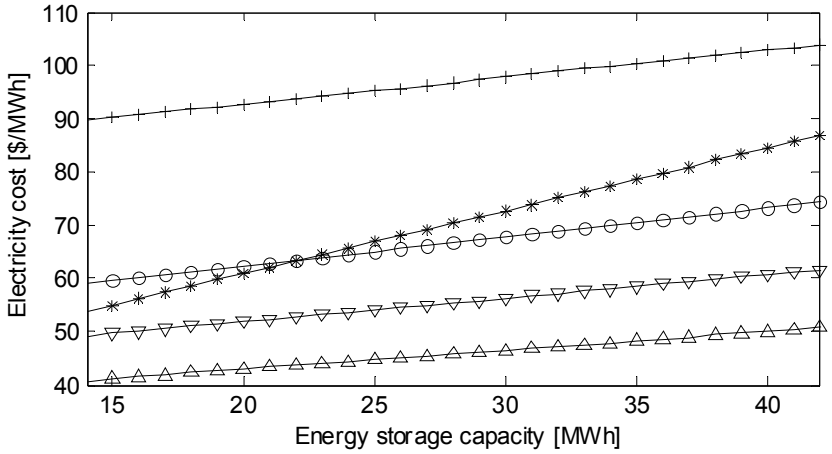

Figure 54. Levelised production cost of electricity as a function of storage capacity for the different energy storage systems. (+) H_2-O_2 with separated electrolyzer and fuel cell; (o) H_2-O_2 with reversible fuel cell; (∇) H_2-Br with reversible fuel cell; (∗) vanadium battery; (Δ) pumped hydro.

4.5 Conclusions

The chapter presented a new method for evaluating the power smoothing capability of energy storage in conjunction with grid-connected wind farms. The method is based on the statistical properties of the wind and a representation of the wind energy conversion system and the energy storage device. To estimate the firm power output of the wind-storage system, it is required that the expected increase in storage level during charging must be equal to the expected decrease in storage level during discharging. Furthermore, it is assumed that the minimum and maximum storage levels are not reached during operation. For an example system based on typical Norwegian wind conditions, it is explained how the necessary storage capacity can be estimated. It is shown that the power rating of the storage device does not need to be more than approximately 50% of rated wind power to provide sufficient smoothing.

A cost assessment has been carried out based on results from the probabilistic model for evaluation of the cost of power smoothing. For the example studied here, firm power must have about twice as high value as fluctuating power to compensate for the investment cost of pumped hydro. Regenerative flow cells, such as the vanadium battery, seem to have too high cost for energy capacity to be a viable option. However, the estimation of the required energy capacity is based on a simplified criterion. It could very well be that the vanadium battery is a viable option for power smoothing with lower energy capacity and thus less investment costs than estimated here. Hydrogen-oxygen systems on the other hand, lead to high

power smoothing cost because of low electrical efficiency. This is especially true for systems with separated electrolyzer and fuel cell. If future goals for cost and performance are realized, hydrogen storage with regenerative fuel cell will clearly be a better option than a system with separated electrolyzer and fuel cell.

To summarize, the model is well suited to study the impact of storage efficiency, charging capacity and discharging capacity on the operation of a grid-connected wind-storage system. Future developments of the model should include improved rules for estimating the required energy capacity.

5 OPERATION AND SCHEDULING OF WIND POWER WITH ENERGY STORAGE IN A MARKET SYSTEM

5.1 Introduction

This chapter describes a method for short-term scheduling of wind power by utilization of energy storage. The method is based on a dynamic programming algorithm for finding the optimal generation scheduling in a day-ahead power market. An operation strategy that seeks to minimize the difference between the actual power output and the scheduled power output has also been developed. The scheduling and operation methods have been implemented in Matlab as a part of a general wind-storage simulation model. The model also includes a local load and takes into account grid constraints.

The chapter shows an application of the model on a case study where the impact of energy storage sizing, efficiency and wind forecasting accuracy on system operation and economics are emphasized. An extension of the operation strategy by the use of stochastic dynamic programming is briefly discussed. Supplementary results for the scheduling problem based on a linear programming formulation are also presented, in order to give more insight in the possibilities of using energy storage to improve the short-term scheduling of wind power.

Chapters 5.1-5.4 are based on the paper "Operation and Sizing of Energy Storage for Wind Power Plants in a Market System", first presented at the 14th PSCC Conference, Sevilla, Spain, 2002. An updated version of the paper was later published in the Int. Journal of Electrical Power and Energy Systems, vol. 25, 2003 and is given in Appendix B.

5.2 System description

The distributed generation and storage system is shown in Figure 55 and it consists of a wind power plant and an energy storage device. It is assumed that the owner of the plant either has a demand for electricity P_l or alternatively have contracts with nearby electricity consumers represented by an aggregated load demand. The system is connected to the main electricity network by a distribution line with limited capacity. Reactive power flow is neglected in the model. The system components and the electricity market model are presented below.

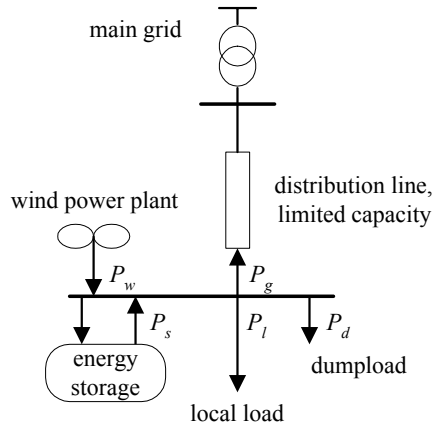

Figure 55. Wind power plant with local energy storage connected to a sparsely populated grid. The direction of the arrows refers to positive values of the variables.

5.2.1 Wind power plant

The wind power generation is calculated from the power curve in Figure 56. For simplicity, it is assumed that the wind power plant consists of identical wind turbines and that the wind conditions are the same for all turbines.

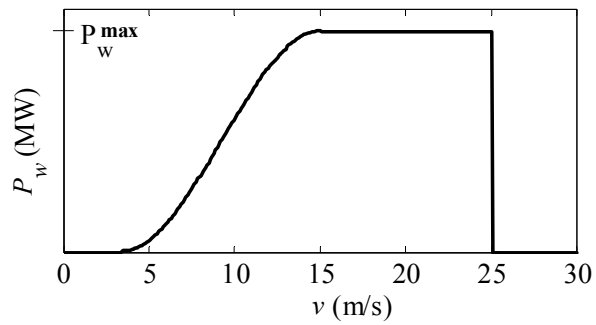

Figure 56. The wind generator input/output characteristics.

5.2.2 Energy Storage

The energy storage device is defined by its power capacity, energy capacity, charging efficiency and discharging efficiency. Different storage types are described chapter 2. The relationship between storage content S and power flow in/out of the storage P_s is defined as follows:

$$S(t+1) = \begin{cases} S(t) - \dfrac{1}{\eta_{dch}} P_s(t)\Delta t & \text{for } P_s(t) \geq 0 \\ S(t) - \eta_{ch} P_s(t)\Delta t & \text{for } P_s(t) < 0 \end{cases} \tag{5.1}$$

$$P_s^{min} \leq P_s(t) \leq P_s^{max} \tag{5.2}$$

$$S^{min} \leq S(t) \leq S^{max} \tag{5.3}$$

where η_{ch} and η_{dch} are the efficiencies of charging and discharging, respectively. The storage level at the beginning of time step t is $S(t)$. The round-trip efficiency of electricity storage is $\eta_{rt} = \eta_{ch} \cdot \eta_{dch}$.

5.2.3 Power export and import

The main grid will act as a power source or sink, depending on the balance between local generation and demand. The power balance is:

$$P_g(t) = P_w(t) + P_s(t) - P_l(t) - P_d(t) \tag{5.4}$$

$$P_g^{min} \leq P_g(t) \leq P_g^{max} \tag{5.5}$$

Power export corresponds to positive values for P_g and is assumed to be measured at the load side of the distribution line. If the net power generation exceeds the line capacity, the excess power is consumed by a dump load P_d that is used only for this purpose. Alternatively, one or more wind turbines could be shut down or downregulated to avoid overloading the grid. The reduction of wind power output is then modeled as a dump load P_d.

The expression for grid losses is based on losses through heat dissipation along the line (RI^2):

$$P_{gl}(t) = \frac{RL}{|V|^2} P_g(t)^2 = a_{gl} \cdot P_g(t)^2 \tag{5.6}$$

where R is the resistance per length, L is the length of the line an V is the voltage. It is assumed that $RL/|V|^2$ can be represented by the constant a_{gl}.

The maximum allowable power export is set equal to the distribution line capacity, while the minimum value (import) is given by:

$$P_g^{min} = -P_g^{max} + a_{gl}(P_{gl}^{max})^2 \tag{5.7}$$

since the line capacity limits the power *injected* into the line.

5.2.4 Electricity market

In the Nordic spot market, daily bids for sale and purchase of energy are provided to the power pool no later than 12 hours before the actual day. After the spot price has been settled, the final schedule for each generator is worked out. During the operation, if a participant does not deliver the contracted amount at the spot market, the discrepancy must be traded in the regulating power market. This normally results in a reduced profit [96]. The market conditions have been considerably simplified in the model. Since the marginal cost of power produced from a wind power plant is zero, it is presumed that wind energy always can be sold at the spot market. The bidding process is not included in the model. Each day at 12:00, the owner of the distributed resource performs the scheduling of the hourly power export P_{sch} for each time step in the scheduling period, which is 24 hours. The hourly income from the spot market is

$$f_{spot}(t) = e(t)P_{sch}(t) \tag{5.8}$$

where e is the spot price of electricity and P_{sch} is the scheduled power export, which is used as the contracted power exchange. Pricing of power losses is based on the spot price:

$$f_{loss}(t) = -e(t)P_{gl}(t) \tag{5.9}$$

An income for supplying electricity to the load is included. It is set equal to the cost for supplying the load with electricity from the spot market:

$$f_{load}(t) = e(t) \cdot (P_l(t) + a_{gl}P_l(t)^2) \tag{5.10}$$

This means that the owner of the wind power plant obtains an extra income due to avoided transmission and distribution costs. Since the focus is on the wind uncertainty and not on demand uncertainty, the load is chosen to be deterministic. In general, it is much easier to predict power consumption in the power system than wind power generation [97]. However, the model could easily be extended to include load uncertainties.

The regulating power market is simplified by using average values for imbalance costs. The prices for sale and purchase of electricity traded in the regulating market are proportional to the spot price:

$$f_{reg}(t) = \begin{cases} (1 - c_{dw}) \cdot e(t) P_{dev}(t) & (P_{dev}(t) \geq 0) \\ (1 + c_{up}) \cdot e(t) P_{dev}(t) & (P_{dev}(t) < 0) \end{cases} \tag{5.11}$$

where the deviation between actual and scheduled power export, defined as

$$P_{dev} = P_g - P_{sch} \tag{5.12}$$

is traded in the regulating power market. In the present Norwegian market, a discrepancy between the actual and planned generation could in fact lead to higher revenue, depending on the overall power balance in the system. This could for instance happen in the cases when the actual power export is higher than scheduled at the same time as there is a power deficit in the system. However, it is presumed that in average, deviations from the schedule are disadvantageous, since they increase the uncertainty of the overall power balance.

The annual revenue is given by the following relationship:

$$AR = \sum_{year} (f_{spot} + f_{loss} + f_{load} + f_{reg}) \tag{5.13}$$

5.3 Operation strategy

The operation strategy consists of three separate parts: 1) forecasting of wind speed, 2) generation scheduling, which determines the power exchange in the spot market and 3) on-line operation of the storage. In the present model, the forecasts of load and spot price are assumed to have 100% accuracy. A flowchart of the model is shown in Figure 57, and the various steps of the algorithm are described below.

5.3.1 Forecasts

An algorithm for computer-generated wind speed forecasts has been developed. The forecasting is performed once each day in advance of the generation scheduling and is based on the prediction of mean wind speed $\overline{v}^{i+1}$ for the next day i+1. The length of the scheduling period is one day, i.e. 24 hours. By using this method, the forecasted wind speed $\hat{v}^{i+1}(t)$ for each hour in the next day is set equal to the mean wind speed $\overline{v}^{i+1}$. This means

that $\hat{v}^{i+1}(t)$ has the same value for every hour in the scheduling period, as illustrated in Figure 58. The forecasting algorithm includes the following steps:

1. Read wind data $v^{i+1}(t)$ for the scheduling period $t = 1..t_{end}$ for day i+1
2. Calculate mean wind speed $\overline{v}^{i+1} = \frac{1}{t_{end}} \sum_{t=1}^{t_{end}} v^{i+1}(t)$
3. Return the predicted wind speed $\hat{v}(t)^{i+1} = \overline{v}^{i+1}$ for $t = 1..t_{end}$

The accuracy of a forecasting method can be measured by the root-mean-squared error (RMSE), which is defined as

$$\text{RMSE} = \sqrt{\frac{1}{N} \sum_{j=1}^{N} \left(\hat{v}(j) - v(j) \right)^2} \tag{5.14}$$

where N is the total number of time steps of the wind series. For the specific wind series used in the simulations, RMSE was found to be 2.5 m/s. The wind series consists of hourly data for one year, and the mean wind speed for the whole year is 8.5 m/s. As a comparison, the average RMSE of the HILRAM/WASP prediction tool was reported to be about 1.5 m/s for a wind series with mean wind speed equal to 3.75 m/s [98].

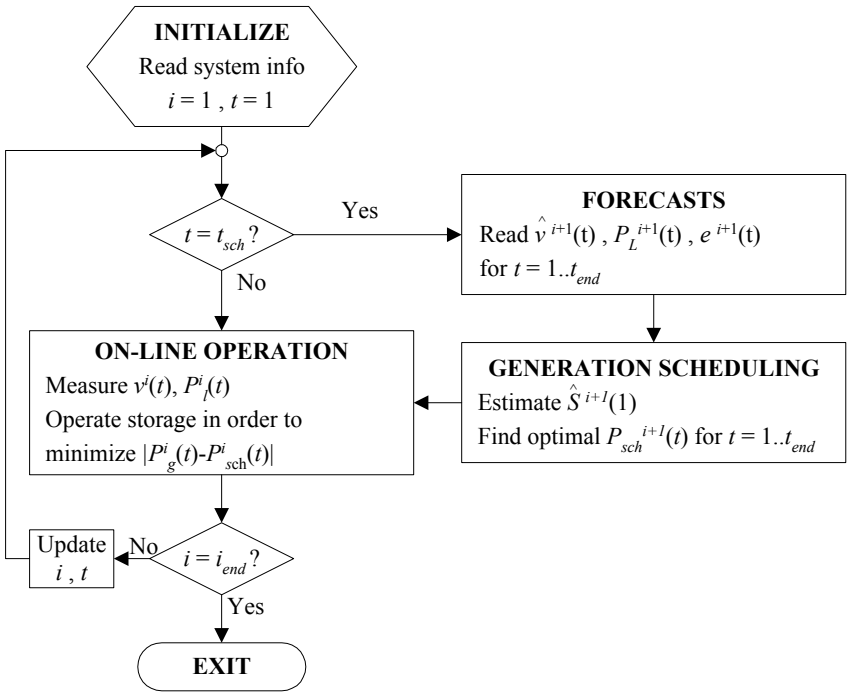

Figure 57. Flowchart of the operation strategy for a wind power plant with energy storage. The index for day and hour is i and t respectively.

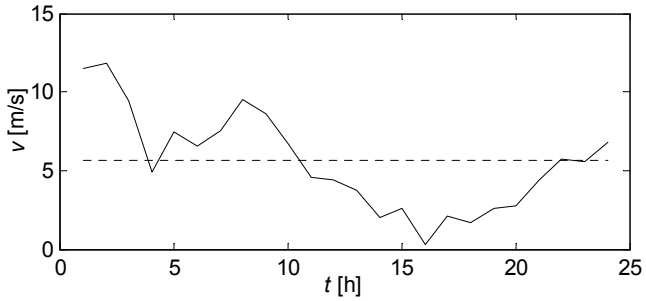

Figure 58. A sample of actual (solid line) and forecasted (dotted line) wind speed.

The basic assumption of the method is that the exact value of the mean daily wind speed is known in advance. It is possible to modify the forecasting method by introducing an uncertainty to the predicted mean value. This could be beneficial if we want to study the impact of lower forecast accuracy. If we represent the uncertainty by the coefficient of variation V, the new prediction of wind speed can be expressed as a random variable with mean $\overline{v}$ and standard deviation $\overline{v} \cdot V$. The modified forecasting algorithm becomes:

1. Read wind data $v^{i+1}(t)$ for the scheduling period $t = 1..t_{end}$ for day i+1
2. Calculate mean wind speed $\overline{v}^{i+1} = \frac{1}{t_{end}} \sum_{t=1}^{t_{end}} v^{i+1}(t)$
3. Draw a random number $\tilde{v}$ from the normal distribution with mean $\overline{v}^{i+1}$ and standard deviation $\overline{v}^{i+1} \cdot V$
4. Return the predicted wind speed $\hat{v}^{i+1}(t) = \tilde{v}$ for $t = 1..t_{end}$

5.3.2 Generation scheduling

Generation scheduling of the wind-storage system is performed at the specified hour t_{sch} each day. The objective is to find the power export for the next day which maximizes the expected profit. Since the wind speed forecast is uncertain, and a penalty is given for trading in the regulating market, the optimization problem should ideally take into account uncertainty. However, at this stage of the modeling work, the forecasted values are treated as deterministic variables. Expected penalties due to deviations between actual and scheduled export are consequently omitted in the scheduling problem.

Given the spot price, load demand and forecast of wind speed, the optimization problem is to determine the hourly trading of electricity in the spot market which maximizes the expected profit over the scheduling period. Mathematically, the scheduling problem is formulated as:

$$\max\left\{F=\sum_{t=1}^{t_{end}} f_{sch}(t)\right\} \tag{5.15}$$

where

$$f_{sch}(t)=e(t)\cdot\left(P_{sch}(t)-a_{gl}P_{sch}(t)^2\right)-c_dP_d(t) \tag{5.16}$$

subject to the system operating constraints (5.1)-(5.7) and the initial storage level. Since there are normally large uncertainties in the prediction of wind speed, the optimization horizon is chosen to be only 24 hours. According to equation (5.15), it is beneficial from an economic point of view to discharge the storage completely at the end of each period. However, if good long-term forecasts for the wind speed exist, the optimization horizon should be increased. Then it could be favorable to store energy at the end of the next day, for instance if there was a risk for long periods with no wind. This is considered in Chapter 6. A special case occurs when the expected local power surplus exceeds the capacity of the distribution line. It is obviously better to store the energy surplus than to use the dump load. This is modeled by introducing a penalty c_d for the dump load. Thus, the value of P_d deviates from zero only when the storage is completely filled or at maximum charging power at the same time as the net local generation exceeds the export capacity.

The generation scheduling is performed 12 hours in advance of the next day, which means that the storage level is unknown at the start of the optimization period. If the wind forecasts were 100% correct, the estimated value $\hat{S}^i(t_{end})$ from the previous optimization could be used. However, there will always be some deviations between the actual wind speed and the forecasted wind speed. To get a better estimate of the initial storage level of day i+1, the following equation is employed:

$$\hat{S}^{i+1}(1)=\hat{S}^i(t_{end})+\Delta S \tag{5.17}$$

where ΔS is a storage level correction based on the measured storage level at the scheduling hour t_{sch} and an improved forecast of the wind speed for the remaining hours of the day. The improved forecast is calculated by using the method described in section 5.3.1 for the remaining hours of the day.

Dynamic programming algorithm

The optimization problem is solved using a dynamic programming (DP) algorithm based on [99, 100], which requires disctretization of the storage

level. The storage level at the beginning of time step t is denoted $S(t) = S^k$, and the storage level at the beginning of time step t+1 is denoted $S(t+1) = S^m$. The profit at time step t can then be expressed as $f_{sch}(t,k,m)$ which is the result of operating the storage so that the storage level is changed from S^k to S^m. Consequently, charging occurs when $m > k$.

A recursive formula for the scheduling problem can be expressed as

$$F^*(t,k) = \max_m \left\{ f_{sch}(t,k,m) + F^*(t+1,m) \right\} \tag{5.18}$$

where $F^*(t,k)$ is the profit obtained by optimal operation from time step t to the end of the scheduling period when the storage level at the beginning of time step t is S^k. We define $F^*(t_{end}+1,m) = 0$ for all m to indicate the end of the scheduling period.

The DP routine returns the optimal values of the storage level for each hour in the scheduling period:

$$\left[\hat{S}^{i+1}(2), \hat{S}^{i+1}(3), ..., \hat{S}^{i+1}(t_{end}) \right]$$

where $\hat{S}^{i+1}(t)$ denotes the *estimated* storage level for hour t in day i+1. By using equations (5.1) and (5.4), the estimated hourly power export to the external grid $\hat{P}_g^{i+1}(t)$ can be found. The scheduled power export $P_{sch}^{i+1}(t)$ is then set equal to $\hat{P}_g^{i+1}(t)$.

5.3.3 On-line operation

A straightforward operation strategy is employed. For each hour, the storage is operated to minimize the difference between the scheduled and the measured power export to the main grid:

$$\min_{P_s(t)} P_{dev}(t) \tag{5.19}$$

subject to the physical constraints (5.1)-(5.7). The control variable is the power output of the storage $P_s(t)$, which can take positive and negative values. The on-line operation problem is solved by a control logic scheme:

if $P_w(t) - P_l(t) > P_{sch}(t)$

Store excess energy until $P_{dev}(t) = 0$

or operational limits are reached

else

Release stored energy until $P_{dev}(t) = 0$

or operational limits are reached

5.4 System simulation

A case study is designed for demonstrating the proposed scheduling and operation strategy of the distributed resource. The parameters for the base case are listed in Table 18. The type of energy storage is not specified, but it could for instance be a redox flow cell.

Table 18. The parameter values for the base case.

Grid capacity	P_g^{max}	4 MW
Wind power capacity	P_w^{max}	10 MW
Power capacity of storage	P_s^{max}	6 MW
Energy capacity of storage	S^{max}	100 MWh
Average load	$\bar{P}_l$	2.6 MW
Average wind power	$\bar{P}_w$	4 MW
Grid losses parameter	a_{gl}	0.01 MW^{-1}
Round trip efficiency of storage	η_{rt}	75%
Wind forecast error	RMSE	2.6 m/s

Hourly values of wind speed for one year are generated by using the computer software WDLTOOLS [101]. The mean wind speed is 8.5 m/s. Time series for electricity load is based the normalized daily load curve in Figure 59. The hourly values in Figure 59 are multiplied by the daily mean load $\bar{P}_l^i$ for day i to calculate the load for each hour of the day. The daily mean load is obtained from a normal distribution $N(\mathrm{E}(\bar{P}_l), \sigma_l)$ where $\mathrm{E}(\bar{P}_l)$ is the expectation value of the daily mean load and σ_l is the standard deviation of the daily mean load. The electrical load is simulated with $\mathrm{E}(\bar{P}_l) = 2.6$ MW and $\sigma_l = 0.52$ MW.

Electricity prices are shown in Figure 60 and are for simplicity chosen to be equal for all days. The mean spot price in the base-case is set to 30 $/MWh. As a comparison, the average spot price in the Nordic power market in year 1996 and year 2000 were 254 NOK/MWh and 103 NOK/MWh,

respectively [102] (1$ ≈ 7 NOK in January 2004). Moreover, the variations in simulated spot price during the day are chosen to be higher than observed in the market today. The simulated average price for purchase of electricity in the regulating market is 25% higher than the spot price, and the average price for sales is 10% lower than the spot price. These values are partly based on [96], assuming a relatively high penetration of wind power in the Nordic market.

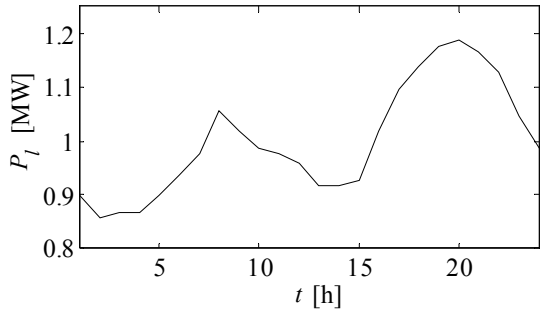

Figure 59. Normalized daily load curve.

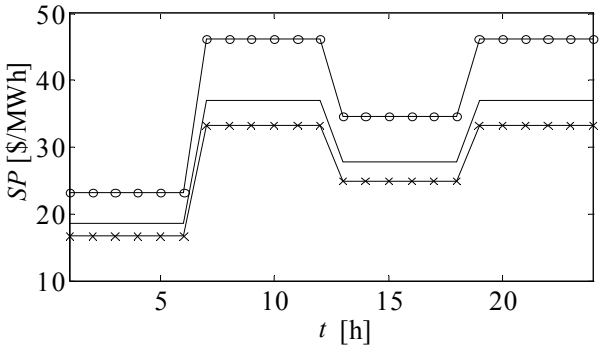

Figure 60. Simulated time series for spot price (-), price for purchase of electricity in the regulating market (o) and price for sale of electricity in the regulating market (x).

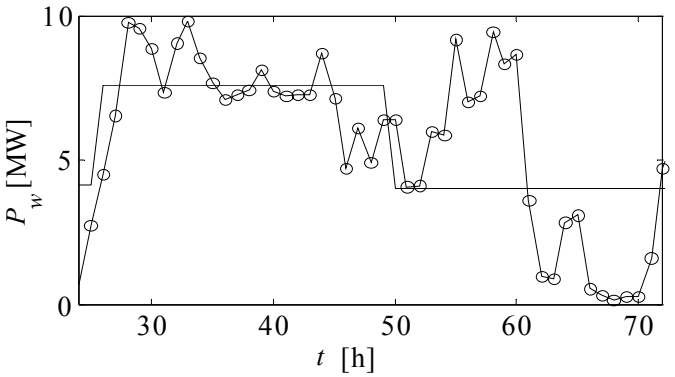

Figure 61. Actual P_w (o) and forecasted $\hat{P}_w$ (-) wind power generation.

5.4.1 Demonstration of daily operation

The scheduling and operation strategy is demonstrated by presenting a 48-hour simulation run of the base case. Forecasted and actual values of hourly wind power generation are shown in Figure 61.

Figure 62 displays the scheduled and actual power export. The plant manages to follow the schedule most of the time except for some hours at the start and end of the simulation period. The discrepancy can be understood by looking at Figure 63, where the estimated and actual storage levels are plotted. At the start and end of the period, the actual storage level is empty for a longer period than estimated. For those hours, the storage cannot compensate if the wind power generation is lower than predicted. Moreover, the actual power export also deviates from the schedule for t=55. The reason for this discrepancy is that the power capacity of the storage is too low to compensate for the wind-forecast error in that hour.

It is important to obtain a good estimate of the initial storage level used in the optimization routine. If the actual storage level is higher than the estimate, the storage can reach its maximum value too early. Likewise, if the storage level is lower than the estimate, the storage can be discharged too early. The latter is observed in Figure 63, where the estimated storage level at the start of day two (t=49) is higher than the actual value. This causes a full discharge of the storage at the end of the period one hour earlier than estimated, and system operation becomes less flexible than expected.

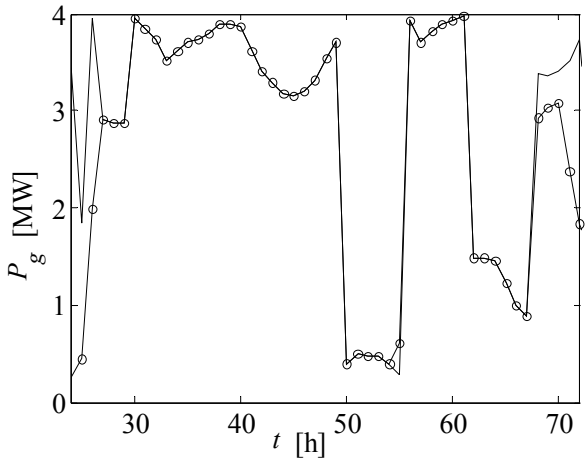

Figure 62. Actual power export P_g (o) and scheduled power export P_{sch} (-).

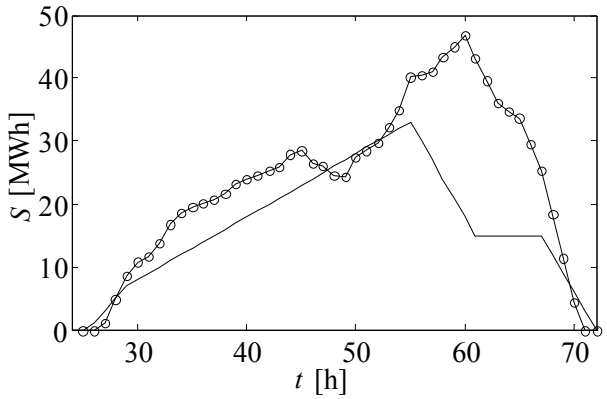

Figure 63. Actual storage level S (o) and estimated storage level $\hat{S}$ (-).

5.4.2 Simulation results

A simulation study has been carried out to gain knowledge about the impact of storage design and wind forecasting error on the performance and economics of the system. The time step is one hour and the length of the time series is 8760 hours, i.e. one year. The parameter values in Table 18 are used as a base case. It should be noted that the modeling method of wind speed and load described above does not take into account seasonal variations. At typical wind farm sites in Norway, there is a close match between the seasonal domestic electricity demand and wind energy [90]. Therefore, the error is assumed to be small in this case where the average wind power output is relatively close to the average demand.

Results from simulation runs with different storage parameters P_s^{max} and S^{max} are presented in Table 19. The relative schedule deviation P_{dev}/P_{sch} varies from 3% to 11% for the largest and smallest storage system, respectively. Thus, unpredictable variations in wind power generation are smoothed by the storage most of the time. The ratio P_d/P_w is a measure of the energy loss due to grid constraints, since the dump load is only used when the net local generation exceeds the line capacity. The relative usage of the dump load is low for all sizing alternatives, although there is a clear correlation with S^{max}. A two-fold increase in energy capacity results in a four-fold reduction of dumped wind energy. Moreover, an interesting effect is observed when comparing the different values of P_d/P_w for S^{max} = 50 MWh. The usage of the dump load actually increases slightly for increasing power capacity, although the opposite could be expected because the ability of the storage to consume excess power also increases. On the other hand, with a higher power capacity it is possible to store more energy during off-peak periods. Consequently, the storage will be completely filled more

often. This situation is undesirable, but can be avoided by adding a limitation on the available power capacity in the scheduling routine.

Table 19. The impact of storage sizing on the performance and economics of the system. AR is annual revenue

Storage sizing		**Results**		
P_s^{max} (MW)	S^{max} (MWh)	P_{dev}/P_{sch} (%)	P_d/P_w (%)	AR (Mill. $)
4	50	11.2	4.7	1.059
4	100	10.2	1.2	1.090
4	150	10.1	0.4	1.096
6	50	7.6	4.8	1.062
6	100	4.9	1.2	1.097
6	150	4.8	0.4	1.101
8	50	6.6	4.8	1.064
8	100	3.5	1.2	1.099
8	150	3.2	0.4	1.104

Table 19 shows that we obtain higher annual revenue by increasing the power and energy capacity of the storage, as expected. On the other hand, the storage device is then likely to be more expensive, which is particularly true for fuel cell systems. Finding an appropriate size of the storage is not only important from an operation point of view but is also of great economic importance due to potential high investment costs. Figure 64 displays the duration curves for charging power, discharging power and storage level, which provides useful information about the utilization of the storage device. It is evident from the charging and discharging curves that a storage unit with separate charging and discharging devices (for instance an electrolyzer and a fuel cell) will have an undesirable low utilization of the total installed capacity. It is interesting to notice the difference between the charging and discharging curve. We see that the charging power is generally higher than the discharging power, which is due to the storage losses. Consequently, the capacity of the fuel cell should be considered to be lower than the electrolyzer capacity for a hydrogen storage system.

The usage of the total energy capacity is also relatively low, as can be seen from the duration curve for storage level in Figure 64. This is beneficial from an operation point of view, since a full storage increases the risk for distribution line overload. In the case of no grid constraints, the required energy capacity would be considerably lower. Moreover, the duration curve also shows that the storage is empty for some periods. As this reduces the flexibility of the storage operation, one should consider setting the minimum allowable storage level in the scheduling routine higher than zero.

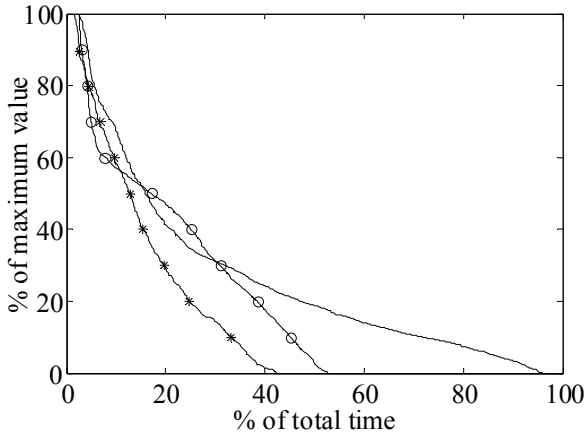

Figure 64. Duration curves for charge (o), discharge (*) and the storage level (-) of the energy storage device. The base case parameters are used for the simulation.

An essential parameter in energy storage design is the round-trip efficiency η_{rt}. The ability to take advantage of electricity price variations is in particular dependent on the storage losses. Consequently, if the storage efficiency is low, the storage will only be used to prevent overloading of the line during periods of high wind speed. This is illustrated in Figure 65, where the utilization factor of the distribution line is plotted as a function of the round-trip storage efficiency. It is clear that the utilization of the power line decreases significantly for low values of η_{rt}. Figure 65 also shows the influence on the annual revenue. A sensitivity analysis gives that 1% improvement in the storage efficiency will lead to about 0.3% higher annual revenue.

The economic value of accurate wind forecasts is illustrated in Table 20. As expected, the revenue is highest for perfect forecasting, since in that case all the energy could be traded in the spot market. As the forecasting error increases, it becomes more difficult to follow the schedule during on-line operation. Hence, more energy must be traded in the regulating market, and the revenue is reduced according to the price curves in Figure 60. This is particularly true when employing the persistence method of forecasting, which is to use the latest measured wind speed as a forecast for all hours in the scheduling period. The persistence method gives RMSE = 5.6 m/s for the wind series used here. Thus, as the forecasting uncertainty increases, it becomes more and more difficult to use the energy storage for exploiting the price variations at the same time as imbalance costs are minimized. If the wind forecasts were poor, it would be better to trade the expected wind power generation in the spot market and use the energy storage to compensate for imbalances.

Table 20. The impact of wind forecast error on annual revenue and schedule deviations.

RMSE (m/s)	0.0	2.5	3.0	3.6	5.6
AR (Mill.$)	1.123	1.097	1.064	1.040	0.931
P_{dev}/P_{sch} (%)	0.0	4.9	12.4	16.9	38.4

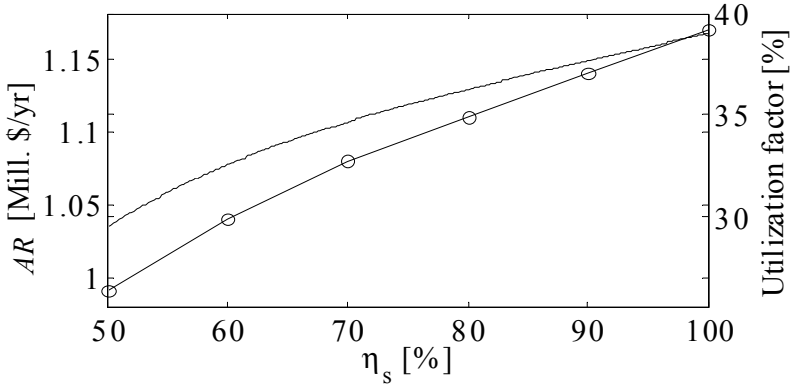

Figure 65. Annual revenue AR (o) and the utilization of P_s^{max} (-) as functions of electrical energy storage efficiency η_{rt}.

5.4.3 Investment potential

The simulation results show that with properly sized energy storage, it is possible for owners of wind power plants to take advantage of hourly price variations in the spot market. The results obtained from the simulations should ultimately be used as a part of an economic assessment, where also investment costs are considered. It is also interesting to compare energy storage with grid reinforcements in areas where the wind power potential exceeds the capacity of the existing network. The annual revenue for the base case with energy storage is 1.1 Mill.$. For comparison, simulation of the system with a new parallel line instead of energy storage gives a yearly revenue of $1,000,000.

The investment potential of energy storage as an alternative to grid reinforcements can be roughly estimated by using the following formula:

$$IP = \frac{AR(wind + storage) - AR(wind + line)}{a_{r,Y}} \tag{5.20}$$

where $a_{r,Y}$ is the annuity factor and AR is the annual revenue. By using equation (5.20) with 7% interest rate and a period of analysis of 20 years, energy storage would be the most economic solution if the difference in

investment cost between energy storage and the new line is less than IP = \$1,000,000. Present cost estimates [95] indicate that electrochemical energy storage systems are likely to be more expensive than grid reinforcements, at least in the near future. On the other hand, for areas where grid expansions lead to unwanted interference with the local environment, energy storage should be considered as a reasonable way to increase the penetration of wind power. Another alternative is to reduce the power output of the wind farm in periods with high wind speed and low load by either shutting down units or downregulating the output. For the system studied here, such a strategy without the usage of energy storage would give yearly revenue of \$900,000 Mill. The energy loss due to downregulation was found to be 16%. A rough estimate of the break-even cost of the energy storage as an alternative to downregulation of wind power is in this case \$15/kWh and \$100/kW. This is lower than the estimated investment costs used in the previous chapter (see Table 16). In a market with higher imbalance costs, the energy storage alternative could turn out to be more attractive.

5.5 Improvement of the operation strategy by stochastic dynamic programming

During the on-line operation, schedule deviations are traded in the regulating market. In the model, the regulating market is represented by average penalties that reflect the cost of downregulating and upregulating conventional power plants. The on-line operation strategy described in section 5.3 was to control the charging and discharging of the energy storage such that schedule deviations were minimized. Here, an extended approach is introduced and briefly discussed.

The generation scheduling is still derived by using the DP-algorithm described in section 5.3 . The new approach is to consider generation uncertainty in the on-line operation problem and to use information of expected future wind speed to obtain an improved operation strategy. This is achieved by employing a Stochastic Dynamic Programming (SDP) algorithm, which returns the optimal storage operation for all possible outcomes of wind power generation during on-line operation. Depending on the actual wind power output and storage level, it may be profitable to allow for deviations from the scheduled power export in some periods to increase the profits at a later stage. The benefit of SDP is that it gives a feedback control of the system, in contrast to a predefined "follow the schedule"-strategy. The optimum storage operation is derived in the form of a "look-up table" for the hourly values of wind power generation and energy storage level. Any application of the method requires that the standard deviation of the generation forecast is known with sufficient accuracy. Bakirtzis and

Gavanidou have earlier developed a similar method for autonomous systems comprising of solar power, wind power, battery storage, diesel generators and stochastic demand [103].

The SDP-algorithm is based on [103, 104] and the DP-algorithm described in 5.3.2 . Wind power is taken as a random variable which is discretizied into a specified number of levels. We define P_w^j as the wind power output related to level *j*. In the DP-formulation, we used the notation *F**(*t*,*k*) for the profit obtained by optimal operation from time step *t* to t_{end}. Since the wind power is treated as a stochastic parameter in the SDP-formulation, we must replace the deterministic profit with the expected profit:

$$\mathrm{E}\left[F^*(t,k)\right] = \sum_j \Pr(t,j) \cdot F^*(t,k,j) \tag{5.21}$$

where Pr(*t*,*j*) is the discrete probability that the wind power output at time step *t* is equal to P_w^j where *j* is the discrete wind power level. $F^*(t,k,j)$ refers to the profit obtained from an optimal operation policy if the realization of the random variable is P_w^j at time step *t*. The optimal storage policy is expressed by the recursive formula

$$F^*(t,k,i) = \max_m \left\{ f_{oper}(t,k,m,i) + \mathrm{E}\left[F^*(t+1,m)\right] \right\} \tag{5.22}$$

where $f_{oper}(t,k,m,i)$ is the profit of operating the storage from state *k* to state *m* if the wind power level is *i* at time step *t*. The profit f_{oper} depends on the penalty for the deviation between scheduled and actual power export, and the grid losses:

$$f_{oper} = f_{reg} + f_{loss} \tag{5.23}$$

where f_{reg} and f_{loss} are defined in equations (5.11) and (5.9).

Simulation runs have been carried out to show the benefits of the improved method. Since the SDP-algorithm requires discrete values of the storage level and the stochastic wind power, some modifications have been made compared to the original case study:

- The wind power and load only occur in steps of 1 MW
- Charging and discharging efficiencies are set to 100%.

It is emphasized that these simplifications are not required for employing the SDP-algorithm, but are chosen in order to obtain fast simulation and for

demonstration of the method. The time-series for wind power generation and forecast used in the example are shown in Figure 66. By the use of the wind forecasting method proposed in section 5.3.1 , it is found that the standard deviation σ_P of wind power forecast is approximately 2 MW. The lower and upper limits of $P_w^j(t)$ are found by the 95% confidence limits of $\hat{P}_w$:

$$P_w^j(low) = \max\left[0, \hat{P}_w - 2\sigma_P\right] \tag{5.24}$$

$$P_w^j(hi) = \min\left[P_w^{max}, \hat{P}_w + 2\sigma_P\right] \tag{5.25}$$

taking into account that the wind power cannot obtain negative values or exceed the rated power. The method of generating the discrete probability distribution of wind power is based on [103].

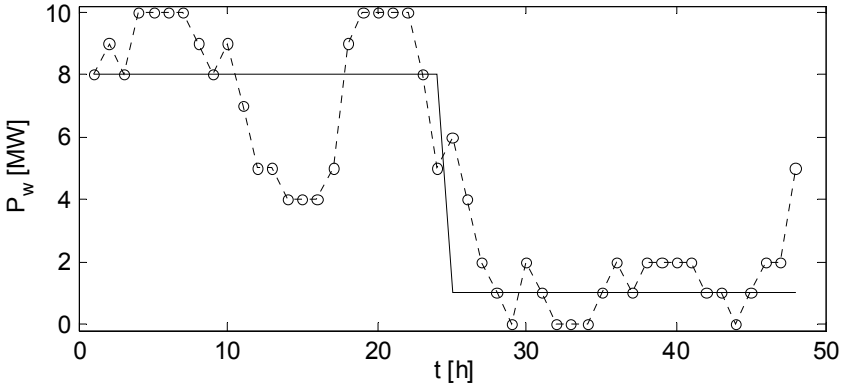

Figure 66. Actual P_w (o) and forecasted $\hat{P}_w$ (-) wind power generation.

Figure 67 shows a comparison between the original operation strategy and the SDP-strategy. In the first part of the simulation period, the power export is equal to the grid capacity for both operation strategies, because the wind power generation is very high. As the wind power decreases, the power export becomes different for the two strategies. For the original operation strategy, the energy storage is operated in order to follow the scheduled power as close as possible. Only some small deviations are observed at t = 32-36 h. For the SDP-strategy, on the other hand, we see that the net power export switches from 4 MW to –4 MW earlier that scheduled (t = 22-23 h). This is due to increased charging of the storage, although such a strategy leads to higher imbalance costs. The interesting result is that it is beneficial to discharge the "extra" stored energy at the end of the period, which increases the profit from \$15,000 to \$20,000. Figure 67 also shows how the storage level varies for the different operation strategies. We see that the storage is completely discharged at the end of the period for the-SDP strategy, in contrast to the original operation strategy.

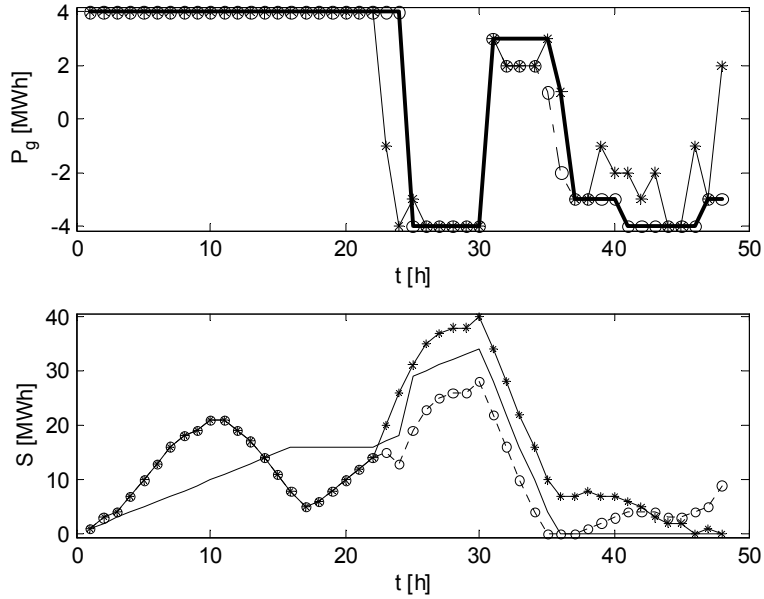

Figure 67. The upper graph shows the scheduled power export (thick dotted line), the actual power export using the SDP-strategy (*) and the actual power export using the original operation strategy (o). The lower graph shows the estimated storage level (-), the storage level using the SDP-strategy (*) and the storage level using the original operation strategy (o).

The example system has also been simulated for one month, in order to give a more correct idea of the operation benefits of the SDP-algorithm. The most important result is that the revenue is increased with approximately 5%. At the same time, the schedule deviations are increased from 12% to 29%. We recall from section 5.4 that the penalty for positive and negative deviations is 10% and 25% of the spot price, respectively. Since the penalties are relatively low, and since the generation scheduling is based on imperfect wind forecasts, the results show that it is beneficial to allow some schedule deviations. However, if the penalties approach 100% of the spot price, the SDP-strategy will approach the original operation strategy, which is to minimize schedule deviations.

The drawback of the SDP-algorithm developed here is that it requires discrete values of both the storage level and the probability density function of wind power. This leads to long computation times. Another problem is that it may be difficult to estimate the standard deviation of short-term wind forecasts. Moreover, during the on-line operation, the power output of the storage P_s is calculated from discrete values of the storage level. Since the actual values of wind power P_w take continuous values, there will be a mismatch between the optimal value of P_g calculated in the SDP-algorithm and the actual value. In order to obtain a satisfactory level of accuracy, one

may run into dimensional problems. There exist advanced methods such as stochastic dual dynamic programming [105], which avoids the tables of the conventional dynamic programming, but it is not considered in this work.

5.6 A linear programming formulation

Section 5.3.2 described the scheduling problem using a dynamic programming (DP) algorithm. The model handles non-linear equations for e.g. power losses and energy conversion efficiencies, but requires discrete states for the storage level. The advantages of DP in this case are that it is easy to implement as computer code and that non-linear equations can be included. Moreover, DP is an efficient tool for problems with long optimization horizon, since the number of calculations needed is proportional to the number of time steps. The obstacle for efficient usage of DP here is the trade-off between the number of discrete storage levels and computational efficiency, known as the "curse of dimensionality" [104]. Therefore, the scheduling problem has also been formulated as a linear programming (LP) problem, and the Matlab Optimization Toolbox [106] has been applied for solving the problem.

This section covers additional studies of using optimization methods for the scheduling problem. The analysis is limited to a 48-hour operation window, rather than e.g. yearly simulations, as this will give better insight about how the model works. The analysis identifies the importance of system parameters like storage efficiency, grid constraints and electricity price variations. Equally important is the study of the model itself, by looking at how the formulation of constraints can be varied to represent different operation regimes.

5.6.1 Basic LP-model

The LP-problem is formulated as

$$\max \; F \tag{5.26}$$

subject to the system constraints

$$A\mathbf{x} = \mathbf{b} \tag{5.27}$$

$$\mathbf{x}^{\min} \le \mathbf{x} \le \mathbf{x}^{\max} \tag{5.28}$$

where F is the objective function, A is the system matrix, $\mathbf{x}$ is the vector containing all variables and $\mathbf{b}$ is the parameter vector. The scheduling problem can then be expressed as

$$\max \; F = \sum_{t=1}^{M} e(t) \cdot \left(P_g(t) - P_{gl}(t) \right) - c_d P_d(t) \tag{5.29}$$

subject to

$$P_g(t) - P_s(t) + P_d(t) = P_w(t) - P_l(t) \quad \text{for} \quad t = 1...M \tag{5.30}$$

$$P_{gl}(t) - a_{gl}^* \cdot \left(P_{imp}(t) + P_{exp}(t)\right) = 0 \quad \text{for} \quad t = 1...M \tag{5.31}$$

$$P_g(t) + P_{imp}(t) - P_{exp}(t) = 0 \quad \text{for} \quad t = 1...M \tag{5.32}$$

$$P_s(t) + P_{ch}(t) - P_{dch}(t) = 0 \quad \text{for} \quad t = 1...M \tag{5.33}$$

$$S(t+1) - S(t) - \eta_{ch} P_{ch}(t) + \eta_{dch}^{-1} P_{dch}(t) = 0 \quad \text{for} \quad t = 2...M \tag{5.34}$$

$$S(t+1) - \eta_{ch} P_{ch}(t) + \eta_{dch}^{-1} P_{dch}(t) = S_1 \quad \text{for} \quad t = 1 \tag{5.35}$$

with bounds

$$0 \le P_{imp}(t) \le P_g^{max} \tag{5.36}$$

$$0 \le P_{exp}(t) \le P_g^{max} \tag{5.37}$$

$$0 \le P_{ch}(t) \le P_{ch}^{max} \tag{5.38}$$

$$0 \le P_{dch}(t) \le P_{dch}^{max} \tag{5.39}$$

$$0 \le S(t) \le S^{max} \tag{5.40}$$

Here, M is the optimization horizon, P_{imp} is power import from the grid and P_{exp} is power export to the grid. Linear grid losses are defined by the parameter a_{gl}^*. The net power generation of the storage P_s is divided into charging power P_{ch} and discharging power P_{dch}. To calculate the profit over the period, we include the income from supplying the local load:

$$\text{profit} = \sum_{t=1}^{M} \left[e(t) \cdot \left(P_g(t) - P_{gl}(t)\right) + e(t) \cdot \left(P_l(t) + a_{gl}^* P_l\right) \right] \tag{5.41}$$

5.6.2 Modeling of grid restrictions

In this section, we focus on how the grid connection model influences the operation strategy. The time series for electricity price shown in Figure 68 is the same as earlier. Wind power and electrical load are plotted in Figure 69. The grid limit is fixed to 4 MW, and the mean load is 2.6 MW. The maximum output of the wind power plant and the energy storage are both 2 MW. Furthermore, 100% storage efficiency is chosen to start with.

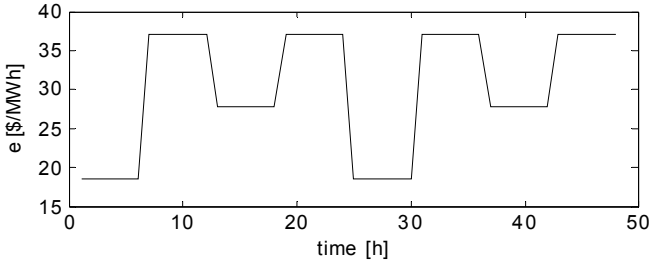

Figure 68. Electricity price.

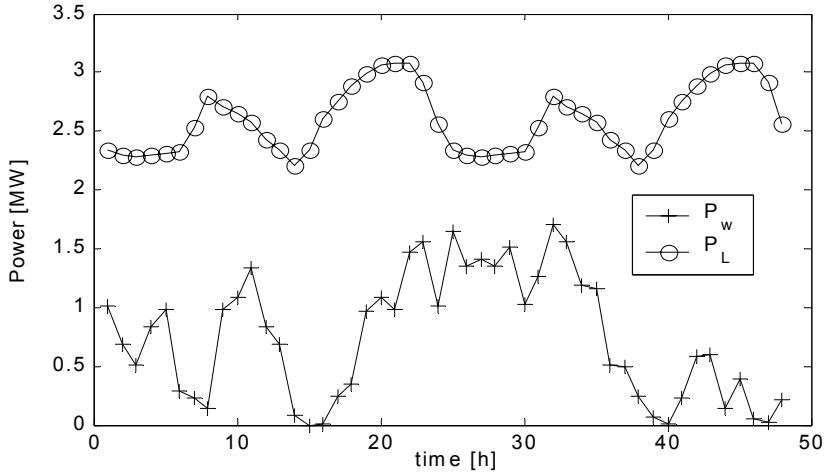

Figure 69. Wind power P_w and electrical load P_l.

CASE A: No grid losses and no restrictions on power import.

In this case, it is allowed to import power from the grid for charging of the storage. As observed by comparing Figure 68 and Figure 70, the charging and the discharging follow the electricity price, as expected. The operation of the storage is independent of the wind power generation since power line losses are neglected and the power line capacity is not reached. The profit was \$1,294. It can be observed from Figure 70 that the energy storage is discharged in the evening of both days, although the electricity price is equally high in the morning. A simulation run with 1 MW discharging capacity gave the same profit, but the storage was discharged in the morning as well as in the evening. This is shown in Figure 71. Since the same profit is obtained for the two cases, it means that there is more than one solution of the optimization problem for $P_{dch}^{max} = 2$ MW.

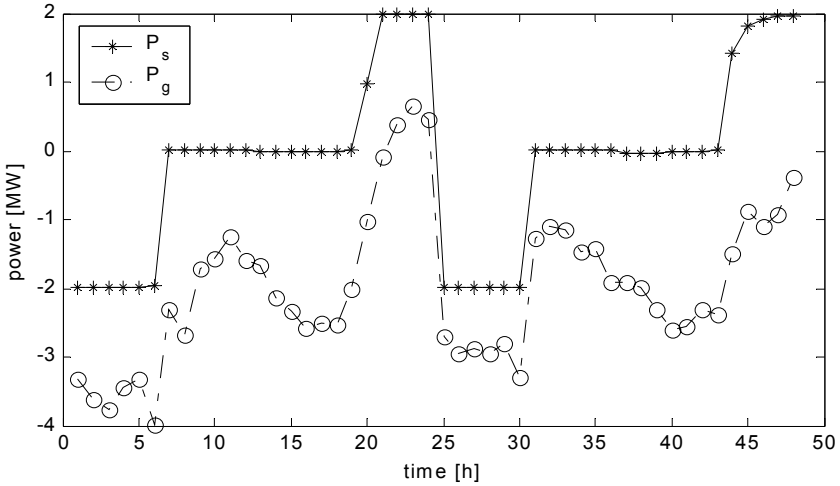

Figure 70. Power export to the grid P_g and power output of the storage P_s in Case A.

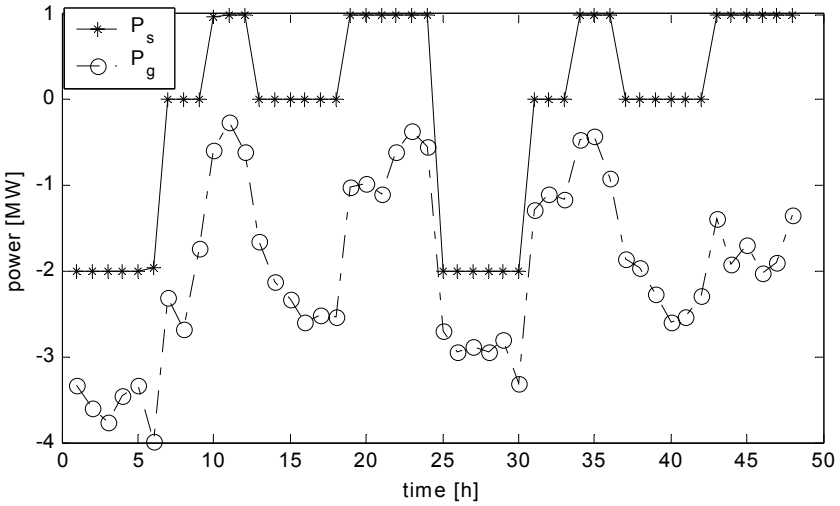

Figure 71. Power export to the grid P_g and power output of the storage P_s in Case A. The discharging capacity is 1 MW.

CASE B: No grid losses, but restrictions on power import.

In this case, the charging power is restricted by the wind power output, so that the stored electricity originates from wind power. This is modeled by replacing (5.38) with the constraint

$$0 \le P_{ch}^{max}(t) \le \min\left\{P_{ch}^{max}, P_w(t)\right\} \tag{5.42}$$

where P_{ch}^{max} is the original charging capacity and $P_{ch}^{max}(t)$ is the updated charging capacity which is dependent on the hourly wind power output. Since the grid losses are zero, it is expected that the profit will be lower than in Case A. The advantage of using this restriction is that the benefits of using energy storage for wind power are then distinguished from the benefits for the power system in general. The grid power and storage output are shown in Figure 72, and we see how the charging power is limited by the wind power output in the different time steps. The profit is now \$1,189, which is lower than in Case A (\$1,294). In the following sections, the import restriction in Case B will be used, in order to study the gain of storing wind energy exclusively.

CASE C: Linear grid losses

Grid losses are now included by setting $a_{gl}^{*} = 0.04$. This means that the grid losses are always 4% of the power input into the power line. The simulation results are shown in Figure 73. As expected, the maximum fuel cell output is reduced compared to Case B, and we see that there is no export of power to the external grid. The profit is \$1,237, which is larger than with no grid

losses. The reason is that the benefit of providing the load with locally produced power is included in the total profits. A local energy source reduces the transmission and distribution losses for supplying power to the local load and thereby also the transmission and distribution costs.

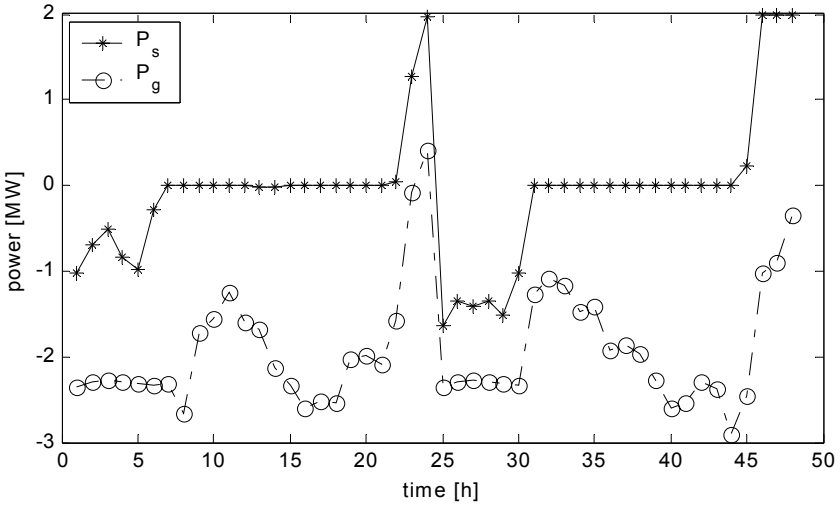

Figure 72. Power export to the grid P_g and power output of the storage P_s in Case B.

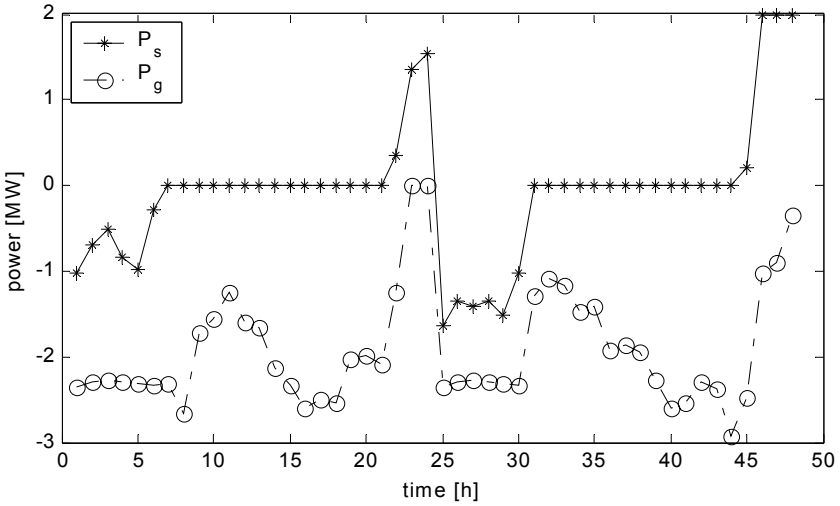

Figure 73. Power export to the grid P_g and power output of the storage P_s in Case C.

CASE D: Linearization of quadratic grid losses

In section 5.2.3 , active power losses in the network were approximated with the quadratic function $P_{gl} = a_{gl} P_g^2$. It is interesting to compare the results with this representation and the linear representation given in Case B. However, the quadratic function must be linearized in the linear

programming model. Figure 74 shows the original quadratic function using a_{gl} = 0.01 MW^{-1} and a linear representation consisting of 3 segments. When running the simulations with linearized function, the storage operation is quite different from Case C. Figure 75 shows that the magnitude of the hourly power import is lower than in Figure 73. In case D, discharging occurs during more hours than in Case C. The total profit is $1,248. It can be concluded that a linearized second order function for power transportation losses gives a smoother power output of the wind-storage system because of the incremental cost of increased losses.

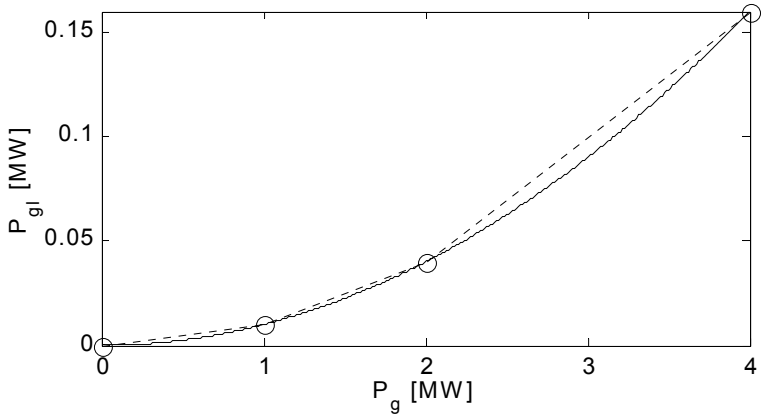

Figure 74. Quadratic power loss function and a linearization in 3 segments.

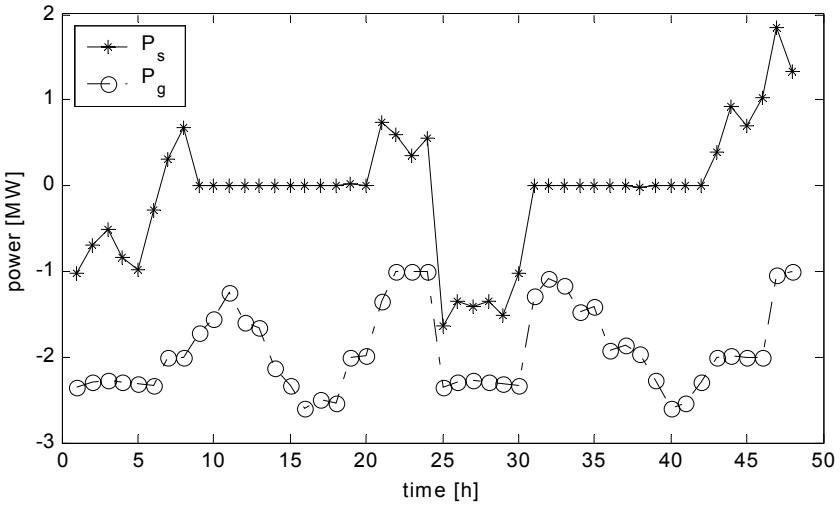

Figure 75. Power export to the grid P_g and power output of the storage P_s in Case D.

5.6.3 Smoothing of the power output

In this section, a 48-hours sample of the spot price from the European Power Exchange (EEX) has been used. The time series is shown in Figure 76. The price varies between 15 €/MWh and 65 €/MWh, which mean that an energy storage device with 75% efficiency would be attractive for price optimization. The rated power of the wind farm is set to 10 MW, and the rated power of the energy storage is set to 6 MW. Results from a 48-hour simulation run of the system are shown in Figure 77. Perfect forecasts of wind, load and electricity price are assumed. As we can see, there are large fluctuations of the power balance with the external grid, especially during the time interval t = 7 - 25. Due to the grid limit of 4 MW, the fluctuations are lower than for the unconstrained wind power output, but not much. For the system operator, it may be beneficial if the hour-to-hour fluctuations from the distributed generator are reduced. Another aspect is the dynamic characteristics of the storage device. If the regulating process is slow relative to the time stepsize, it could be difficult to e.g. switch from –4 MW to 4 MW output within a time step.

In order to put limitations on power fluctuations, the following restriction has been included in the LP-model:

$$\left|P_g(t) - P_g(t-1)\right| \leq \alpha \quad \text{for} \quad t = 2...T \tag{5.43}$$

where α is the maximum difference between the power sales for two following time steps. Thus, α can be used for regulating the output of the wind-storage system. The absolute value in (5.43) is reformulated in the LP model by using the variables P_{imp} and P_{exp}. Figure 78 illustrates this operation principle. Simulations with three different values of α are presented.

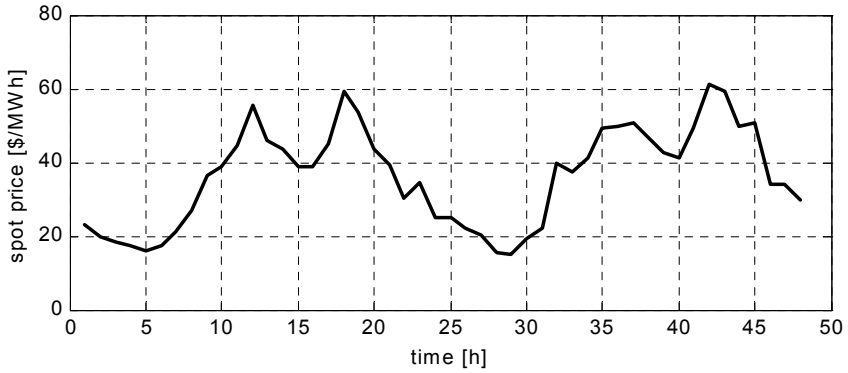

Figure 76. Electricity price sample from the German EEX-market. The price is converted from €/MWh to $/MWh.

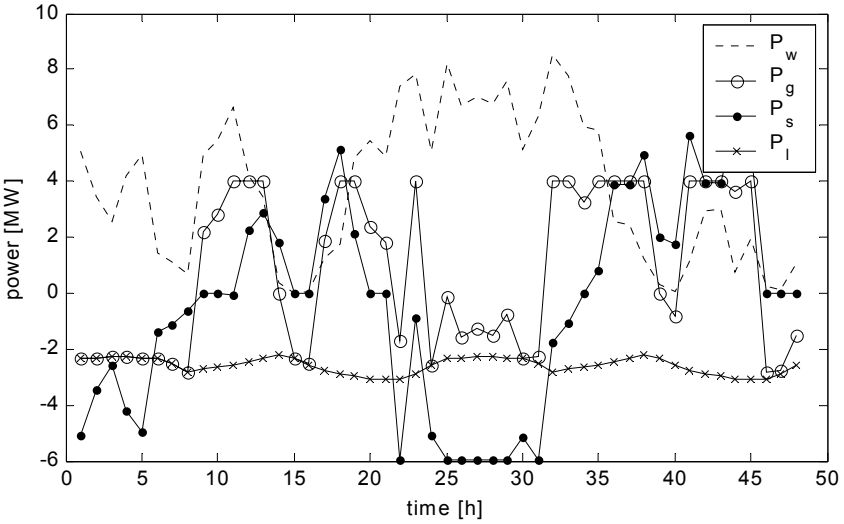

Figure 77. Power balance in the system. P_w is wind power, P_g is net power export to the grid, P_s is net power output of the storage, P_l is load.

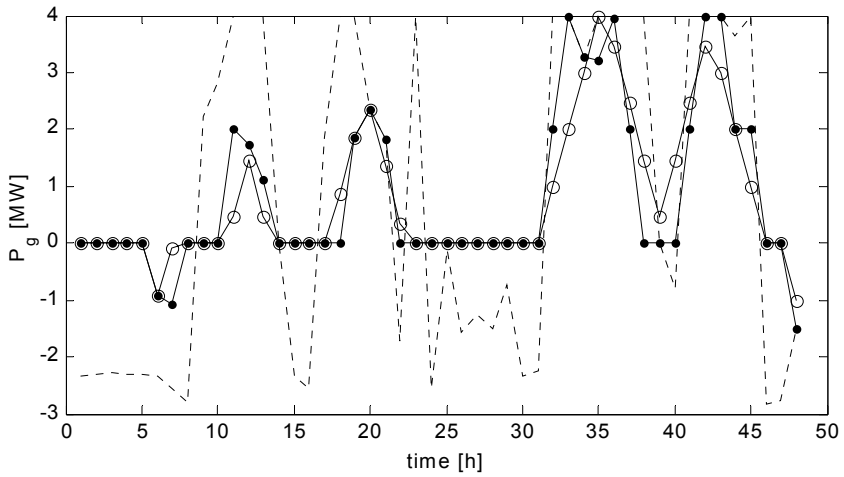

Figure 78. The effect of varying the power-smoothing parameter α. (--) : α=infinity, (•) : α=2 MW, (o) : α=1 MW. The profit is decreasing; $7,342 - $6,734 - $6,645.

5.6.4 Control of the wind power output

As in the previous section, the wind power rating and grid capacity are set to 10 MW and 4 MW, respectively. Since the wind power rating is 2.5 times the grid capacity, congestion situations are likely to occur. This can happen if the storage is completely filled up, or if the power rating of the storage is too low. The simplest way to model this situation is to include a controllable dump-load, which can be switched on when needed. This could for instance

be an electrical heater. Some wind turbine types have the possibility of reducing the output by blade pitching. In the model, these control mechanisms are equivalent. Another method is to shut down individual wind turbines when it is a danger for overloading the network. In Figure 79, the difference between the control mechanisms is illustrated. The power rating of the storage is set to only 1 MW here, so the wind power output is forced to be reduced at some hours. Moreover, the rating of individual wind turbines is chosen to be 2 MW. The profit is 2.5% lower for the shutdown-alternative.

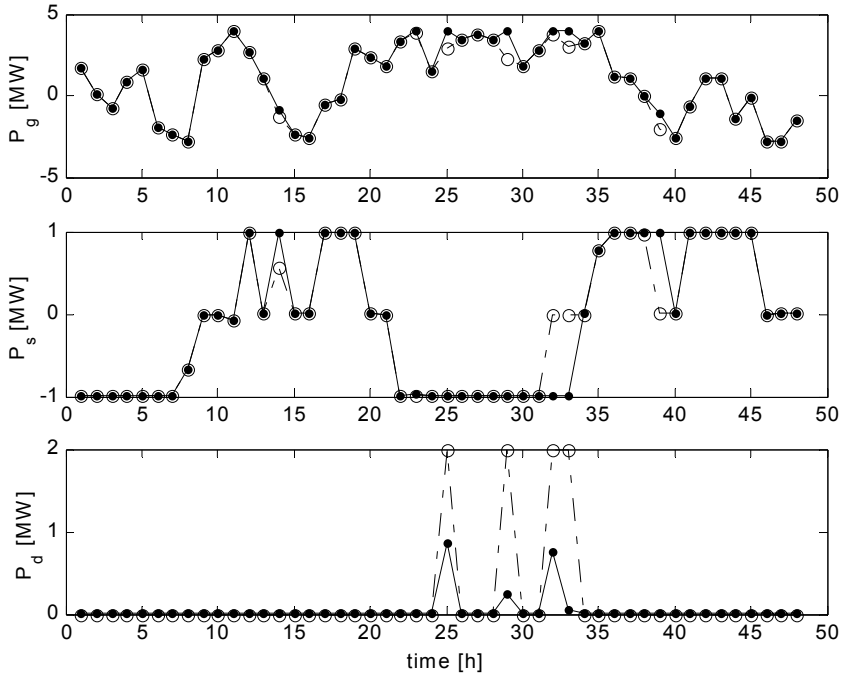

Figure 79. Simulations with dumping of excess wind power (•) and with shutdown of individual wind turbines (o). The upper graph shows net grid power P_g. The middle graph shows net storage output P_s. The bottom graph shows the dissipated wind power P_d for the two control mechanisms.

5.6.5 Storage efficiency

The ability of the energy storage to exploit spot price differences depends on the magnitude of price variations relative to the round-trip efficiency of energy storage η_{rt}. The relation between the prices in two hours, t_1 and t_2, must be at least $1/\eta_{rt}$ in order to make profits by storing wind power at t_1 and release the stored energy at t_2. In Figure 80, the impact of storage efficiency is illustrated. We see that the storage is not in use for η_{rt} lower than = 24%. At this point, the storage "moves" wind energy from the lowest

price hour to the highest price hour. This happens exactly at $\eta_{rt} = e^{min}/e^{max}$, as expected. The effect of limited grid capacity (4 MW) is also shown in the figure. In this case, the storage is used even for η_{rt} = 1% because of the grid limit. Therefore, the power export increases slowly until the hour is reached when wind power is moved from low price to high price. It is noticeably that at this point, the power export suddenly drops because of the increased usage of the storage, but the profit is higher because of the price difference.

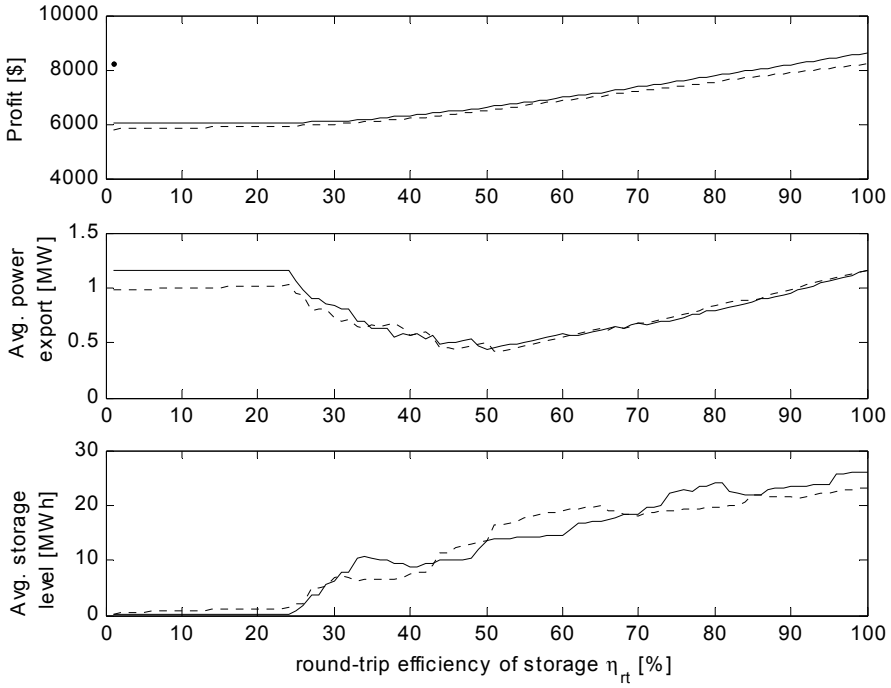

Figure 80. Simulations with increasing storage efficiency for a case with no grid restrictions (solid line) and a case with grid limit of 4 MW (dotted line). The upper graph shows the profit, the middle graph shows the exported power to the grid and the lower graph shows the average energy storage level.

5.7 Conclusions

A method for scheduling and operation of a wind power plant with energy storage in a market system has been presented. The method is suitable for any type of electrical energy storage and is also useful for other intermittent energy resources than wind. By implementing the method in a computer simulation model, valuable knowledge about the impact of energy storage sizing on system performance is obtained. Simulation results of a case study show that with properly sized energy storage, owners of wind power plants can take advantage of variations in the spot price of electricity, thus increasing the value of wind power in electricity markets. In addition, energy storage makes it possible to reduce imbalances due to wind

forecasting errors and to reduce dumping of wind energy due to grid constraints. For a case with 10 MW wind power capacity, 2.6 MW average local load and 4 MW grid capacity, an energy storage system rated at 6 MW/ 100 MWh is suitable for all three purposes. Application of energy storage increased the annual revenue with 22% compared to wind only. With available technology and existing price estimates, energy storage devices such as reversible fuel cells are likely to be a more expensive alternative than grid expansions.

The short-term scheduling problem is implemented by using a general dynamic programming algorithm. It has been shown how it is possible to improve the economic gain of energy storage by taking into account the stochastic properties of wind in the operation problem. This is obtained by employing a stochastic dynamic programming formulation. For the case study, the improved operation strategy increased the annual revenue with 5%, but also caused larger deviations between actual and scheduled power export.

A modified version of the short-term scheduling model based on linear programming is also presented. It is shown how the restrictions of the optimization problem can be modified to represent different scheduling strategies and operating conditions. It is shown that the value of the distributed generation and storage system is highest in remote areas with high grid losses for import of electricity. Moreover, a sensitivity analysis of the round-trip efficiency of the energy storage has been carried out. It is shown that although large variations in electricity price makes it profitable to utilize the energy storage, the economic gain is damped by the reduced net power output due to storage losses.

6 OPTIMUM OPERATION POLICY FOR WIND-HYDROGEN ENERGY SYSTEMS

6.1 Introduction

In chapter 5, an operation strategy for energy storage in connection with wind farms in a market system was presented. A Dynamic Programming algorithm was used for the daily scheduling. The on-line operation strategy was to control the charging and discharging of the energy storage in order to follow the scheduled power export. An extension of the method is presented in this chapter. Hydrogen is used as the storage medium, and a hydrogen load is included. In the example considered here, no other sources of hydrogen are present. Thus, the challenge is to find the optimal operation strategy, given that the hydrogen storage system always must be able to supply hydrogen to the load. In addition, an oxygen load is included. The chapter describes a methodology for the on-line operation of such a system, using principles from optimization theory and model predictive control. Examples on the utilization of the method are given both for grid-connected and isolated systems.

The model presented in this chapter is a modified version of the model described in "Optimal Operation of Hydrogen Storage for Energy Sources with Stochastic Input", which was presented at the 2003 IEEE Bologna Power Tech Conference. The paper is given in Appendix B.

6.2 Method

6.2.1 Description of the concept

The distributed wind-hydrogen system is shown in Figure 81. The wind power plant is connected to a local grid, which feeds electricity to one or more consumers. The wind power plant is the main energy source for electricity and heat, as well as for splitting water into hydrogen and oxygen

in the electrolyzer. A fuel cell converts hydrogen back to electricity, also producing heat that can be utilized. Several backup solutions can be considered, depending on the location. In a remote area with no grid-connection, a short-term energy storage device and/or a backup generator are required. If the electricity consumers are connected to the utility, the grid can be used for both power export and import. The value of interacting with the grid is determined by the electricity market conditions. If the installed wind generation capacity is larger than the grid limit it may sometimes be necessary to dump excess power or decrease the output of the generator.

The hydrogen storage system consists of power conversion systems, electrolyzer, fuel cell, hydrogen compressors and high-pressure storage tanks. Alternatively, the electrolyzer and fuel cell can be combined in a reversible fuel cell. A hydrogen load is included, which for instance can be a hydrogen filling station for hydrogen-fueled vehicles or ships. The oxygen produced from electrolysis is a by-product, which is either vented into the air or compressed and stored for later usage.

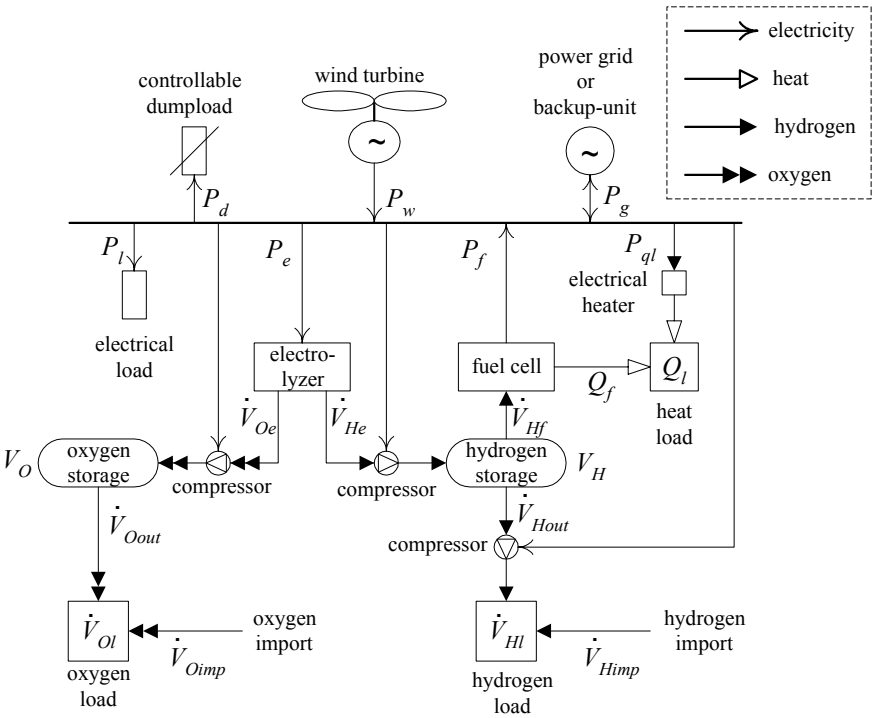

Figure 81. Schematic figure of the distributed energy system. Power export corresponds to positive values of P_g while power import corresponds to negative values of P_g.

6.2.2 Operation strategy

Power export and import are traded in a day-ahead electricity market. A simple market model is employed here. Each day at a specified hour t_{sch}, the owner of the plant establishes a schedule of the net power export to the grid for each hour the day ahead. The scheduled power export is traded at the day-ahead market. This generation scheduling is based on forecasts of electricity price, loads and wind power generation for the next day. Due to unforeseen wind and load variations, and limited regulating flexibility of the electrolyzer and the fuel cell, there would be periods during the real-time operation with imbalances between the actual and scheduled export. Depending on the electricity market conditions, imbalances between the measured export and contracted power result in a penalty which reflects the regulating costs of other plants. In the text, the contracted power is referred to as the scheduled power export. Moreover, the regulating costs of other plants are referred to as imbalance costs. For each hour, the scheduled power export, imbalance costs, and new forecasts of loads and generation are taken into account for finding the optimal operation of the electrolyzer and the fuel cell. The operation strategy is illustrated in Figure 82.

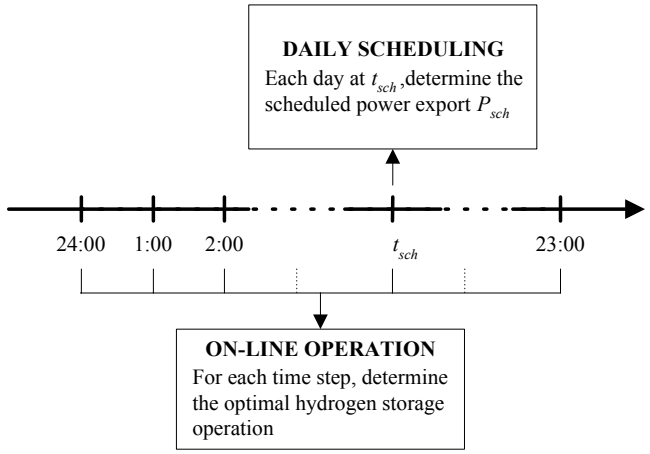

Figure 82. Illustration of the operation strategy.

6.2.3 Plant model

A mathematical model based on Linear Programming has been developed based on the proposed operation strategy. The system equations consist of linear equations for power, heat and mass balances, and the main symbols used in the equations are displayed in Figure 81. The storage balances for time step *t* are expressed as:

$$V_H(t+1) - V_H(t) = \left(\dot{V}_{He}(t) - \dot{V}_{Hf}(t) - \dot{V}_{Hout}(t)\right) \cdot \Delta t \quad (6.1)$$

$$V_O(t+1) - V_O(t) = \left(\dot{V}_{Oe}(t) - \dot{V}_{Oout}(t)\right) \cdot \Delta t \quad (6.2)$$

where $V_H(t)$ refers to the hydrogen storage level at the beginning of time step t. The hydrogen and oxygen load are covered either by extracting gas from the storage or by import:

$$\dot{V}_{Hout}(t) + \dot{V}_{Himp}(t) = \dot{V}_{Hl}(t) \quad (6.3)$$

$$\dot{V}_{Oout}(t) + \dot{V}_{Oimp}(t) = \dot{V}_{Ol}(t) \quad (6.4)$$

Hydrogen and oxygen gas are produced in the electrolysis process, with the following relations:

$$P_e(t) = \eta_e \cdot \dot{V}_{He}(t) \quad (6.5)$$

$$\dot{V}_{Oe}(t) = r \cdot \dot{V}_{He}(t) \quad (6.6)$$

where r is the amount of oxygen produced per unit of hydrogen, and η_e is a linear approximation of the electrical efficiency of the electrolyzer (kWh/Nm^3), taking into account stack losses and power conversion losses. Hydrogen and oxygen are compressed and then stored in pressurized tanks. For the usage of hydrogen in vehicles, it may be necessary to compress the stored hydrogen to a higher pressure at the filling station. The total compression power becomes

$$P_c(t) = \eta_{Hc} \cdot \dot{V}_{He}(t) + \eta_{Hc2} \cdot \dot{V}_{Hout}(t) + \eta_{Oc} \cdot \dot{V}_{Oe}(t) \quad (6.7)$$

where η_{Hc} and η_{Oc} are the efficiencies of the compressors between the electrolyzer and the hydrogen and oxygen tanks, respectively. The efficiency of the compressor used for providing the necessary pressure to the filling station is denoted η_{Hc2}.

Similarly to the electrolyzer power, the fuel cell power is expressed by

$$P_f(t) = \eta_f \cdot \dot{V}_{Hf}(t) \quad (6.8)$$

Depending on the type of fuel cell and the operating conditions, it may be possible to utilize heat from the fuel cell process. Combined heat and power from low-temperature PEM fuel cells (PEM: Proton Exchange Membrane) has been given increasing attention the last years [107]. The heat balances in the model are

$$Q_f(t) = \eta_{fq} \cdot \dot{V}_{Hf}(t) \tag{6.9}$$

$$Q_f(t) + \eta_{ql} \cdot P_{ql}(t) - Q_d(t) = Q_l(t) \tag{6.10}$$

where η_{fq} is the heat efficiency of the fuel cell and η_{ql} is the efficiency of electrical heating. If the usable heat production in the fuel cell exceeds the heat demand, it is assumed that excess heat can be dumped, given by Q_d. In real systems, the relationship between heat Q_f and hydrogen flow $\dot{V}_{Hf}$ is not linear [47]. Nevertheless, a linear equation will give useful information about the potential advantages of increasing the total fuel cell efficiency and is therefore assumed to be sufficient at this stage of modeling.

The power balance is

$$P_f(t) - P_e(t) - P_g(t) - P_{ql}(t) - P_d(t) - P_c(t) = P_l(t) - P_w(t) \tag{6.11}$$

where dumping (or dissipation) of excess wind power P_d is necessary if the local power surplus exceeds the transmission capacity to the external grid. Grid losses are positive for both power import and power export and are calculated from the equations

$$P_{gl}(t) = a_{gl}^{*} \cdot \left(P_{imp}(t) + P_{exp}(t) \right) \tag{6.12}$$

$$P_g(t) = P_{exp}(t) - P_{imp}(t) \tag{6.13}$$

where P_{imp} is power import from the grid and P_{exp} is power export to the grid. A linear approximation of line losses is given by the parameter a_{gl}^{*}. The power exported to the external grid P_g can thus have positive or negative values, which represent export respectively import of power. It is possible to simulate isolated operation by fixing P_{exp} to zero. In this mode, power import P_{imp} is equivalent to the power generation of a backup unit, for example a diesel generator.

Some of the variables in the plant model are restricted by upper and lower bounds:

$$V_H^{min} \le V_H(t) \le V_H^{max} \tag{6.14}$$

$$V_O^{min} \le V_O(t) \le V_O^{max} \tag{6.15}$$

$$P_e^{min} \le P_e(t) \le P_e^{max} \tag{6.16}$$

$$P_f^{min} \le P_f(t) \le P_f^{max} \tag{6.17}$$

$$P_g^{min} \le P_g(t) \le P_g^{max} \tag{6.18}$$

$$0 \le P_{exp}(t) \le P_g^{max} \tag{6.19}$$

$$0 \le P_{imp}(t) \le -P_g^{min} \tag{6.20}$$

where $-P_g^{min}$ is equal to P_g^{max} in grid-connected mode and equal to the capacity of the backup generator in isolated operation mode. The value of P_g^{max} is set to zero in isolated mode.

A special case is the minimum bounds of electrolyzer power and fuel cell power. With present technology, these devices have a minimum operating point ranging from 10% to 50% of nominal power, depending on the manufacturer. In periods when hydrogen production is not necessary, the electrolyzer must either be switched completely off or be running at minimum power. The on/off-switching is modeled using binary variables:

$$P_e^{min}(t) \cdot \gamma_e(t) \le P_e(t) \le P_e^{max}(t) \cdot \gamma_e(t) \tag{6.21}$$

$$P_f^{min}(t) \cdot \gamma_f(t) \le P_f(t) \le P_f^{max}(t) \cdot \gamma_f(t) \tag{6.22}$$

$$\gamma_e(t) \in \{0,1\} \tag{6.23}$$

$$\gamma_f(t) \in \{0,1\} \tag{6.24}$$

where γ_e and γ_f represents the on/off state of the electrolyzer respectively the fuel cell. A simple method for solving the binary variable problem is employed. In the linear programming formulation used here, all variables are represented as continuous variables. If the optimum electrolyzer power is found to be between zero and the minimum power level, the electrolyzer power is rounded to the nearest of these values, and the optimization is carried out once more with fixed electrolyzer power. The fuel cell power is modeled in the same way.

6.2.4 Market model

The wind-hydrogen system is operating in two electricity markets, the day-ahead spot market and the regulating power market. The profit from the spot market is given by the spot price and the scheduled power export:

$$f_{spot}(t) = e(t) \cdot P_{sch}(t) \tag{6.25}$$

which is fixed before the actual day. Grid losses are assumed to be paid by spot price:

$$f_{loss}(t) = -e(t) \cdot P_{gl}(t) \tag{6.26}$$

During real-time operation, any schedule deviations must be settled in the regulating market:

$$f_{reg}(t) = e_{reg}(t) \cdot \left(P_g(t) - P_{sch}(t) \right) \tag{6.27}$$

where

$$e_{reg}(t) = \begin{cases} (1 + c_{up}) \cdot e(t) & , \left(P_g(t) - P_{sch}(t) \right) \le 0 \\ -(1 - c_{dw}) \cdot e(t) & , \left(P_g(t) - P_{sch}(t) \right) \ge 0 \end{cases} \tag{6.28}$$

is the imbalance cost due to upregulation or downregulation of other generators in the power system. The regulating market is simplified by introducing constants c_{up} and c_{dw} for the cost of upregulation or downregulation, so that the imbalance cost is proportional to the spot price. In the LP model, the imbalance between actual and scheduled export is represented by

$$P_{dw}(t) - P_{up}(t) = P_{exp}(t) - P_{imp}(t) - P_{sch}(t) \tag{6.29}$$

so that upregulation of other generators P_{up} is distinguished from downregulation P_{dw}. A power market with negligible imbalance costs can be simulated by omitting the scheduling and setting $P_{sch}(t) = 0$ for all t. Imbalance costs are then omitted by setting c_{up}=0 and c_{dw}=2 in (6.28) so that the profit of operating in the market at time step t becomes $e(t) \cdot P_g(t)$.

A variation of the market model can be defined for isolated systems by replacing the time series for electricity price with a cost function of a backup generator. In the model presented here, generation scheduling is omitted in isolated mode. By assuming constant, linear generation costs e_{bg}, the (negative) profit of operating the isolated system at time step t becomes equal to $-e_{bg} \cdot P_{imp}(t)$.

If the hydrogen load or oxygen load cannot be entirely supplied by the wind-hydrogen system, it is necessary to import the gases from external sources. The profit (in this case negative) is given by

$$f_H(t) = -c_H \cdot V_{Himp}(t) \tag{6.30}$$

$$f_O(t) = -c_O \cdot V_{Oimp}(t) \tag{6.31}$$

where it is assumed that the price of imported hydrogen and oxygen is constant and that it is not possible export hydrogen or oxygen.

The upper and lower bounds of the variables introduced in the market model are

$$P_g^{min} \le P_{sch}(t) \le P_g^{max} \tag{6.32}$$

$$0 \le P_{up}(t) \le P_g^{max} - P_g^{min} \tag{6.33}$$

$$0 \le P_{dw}(t) \le P_g^{max} - P_g^{min} \tag{6.34}$$

6.2.5 State variable notation

To make the notation compact, the variables and parameters are arranged into vectors of state variables $\mathbf{x}(t)$, control variables $\mathbf{u}(t)$, dependent variables $\mathbf{w}(t)$ and time-varying parameters $\mathbf{p}(t)$. The state variables are the variables that have inter-temporal links, which are the storage levels of hydrogen and oxygen. The controllable variables are the power consumption of the electrolyzer, the power output of the fuel cell, the outflow rate of hydrogen from the storage to the hydrogen load and the outflow rate of oxygen from the storage to the oxygen load. Dependent variables are the variables that are calculated from the system equations, but do not have inter-temporal links. The time-varying parameters are the external inputs to the plant model and the market model, which comprise wind power generation, electrical load, heat load, hydrogen load, oxygen load, scheduled power export and spot price of electricity. The vectors are defined below:

$$\mathbf{x} = \begin{bmatrix} V_H & V_O \end{bmatrix}^T \tag{6.35}$$

$$\mathbf{u} = \begin{bmatrix} P_f & P_e & \dot{V}_{Hout} & \dot{V}_{Oout} \end{bmatrix}^T \tag{6.36}$$

$$\mathbf{w} = \begin{bmatrix} P_g & P_{gl} & P_{exp} & P_{imp} & P_d & Q_d & P_{dw} & P_{up} & \dot{V}_{Himp} & \dot{V}_{Oimp} \end{bmatrix}^T \tag{6.37}$$

$$\mathbf{p} = \begin{bmatrix} P_w & P_l & Q_l & \dot{V}_{Hl} & \dot{V}_{Ol} & P_{sch} & e \end{bmatrix}^T \tag{6.38}$$

By the use of this notation, the system equations and variable bounds can be reduced to the following compact form

$$\mathbf{x}(t+1) = A\mathbf{x}(t) + B\mathbf{u}(t) \tag{6.39}$$

$$C\mathbf{w}(t) = D\mathbf{u}(t) + E\mathbf{p}(t) \tag{6.40}$$

$$\mathbf{x}^{\min} \le \mathbf{x}(t) \le \mathbf{x}^{\max} \tag{6.41}$$

$$\mathbf{u}^{\min} \le \mathbf{u}(t) \le \mathbf{u}^{\max} \tag{6.42}$$

$$\mathbf{w}^{\min} \le \mathbf{w}(t) \le \mathbf{w}^{\max} \tag{6.43}$$

where the matrixes A, B, C, D and E are given by

$$A = \begin{bmatrix} 1 & 0 \\ 0 & 1 \end{bmatrix} \tag{6.44}$$

$$B = \begin{bmatrix} (-\frac{\Delta t}{\eta_f}) & \frac{\Delta t}{\eta_e} & (-\Delta t) & 0 \\ 0 & \frac{r \cdot \Delta t}{\eta_e} & 0 & (-\Delta t) \end{bmatrix} \tag{6.45}$$

$$C = \begin{bmatrix} 1 & 0 & (-1) & 1 & 0 & 0 & 0 & 0 & 0 & 0 \\ 0 & 1 & (-a_{gl}^{*}) & (-a_{gl}^{*}) & 0 & 0 & 0 & 0 & 0 & 0 \\ 1 & 0 & 0 & 0 & 1 & (1/\eta_{ql}) & 0 & 0 & 0 & 0 \\ 0 & 0 & (-1) & 1 & 0 & 0 & 1 & (-1) & 0 & 0 \\ 0 & 0 & 0 & 0 & 0 & 0 & 0 & 0 & 1 & 0 \\ 0 & 0 & 0 & 0 & 0 & 0 & 0 & 0 & 0 & 1 \end{bmatrix} \tag{6.46}$$

$$D = \begin{bmatrix} 0 & 0 & 0 & 0 \\ 0 & 0 & 0 & 0 \\ (1+\frac{\eta_{fq}}{\eta_{ql} \cdot \eta_f}) & (-1-\frac{\eta_{Hc}}{\eta_e}-\frac{r \cdot \eta_{Oc}}{\eta_e}) & (-\eta_{Hc2}) & 0 \\ 0 & 0 & 0 & 0 \\ 0 & 0 & -1 & 0 \\ 0 & 0 & 0 & -1 \end{bmatrix} \tag{6.47}$$

$$E = \begin{bmatrix} 0 & 0 & 0 & 0 & 0 & 0 & 0 \\ 0 & 0 & 0 & 0 & 0 & 0 & 0 \\ 1 & (-1) & (-\frac{1}{\eta_{ql}}) & 0 & 0 & 0 & 0 \\ 0 & 0 & 0 & 0 & 0 & -1 & 0 \\ 0 & 0 & 0 & 1 & 0 & 0 & 0 \\ 0 & 0 & 0 & 0 & 1 & 0 & 0 \end{bmatrix} \tag{6.48}$$

6.2.6 Generation scheduling

In the generation scheduling problem, the objective is to maximize the expected profit from power trading in the day-ahead market based on forecasts of generation, loads and electricity price. The generation scheduling is performed at time step t_{sch}, which is L time steps ahead of the next day. The length of the scheduling period is M, and the scheduling problem can be formulated as

$$\max \left\{ \sum_{k=t_{sch}+L}^{t_{sch}+L+M} \left[f_{spot}\left(\hat{P}_g(k), \hat{e}(k)\right) + f_{loss}\left(\hat{P}_{gl}(k), \hat{e}(k)\right) + \ldots \right.\right. \\ \left.\left. + f_H\left(\hat{\dot{V}}_{Himp}(k)\right) + f_O\left(\hat{\dot{V}}_{Oimp}(k)\right) \right] \right\} \tag{6.49}$$

where the notation $\hat{P}_g(k)$ is used in order to distinguish a future estimated (or forecasted) value within the optimization horizon from the actual value $P_g(k)$ at time step k. The estimated values of the power export to the grid $\hat{P}_g$ for all time steps of the next day are chosen as the scheduled export P_{sch}. On compact form, the scheduling problem can be expressed as:

$$\max \left\{ \sum_{k=t_{sch}+L}^{t_{sch}+L+M} f_{sch}\left(\hat{\mathbf{w}}(k), \hat{\mathbf{p}}(k)\right) \right\} \tag{6.50}$$

subject to the system constraints

$$\hat{\mathbf{x}}(k+1) = A\hat{\mathbf{x}}(k) + B\hat{\mathbf{u}}(k) \tag{6.51}$$

$$C\hat{\mathbf{w}}(k) = D\hat{\mathbf{u}}(k) + E\hat{\mathbf{p}}(k) \tag{6.52}$$

$$\mathbf{x}^{\min} \le \hat{\mathbf{x}}(k) \le \mathbf{x}^{\max} \tag{6.53}$$

$$\mathbf{u}^{\min} \le \hat{\mathbf{u}}(k) \le \mathbf{u}^{\max} \tag{6.54}$$

$$\mathbf{w}^{\min} \le \hat{\mathbf{w}}(k) \le \mathbf{w}^{\max} \tag{6.55}$$

$$k \in [t_{sch} + L : t_{sch} + L + M]$$

where f_{sch} is given by the bracketed expression in (6.49).

6.2.7 On-line operation

In the on-line operation problem, the control sequence for a specified time horizon N is optimized for maximizing profits. The control variables are electrolyzer power, fuel cell power, the outflow rate of hydrogen from the

storage to the hydrogen load, and the outflow rate of oxygen from the storage to the oxygen load. Only the values for the first time step t in the control sequence are applied, before moving to the next time step. In the next time step, the optimization is repeated, and new values for the control variables are calculated. This method of receding-horizon strategy is known as model predictive control [108], which frequently been applied in the control of large industrial plants and especially in the chemical process industry.

During the on-line operation, the mismatch between the actual power export and the contracted power is traded in the regulating market. The profit function for on-line operation at time step t is defined as:

$$\begin{aligned} f_{oper}\left(\mathbf{w}(t),\mathbf{p}(t)\right) = f_{reg}\left(P_g(t),P_{sch}(t),e(t)\right) + f_{loss}\left(P_{gl}(t),e(t)\right) + \ldots \\ + f_H\left(\dot{V}_{Himp}(t)\right) + f_O\left(\dot{V}_{Oimp}(t)\right) \end{aligned} \tag{6.56}$$

where the individual terms are defined in (6.26), (6.27), (6.30) and (6.31). The on-line operation problem with N time steps horizon is formulated as

$$\max\left\{ f_{oper}\left(\mathbf{w}(t),\mathbf{p}(t)\right) + \sum_{k=t+1}^{t+N} f_{oper}\left(\hat{\mathbf{w}}(k),\mathbf{p}(k)\right) \right\} \tag{6.57}$$

subject to the system constraints (6.39)-(6.43) for the present time step t and the system constraints (6.51)-(6.55) for the rest of the optimization period:

$$k \in [t+1 : t+N]$$

It should be noticed that the actual parameter vector **p**(k) is used in the objective function instead of estimated values. This is because the parameters used in the objective function are the spot price $e(k)$ and the scheduled power export $P_{sch}(k)$ which both are assumed to be known for the whole optimization period. If the optimization horizon N exceeds the last hour of the next day, it will be necessary to use estimates for $e(k)$ and $P_{sch}(k)$ for the exceeding time steps.

The output of the optimization routine comprises the real-time values of the state variables, control variables and depended variables for time step t. Furthermore, the optimization routine estimates the variables for k=t+1:t+N. At the scheduling hour t_{sch}, the estimated values of the state variables at the start of the scheduling period, $\hat{\mathbf{x}}(t_{sch}+L)$, are used as inputs to the scheduling problem (6.50).

6.3 Example

An example system as shown in Figure 81 has been constructed for demonstrating the operation strategy. The parameters that were introduced in the case study in chapter 3.3 are also used here, with the addition of oxygen demand and heat demand. The filling of hydrogen vehicles takes place during the period 2:00-6:00 every night, while the oxygen demand is for simplicity set to a constant value throughout the day and year. The stationary energy demand is divided equally between electricity demand and heat demand. The demand patterns for heat and electricity are decided to be identical, which is a rough simplification of real systems. But since the point here is to demonstrate operation principles, the simplification is assumed to be sufficient. The yearly average values for the different loads are shown in Table 21. The time series for the total stationary energy demand is the same as introduced in the case study in chapter 3.3.

Table 21. Average values of the different loads.

Electrical load	Heat load	Hydrogen load	Oxygen load
625 kW	625 kW	2,500 Nm^3/day	1,250 Nm^3/day

The time series for wind speed is also the same as used in chapter 3.3. Forecasts are based on results from [97], which describes the Danish Wind Power Prediction Tool (WPPT). The paper shows a graph of the prediction error for the WPPT and for the persistence method for one year, which are reproduced in Figure 83. It is clear from the graph that WPPT outperforms the persistence method for forecasts more than 5 hours ahead.

Here, a method for constructing wind power forecasts based on the actual hourly values is presented. The procedure is as follows:

1. Calculate the absolute error of wind power by multiplying the prediction error in Figure 83 with the average yearly wind power generation for the location. The error is used as an estimate for the standard deviation $\sigma_P(t)$ of the difference between actual and forecasted wind power output [94].
2. Draw random numbers $P_{w,err}(t)$ from a normal distribution with zero mean and standard deviation equal to $\sigma_P(t)$.
3. Read the actual wind power data $P_w(t)$ for t = 1...N and calculate the mean wind power $\overline{P}_w$ for $t = 1...N$ where N is the prediction horizon.
4. For $P_w(t) \geq \overline{P}_w$, the forecasted wind power is $\hat{P}_w(t) = P_w(t) - \left|P_{w,err}(t)\right|$
5. For $P_w(t) < \overline{P}_w$, the forecasted wind power is $\hat{P}_w(t) = P_w(t) + \left|P_{w,err}(t)\right|$

The motivation for introducing the mean wind power $\overline{P}_w$ is to avoid that the forecasted values fluctuate too much. This is demonstrated in Figure 84, which shows the result of multiple runs of the forecasting procedure. Steps 4 and 5 force the forecasted values to seek towards the mean value. Thus, it is possible to obtain smoother and more realistic values than using a forecasting model of the type $\hat{P}_w(t) = P_w(t) + P_{w,err}(t)$.

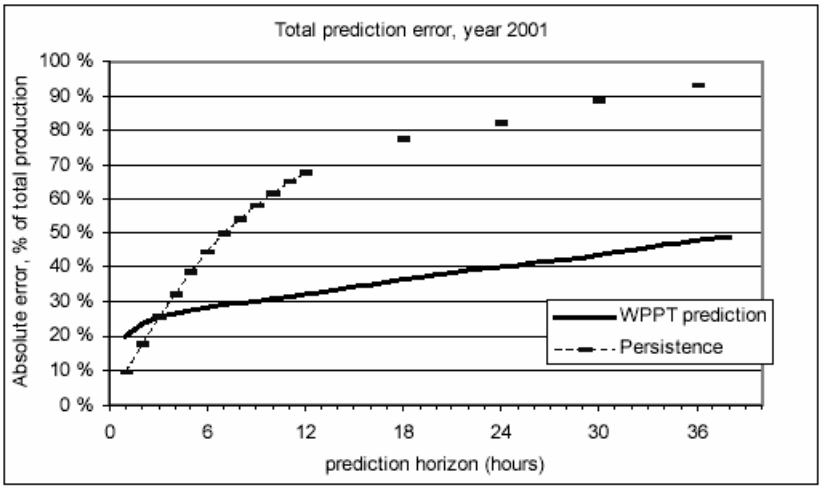

Figure 83. The total absolute prediction error of wind in the Eltra area (western Denmark). Source: Holttinen, Nielsen and Giebel [97].

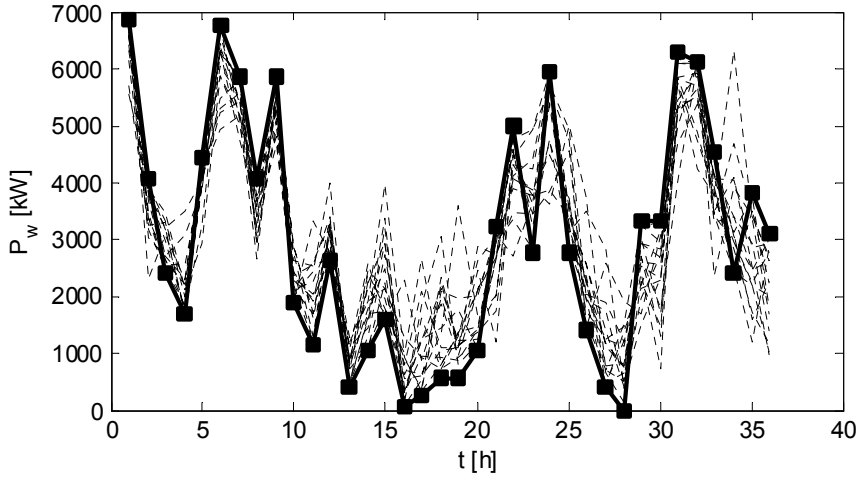

Figure 84. Illustration of the forecasting method used in the example. The actual wind power generation is shown with thick line and boxes. Different realizations of the forecast are shown with thin, dotted lines.

Three different market conditions for power import and export have been considered. CASE 1 is a grid-connected case with large daily variations in the spot price of electricity. Spot prices for the European Energy Exchange (EEX) from 2002 are used in this example. Each day at 12:00, the plant owner determines the hourly power sales and purchase for the next day, which gives the scheduled power export P_{sch}. Imbalance costs will have large variations from hour to hour and from day to day in real markets. In order to simplify the representation of the power system operation, constant imbalance costs are assumed in this example. The imbalance cost for upregulation is chosen to be 150% of the hourly spot price, which corresponds to c_{up} = 0.5 in equation (6.28). It is assumed a wind farm controller is installed, which limits the production if the electrolyzer cannot consume the all of the power surplus. The constant c_{dw} is set to 1 in (6.28) so that e_{reg} = 0 when the schedule deviation is positive. A similar market model is employed in [109].

CASE 2 is based on present Norwegian market conditions, where the spot price variations are small and the imbalance costs for wind power are assumed to be diminutive [110]. Spot prices for the Oslo-area from 2001 have been used, with no imbalance costs. Since this means that there are no economic penalties for deviation between scheduled and actual power export, the daily scheduling is omitted.

In CASE 3, isolated operation of the wind-hydrogen plant is simulated, with no possibility for power export. A backup generator with constant operation cost equal to 0.65 NOK/kWh is used when the wind-hydrogen system is not able to cover the loads. As for CASE 2, day-ahead scheduling is omitted in CASE 3, since the imbalance costs are set to zero. In actual isolated systems with several diesel generators, it will be necessary to perform a diesel unit commitment in order to decide which generators that should be operating the next day, see e.g. [103]. It should also be stressed that the operation of the isolated system is simplified here compared to what is required in a real isolated power system with high wind energy penetration. The purpose of CASE 3 is to show that the *principles* of on-line operation optimization also are relevant for isolated systems.

Table 22 lists the efficiencies of the different components. Compression work from electrolyzer to the storage tanks is not included, since it is assumed that the electrolyzer is pressurized (>15 bar). Compression work for the filling station is set to 0.2 kWh/Nm^3. In the base case, it is assumed that waste heat from the fuel cell cannot be utilized. The impact of heat utilization is assessed in section 6.4.2 .

Table 22. Component efficiencies

η_e	4.0 kWh_{el}/Nm^3
η_f	2.0 kWh_{el}/Nm^3
η_{Hc2}	0.2 kWh_{el}/Nm^3
η_{gl}	1.0 kWh_{heat} / kWh_{el}

Simulations of the system for 48 hours of operation are carried out for the three different cases. The idea is to give insight in how the operation strategy works, by comparing simulation runs with different parameter settings. The 48-hour time series of wind power and the different loads are plotted in Figure 85. Normalized values of the electricity price used in CASE 1 and CASE 2 are plotted in Figure 86. The hourly variations of the electricity price in CASE 1 are much larger than in CASE 2, which will influence the optimal usage of the hydrogen storage components.

Different results from simulation runs of one year are also presented for CASE 1. The yearly simulations are performed in order to gain knowledge about the impact of component sizing, energy conversion efficiencies, heat utilization and forecast uncertainty.

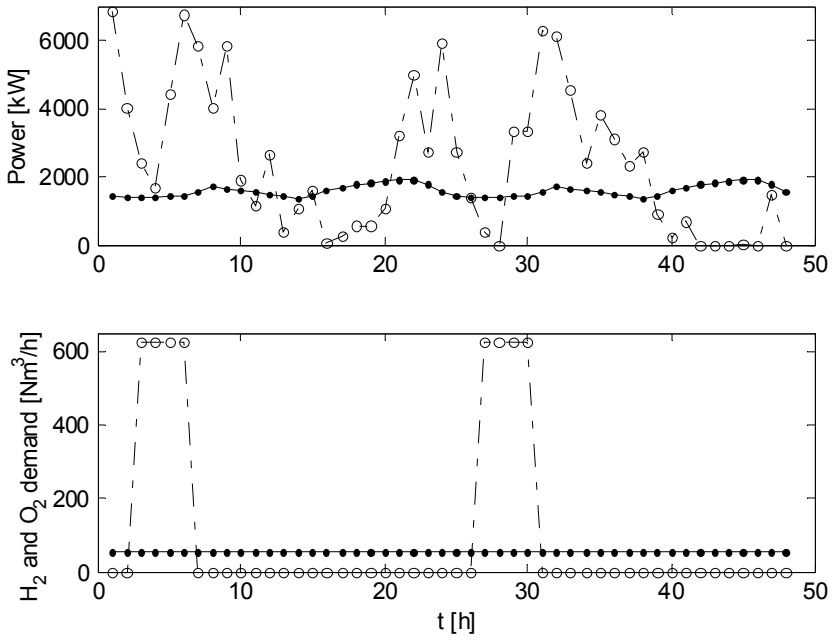

Figure 85. The upper figure shows time series for wind power (o) and the sum of electrical load and heat load (•). The lower figure shows time series for hydrogen demand (o) and oxygen demand (•).

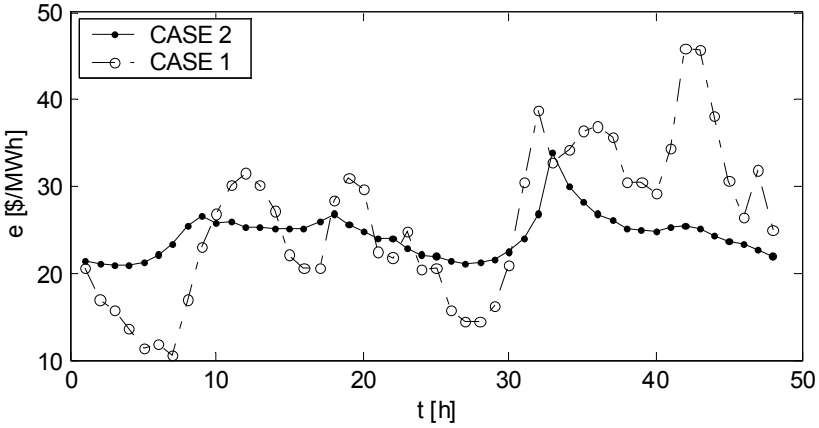

Figure 86. Sample of the spot price of electricity in EEX (CASE 1) and Nordpool (CASE 2).

6.4 Results from CASE 1: Thermal system

6.4.1 Demonstration of daily operation

In this case, the generation scheduling is performed each day at a specified hour. As a first approach, it is assumed that the scheduling takes place at the start of each day, so that there is no delay between the scheduling hour and the first hour of the scheduling period. Furthermore, perfect forecasts of wind power are used to start with.

Optimization horizon

The first parameter to be investigated is the optimization horizon that is used for finding the optimal generation scheduling. In chapter 5.4, the optimization horizon was set equal to the scheduling period, which is 24 hours. This is not necessarily a good choice, since information about the wind conditions for the following days will influence on how the system should be operated the current day. We see that this is true for the system studied here by observing the differences between 24-hour and 48-hour optimization horizon shown in Figure 87. Since the total time period is 48 hours, it is necessary to perform two optimizations when choosing 24-hour optimization horizon. For the 48-hour alternative, only one optimization is performed. An explanation to the different behavior is that the value of storing hydrogen and oxygen beyond the optimization horizon is set to zero. Therefore, it is optimal to use all the hydrogen and oxygen that is produced in the optimization period. An optimization horizon of 24 hours gives therefore less flexibility in the usage of the storage than 48-hour horizon.

The difference between 24-hour and 48-hour horizon becomes clearer if we examine the storage levels plotted in Figure 88. The hydrogen storage level

reaches zero at $t = 20$ when the optimization horizon is 24 hours, but this is not the case for 48-hour horizon. The difference emphasizes that the length of the optimization period is important in generation scheduling. Sometimes it would be beneficial to store hydrogen for longer periods than one day, for instance if the predicted values for wind speed are declining over time or if it is expected that the spot price is going to be higher at a later stage. The problem is that forecasts of wind speed, electricity price and loads increase in uncertainty for longer optimization horizons. This is especially true for wind speed prediction.

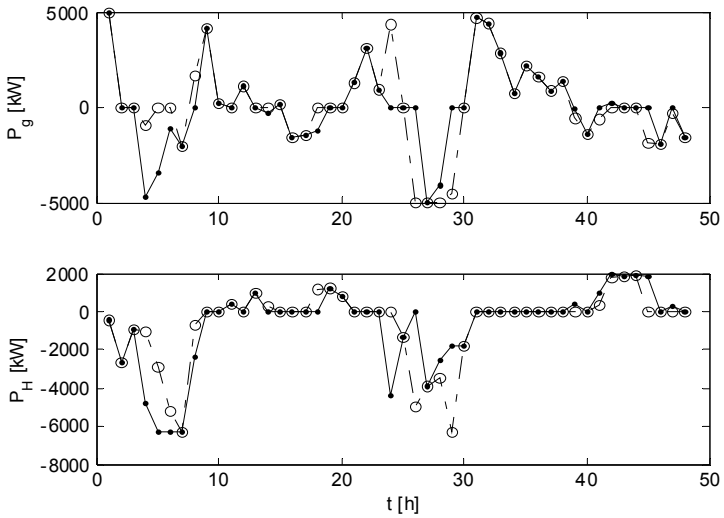

Figure 87. Power export to grid (upper figure) and net power flow out of the storage (lower figure). The graphs represent 24-hour (o) and 48-hour (•) optimisation horizon.

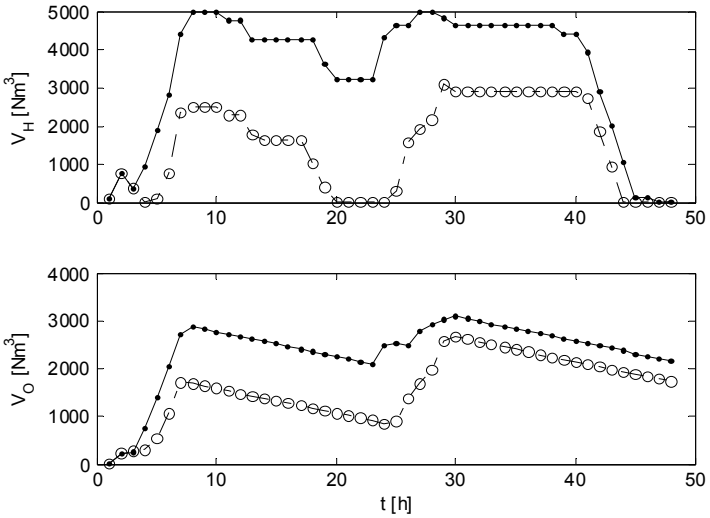

Figure 88. Hydrogen storage level (upper figure) and oxygen storage level (lower figure). The graphs represent 24-hour (o) and 48-hour (•) optimization horizon.

Wind forecast uncertainty

Simulation runs have been carried out to illustrate how the wind forecast uncertainty influences the on-line operation. The forecasting method described in section 6.3 is used with 36 hours look-ahead time. Updated forecasts are decided to be available every sixth hour, as for the Danish Wind Power Prediction Tool. The actual and forecasted wind power curves are plotted in Figure 89. The figure also shows the actual and scheduled power export. The reduction in profit compared to perfect forecast was 7%, and the deviations from the schedule are relatively small. The deviations are most distinct at around $t = 15$ and at the end of the period. By looking at the hydrogen storage level shown in Figure 90, we see that the hydrogen storage gets empty before the end of the simulation period. Since there was no hydrogen left to run the fuel cell, it was not possible to follow the scheduled power export. There are no positive deviations from schedule, since the price of excess power is zero. In periods when the wind power output is higher than forecasted, the excess wind power is used for hydrogen production. If the maximum capacity of the electrolyzer or the hydrogen storage is reached, the wind farm controller limits the power output.

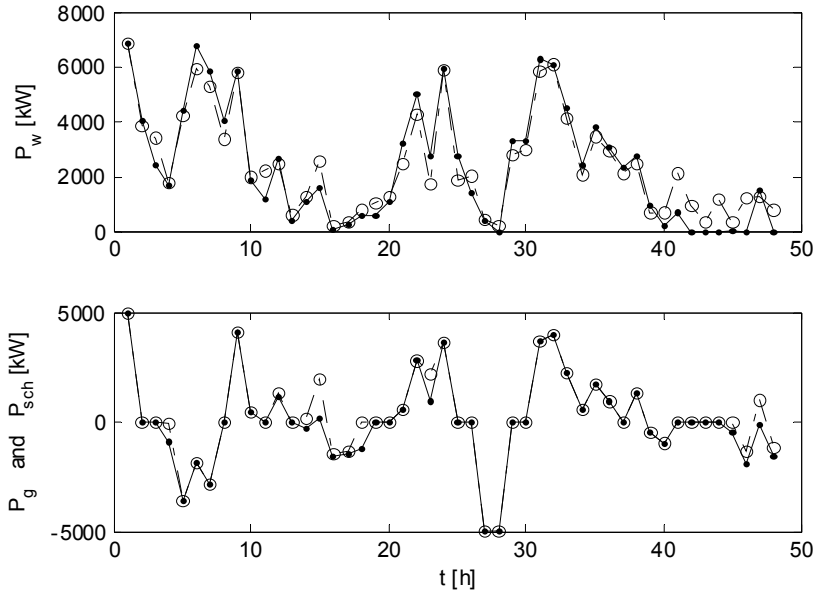

Figure 89. Upper figure shows actual (•) and forecasted (o) wind power generation. Lower figure shows actual power export (•) and the scheduled export (o) using 36 hour wind forecast and hourly on-line optimization.

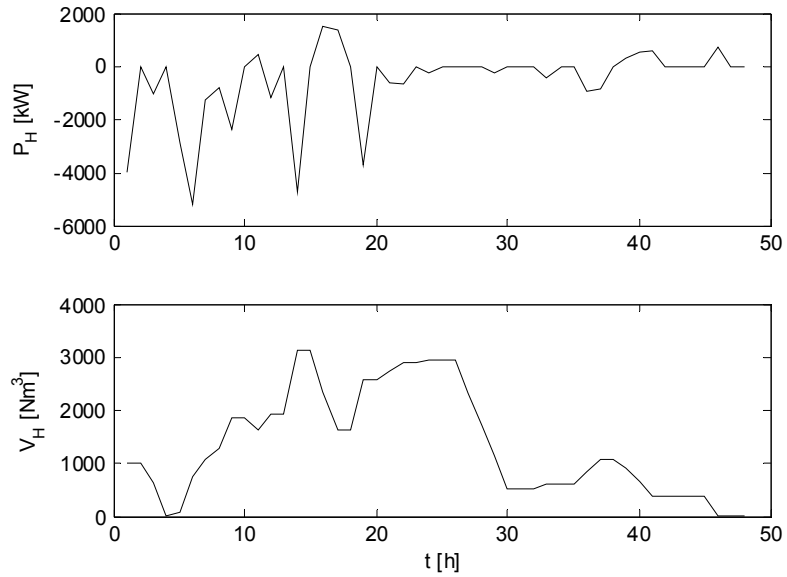

Figure 90. Net power output of hydrogen storage (upper) and hydrogen storage level (lower) using 36-hour wind forecast and hourly on-line optimization.

6.4.2 Simulation of one year

Component sizing

Yearly simulations are first carried out to show the impact of component sizing on the annual revenue. An income for supplying electricity to the load is included in the annual revenue, as in chapter 5. Perfect wind forecasts are used, so that imbalance costs are not taken into account. An optimization horizon of 48 hours is used in the simulations, and the optimization is updated every 24 hour. In Figure 91, the annual revenue is plotted as a function of component capacities. We observe that it is possible to reduce the component sizing considerably and still obtain a relatively high profit. Without going further into details about optimal component sizing here, the following component capacities are found to be appropriate for yearly simulations of CASE 1:

- P_e^{max} = 3,000 kW (Electrolyzer capacity)
- P_f^{max} = 1,000 kW (Fuel cell capacity)
- V_H^{max} = 5,000 Nm^3 (Hydrogen storage capacity)
- P_w^{max} = 7,000 kW (Wind power capacity)
- P_g^{max} = 5,000 kW (Grid capacity)

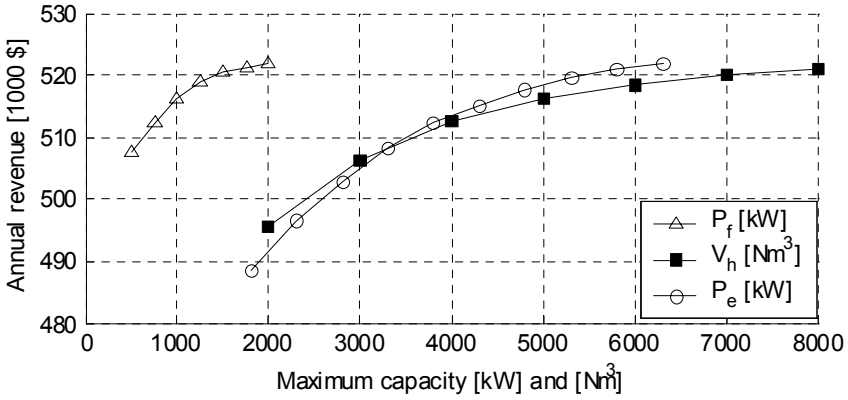

Figure 91. Annual revenue as a function of component sizing. The reference values are P_f^{max} *= 2,000 kW,* P_e^{max} *= 6,300 kW and* V_H^{max} *= 8000* Nm^3.

Fuel cell operation

In some cases, it might be possible to utilize heat produced from the fuel cell. The stationary energy demand in the example is divided into 50% electricity demand and 50% heat demand. By making use of hydrogen as a source of both electricity and heat, it would be possible to increase the overall efficiency of hydrogen storage. Another option is to apply a hydrogen burner [84] for direct conversion of chemical energy into heat, although not considered here. The main results from yearly simulations with and without utilization of fuel cell heat are shown in Table 23. In addition, results from a simulation with no fuel cell are included in the table.

Table 23. Simulations of one year with perfect forecasting of wind power. AR = annual revenue; UF = utilization factor; P = power. CHP = Combined Heat and Power. Subscript "e" means electrolyzer, "f" means fuel cell, "HV" means hydrogen storage tank and "g" means "grid".

	no fuel cell	**fuel cell**	**fuel cell CHP**
AR [1000 $]	482	497	511
UF_e [%]	14	23	26
UF_f [%]	-	13	19
UF_{HV} [%]	24	31	41
UF_g [%]	38	39	38
$\bar{P}_g$ [kW]	757	635	624

The annual revenue increases by 3% if we install a fuel cell. By utilizing the heat of the cooling water from the fuel cell, the revenue increases further by 3%. The reason why the value of the fuel cell installation is low is that the

round trip efficiency of hydrogen storage is only 50% with no heat utilization. It is only economic to produce hydrogen for stationary purposes if the price difference between the hours of hydrogen production and combustion can compensate for the losses. Therefore, the fuel cell is in stand-by mode (zero power output) much of the time, which is evident from the low utilization factor as shown in the table. An important consequence of operating the fuel cell is that the overall losses increase, which gives a lower total volume of exported energy. By installing a fuel cell, the average power export is reduced by 16%. At the same time, the utilization of the cable that connects the distributed system to the main grid increases, because of the increased hydrogen production in low price periods.

Start/stop of electrolyzer and fuel cell

The minimum operating power of the electrolyzer and the fuel cell has been set to zero in the simulations. Moreover, the efficiencies are modeled as constant values over the whole operating range. In practice, the relation between power consumption and hydrogen production can be a highly nonlinear in the lower operating range of the electrolyzer. This is mainly due to parasitic loads and operation characteristics of the power conversion unit. This is also true for the relation between power output and hydrogen consumption in fuel cells. If a restriction is put on the operating range of the electrolyzer and the fuel cell so that operation between 0% and 10% of rated power is prohibited, the annual revenue decreases by only 1%. The reason for the low impact is that the devices normally operate above 10% of the rated power. This is evident from Figure 92, which displays the duration curves for the electrolyzer power and fuel cell power.

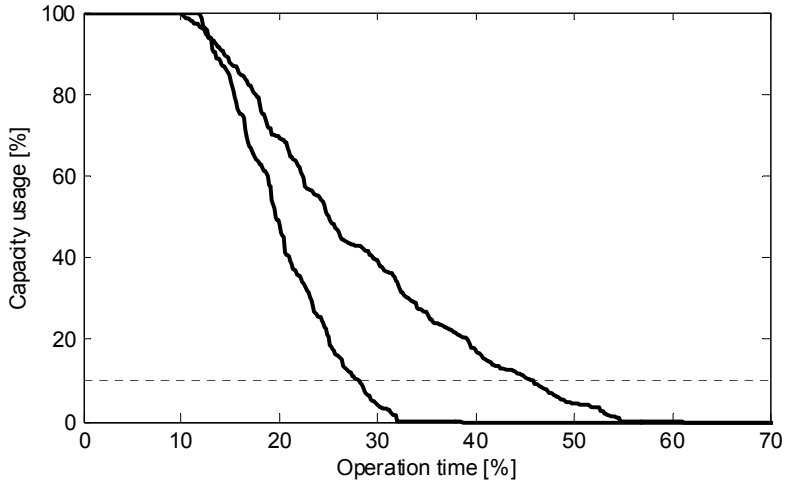

Figure 92. Duration curve of electrolyzer (solid line) and fuel cell (dashed line). The thin, dotted line is the minimum operation level when including on/off switching of the components.

Another important issue is that electrolyzers may have a relatively long response time from start-up to normal operation. Therefore, to manage sudden changes in power balance it could be necessary to keep the electrolyzer running at minimum power even if hydrogen is not needed. By setting the minimum power of the electrolyzer to 10% (i.e. it is never switched off), the annual revenue is reduced by 6%. To get a more correct idea of the impact of on/off switching, it is necessary to increase the modeling detail of the electrolyzer, fuel cell and power conversion units. For instance, it would be convenient to include a relation between efficiency and number of hours of continuous operation. If available, start/stop costs of the devices could be included in the optimization model.

Compression of hydrogen and oxygen

It has been assumed that the electrolyzer operates at high pressure (~30-40 bar) so that further compression is not necessary for storage of hydrogen and oxygen. The only compression work needed is to supply hydrogen for the filling station. Another possibility is to store hydrogen locally at higher pressure (e.g. 200-400 bar), so that it can be discharged directly to the filling station without further compression. At some locations, it may be required that hydrogen and oxygen are stored at high pressure to reduce the size of the storage system and thus reduce the area usage. This leads to increasing electricity consumption which gives a lower round-trip efficiency of hydrogen storage. Consequently, it will be fewer hours in which it is profitable to store hydrogen for power generation later on. Moreover, if the oxygen amount in the storage is sufficiently high to cover the demand within the optimization horizon, it will be better in some cases to release the oxygen to the air than to use electricity for oxygen compression. By setting the hydrogen compression work equal to 0.2 kWh/Nm^3 and the oxygen compression work equal to 0.4 kWh/Nm^3, it is found that the annual revenue decreases by 3%, and the usage of fuel cell becomes 14% lower than with the original assumptions.

Uncertainty of wind forecasts

We now look at how the uncertainty of wind forecasts influences the operation of the system. In e.g. the present Nordic market, bids must be given until 12:00 the previous day. The long lead-time causes large errors in wind power predictions. As more wind power is introduced in the power system, it would be beneficial to create a more flexible market [97]. Following the suggestions made by Holttinen et.al [97], two different market options are analyzed:

- MARKET 1: Scheduling 13-37 hours ahead
- MARKET 2: Scheduling 7-13 hours ahead

The first option is similar to the actual Nordic power market, where bids for every hour the next day must be delivered to the market operator before 12:00. The other option represents a more flexible market with shorter time span between scheduling and operation of the power system. Because of the reduced wind uncertainty, it is expected that the hydrogen storage will be less frequently used for balancing purposes in the flexible market. Thus, the value of installing a fuel cell will also be reduced. Results from simulation runs of the two market options with different fuel cell configurations are displayed in Table 24. The simulations give 15% gain in revenue by using a fuel cell in MARKET 1, compared to 13% in MARKET 2. The economic gain of utilizing fuel cell heat is slightly higher in MARKET 1 than in MARKET 2.

Table 24. Simulations of one year with imperfect forecasting of wind power in two different market systems. NO FC = no fuel cell; FC = fuel cell; FC CHP = fuel cell with combined heat and power; AR = annual revenue; UF = utilization factor.

	MARKET 1: 13-37 h			**MARKET 2: 7-13 h**		
	NO FC	FC	FC CHP	NO FC	FC	FC CHP
AR [1000 $]	355	408	426	382	430	448
UF_e [%]	16	29	30	15	27	28
UF_f [%]	-	22	24	-	19	21
UF_{VH} [%]	91	36	39	90	33	40
UF_g [%]	33	32	32	33	33	32
$\overline{P}_g$ [kW]	378	341	367	451	433	445
P_{dev}/P_{sch}[%]	24	14	14	17	11	10
P_d/P_w [%]	13	8	9	11	6	7

By comparing the utilization factors in Table 24 with Table 23 it is evident that both the fuel cell and the electrolyzer are operating more frequent as the wind uncertainty increases. Hydrogen is produced when the actual wind power generation exceeds the forecasted value. With no fuel cell, the hydrogen storage fills up rapidly, which results in a high average storage volume. When the storage is completely filled up, the wind farm controller reduces the power output so that imbalance costs are avoided. The high utilization factor of the hydrogen storage in the case of no fuel cell indicates that it would be beneficial to increase the hydrogen load, if possible. Then the extra amount of hydrogen would be produced almost merely from wind power that otherwise would have been dissipated. However, it would also be necessary to increase the storage volume in order to store excess hydrogen over a longer period.

Estimation of electricity price

So far, the actual spot price of electricity has been applied in the generation scheduling problem. In a real power pool, the actual price is not known in beforehand, but will be settled based on the bids for sales and purchase of power. To get a more realistic representation of the market, price forecasts are now used instead of the actual price when performing the generation scheduling. For simplicity, the available hourly prices for the previous day are chosen as forecast. Figure 93 displays a sample of the actual and forecasted price based on this method. The interesting result is that the forecast error leads to only 2.3% reduction in the annual revenue compared to perfect forecasting. This can be explained by the fact that the generation scheduling is influenced by the relative daily price variations, which maintain more or less the same shape for different days. Furthermore, the actual electricity price is used in the on-line optimization problem, which makes it possible to correct for unexpected price fluctuations.

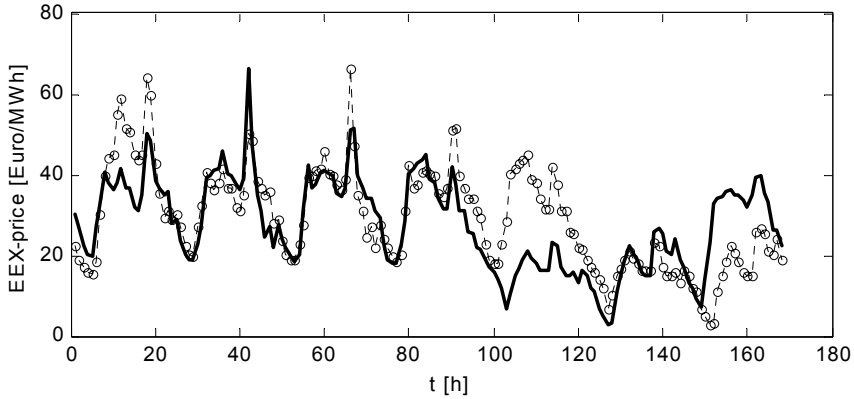

Figure 93. Actual EEX-price (thick line) and price forecast (dotted line with circles) for 15-21 January 2002.

6.5 Results from CASE 2: Hydro dominated system

There are no imbalance costs in CASE 2, and the hourly electricity price variations are lower than in CASE 1. Generation scheduling is omitted in this case, so the system operation is optimized from hour to hour based on the spot price of electricity and wind forecasts. The 48-hour time series for the external inputs (wind power, loads and electricity price) are given in section 6.3 . Three different alternatives for wind power forecasting have been used here:

- Perfect forecast with 48-hour horizon.
- Imperfect forecast with 36-hour horizon as shown in Figure 81.
- Persistence method with 36-hour horizon.

The latter method uses the last available wind power measurement as forecast. The net power export to the grid and net power output of the hydrogen storage system are shown in Figure 94 for the three forecast methods. It is interesting to notice that the fuel cell is almost of no use. The reason is that the hourly electricity price variations cannot compensate for the losses in the hydrogen storage chain. This indicates that for such market conditions, it will be adequate to install a hydrogen storage system without a fuel cell. Hydrogen will then be produced merely for the filling station. Furthermore, the power balance with the external grid is almost the same when simulating with perfect forecast and imperfect forecast. The difference in profit was therefore found to be insignificant. Even with the persistence method, there is not a big reduction in profit over the period compared to perfect forecast, namely 5%. The differences are due to grid losses. Figure 94 shows that the power export and power import are higher for the persistence method at some hours.

It is remarkable that the forecasting error has so little effect on the profit. The most important factor that explains this behavior is that there are no imbalance costs in CASE 2. Thus, the electrolyzer power is practically independent of the wind power generation. The only motive for not importing power from the grid is to reduce costs for grid losses. Therefore, good wind forecasts are not crucial, and the electrolyzer usage is mostly depending on electricity price variations.

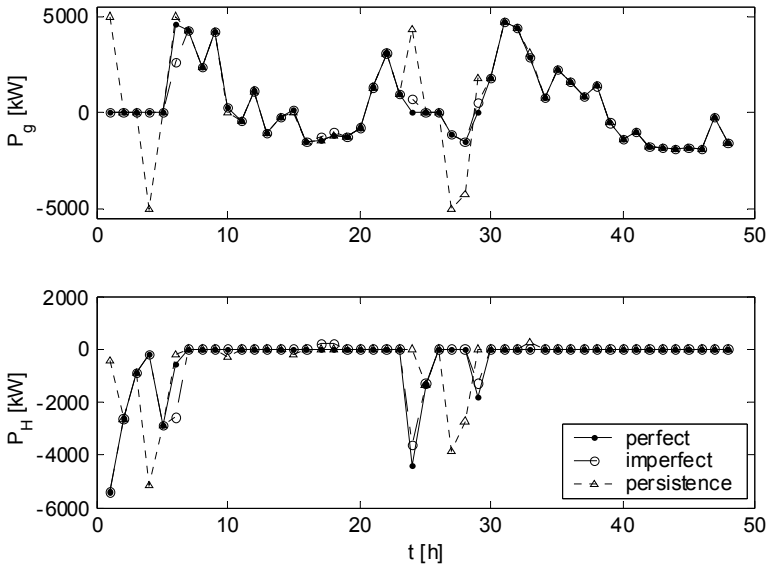

Figure 94. Power export to grid P_g (upper figure) and net power flow out of the hydrogen storage P_H (lower figure). The graphs represent perfect forecast, imperfect forecast and the persistence method of forecasting.

6.6 Results from CASE 3: Isolated operation

Isolated operation is examined in this case. The objective is to minimize the operation cost of the backup generator over the period. A simple representation of a diesel generator has been employed; linear cost curve and no startup or shutdown cost. Although simple, such a model will give important insight in optimal coordinated operation of the backup generator, electrolyzer and fuel cell. In order to demonstrate the operation principles, the 48-hour time-series for the loads shown in Figure 85 are applied. The wind power series is shown in Figure 95 and is slightly different than the wind power series used for CASE 1 and 2. The average wind power is slightly lower for the new series, so that the backup generator is more in use. This makes it easier to illustrate the optimal operation of the backup generator under different conditions.

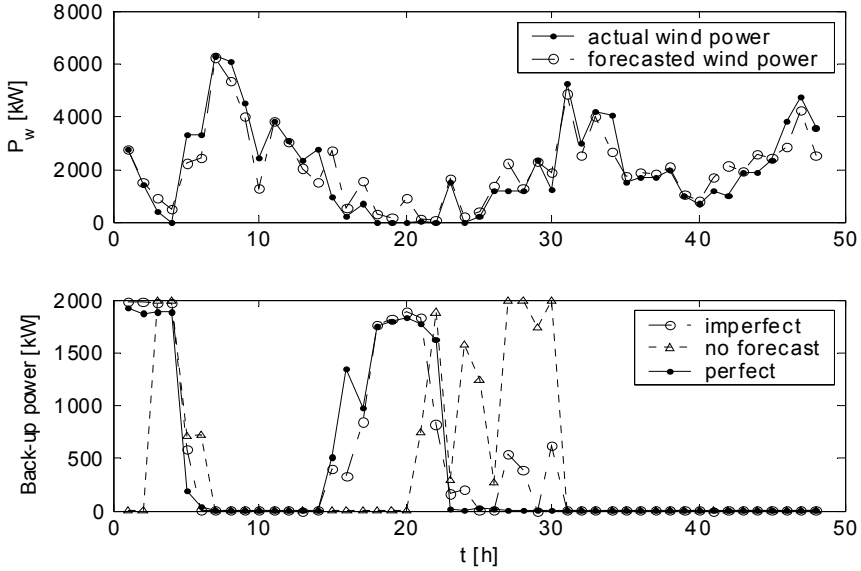

Figure 95. Forecasted (-o-) and actual (-.-) wind power generation are shown in the upper figure. The usage of the backup generator is shown in the lower figure, the graphs represent perfect forecast, imperfect forecast and no forecasts (load-following strategy).

Three different forecast options have been investigated:

- Perfect forecast for the whole 48-hour period.
- Imperfect forecasts using the model described in section 6.3
- No forecasts (load-following).

The latter method is equivalent to a load-following strategy, where power surplus is used to produce hydrogen that is combusted in the fuel cell when the wind power is less than the load. With the load-following strategy, the backup generator is operated whenever there is a deficit of wind power and

hydrogen for supplying the different loads. Figure 95 shows the backup-power for the three forecast assumptions. What happens with the load-following strategy (no forecast) in the first few hours is that the backup generator is not operated until it is suddenly needed. But when the filling of hydrogen vehicles start at $t = 4$, there is no wind power generation. Even though the backup generator is operated at maximum power, the electrolyzer cannot produce enough hydrogen, since most of the electricity is consumed by the stationary loads. This causes a deficit of hydrogen to the vehicles, which is represented in Figure 96 as a negative level of hydrogen storage. A similar situation occurred at $t = 27$. For the load-following strategy, the backup generator provided 25% of the stationary energy consumption. As much as 10% of the hydrogen needed for the filling station was not supplied. A way of preventing that hydrogen is not supplied is to introduce a trigger level for the hydrogen storage, which is above the minimum allowable storage level. If the storage amount gets below this level, the electrolyzer power is set to maximum whether wind power is available or not. Thus, the backup generator will be operated to meet the demand for hydrogen in periods with low wind speed. This strategy is similar to the control strategy presented in chapter 3.2.4.

By applying forecasts of wind power for several hours ahead, it is also possible to prevent a situation where hydrogen is not supplied. Figure 95 shows that the backup generator is operated at rated power the first two hours of the simulation, so that it is possible to produce a sufficient amount of hydrogen for later use in the filling station. Imperfect forecasts of wind power cause only a small increase in the total electricity generation of the backup generator (3%). The most important impact of forecasts is that improved accuracy can prevent that surplus hydrogen, which optimally should have stored for a longer period, is too quickly combusted in the fuel cell. This is exemplified in Figure 96, where the net power output of the hydrogen storage is shown for the different forecasts. If perfect forecasts of wind were available, the fuel cell would not have been used between $t = 15$ and $t = 20$. With imperfect forecasts, the fuel cell is operated in this period, but this will increase the total energy losses since the hydrogen optimally should have been stored until $t = 28$, when the filling of hydrogen vehicles takes place.

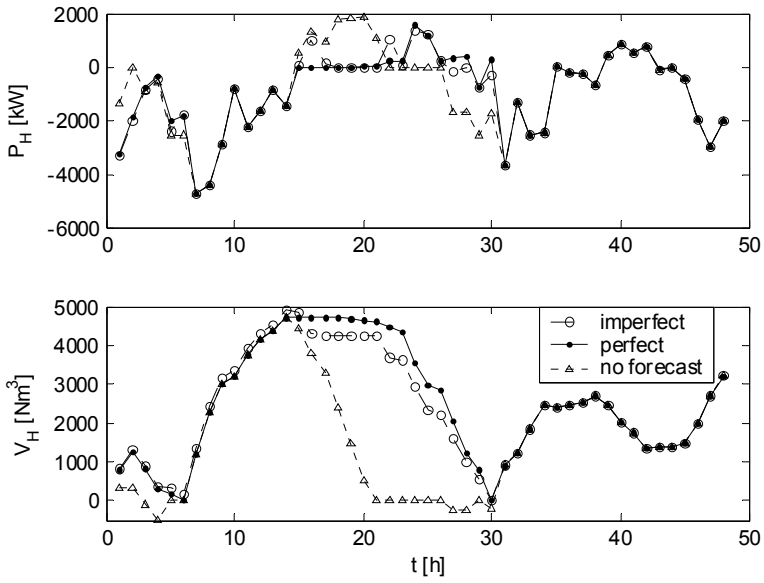

Figure 96. Net power output of the hydrogen storage (upper figure) and hydrogen storage level (lower figure). The graphs represent simulations with imperfect wind forecasts, perfect wind forecasts and no forecasts (load-following strategy).

6.7 Conclusions

A useful method for managing uncertainties

A novel method for the optimum operation of wind-hydrogen systems has been presented in this chapter. The method is based on principles of model predictive control for continuously updating the hourly operation of fuel cell and electrolyzer as new information on wind, loads, storage levels and electricity price are available. The problems related to wind speed uncertainties are managed by updating the optimization of hydrogen storage operation every time step. An algorithm for constructing synthetic time-series for forecasting of wind power has been constructed. Results from three case studies have demonstrated that the method is useful for analyzing the performance of the wind-hydrogen system with respect to component usage and generation uncertainty. CASE 1 simulates a thermal power system with high imbalance costs and large hourly spot price variations. CASE 2 is based on a power system dominated by hydropower, with negligible imbalance costs and small variations in spot price. CASE 3 represents isolated operation of the wind-hydrogen system with a backup generator.

Isolated systems: Optimum usage of the hydrogen product

In the isolated case, the proposed operating strategy is compared with a load following strategy. The motivation of using on-line optimization in isolated

operation mode rather than a load-following strategy is to prevent usage of hydrogen for power generation that rather should be stored for supplying the hydrogen filling station at a later point of time. Thus, the energy efficiency of the system could be increased.

Hydro-dominated systems: Optimum electrolyzer operation based on electricity price variations

In the hydro-dominated case, the price variations are too small to compensate for the losses in the hydrogen chain. The utilization factor of the fuel cell becomes very low and the electrolyzer is therefore used mainly for providing hydrogen to the filling station. Since the imbalance cost for wind power is set to zero, the optimum electrolyzer operation will be more dependent on good predictions of electricity price and hydrogen load than wind speed.

Thermal systems: Exploiting the price variations and reducing uncertainties

The case based on thermal power system conditions with large price variations is best suited to illustrate the usefulness of the operating principles for the wind-hydrogen system. Even though 50% of the energy is lost in the hydrogen chain, simulations show that the fuel cell is operated at a daily basis to increase profits. By the use of a hydrogen storage system, wind power is moved from periods with low price to peak price periods.

Generation scheduling is performed for a day-ahead market at a specific hour each day. Simulations with perfect forecasting of wind power show that it is beneficial to increase the optimization horizon beyond the scheduling period in order to obtain a value for hydrogen that is stored at the end of the scheduling period. Thus, good tools for medium-term wind forecasts are crucial to obtain a robust generation plan. This is further emphasized by the fact that deviations from scheduled export can lead to high imbalance costs. The introduction of uncertain wind forecasts gave 18% reduction of the annual revenue in the case study. Imbalances are in some degree avoided by controlling the fuel cell power output and electrolyzer power consumption, but this causes higher energy losses. Deviations from the scheduled export are significantly lower than for a wind-hydrogen system with no fuel cell. By installing a stationary fuel cell system, and thus use hydrogen for power generation in addition to the filling station, the revenue is increased by 15%. By assuming 20 years lifetime and 7% discount rate on investment, the investment cost (break-even cost) of the fuel cell should not be more than about $500/kW in order not to exceed the extra operational profits obtained by including the fuel cell. This is unfortunately far lower than present retail prices of fuel cells, but it is for

instance comparable with the long-term goal for reversible PEM-cells set by the U.S. Department of Energy, which is $600/kW by 2030 [34]. Moreover, by making use of waste heat from the fuel cell, and thus increase the value of hydrogen, the break-even cost is roughly $750/kW. Even though these cost calculations have been made simple, the results indicate that it can be economically viable to use renewable hydrogen not only as a fuel for transportation, but also for stationary energy supply.

7 DISCUSSION AND CONCLUSIONS

7.1 Discussion of the evaluated systems

Motivations for local energy storage

Three somewhat independent motivations for energy storage in connection with wind power are evaluated in the thesis. First, wind is intermittent and difficult to predict. Energy storage could be valuable for matching wind power with demand and for reducing generation uncertainty. Secondly, good wind sites are often located in remote areas. Storage of wind energy could defer grid upgrades in weak grids and reduce the dependency of fossil fuels in isolated power systems. Thirdly, hydrogen as a storage medium for wind energy could provide clean fuel for transportation. Thus, hydrogen energy storage is applicable to all three purposes. Storage solutions such as pumped hydro and compressed air are useful for the first purpose and in some cases for the second purpose, depending on the geographical conditions. Redox flow cells are modular devices that are useful for the two first purposes. Conventional (secondary) batteries are applicable to the first two purposes and in fact also for the third purpose, although not considered in the thesis. Electrical vehicles with rechargeable battery could act as a storage medium for wind power, by using the batteries as flexible loads that could follow wind power generation. This opportunity has for example been considered for the Danish energy system [111].

Hydrogen storage and grid constraints

In chapter 3, hydrogen storage is proposed as a solution to transmission constraint problems for areas with good wind energy resources but low electricity consumption and limited export capacity. Without energy storage, grid reinforcements or controllable loads, it is necessary to reduce the wind power output in periods with high wind speed and low loads. If proper control mechanisms for the power output are installed, this option is certainly attractive. However, the electricity cost increases rapidly as a function of installed wind power because of the increased amount of

dissipated wind energy. If the thermal capacity of the power line or cable is the limiting factor, dissipation of wind power is most likely to occur in winter for Norwegian conditions because of the strong seasonal variations of the wind. This could also be the case where voltage rise limits the acceptable wind power output, if the installed wind power is high relative to the local load. The seasonal variations also affect the cost of hydrogen if excess wind energy is used for electrolytic hydrogen production. The storage costs tend to be very high if all the excess energy should be used to supply a constant daily hydrogen demand. On the contrary, if the hydrogen demand instead followed the seasonal wind variations, the cost of hydrogen could be reduced by about 40%. In areas where seasonal hydrogen storage is possible in underground caverns, the storage costs would be negligible compared to the cost of producing hydrogen. Hydrogen storage in natural underground caverns is estimated to be two orders of magnitude cheaper than compressed storage in cylinders [43, 44].

If wind-derived hydrogen is not utilized as a separate product, but instead powers a stationary fuel cell, the hydrogen solution tends to be less attractive for the grid constraint problem. In the example studied in chapter 3, storage of excess wind energy in the form of hydrogen resulted in almost twice as high electricity cost as the "wind energy dissipation"-alternative for the same amount of annual delivered energy. In addition to the high investment costs, at least 50% of the energy will be lost through the hydrogen chain. However, if there is a good reason for avoiding power exports and imports, for example in the case of unattractive market conditions or if there is no electrical connection to the main grid, hydrogen might be a viable alternative for providing the electrical load with electricity from wind. However, according to the calculations made here, one must in that case expect to pay more than six times the cost of wind energy in the grid today. On the positive side, considerable cost savings could be obtained by using the same hydrogen storage system for providing energy for stationary use and for transportation since the same electrolyzer then serves two functions. Thus, it is important to exploit the flexibility of the hydrogen storage system in order to make it viable in conjunction with wind energy.

Hydrogen storage as balancing device in a market system

Chapter 6 shows how hydrogen storage can be applied for several purposes in a market based system. The system contains both a hydrogen filling station and a stationary fuel cell. By smart operation of the electrolyzer and the fuel cell, it is possible to increase the value of wind power both by “moving” electricity from low price hours to high price hours and also by reducing imbalance costs of intermittent generation. Simulation results showed that the economic gain is small in a hydro dominated system such

as in Norway, because of small price variations and low imbalance costs. In thermal systems, on the other hand, the economic gain is significant. However, in order to justify the investments of the hydrogen storage tanks, it must be a demand for hydrogen as an own product, presumably as a fuel for transportation. The extra economic gain by installing a fuel cell unit will balance the fuel cell investment if a cost goal of $300-600/kW is achieved in the future. It should be emphasized that as more unconventional sources like wind are introduced in the power system, the usefulness of using hydrogen for balancing purposes and for spot price optimization will increase.

Small-scale niche application for hydrogen

An attractive location for small-scale wind-hydrogen systems is nearby local industry such as fish farms at the windy coast of Norway. In addition to providing hydrogen for local vehicles and electricity consumers, the system could also provide oxygen for use at the fish farm. Moreover, waste heat from the fuel cell and perhaps also from the electrolyzer could to some extent cover the heat demand of the fish farm. In such cases, the wind-hydrogen system becomes truly multifunctional and is an exciting concept.

Comparison of storage systems for increasing the value of wind power

If hydrogen is not used in transportation, but merely as an energy carrier for stationary electricity, it should be evaluated in comparison with other relevant energy storage options. In chapter 4, several storage solutions are compared for the purpose of smoothing fluctuating wind power. Pumped hydro was clearly the most economic of the storage methods that were considered. Results for compressed air storage are not included in the chapter, but it is likely to be just slightly more expensive than pumped hydro. Unfortunately, these systems require special geographical conditions which limits their use in conjunction with wind power. Redox flow cells, on the other hand, are modular and are advantageous over hydrogen-oxygen storage systems regarding electrical efficiency. Furthermore, the fuel cell unit of for example vanadium batteries is expected to be cheaper than separate hydrogen fuel cell and electrolyzer. Consequently, redox-flow cells seem more attractive for wind power smoothing. On the other hand, an interesting result was obtained for reversible hydrogen fuel cells. If such units achieve the near-future goals for cost and performance, the electricity cost of the wind-hydrogen system becomes comparable with the more energy efficient wind-vanadium system. The reason is that the relative cost of the energy component is in favor of the hydrogen storage system. Since the discharging time in the example turned to be long (about 50 hours of full power generation), the energy cost component turned out to be very important for the economic result. According to the results shown in chapter

4, the value of firm power delivered to the grid must be about 2-3 times higher than fluctuating wind power in order to cover the extra investments.

If the operator of the combined wind-storage plant participates in a market system where the electricity price varies throughout the day, the round-trip efficiency of energy storage becomes especially important. The relation between the prices in two hours must be at least as high as the inverse of the round-trip efficiency to achieve economic gains. When simulating the participation in a day-ahead market, the results indicate that the discharging time of the storage need not to be higher than about 10-20 hours, even when the wind power plant is located behind a bottleneck in the grid. Thus, redox flow cells would in this case turn out to be more attractive than reversible hydrogen fuel cells, which have lower cost of energy capacity but also lower efficiency.

7.2 Discussion of the developed methods

Several methods for analyzing distributed energy systems with wind energy and energy storage have been developed during the doctoral study. The choice of method is dependent on what aspects of the combined wind-storage operation that are being studied. In addition, the ideas have been developed over time. For instance, the method presented in chapter 6 is an improved version of the method presented in chapter 5. This section summarizes the characteristics of the different methods as they appear in the thesis and points out benefits and limitations. Possible extensions of the methods are also discussed.

Time sequential simulation model with simple operation principles

In chapter 3, different means of utilizing hydrogen storage for exploitation of wind resources are proposed. The analysis is based on a time sequential simulation model, combined with cost assessment. The basic operation strategy is to avoid dissipation of wind energy due to grid constraints and to ensure that a sufficient amount of hydrogen fuel is supplied to the filling station every day. Hydrogen production primarily follows the wind power generation, but power import from the main grid is sometimes necessary to supply hydrogen to the filling station in periods with low wind and low hydrogen storage level. By making small adjustments of the operation strategy, it is possible to simulate many different operating alternatives, such as using local power surplus or wind power directly for hydrogen production. Further operation variations are made possible by including a fuel cell in the model. The operating strategies are simple in the sense that no forecasting and generation planning or other advanced methods are employed. Operation of the electrolyzer and fuel cell depends merely on the hourly electrical energy balance and the measured hydrogen storage level. It

would be easy to extend the method with operating strategies based on the difference between the electricity price in peak hours and off-peak hours, as done by e.g. Amos [29].

By using simple models for the different components, we obtain fast simulations. Moreover, the model is easy to implement and modify in a programming language such as Matlab. Because of the fast simulation time and model flexibility, it is easy to do a comprehensive study of component sizing by yearly simulations with one-hour time step. It is shown how the model can be used to find e.g. the optimum fuel cell size or the optimum combination of wind power sizing and storage sizing. This is obtained by comparing the total cost of selected systems with different component sizing. More sophisticated search algorithms could be implemented to reduce the number of trials for finding the optimum component sizing.

Probabilistic model

Chapter 4 presents a different modeling approach. Instead of using measured or modeled time-series of wind, the statistical properties of wind are used for establishing a model of wind-storage systems. Moreover, the motivation for applying energy storage for wind power is different. In the probabilistic model, the objective of installing a storage device is to smooth wind power fluctuations by providing a constant (firm) power output over a specified period.

The probabilistic model is developed for electrical energy storage. It does not include an option for hydrogen load in the case where hydrogen is used as storage medium. Future developments of the model could include such a function, thus enhancing the value of the hydrogen storage equipment. At the Norwegian University of Science and Technology, a probabilistic model of an isolated wind-electrolyzer plant for hydrogen supply is being developed [91]. The principles for operation of the electrolyzer described in [91] could be modified to fit in with the model described in chapter 4, in order to study the combined supply of electricity and hydrogen from a grid-connected wind-hydrogen system by a probabilistic approach.

The criterion of storage operation is that the expected energy flow into the storage is equal to the expected energy flow out of the storage. By this criterion, we ensure that there is no net increase or decrease in the storage level over the specified period. In the example presented in chapter 4, the criterion for the energy storage balance is applied for each week of the year, by assuming that the weekly wind speed variation follows a Weibull distribution. The required size of the energy storage for power smoothing was calculated from the week with highest expected wind speed. Since the

net power output of the combined wind-storage system does not exceed the firm power level for this week, the firm power level can also be regarded as the minimum transmission capacity that causes no dissipation of wind energy. The time resolution was chosen to be one week, because it is then possible to study the seasonal variations of wind, which is significant in many places in Norway. If the seasonal wind variations are negligible, the calculations could be based on the stochastic properties of the yearly wind speed.

The probabilistic model gives information on the expected performance of energy storage regarding smoothing of wind power. One of the outputs of the model is the expected value of the firm power that can be provided by the wind-storage system. To be usable with respect to on-line operation, the probabilistic model should be combined with a sequential simulation model with e.g. one-hour simulation time step. If we have a wind forecast for the next day with an estimate of the forecast error, it is possible to use the probabilistic model to find a generation schedule of the wind-storage system that minimizes the expected deviation between the scheduled and actual power output. Sample results from simulation runs with such an operation strategy are given in Table 25, which shows the average schedule deviation as a function of wind forecast error for a wind power plant with and without energy storage. The results show that energy storage greatly reduces the need for accurate wind predictions if the objective is to minimize the expected deviation between the scheduled and actual power output.

Table 25. Average deviation from scheduled power output as a function of wind forecasting uncertainty for a wind power plant with and without energy storage. The wind power capacity is 1 MW, the power capacity of the storage is 0.5 MW and the energy capacity of the storage is 5 MWh. Seasonal wind variations are not taken into account.

Forecast error	Wind power plant	Wind-storage plant
1 m/s	12.5 %	0.06 %
2 m/s	25.0 %	0.12 %
3 m/s	47.5 %	0.26 %
4 m/s	50.0 %	0.66 %

Time sequential simulation model with generation scheduling

Chapter 5 describes a variant of the simulation method introduced above. The objective of the energy storage operation here is not only to reduce unwanted wind power fluctuations, but also to increase profits by operating in a market-based system. The basis is a simplified day-ahead market model where a generation schedule is submitted to the market operator. Instead of using the statistical properties of wind forecasts to find a firm power output in the scheduling routine, this model optimizes the energy storage operation

with respect to the hourly price variations. In cases when the wind power output is below the grid limit, the storage level at the end of the scheduling period will be zero. On the other hand, if the wind power generation in the last part of the scheduling period exceeds the grid limit, it is more valuable to store the excess energy than to reduce the power output of the wind turbines. Therefore, dissipated wind power is given a negative value so that dissipation of wind power does not occur until the storage is completely filled up.

The operating strategy is to avoid imbalance costs by controlling the power generation and consumption of the energy storage unit. In the optimization problem for the day-ahead spot market participation, the wind forecasts are regarded as deterministic. The available power and energy capacities of the storage system, i.e. the full flexibility of the storage system, are used for maximizing the profit based on the forecast. In some cases, this could have negative economic impact during on-line operation. As an example, if the forecasted wind power output is 5 MW, and the optimum power output of the energy storage is found to be 4 MW for the same hour, the scheduled power output of the wind-storage system is 9 MW. What happen if the actual wind power output is not 5 MW, but 4 MW instead? The storage is operated to follow the scheduled power ouput, but if the maximum capacity of the storage is only 4 MW, there will be a deviation of 1 MW. On the other hand, if the available power capacity in the optimization routine was set to 3 MW instead of 4 MW, there would be no schedule deviations, since we have 1 MW as reserve capacity for handling imbalances. The consequence is that the expected profit from the scheduling is reduced, but so are also the imbalance costs. A similar reserve capacity for the energy capacity of the storage would also be beneficial. In the case study in chapter 5.4, the economic gain of improving the operation strategy by this method was found to be 3-5% of the total yearly profit.

Time sequential simulation model with generation scheduling and on-line optimization

The operating strategy in the model presented in chapter 5 was to follow the generation schedule as close as possible by charging and discharging the energy storage. However, since the generation planning is based on wind forecasts that can be very uncertain, it may happen that the scheduled power export is far from optimal with respect to the actual wind speed. Moreover, since the operation of the storage will depend on the difference between actual and forecasted wind power output, the storage level during on-line operation may be very different from the storage level which was estimated in the generation scheduling routine. Therefore, chapter 6 presents an improvement of the on-line operation strategy from chapter 5, by optimizing

the storage operation every time-step. Thus, an on-line adjustment of the optimal storage operation is obtained by taking into account the original generation schedule and imbalance costs for schedule deviations. An advantage of this method is that also new information on the present storage level is taken into account, as well as new wind forecasts and price forecasts if available. It was also found that it is beneficial to use a long optimization horizon for generation scheduling (*if* forecasts are available), since economic gains can be achieved by storing wind energy beyond the next day. By using a long optimization horizon and updating the optimization each time step, the problem of assigning a value of stored energy at the end of the optimization horizon gets less important. The value of stored energy at the end of the optimization period was set to zero, since it is assumed that it exist no information on wind conditions beyond the optimization horizon. It would be possible to estimate a value of stored hydrogen based on long-term forecasts as done in hydro power planning [112], but this has not been considered further here.

Hydrogen is chosen as the energy storage medium in chapter 6. A hydrogen filling station is therefore included, so that the stored energy can be used both as fuel for transportation and for stationary electricity production. Moreover, a demand for the oxygen produced in the electrolysis process is also included. The hydrogen and oxygen loads are regarded as "high priority" loads in the model, by assigning a high penalty for not supplying the loads. If the operation strategy was to follow the scheduled power export as close as possible, it could happen that less hydrogen and oxygen were stored than needed for the loads, for instance if the actual wind power output was lower than the predicted value. Such situations are avoided by updating the operation strategy each time step, so sufficient amounts of hydrogen and oxygen are produced and stored for supplying the loads.

In chapter 6, the problem of maximizing the operational profit is formulated as a linear programming (LP) problem. Since two different storage systems (hydrogen *and* oxygen) are included, a dynamic programming (DP) formulation would have resulted in an unsatisfactory number of states and thus long computational times. The LP formulation does not have this drawback. In the LP model, start/stop operation of the electrolyzer and the fuel cell is handled by including a minimum operating power level. The devices must be operated with higher power than this level, or be switched off (or set in standby mode with negligible power consumption). Thus, two discrete states for the electrolyzer and the fuel cell are introduced. In the LP model, all variables are represented as continuous variables. If the optimum electrolyzer power is found to be between zero and the minimum power level, the electrolyzer power is rounded to the nearest of these values, and

the optimization is carried out once more. The fuel cell power is handled in a similar manner. In order improve the operation strategy, it is possible to formulate the problem as mixed-integer LP. It would then also be possible to include start/stop costs of the devices, which could represent electrochemical degradation and mechanical wear.

7.3 Conclusions

This thesis has treated different applications of energy storage in conjunction with wind power. The motivations for applying energy storage are that wind power generation is intermittent and generally difficult to predict and that good wind energy resources are often found in areas with limited grid capacity. Moreover, if hydrogen is used as a storage medium, wind energy can be a source of hydrogen fuel for clean transportation.

Simulation provides useful insight and knowledge

Chapter 3 presented a sequential simulation model of a wind-hydrogen energy system. The model is useful for gaining knowledge of the benefits and limitations of different integration alternatives that exist within a wind-hydrogen framework. Combined with a cost model for electricity and hydrogen supply, it is possible to give suggestions for feasible sizing of the different system components for different integration alternatives. The results point out that an electrolyzer rating of about 50% of the wind power rating is appropriate for most applications, even if the value of excess wind power is low or zero. Wind-hydrogen systems with reversible fuel cell and systems with separate electrolyzer and fuel cell are found to be equivalent with respect to electricity cost if applied to cover the electricity demand in areas with weak or no connection to the main grid.

Smoothing of wind power fluctuations

In the model presented in chapter 4, the stochastic properties of wind speed are used as a basis for evaluating the ability of energy storage to smooth wind power fluctuations. The model takes into account power capacity constraints of the energy storage and the expected impact on the smoothing capability. The method is also useful for estimating the minimum transmission capacity that is required for avoiding dissipation of wind energy.

Wind power in electricity markets

In chapter 5, energy storage is proposed for increasing the value of wind power in a market-based system. A method for optimum generation scheduling of the wind-storage system in a market with varying electricity price has been developed. The basic model employs a dynamic programming algorithm for the scheduling problem, and it is shown how

stochastic dynamic programming can be applied for the on-line operation problem. Moreover, different variants of the scheduling problem by the use of a linear programming formulation are presented.

The model presented in chapter 6 extends and improves the model presented in chapter 5. Optimization principles are used for on-line operation as well as for generation scheduling. A receding-horizon operation strategy is employed for effective management of uncertainties. The method is applied to a wind-hydrogen system with the possibility of supplying electrical loads, heat loads and demand for hydrogen and oxygen.

Justification for high cost storage systems

In the cases where wind-derived hydrogen is not considered as a fuel for transportation, but merely for stationary energy supply, the hydrogen option should be evaluated against other and more energy efficient storage alternatives for wind energy, such as pumped hydro and redox flow cells. In order to exploit the opportunities for energy storage in electricity markets, it is crucial that the electrical efficiency of the storage is as high as possible. Energy storage combined with tools for wind power prediction opens the possibilities of taking advantage of varying electricity prices as well as reducing imbalance costs. If there are large errors related to short-term wind forecasts, it turns out to be difficult to use energy storage both for exploiting price variations and for minimizing imbalance costs.

The results indicate that the difference between electricity prices in peak hours and off-peak hours, as well as the imbalance costs of wind power must be high to justify the installation of a cost-intensive energy storage system. Thus, energy storage could be feasible for wind power integration in power systems with high-cost peaking units and regulating units. Moreover, energy storage would become more attractive as the amount of wind power in the power system increases, because of the increased difficulty of matching supply and demand.

Hydrogen as a carrier of wind energy

Hydrogen fuel cells are not yet cost competitive, but hydrogen is nevertheless a promising alternative as a carrier of wind energy. Hydrogen can be a viable storage medium for wind energy if hydrogen is introduced into the transportation sector. Furthermore, it would be important to make use of the flexibility that the hydrogen alternative offers regarding sizing, operation and utilization of oxygen and heat as by-products.

It should be emphasized that seasonal wind speed variations could lead to high storage costs if compressed hydrogen storage cylinders are used for

long-term storage. Seasonal storage of hydrogen in underground caverns should therefore be considered in areas where this is possible. The simulation results indicate that reduction of hydrogen storage costs would be more important than obtaining low-cost and high-efficient fuel cells and electrolyzers. Regarding fuel cells and electrolyzers, it would be important to further develop reliable, large-scale systems that can handle power fluctuations in order to make wind-hydrogen systems attractive.

Overall conclusion
Local storage systems are recommended for managing the intermittent and stochastic character of wind energy, either in electric isolated systems or in areas with weak grid connection. Moreover, energy storage is also advantageous in interconnected power systems with high proportions of wind power. Substantial operational benefits have been documented by simulations and optimization algorithms. Hydrogen as a storage medium and carrier of wind energy provides additional benefits as this technology matures and gets cost-effective.

7.4 Directions for further work

There is at present a rapid development within the field of hydrogen storage and other energy storage systems. It is expected that energy storage, and hydrogen storage in particular, will play an important role as the share of wind energy and other intermittent renewable energy sources continues to grow within the energy mix. Further development of simulation tools is important for a better understanding of the benefits and limitations of the different integration alternatives. Among the methods introduced in the thesis, one may consider the following extensions and improvements:

- Since the focus of the work has been on developing operation strategies for different integrated energy systems, general models of the individual subcomponents have been used. A logical extension of the models would be to represent electrolyzers, fuel cells and power converters by efficiency curves instead of constant efficiencies. Moreover, modeling of startup and shutdown of electrolyzer and fuel cell systems could be improved.

- Methods for short-term generation scheduling of wind-storage systems have been developed. The value of stored energy at the end of the scheduling period has been set to zero. An improvement of the method could be to link the short-term generation scheduling with medium-term scheduling. Thus, it should be possible to obtain an estimate of the value of stored energy at the last time step of the short-term optimization period.

- The impact of component sizing has been studied by systematically comparing the performance of selected systems with different sizing. More sophisticated search algorithms could be implemented to reduce the number of trials for finding optimum sizing.

- Wind energy has been chosen as energy source, but the developed methods are applicable to any intermittent energy source. Submodels for solar panels, micro hydro and wave power converters could easily be implemented.

- The different case studies that are presented in the thesis are general and not related to specific geographical areas. However, as discussed in chapter 2, the usage of energy storage and hydrogen in conjunction with wind energy has already been considered for several locations in Norway and other areas of the world. A reasonable next step of research is to apply the methods to a particular case with site-specific representation of wind speed, electrical load, electricity market conditions and a possible demand for hydrogen in transportation.

REFERENCES

[1] European Renewable Energy Council (2004) Renewable energy target for Europe – 20% by 2020. Briefing paper. Available at http://www.erec-renewables.org.

[2] Árnason B. and Sigfússon T.I. (2000) Iceland - a future hydrogen economy. *Int J Hydrogen Energy 25*, 389-394.

[3] Ackermann T., Garner K. and Gardiner A. (1999) Embedded wind generation in weak grids - economic optimisation and power quality simulation. *Renewable Energy 18*, 205-221.

[4] Vogstad K.-O. (1997) Energy resource planning - A systems engineering approach. Master Thesis. Norwegian University of Science and Technology, Trondheim, Norway.

[5] Carpinelli G., Celli G., Pilo F. and Russo A. (2001) Distributed generation siting and sizing under uncertainty. In *Proc. 2001 IEEE Porto Power Tech Conf*., Porto, Portugal.

[6] European Commission (1999) *Wind energy - The facts*. ISBN 92-828-4571-0. Office for Official Publications of the European Communities, Luxembourg.

[7] Zaininger H.W. and Barnes P.R. (1997) Applying wind turbines and battery storage to defer Orcas Power and Light Company distribution circuit upgrades. ORNL-Sub/96-SV115/1. Oak Ridge National Laboratory, Oak Ridge, TN - USA.

[8] Sørensen J. and Bugge O. (2002) Wind-hydrogen system on the island of Røst, Norway. In *Proc. 14th World Hydrogen Energy Conf*., Montreal, Canada.

[9] Tande J.O.G., Bindner H. and Murphy P. (1997) Power control for wind turbines in weak grids. In *Proc. 1997 European Wind Energy Conf*., Dublin, Ireland.

[10] Persaud S., Fox B., Flynn D. and Hodgkinson G. (1999) Optimising wind power penetration in rural distribution networks. In *Proc. 1999 European Wind Energy Conf*., Nice, France. pp 805-808.

[11] Mørk E., Rødskog M., Hystad J. and Jenssen B.H. (2003) Vindkraft i Nord-Norge, konsekvenser for sentralnettet (E. Wind power in northern Norway, consequences for the central grid). Statnett Grid development division, Oslo, Norway.

[12] Pálsson M., Toftevaag T., Uhlen K. and Tande J.O.G. (2002) Large-scale wind power integration and voltage stability limits in regional networks. In *IEEE Power Engineering Society Summer Meeting,* Chicago, USA. pp 762-769.

[13] Liew S.N. and Strbac G. (2002) Maximising penetration of wind generation in existing distribution networks. *IEE Proc-Gener Transm Distrib 149*, 256-262.

[14] Tande J.O.G. (2000) Exploitation of wind-energy resources in proximity to weak electric grids. *Applied Energy 65*, 395-401.

[15] Bindner H. and Lundsager P. (2002) Integration of wind power in the power system. In *IEEE 28th Annual Conf. of the Industrial Electronics Society, IECON 02*, Sevilla, Spain. pp 3309-3016.

[16] Gardner P., McGoldrick S., Higgins T. and Gallachóir B. (2003) The effect of increasing wind penetration on the electricity systems of the Republic of Ireland and Northern Ireland. In *Proc. 2003 European Wind Energy Conf*. and Exhibition, Madrid, Spain.

[17] Hansen L.H., Madsen, P.H., Blaabjerg F., Christensen H.C., Lindhard U. and Eskildsen K. (2001) Generators and power electronics technology for wind turbines. In *IEEE 27th Annual Conf. of the Industrial Electronics Society, IECON 01*, Denver, CO - USA. pp 2000-2005.

[18] Scott N.C. and Atkinson D.J. (1999) Using load management to limit steady state voltage rise on weak networks. In *Proc. 1999 European Wind Energy Conf*., Nice, France. pp 758-761.

[19] Bindner H. (1999) Power control for wind turbines in weak grids: Concepts development. Risø-R-1118(EN). Risø, Roskilde, Denmark.

[20] González A., McKeogh E. and Gallachóir B.O. (2003) The role of hydrogen in high wind energy penetration electricity systems: The Irish case. *Renewable Energy 29*, 471-489.

[21] Gallagher P., McKeogh E., González A. and Deane P. (2003) Computer simulation of planned 100 % renewable generation on an island off the west coast of Ireland. In *Proc. Int. Conf. RES for islands. Tourism & Water*, Crete, Greece. pp 87-96.

[22] Keith G. and Leighty B. (2002) Transmitting 4,000 MW of new windpower from North Dakota to Chicago: New HVDC electric lines or hydrogen pipeline. In *IEEE Power Engineering Society Summer Meeting*, Chicago, USA. pp 510-511.

[23] Gamallo F. (2001) Patagonian wind exported as liquid hydrogen. In *Proc. Hypothesis IV*, Stralsund, Germany.

[24] Gallachóir B. (2003) Energy from the ocean. *Irish Engineers J 57*, 24-27.

[25] Ackermann T. (2002) Transmission systems for offshore wind farms. *IEEE Power Engineering Review,* December, 23-27.

[26] Altmann M. and Richert F. (2001) Hydrogen production at offshore wind farms. In *Proc. Offshore Wind Energy Special Topic Conf.*, Brussels, Belgium.

[27] Homepages of Eltra, Transmission system operator in Western Denmark. http://www.eltra.dk.

[28] Castronouvo E.D. and Pecas Lopes J.A. (2003) Wind and small-hydro generation: An optimisation approach for daily integrated operation. In *Proc. 2003 European Wind Energy Conf. and Exhibition*, Madrid, Spain.

[29] Amos W.A. (2000) Economic assessment of wind energy coupled with a reversible hydrogen fuel cell. Milestone Type P report. National Renewable Energy Laboratory, Golden, CO - USA.

[30] Cruden A. and Dudgeon G.J.W. (2000) Opportunities for energy storage devices operating with renewable energy systems. In *Proc. EESAT 2000*, Orlando, FL - USA.

[31] Cruden, A. and Dudgeon G.J.W. (2001) The impact of energy storage devices used in conjunction with renewable embedded generators, on the protection and control system. In *IEE 7th Int. Conf. on Developments in Power System Protection*, Amsterdam, Netherlands. pp 230-233.

[32] Bathurst G.N. and Strbac G. (2003) Value of combining energy storage and wind in short-term energy and balancing markets. *Electric Power Systems Research 67*, 1-8.

[33] Eriksen P.B. (2003) Personal communication. December, Eltra, Denmark.

[34] Petersen A.H., Juhl C., Pedersen T.E., Ravn H., Søndergren C., Simonsen P., Jørgensen K., Nielsen L.H., Larsen H.V., Morthorst P.E., Schleisner L. Sørensen F. and Sørensen B. (2001) Scenarier for samlet udnyttelse af brint som energibærer i Danmarks fremtidige energisystem (E. Scenarios for the utilisation of hydrogen as an energy carrier in the future energy system in Denmark). IMFUFA text no. 390*,* Roskilde University, Denmark.

[35] Andreassen K. (1998) Hydrogen production by electrolysis. In *Hydrogen Power: Theoretical and Engineering Solutions*. Edited by Saetre T.O. Kluwer Academic Publishers, Netherlands. pp 91-102.

[36] Rasten E. (2000) Personal communication, March. Norwegian University of Science and Technology.

[37] Schnurnberger W., Seeger W. and Steeb H. (1988) Selected hydrogen production systems. In *Hydrogen as an energy carrier: Technologies, systems, economy*. Edited by Winter C.-J. and Nitsch J. Springer Verlag, Berlin, Germany. pp 209-248.

[38] Schug C.A. (1998) Operational characteristics of high-pressure, high-efficiency water-hydrogen-electrolysis. *Int J Hydrogen Energy 23*, 1113-1120.

[39] Dutton A.G., Bleijs J.A.M., Dienhart H., Falchetta M., Hug W., Prischich D. and Ruddell A.J. (2000) Experience in the design, sizing, economics, and implementation of autonomous wind-powered hydrogen production systems. *Int J Hydrogen Energy 25*, 705-722.

[40] Børresen B. (2003) Personal communication, December. Norwegian University of Science and Technology.

[41] Rasten E. (2001) Electrocatalysis in water electrolysis with Solid Polymer Electrolyte. Doctoral Thesis. Norwegian University of Science and Technology, Trondheim, Norway.

[42] Hemmer P.C. (1989) Termisk fysikk (E. Thermal physics). Tapir, Trondheim, Norway.

[43] Carpetis C. (1988) Storage, transport and distribution of hydrogen. In *Hydrogen as an energy carrier: Technologies, systems, economy*. Edited by Winter C.-J. and Nitsch J. Springer Verlag, Berlin, Germany. pp 249-290.

[44] Amos W.A. (1998) Costs of storing and transporting hydrogen. NREL/TP-570-25106. National Renewable Energy Laboratory, Golden, CO - USA.

[45] Cleghorn S.J.C., Ren X., Springer T.E., Wilson M.S., Zawodzinski C., Zawodzinski T.A. and Gottesfeld S. (1997) PEM fuel cells for transportation and stationary power generation applications. *Int J Hydrogen Energy 22*, 1137-1144.

[46] Aaberg R.J. (1999) Fuel cells - Fundamentals and technologies. Lecture notes 23. April. Norwegian University of Science and Technology, Trondheim, Norway.

[47] Hamelin J., Agbossou K., Laperrière A., Laurencelle F. and Bose T.K. (2001) Dynamic behavior of a PEM fuel cell stack for stationary applications. *Int J Hydrogen Energy 26*, 625-629.

[48] Schnurnberger W. (1999) Renewable energy systems with hydrogen storage and fuel cells: System efficiency and implementation strategies. In *Proc. Hydrogen - Electrochemistry and Energetics*,

Trondheim, Norway. pp 91-98.

[49] Mitlitsky F., Myers B., Weisberg A.H., Molter T.M. and Smith W.F. (1999) Reversible (unitised) PEM fuel cell devices. *Fuel cells Bullentin 11*, 6-11.

[50] Ioroi T., Kitazawa N., Yasuda K., Yamamoto Y. and Takenaka H. (2000) Iridium oxide/platinum electrocatalysts for unitized regenerative polymer electrolyte fuel cells. *J Electrochem Soc 147*, 2018-2022.

[51] Ledjeff K., Mahlendorf F., Peinecke V. and Heinzel A. (1995) Development of electrode/membrane units for the reversible solid polymer fuel cell (RSPFC). *Electrochim Acta 40*, 315-319.

[52] Gileadi E., Srinivasan S., Salzano F.J., Braun C., Beaufrere A. and Gottesfeld S. (1977) An electrochemically regenerative hydrogen-chlorine energy storage system for electric utilities. *J Power Sources 2*, 191-200.

[53] Yeo R.S., McBreen J., Tseung A.C.C. and Srinivasan S. (1980) An electrochemically regenerative hydrogen-chlorine energy storage system: electrode kinetics and cell performance. *J Applied Electrochemistry 10*, 393-404.

[54] Skolnik E.G. and DiPietro J.P. (1998) Technical and systems evaluations. In *Proc. 1998 U.S DOE Hydrogen Program Review*. National Renewable Energy Laboratory, Golden, CO - USA.

[55] Thomassen M., Børresen B., Hagen G. and Tunold R. (2003) H_2/Cl_2 fuel cell for co-generation of electricity and HCl. *J Applied Electrochemistry 33*, 9-13.

[56] Hernes M. (1999) Kraftelektronikkteknologi for nettintegrasjon av ulike energikilder og lagringsmedia (E. Power electronics for grid-integration of different energy sources and storage mediums). TR A4994. Sintef Energy Research, Trondheim, Norway.

[57] Mohan N., Undeland T.M. and Robbins W.P. (2003) *Power electronics - Converters, applications, and design*. John Wiley & Sons, Inc.

[58] Ter-Gazarian A. (1994) Energy storage for power systems. *IEE Energy Series 6*. Peter Peregrinus Ltd., London, UK.

[59] Price A., Thijssen G. and Symons P. (2000) Electricity storage, a solution in network operation? In *Proc. Distributech Europe*, Vienna, Austria.

[60] Ringheim N.A. (2002) Overview on different types of energy storages. TR A5610. Sintef Energy Research, Trondheim, Norway.

[61] Dell R.M. and Rand D.A.J. (2001) Energy storage - a key technology for global energy sustainability. *J Power Sources 100*, 2-17.

[62] Denholm P. and Kulcinski G.L. (2003) Life cycle energy requirements and greenhouse gas emissions from large scale energy storage systems. *Energy Conversion and Management*. In press.

[63] Kondoh J., Ishii I., Yamaguchi H., Murata A., Otani K., Sakuta K., Higuchi N., Sekine S. and Kamimoto M. (2000) Electrical energy storage systems for energy networks. *Energy Conversion & Management 41*, 1863-1874.

[64] Kodama E. and Kurashima Y. (1999) Development of a compact sodium-sulphur battery. *Power Engineering Journal 13*, 136-141.

[65] McDowall J.A. (2001) Opportunities for electricity storage in distributed generation and renewables. In *IEEE/PES Transmission and Distribution Conf. and Exposition*, Atlanta, GA-USA. pp 1165-1168.

[66] Price A., Bartley S., Male S. and Cooley A. (1999) A novel approach to utility scale energy storage. *Power Engineering J 13*, 122-129.

[67] Shibata A. and Sato K. (1999) Development of vanadium redox flow battery for electricity storage. *Power Engineering J 13*, 130-135.

[68] Vanhanen J.P., Lund P.D. and Tolonen J.S. (1998) Electrolyser-metal hydride-fuel cell system for seasonal energy storage. *Int J Hydrogen Energy 23*, 267-271.

[69] Kauranen P.S., Lund P.D. and Vanhanen J.P. (1994) Development of a self-sufficient solar-hydrogen energy system. *Int J Hydrogen Energy 19*, 99-106.

[70] Lehman P.A., Chamberlin C.E., Pauletto G. and Rocheleau M.A. (1997) Operating experience with a photovoltaic-hydrogen energy system. *Int J Hydrogen Energy 22*, 465-470.

[71] Abaoud H. and Steeb H. (1998) The German-Saudi HYSOLAR program. *Int J Hydrogen Energy 23*, 445-449.

[72] Szyszka A. (1996) Review of the Neunburg vorm Wald solar hydrogen demonstration project. *Power Engineering Journal*, October, 226-232.

[73] Barthels H., Brocke W.A., Bonhoff K., Groehn H.G., Heuts G., Lennartz M., Mai H., Mergel J., Schmid L. and Ritzenhoff P. (1998) Phoebus-Jülich: An autonomous energy supply system comprising photovoltaics, electrolytic hydrogen, fuel cell. *Int J Hydrogen Energy 23*, 295-301.

[74] Dutton A.G., Rudell A.J., Dienhart H., Hug W., Seeger W. and Bleijs J.A.M. (1996) Electrolyser and system operation in wind/hydrogen electrolysis systems. In *Proc. 1996 European Union Wind Energy Conf.*, Göteborg, Sweden. pp 357-360.

[75] Menzl F., Wenske M. and Lehmann J. (1999) Windmill-electrolyser system for a hydrogen based energy supply. In *Proc. 1999 European Wind Energy Conf*., Nice, France. pp 911-914.

[76] Agbossou K., Chahine R., Hamelin J., Laurencelle F., Anouar A., St-Arnaud J.-M. and Bose T.K. (2001) Renewable energy systems based on hydrogen for remote applications. *J Power Sources 96*, 168-172.

[77] Kolhe M., Agbossou K., Kelouwani S., Anouar A., Fournier M., Hamelin J. and Bose T.K. (2002) Long-term performace of stand-alone renewable energy system for hydrogen production. In *Proc. 14th World Hydrogen Energy Conf*., Montreal, Canada.

[78] Yde L., Poulsen B. and Maegaard P. (2003*) Brintbil med forbrændingsmotor* (E. Hydrogen car with combustion engine). ISBN 87-7778-142-2. Folkecenter for Renewable Energy, Hurup Thy, Denmark.

[79] Windpower Monthly (2001) *Harnessing Antarctic energy*. December 2001.

[80] Magill P. (2003) Construction and operation of a high-penetration wind-diesel system at Mawson, Antarctica. Presented at *Yukon Int. Wind Conf*., Whitehorse, Canada.

[81] Windpower Monthly (2003) *Hydrogen myths and wind realities*. May 2003.

[82] Homepages of IFE, Institue for energy technology. http://www.ife.no.

[83] Homepages of HiA, Agder University College. http://www.hia.no.

[84] Glöckner R., Kloed C., Nyhammer F. and Ulleberg Ø. (2002) Wind/hydrogen systems for remote areas - A Norwegian case study. In *Proc. 14th World Hydrogen Energy Conf*., Montreal, Canada.

[85] Norsk Hydro ASA (2003) Hydrogen society on the island of Utsira. Press Release, May 2003. Available at http://www.hydro.com.

[86] EHN (2003) EHN signs an agreement with the largest Norwegian electricity company and the world leader in hydrogen-based installations. Press Release, October 2003. Available at http://www.ehn.es.

[87] Ulleberg Ø. (1998) Stand-alone power systems for the future: Optimal design, operation & control of solar-hydrogen energy systems. Doctoral thesis. Norwegian University of Science and Technology, Trondheim, Norway.

[88] IEA (1994) *2. Estimation of cost of energy from wind energy conversion systems*. Expert group study on Recommended practices for wind turbine testing and evaluation. (2.ed). Edited by Tande

J.O.G. and Hunter R., Roskilde, Denmark.

[89] Vogstad K.-O., Belsnes M.M., Tande J.O.G., Hornnes K.S. and Warland G. (2001) Integrasjon av vindkraft i det norske kraftsystemet (E. Integration of wind power in the Norwegian power system). TR A5447. Sintef Energy Research, Trondheim, Norway.

[90] Tande J.O.G. and Vogstad K.-O. (1999) Operation implications of wind power in a hydro based power system. In *Proc. 1999 European Wind Energy Conf*., Nice, France. pp 425-428.

[91] Grimsmo L.N., Korpaas M., Gjengedal T. and Møller-Holst S. (2004) A study of a stand-alone wind and hydrogen system. In *Proc. Nordic Wind Power Conf*., Göteborg, Sweden.

[92] Gavanidou E.S., Bakirtzis A.G. and Dokopoulos P.S. (1992) A probabilistic method for the evaluation of the performance of wind-diesel energy systems. *IEEE Transactions on Energy Conversion 7*, 418-425.

[93] Karaki S.H., Chedid R.B. and Ramadan R. (1999) Probabilistic performance assessment of wind energy conversion systems. *IEEE Transactions on Energy Conversion 14*, 217-224.

[94] Dougherty E.R. (1990) Probability and statistics for the engineering, computing and physical sciences. Prentice-Hall, Englewood Cliffs, NJ-USA.

[95] Korpaas M., Hildrum R. and Holen A.T. (2001) Hydrogen energy storage for grid-connected wind farms. In *Proc. 6th IASTED Int. Conf., Power and Energy Systems*., Rhodes, Greece. pp 590-594.

[96] Nielsen L.H. and Morthorst P.E. (Editors) (1998) Fluktuerende vedvarende energi i el- og varmeforsyningen - det mellemlange sigt (E. System integration of wind power on liberalised electricity market conditions. Medium term aspects). Risø-R-1055(DA). Risø, Roskilde, Denmark.

[97] Holttinen H., Nielsen T.S. and Giebel G. (2002) Wind energy in the liberalised market – forecast errors in a day-ahead market compared to a more flexible market mechanism. In *Proc. 2nd Int. Symposium on Distributed Generation*, Stockholm, Sweden.

[98] Landberg L. and Watson S.J. (1994) Short-term prediction of local wind conditions. *Boundary-Layer Meteorology 70*, 171-195.

[99] Faanes H.H. (2000) Energiplanlegging (E. Energy planning). Lecture notes. Norwegian University of Science and Technology, Trondheim, Norway.

[100] Smith D.K. (1991) *Dynamic programming - a practical introduction*. Ellis Horwood, Chichester, UK.

[101] Infield D., Scotney A., Lundsager P., Bindner H., Pierik J., Uhlen

K., Toftevaag T., Falchetta M., Manninen L. and Van Dijk V. (1995) Engineering design tools for wind diesel systems - Volume 6B. EFI Technical Report No. A4330. Sintef Energy Research, Trondheim, Norway.

[102] Homepages of Nordpool The Nordic Power Exchange. http://www.nordpool.no.

[103] Bakirtzis A.G. and Gavanidou E.S. (1992) Optimum operation of a small autonomous system with unconventional energy sources. *Electric Power Systems Research 23*, 93-102.

[104] Rao S.S. (1996) *Engineering Optimization – Theory and Practice*. (3.ed). Wiley, New York, USA.

[105] Pereira M.V.F. (1989) Optimal stochastic operations scheduling of large hydroelectric systems. *Int J Electrical Power and Energy Systems 11*, 161-169.

[106] The Mathworks (2003) Optimization Toolbox User's Guide. Available at http://www.mathworks.com. The Mathworks, Inc.

[107] Wallmark C. and Alvfors P. (2002) Design of stationary PEFC system configurations to meet heat and power demands. *J Power Sources 106*, 83-92.

[108] Roberts P.D. (2000) A brief overview of model predictive control. *IEE Seminar on Practical Experiences with Predictive Control.* Ref No 2000/023.

[109] Roulston M.S., Kaplan D.T., Hardenberg J. and Smith L.A. (2003) Using medium-range weather forcasts to improve the value of wind energy production. *Renewable Energy 28*, 585-602.

[110] Gustafsson M. (2002) Wind power, generation imbalances and regulation cost. Presented at *Int. Workshop on Wind Power and the Impacts on Power Systems*, Oslo, Norway.

[111] Nielsen L.H. and Jørgensen K. (2000) Electric vehicles and renewable energy in the transport sector – energy system consequences. Risø-R-1187(En). Risø, Roskilde, Denmark.

[112] Fosso O.B., Gjelsvik A., Haugstad A., Mo B. and Wangensteen I. (1999) Generation Scheduling in a deregulated system. The Norwegian Case. *IEEE Transactions on Power Systems 14*, 75-81.

APPENDIX A: SYMBOLS AND ABBREVIATIONS

Below is a list of the main symbols that appear in the text. The symbols are also described as they appear in the text. The notation in the papers in Appendix B differs from the symbol list.

Arabic uppercase letters

AR	Annual revenue [$/yr]
E(x)	Expectation value of variable x
E	Electrical energy [kWh] or [MWh]
E_d	Electrical energy consumed by dump load (Dissipated wind energy)
E_{def}	Energy deficit
E_e	Electrical energy consumed by electrolyzer
E_{exp}	Electrical energy export
E_f	Electrical energy produced by fuel cell
E_g	Net electrical energy exported to the grid
E_{imp}	Electrical energy import
$E_{imp,e}$	Electrical energy import to electrolyzer
E_l	Electrical energy consumed by local load
E_{sp}	Spilled (or excess) wind energy
E_w	Electrical energy produced by wind power plant
F	Faraday number (96,485 As/mol)
F	Objective function
$F_P(P_w)$	Cumulative distribution function of wind power
$F_v(v)$	Cumulative distribution function of wind speed
$H_p(P_w)$	Duration curve of wind power
I	Cell current [A]
IP	Investment potential [$]
IC	Investment cost [$]

L	Lifetime of a component [yr]
L	Number of time steps left before the next day [h]
LPC_{el}	Levelised production cost of electricity [$/kWh]
LPC_{H2}	Levelised production cost of hydrogen [$/Nm^3]
M_r	Relative molecular mass of hydrogen (2.016 g/mol)
M	Optimization horizon of scheduling problem [h]
N	Optimization horizon of on-line operation problem [h]
OM	Operation and maintenance cost [$/yr]
P	Power [kW] or [MW]
P_c	Total power consumption for gas compression
P_{ch}	Charging power
P_d	Dump load (dissipated wind power)
P_{dch}	Discharging power
P_{dev}	Deviations from scheduled generation (P_{dev}=P_g - P_{sch})
P_{dw}	Downregulation of other generators
P_e	Power consumption of electrolyzer
P_{exp}	Power export
P_f	Power output of fuel cell
P_{fp}	Firm power output
P_g	Power exported to the grid
P_{gl}	Grid losses
P_H	Net power output of hydrogen storage system
P_{imp}	Power import
$P_{imp,e}$	Power import to electrolyzer
P_l	Electrical load
P_{ql}	Power consumption of electrical heater
P_s	Power flow in (-) or out (+) of energy storage unit
P_{sch}	Scheduled generation
P_{up}	Upregulation of other generators
P_w	Wind power output
$P_{w,err}$	Forecast error of wind power
Pr	Probability
Q	Reactive power [MVARs]
Q_d	Dumped (excess) heat [kW]
Q_f	Useful heat from fuel cell [kW]
Q_l	Heat load [kW]
R	Resistance per length in power lines [Ohm/km]
R	Cell resistance [Ohm]

R	Rest period [yr]
RI	Reinvestment cost [$]
S	Storage level [MWh]
$\hat{S}^{i+1}(t)$	Estimated storage level at the hour t in the next day i+1 [MWh]
S^{max}	Maximum storage content [MWh]
$\dot{S}_{ch}$	Energy flow into storage [kW]
$\dot{S}_{dch}$	Energy flow out of storage [kW]
SV	Salvage value of a component (rest value) [$]
T	Total simulation time [h]
TC	Discounted present value of the total cost [$]
U_{an}	Anode potential [V]
U_{cat}	Cathode potential [V]
U_{cell}	Cell potential [V]
U_{rev}	Reversible cell potential [V]
UF	Utilization factor [%]
UF_{ch}	Utilization factor of charging device
UF_{dch}	Utilization factor of discharging device
UF_{e}	Utilization factor of electrolyzer
UF_{f}	Utilization factor of fuel cell
UF_{g}	Utilization factor of power line or cable
UF_{rfc}	Utilization factor of reversible fuel cell
UF_{VH}	Utilization factor of hydrogen storage tank
UF_{w}	Utilization factor of wind power plant
V	Grid voltage [V]
V	Coefficient of variation
V_H	Hydrogen content in pressure tank [Nm^3]
V_H^*	Lower supply security limit for hydrogen storage [Nm^3]
V_O	Oxygen content in pressure tank [Nm^3]
V_{Hl}	Yearly hydrogen load [Nm^3]
$\dot{V}_H$	Hydrogen flow rate [Nm^3/h]
$\dot{V}_{He}$	Hydrogen production in electrolyzer
$\dot{V}_{Hf}$	Hydrogen consumption in fuel cell
$\dot{V}_{Himp}$	Import of hydrogen
$\dot{V}_{Hl}$	Hydrogen load
$\dot{V}_{Hout}$	Hydrogen flow rate from storage to load

$\dot{V}_O$ Oxygen flow rate [Nm^3/h]

$\dot{V}_{Oe}$ Oxygen production in electrolyzer

$\dot{V}_{Oimp}$ Import of oxygen

$\dot{V}_{Ol}$ Oxygen load

$\dot{V}_{Oout}$ Oxygen flow rate from storage to load

Y Analysis period [yr]

Arabic lowercase letters

a_{gl} Constant in quadratic equation for grid losses [MW^{-1}]

a_{gl}^* Constant in linear equation for grid losses

$a_{r,Y}$ Annuity factor for discount rate r and Y years

c Scale parameter [m/s]

c_d Penalty for dumping wind power [$/MWh]

c_{dw} Downregulating cost in regulating market [$/MWh]

c_H Import cost of hydrogen [$/$Nm^3$]

c_O Import cost of oxygen [$/$Nm^3$]

c_{up} Upregulating cost in regulating market [$/MWh]

e Electricity spot price [$/MWh]

e_{bg} Operating cost of backup generator [$/MWh]

e_{reg} Regulating power price (imbalance cost) [$/MWh]

$f_v(v)$ Probability density function of wind speed

f Profit [$/h]

f_H Profit for hydrogen import (negative)

f_{load} Profit for supplying local load with wind power

f_{loss} Profit of grid losses (negative)

f_O Profit for oxygen import (negative)

f_{oper} Profit from on-line operation

f_{reg} Profit from regulating market

f_{sch} Profit from scheduled generation (power exchange with market)

f_{spot} Profit from spot market

h Tower height [m]

i Day (chapter 5)

i_{end} Last simulation day (chapter 5)

k Shape parameter

n Number of moles in a reaction

$\dot{n}_{He}$ Molar production rate of hydrogen in electrolyzer [mol/s]

p	Parameter vector
r	Roughness factor [m]
r	Discount rate
r	Amount of oxygen produced per unit of hydrogen
t	Hour of the day (chapter 5)
t_{end}	Last hour of the day (chapter 5)
t	Time step [h]
t_{sch}	Scheduling hour [h]
u	Control variable vector
v	Wind speed [m/s]
v_i	Cut-in wind speed of wind turbine
v_o	Cut-out wind speed of wind turbine
v_r	Rated wind speed
$\overline{v}$	Mean wind speed
$\hat{v}$	Forecast (estimate) of future wind speed
x	State variable vector
w	Dependent variable vector

Greek letters

α	Constant in power smoothing equation [MW]
$\Phi(v)$	Wind power curve between cut-in and rated wind speed [MW]
γ_e	Operating state of electrolyzer (on/off)
γ_f	Operating state of fuel cell (on/off)
η_{ch}	Charging efficiency [%]
η_{dch}	Discharging efficiency [%]
η_e	Specific power consumption of electrolyzer plant [kWh/Nm^3]
η_f	Specific power generation of fuel cell plant [kWh/Nm^3]
η_{fq}	Heat conversion efficiency of fuel cell [kWh/Nm^3]
η_{Hc}	Efficiency of first hydrogen compressor [kWh/Nm^3]
η_{Hc2}	Efficiency of second hydrogen compressor [kWh/Nm^3]
η_I	Current efficiency [%]
η_{Oc}	Efficiency of oxygen compressor [kWh/Nm^3]
η_{ql}	Efficiency of electrical heater [kWh$_{heat}$/ kWh$_{el}$]
η_{rt}	Round-trip efficiency of energy storage [%]
η_{sys}	Electrical efficiency of wind-storage system [%]
η_U	Voltaic efficiency [%]
ρ	Density of hydrogen (0.08988 kg/m^3)

σ_l Standard deviation of the daily mean load [MW]
σ_P Standard deviation of wind power [MW]

Abbreviations

CAES Compressed air energy storage
cdf Cumulative distribution function
CHP Combined heat and power
DP Dynamic programming
EEX European Energy Exchange
ELY Electrolyzer
FC Fuel cell
HHV Higher heating value (3.5 kWh/Nm^3 for H_2)
HVDC High Voltage Direct Current
LHV Lower heating value (2.995 kWh/Nm^3 for H_2)
LP Linear programming
NETA New electricity trading arrangements (UK)
NORDPOOL The Nordic Power Exchange
pdf Probability density function
PEM Polymer Exchange Membrane
RMSE Root mean squared error
SDP Stochastic dynamic programming
SPE Solid Polymer Electrode
WECS Wind energy converter system
WPPT Wind Power Prediction Tool

APPENDIX B: PAPER 1-3

Paper 1

"Hydrogen energy storage for grid-connected wind farms"

The paper appears in the Proceedings of the Sixth IASTED International Conference on Power and Energy Systems, Rhodes, Greece, July 2001, pp 590-594.

Paper 2

"Operation and sizing of energy storage for wind power plants in a market system"

This paper is published in the International Journal of Electrical Power & Energy Systems, vol. 25, 2003, pp 599-606.

Paper 3

"Optimal operation of hydrogen storage for energy sources with stochastic input"

This paper appears in the Proceedings of the 2003 IEEE Bologna PowerTech, Bologna, Italy, June 2003.

Proceedings of the IASTED International Conference
POWER AND ENERGY SYSTEMS
July3-6, 2001, Rhodes, Greece

HYDROGEN ENERGY STORAGE FOR GRID-CONNECTED WIND FARMS

MAGNUS KORPÅS
Dept. of Electrical Power Engineering
Norwegian University of Science and Technology, NOR-7491 Trondheim

RAGNE HILDRUM
Statkraft SF
NOR-1323 Høvik

ARNE T. HOLEN
Dept. of Electrical Power Engineering
Norwegian University of Science and Technology, NOR-7491 Trondheim

ABSTRACT

In this paper, local hydrogen energy storage is proposed as an alternative to grid reinforcements in rural areas with high wind power potential and weak distribution lines. Present and future production cost estimates of electricity are calculated for different wind-storage systems assuming optimal operation in a competitive power market. It is shown that hydrogen energy storage could become an economically feasible alternative to grid expansions if cost and performance goals of hydrogen technology are obtained. The controllable power from the wind-storage system must then be valued 2-3 times higher than fluctuating power in the market. The results are based on a simple probabilistic model. Further work on a comprehensive simulation model will be carried out, in order to investigate different operation strategies and design criteria for wind-storage systems.

KEYWORDS:

Wind Energy, Energy Storage, Hydrogen Energy

1. INTRODUCTION

One of the most difficult challenges in the field of wind energy and other renewable energy sources is the fluctuating power output. Regulation of conventional power plants is absolutely essential to balance the loads. For that reason several sources have claimed that the installed wind power should not exceed 20% of the total installed capacity in an electricity network [1]. In addition locations with high wind potential are often found in rural areas with weak distribution lines. Development of wind power plants in such areas could require extensive grid expansions, which results in low utilization of the grid capacity due to the low capacity factor of wind power plants. Grid expansions may also lead to unwanted interference with the local environment.

By using a locally sited energy storage for power smoothing conventional generators could be relieved from some of their power smoothing functions. As a result, this would increase the potential wind power penetration in electricity networks. In rural areas with weak grid connection, a properly dimensioned energy storage could also be an alternative to grid expansions. The management of daily and weekly wind variations requires both high energy capacity and power capacity of the storage devices, especially for wind power plants consisting of generators in the MW range. Technologies like conventional batteries, flywheels and superconductive magnetic energy storage have the disadvantage that the energy capacity is related to the power capacity. Moreover, the usage of pumped hydro and compressed air storage is limited to certain sites. On the contrary, fuel cell systems with hydrogen storage are modular devices with separated power and energy capacity, and are promising alternatives for large-scale energy storage. Hydrogen-oxygen systems are the most commonly known, but there are also other favourable hydrogen-based systems such as hydrogen-bromide and hydrogen-chloride regenerative fuel cells which use one and the same electrochemical cell for charging and discharging. A different regenerative fuel cell technology known as Regenesys, which is commercially available today, is based on a polysulphide/bromide redox-couple [2].

Several authors have emphasized the usefulness of wind-hydrogen systems for power supply in isolated grids, but rather limited research has been published on grid-connected systems. In the literature, large-scale energy storage is occasionally mentioned as a possibility for wind power plant owners to increase their revenue by operating strategically in the electricity market. Amos [3] has investigated the possibility to store electricity at night, and to sell at daytime when the prices are higher. Cruden et al. have investigated potential trading benefits using optimization techniques [4]. In this paper, local energy storage is proposed as an alternative to grid reinforcements in rural areas with high wind potential. The electricity production costs of different wind-storage systems operating optimally in a competitive power market are estimated using a simple probabilistic model. At the end of the paper complementary results from a detailed simulation model are briefly presented.

2. SYSTEM DESCRIPTION

The system studied is presented in figure 1 and table 1. The wind farm is located near a rural distribution network, and grid expansions are expected to be necessary to fully utilize the wind power potential at the location. A local energy storage is suggested as a different method for increasing the wind power penetration. Since energy storage systems have power losses and significant capital costs, controllable power must be economically awarded in the electricity market compared to fluctuating power.

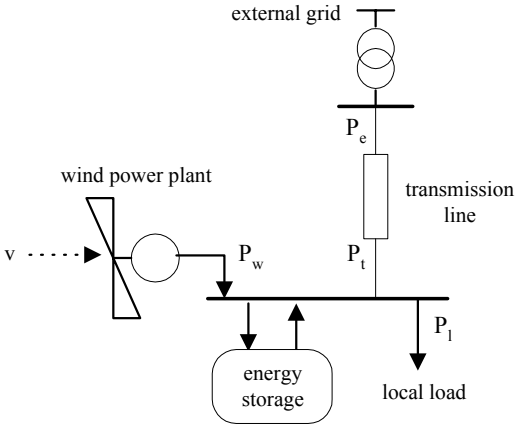

Figure 1. Hybrid wind-storage system connected to a rural distribution grid. P_w is wind power, P_l is the local load, P_t is power to the grid and P_e is the net exported power.

Table 1. Network parameters for the distribution system in figure 1.

Transmission line type	11 kV FeAl 25
Transmission line length	8 km
Transmission line capacity, $P_{t,max}$	4.4 MVA
Maximum local load, $P_{l,max}$	4.0 MW
Minumum local load, $P_{l,min}$	1.5 MW
Mean local load, $\overline{P}_l$	2.6 MW

The stochastic properties of wind velocity are used to determine the energy equations of the system. It is assumed that the energy storage does not reach its upper and lower limits, which will be true only if the storage is unrealistically large. However, this simplification makes it possible to formulate a simple probability model of the system, which can be used in addition to more detailed chronological simulations. For a given wind power rating the power export to the external grid is calculated so that the expected energy amount into and out of the storage during a time period is equal. The energy equations for the storage can be expressed as:

$$E_{ch} = \eta_{ch}\bar{P}_{ch}T_{ch} \quad (1)$$

$$E_{dch} = \frac{1}{\eta_{dch}}\bar{P}_{dch}T_{dch} \quad (2)$$

where

E_{ch}, E_{dch} = Energy into (charging) and out of (discharging) the storage;

$\bar{P}_{ch}$, $\bar{P}_{dch}$ = Mean power into (charging) and out of (discharging) the storage;

η_{ch}, η_{dch} = Efficiency of charging and discharging;

T_{ch}, T_{dch} = Amount of time of charging and discharging.

The wind power potential in the case study is assumed to be 10 MW. Data for the transmission line and the local load are given in table 1. Two alternatives for utilizing the wind power potential are investigated:

1. Construction of a parallel transmission line of type FeAl 50 with 6.9 MVA capacity.
2. Installation of an electrochemical energy storage at the wind power plant site.

The power capacity of the storage system is dimensioned in order to balance the local load in the extreme cases of no wind during maximum load and maximum wind during minimum load;

$$P_{ch,max} = P_{w,max} - P_{l,min} \quad (3)$$

$$P_{dch,max} = P_{l,max} \quad (4)$$

where

$P_{ch,\max}$, $P_{dch,max}$ = Installed charging power and discharging power respectively;

$P_{l,\max}$, $P_{l,\min}$ = Maximum and minimum local load;

$P_{w,\max}$ = Installed wind power.

For regenerative fuel cells where the power rating is equal in both directions, the larger of $P_{ch,max}$ and $P_{dch,max}$ is used. The size of the energy storage is dimensioned to cover mean local load for 4 days, which means that the necessary storage is smaller for systems with high discharging efficiency than for systems with low discharging efficiency. It is emphasized that because of the possibility to export and import power from the external grid, other values for power capacity and energy capacity could be used. Thus, it should be possible to find a more optimal design by optimization techniques or chronological simulations.

Present and future cost estimates and efficiency estimates for the different components are given in table 2 and table 3, respectively. Cost estimations of the Regenesys fuel cell and regenerative hydrogen-oxygen fuel cells are not considered due to lack of data. The controllable power output from the wind-storage system should be reflected in the price for the electricity delivered. It is therefore assumed that the electricity from the wind-storage plant is valued higher than fluctuating wind power in a competitive power market. In both cases the electricity price which gives zero net revenue, i.e. the production cost, is calculated employing the annuity method with 7% interest rate and 20 years depreciation.

Table 2. Present (2000) and future (2010) capital cost estimates for major system components. Operation and maintenance costs is assumed to be 3% of capital costs. Power electronic costs are included in the cost estimations.

	present	future
H_2-O_2 Electrolyser [5] ($/kW)	600	300
H_2-O_2 Fuel cell [6] ($/kW)	3000	1000
H_2-Br reversible fuel cell [7] ($/kW)	-	525
Hydrogen storage [8] ($/kWh)	15	15
Hydrogen compressor [8] ($/($kW_{H2}$))	80[a]	80
Wind power converter [5] ($/kW)	900	700
Transmission line [9] ($/(km kW))	6.5	6.5

a. Energy consumption=0.05 kWh / kWh H2

Table 3. Present (2000) and future (2010) estimates of mean energy efficiency for electrochemical devices. The round trip efficiency for the reversible fuel cell is defined as the electricity-to-electricity efficiency.

	present	future
H_2-O_2 Electrolyser (lower heating value) [5]	69%	74%
H_2-O_2 Fuel cell (lower heating value) [6]	55%[a]	70%[b]
H_2-Br Reversible fuel cell (round trip) [7]	-	72%

a. Phosphoric acid fuel cell
b. Solid polymer fuel cell

3. RESULTS

Main results are presented in table 4. For a wind-hydrogen system today, an unreasonably high price for controllable power is necessary to be competitive to grid reinforcements, due to high fuel cell investment costs and low storage efficiency. Projected future values show that H_2-O_2 systems with separate fuel cell and electrolyser will still have a high production cost of electricity, even with significant cost reductions. On the other hand, the capacity factor of the fuel cell and the electrolyser is unsatisfactory low, which indicates that the devices are overdimensioned. A more optimal sizing of the electrolyser and the fuel cell could bring the electricity costs down. The capacity factor of the regenerative H_2-Br system is higher, since the same electrochemical cell is used for charging as well as discharging. The results for the H_2-Br system indicates that regenerative storage systems can be competitive to grid reinforcements in rural networks, but the controllable power would then have to be 2-3 times more worth than fluctuating power in the market. The value of storing the wind power depends heavily on the conditions in the power market to which the local system is connected. Thermal systems with high price fluctuations between day and night increases the value of beeing able to control the power delivery from the local system. The regulations of the power market also influence on the profitability of the hydrogen storage. Capacity credits will for instance increase the value of the storage system considerably.

The mean power exported to the external grid is low for all cases, and even lower for the local storage alternative than for the grid expansion alternative. However, with a local storage it should be possible to maximize the utilization of the line capacity by installing more wind power and at the same time increase the storage. Theoretically one could have installed about 20MW wind power with a properly designed storage. Without an energy storage further grid reinforcements would be unavoidable.

Table 4. Results from the case study based on the data from table 1,2 and 3. The capacity factor of a device is the ratio between mean power and power capacity. System efficiency is the ratio between energy delivered and total wind energy.

	H_2-O_2 present / future	H_2-Br future	Grid expansions present / future
Production cost of electricity ($/MWh)	135 / 69	52	25 / 20
Mean power export P_e (MW)	0.1 / 0.5	1.0	1.5 / 1.5
Transmission line losses (%)	0.6 / 3	5	3 / 3
Capacity factor, transmission line (%)	2 / 12	23	14
Capacity factor, electrolyser (%)	27 / 25	-	-
Capacity factor, fuel cell (%)	21 / 26	-	-
Capacity factor, reversible fuel cell (%)	-	38	-
System efficiency (%)	65 / 75	86	100 / 100

The system efficiency is relatively high for all systems, even for the present H_2-O_2 system with only 38% round-trip efficiency. This effect is illustrated in figure 2, which shows the mean power export as a function of the round-trip efficiency of storage. It can be seen from the figure that the power export to the external grid is relatively independent of small differences in efficiency, and especially for high efficiencies. On the other hand, figure 3, where reduction in electricity cost is plotted against technology improvement, shows that the overall electricity cost of the wind-storage plant is strongly dependent on the electrochemical efficiencies, and the fuel cell efficiency in particular. The reason for this strong relationship is that the size of the energy storage is dimensioned to cover the load for a certain number of hours. Therefore, as the efficiency increases a smaller energy storage is necessary since less heat will be wasted in the energy conversion. Comparing the curves in figure 3, improvements in electrolyser costs are the least important factor for lowering the electricity cost. An effort to reduce hydrogen storage costs would be more beneficial. The main conclusion to be drawn from figure 3 is the importance of further fuel cell improvements, according to both performance and capital costs.

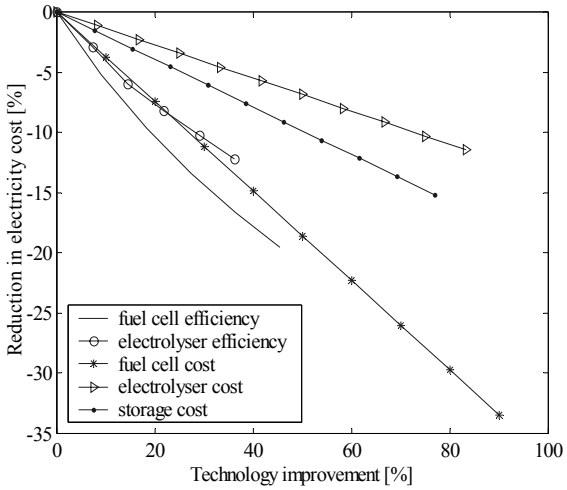

Figure 3. The influence on electricity production costs by improvement in efficiency and cost of different hydrogen technologies for a wind farm with H_2-O_2.

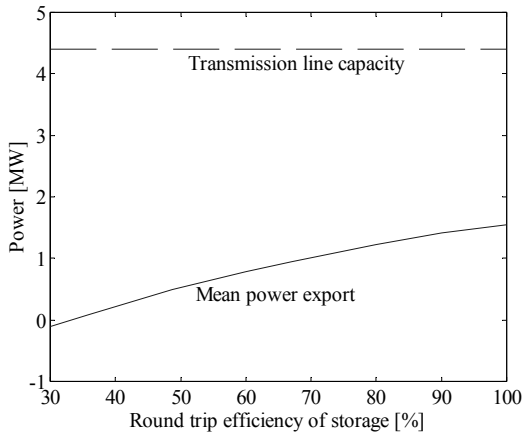

Figure 2. Mean power export to the external grid as a function of storage efficiency.

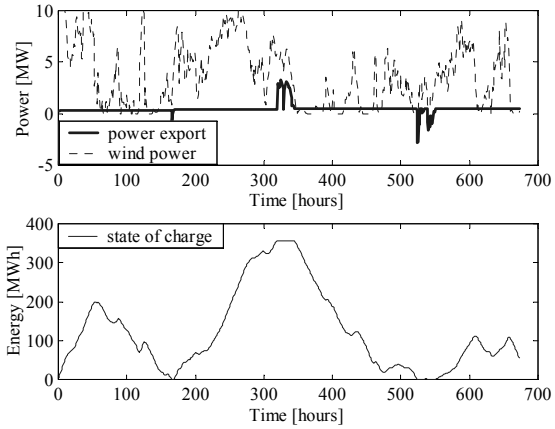

Figure 4. Simulation of the wind-storage system for one month of operation.

4. FURTHER WORK

In the model presented above, it is assumed that the storage tank will neither reach its upper nor its lower limits during a year, and that the plant is operated optimally in the market. To evaluate these assumptions, chronological simulations must be employed. Work on such a simulation model has been started in co-operation with SINTEF Energy Research [10], and preliminary results are discussed shortly here. Figure 4 shows the wind power production, the power export and the state of charge of the storage for one month of operation of a wind-hydrogen system in the power network presented in figure 1 and table 1.

The chosen operational strategy is simple; run the electrolyser whenever the wind power production exceeds the sum of projected weekly mean load and the desired power export for that week. As can be seen, the storage reaches both its lower and upper limits during the time period, which results in a different amount of power exported than desired. In a competitive power market, a smaller reward for the power will then be obtained, which indicates that the results in table 4 are optimistic. However, this situation could to some extent be avoided by putting a more advanced operation strategy to use, rather than increasing the size of the storage. Moreover keeping in mind the low capacity factors of the electrochemical devices, simulations with lower power capacities, leading to lower capital costs, should also be investigated.

5. CONCLUSIONS

Hydrogen energy storage could be an economical feasible alternative to grid expansions for the penetration of wind power in rural networks if future cost and performance goals of hydrogen technology are obtained. The controllable power from a wind-storage system must then be about 2-3 times as much worth as fluctuating power in the power market. Today, the main obstacle for using hydrogen-oxygen based systems in connection with grid-connected wind farms are high capital costs and relatively poor performance of fuel cells. The results indicate that it may be convenient to increase ongoing research on regenerative fuel-cells based on other redox-couples, such as hydrogen-bromide, rather than hydrogen-oxygen systems for stationary purposes.

The results are based on the assumption of optimal operation in a competitive power market. In order to investigate different operation strategies, further work on a detailed simulation model will be carried out. This simulation model will also be employed for finding optimal criteria for the sizing of a wind-storage system.

REFERENCES

[1] B.E.Everett & G.Boyle, Integration, in G.Boyle (Ed.) *Renewable Energy - Power for a Sustainable Future*, (Oxford: Oxford University Press, 1996) 393-433.

[2] A.Price, S.Bartley, S.Male, & A.Cooley, A novel approach to utility scale energy storage, Power Engineering Journal, June 1999, 122-129.

[3] W.A.Amos, Economic Assessment of Wind Energy Coupled with a Reversible Hydrogen Fuel Cell, National Renewable Energy Laboratory, Golden, CO, Milestone Type P report, February 2000.

[4] A.Cruden & G.J.W.Dudgeon, Opportunities for Energy Storage operating with Renewable Energy Systems, *Proceedings of Electric Energy Storage Applications & Technology (EESAT)*, Florida, 2000.

[5] M.K.Mann, V.L.Putsche, & W.A.Amos, The Delivered Cost of Hydrogen from PV and Wind Electrolysis Systems, National Renewable Energy Laboratory, Golden, CO, Milestone Type P report, August 1999.

[6] C.E.G.Padró & V.Putsche, Survey of the Economics of Hydrogen Technologies, National Renewable Energy Laboratory, Golden, CO, Report no. NREL/TP-570-27079, September 1999.

[7] E.G.Skolnik & J.P.DiPietro, Technical and Systems Evaluations, *Proceedings of the 1998 U.S DOE Hydrogen Program Review: Volume 1,* National Renewable Energy Laboratory, Golden, CO, report no. NREL/CP-570-225315.

[8] W.A.Amos*,* Costs of Storing and Transporting Hydrogen*,* National Renewable Energy Laboratory, Golden, CO, NREL/TP-570-25106, November 1998.

[9] SINTEF Energy Research, *Network planning handbook* (in Norwegian), 1999.

[10] M.T.Palsson, A tool for modelling and simulation of grid-connected wind farms, *NEF Technical Meeting*, Trondheim, Norway, November 2000, 31-37.

ELSEVIER

Electrical Power and Energy Systems 25 (2003) 599–606

ELECTRICAL POWER & ENERGY SYSTEMS

www.elsevier.com/locate/ijepes

Operation and sizing of energy storage for wind power plants in a market system

Magnus Korpaas[a,*], Arne T. Holen[a], Ragne Hildrum[b]

[a]*Department of Electrical Power Engineering, Norwegian University of Science and Technology, 7491 Trondheim, Norway*
[b]*Statkraft SF, P.O. Box 200 Lilleaker, 0216 Oslo, Norway*

Abstract

This paper presents a method for the scheduling and operation of energy storage for wind power plants in electricity markets. A dynamic programming algorithm is employed to determine the optimal energy exchange with the market for a specified scheduling period, taking into account transmission constraints. During operation, the energy storage is used to smooth variations in wind power production in order to follow the scheduling plan. The method is suitable for any type of energy storage and is also useful for other intermittent energy resources than wind. An application of the method to a case study is also presented, where the impact of energy storage sizing and wind forecasting accuracy on system operation and economics are emphasized. Simulation results show that energy storage makes it possible for owners of wind power plants to take advantage of variations in the spot price, by thus increasing the value of wind power in electricity markets. With present price estimates, energy storage devices such as reversible fuel cells are likely to be a more expensive alternative than grid expansions for the siting of wind farms in weak networks. However, for areas where grid expansions lead to unwanted interference with the local environment, energy storage should be considered as a reasonable way to increase the penetration of wind power.

Keywords: Wind power; Energy storage; Operation scheduling

1. Introduction

Wind energy is a valuable supplement to conventional energy sources, as wind power technology has become mature. However, the maximum penetration of wind power in electricity networks is limited by the intermittent nature of the energy input. Fluctuations in wind power production also makes it difficult for owners of wind power plants to compete in electricity markets. Energy storage devices with the ability to store large amounts of energy for several hours or more, such as flow cells and fuel cell systems [1], could provide the necessary flexibility for smoothing of wind power. In this way, the possibilities for market operation can be improved. Moreover, for potential wind farm sites remote from a strong electrical connection point, energy storage could provide an alternative to grid reinforcements.

There is a growing research interest in using energy storage to increase the value of intermittent energy sources in electricity markets [2–4]. However, important issues such as the impact of market mechanisms, network constraints and forecasting accuracy of wind power must be further explored to fully determine the advantages and limitations of energy storage for this purpose. Therefore, a method for the scheduling and operation of such a distributed resource in a market system has been developed and implemented in a computer model. This paper aims to describe the proposed method, and to show an application of the method on a case-study, where the impact of energy storage sizing and wind forecasting accuracy on system operation and economics are emphasized.

2. System description

The distributed resource is presented in Fig. 1, and consists of a wind power plant and an energy storage device. The owner of the resource is assumed either to have a demand for electricity P_1 or, alternatively, to have contracts with nearby electricity consumers represented by an aggregated load demand. The system is connected to the main electricity network by a transmission line with limited capacity. Reactive power flow is neglected in the model. The system components and the electricity market model are presented below.

* Corresponding author. Tel.: +47-735-50240; fax: +47-735-94279.
E-mail address: magnusk@elkraft.ntnu.no (M. Korpaas).

0142-0615/03/$ - see front matter © 2003 Elsevier Science Ltd. All rights reserved.
doi:10.1016/S0142-0615(03)00016-4

Nomenclature

P_l	load demand (MW)
P_w	output of wind power plant (MW)
P_e	power exchange with market (MW)
P_s	power output of energy storage (MW)
P_d	dumpload (MW)
P_{sch}	scheduled power exchange with the market (MW)
P_{dev}	deviation between actual and scheduled power exchange (MW)
S	energy storage level (MWh)
η_s	round-trip efficiency of energy storage
η_c	charging efficiency of energy storage
η_d	discharging efficiency of energy storage
v	wind velocity (m/s)
$\hat{x}$	estimated value of variable x
$\bar{x}$	mean value of variable x
f	hourly revenue ($/h)
F	expected revenue over the scheduling period ($)
AR	annual revenue (Mill. $)
I	investment potential (Mill. $)
a	annuity factor
c_t	transmission losses coefficient (1/MW)
SP	spot price of electricity ($/MWh)
c_{rs}	relative difference between spot price and sales price in the regulating market
c_{rp}	relative difference between spot price and purchase price in the regulating market
σ	standard deviation of random variables
V	coefficient of variation of random variables
k_w	weibull shape parameter
RMSE	root-mean-squared error of wind forecast (m/s)
t	index for time
Δt	time step (h)
i	index for day

2.1. Wind power plant

The power output of the wind power plant is calculated from the power curve in Fig. 2. It is assumed that the wind power plant consists of identical wind turbines, and that the wind conditions are the same for all turbines.

2.2. Energy storage

The energy storage device is defined by its energy capacity, charging efficiency, discharging efficiency, charging power capacity, and discharging power capacity. The relationship between storage content S and power flow in/out of the storage P_s is as follows:

$$S(t+1) = \begin{cases} S(t) - \dfrac{1}{\eta_d} P_s(t)\Delta t & (P_s(t) \geq 0) \\ S(t) - \eta_c P_s(t)\Delta t & (P_s(t) < 0) \end{cases} \quad (1)$$

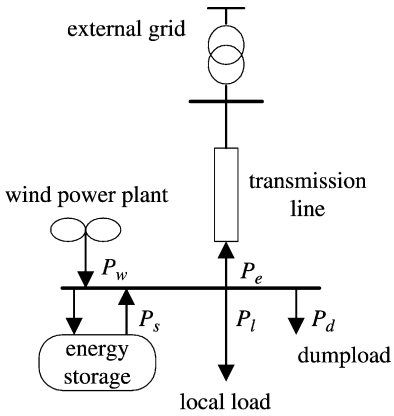

Fig. 1. Wind power plant with local energy storage connected to a scarcely populated grid. The direction of the arrows refers to positive values of the variables.

$$P_s^{min} \leq P_s(t) \leq P_s^{max} \quad (2)$$

$$S^{min} \leq S(t) \leq S^{max} \quad (3)$$

where η_c and η_d are the efficiencies of charging and discharging, respectively. The round-trip efficiency of electricity storage is $\eta_s = \eta_c \cdot \eta_d$.

2.3. External grid

The external grid will act as a power source or sink, depending on the balance between local load and generation. The power exchanged with the marked system is calculated from the power balance:

$$P_e(t) = P_w(t) + P_s(t) - P_l(t) - P_d(t) \quad (4)$$

$$P_e^{min} \leq P_e(t) \leq P_e^{max} \quad (5)$$

Power export corresponds to positive values for P_e and is measured at the load side of the transmission line. If the net power production exceeds the line capacity, the excess power is consumed by a dumpload P_d that is used only for this purpose.

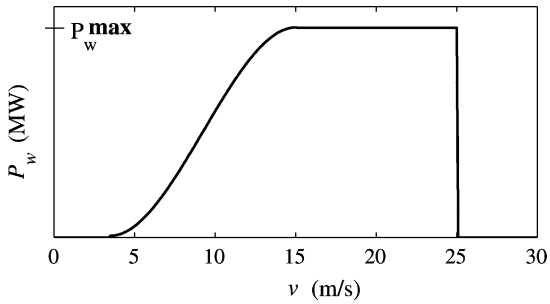

Fig. 2. The wind generator input/output characteristics.

The expression for power losses is:

$$P_{e,loss}(t) = c_t P_e(t)^2 \quad (6)$$

The maximum allowable power exchange (export) is equal to the transmission line capacity, while the minimum value (import) is given by:

$$P_e^{min} = -P_e^{max} + c_t (P_e^{max})^2 \quad (7)$$

2.4. The electricity market

In the Nordic spot market, daily bids for sale and purchase of energy are provided to the power pool no later than 12 h before the actual day. After the spot price has been settled, the final schedule for each generator is worked out. During the operation, if a participant does not deliver the specified amount at the spot market, then the discrepancy must be settled on the regulating power market, which normally results in a reduced income [5].

Market operation is simplified considerably in the model. Since the marginal cost of power produced from a wind power plant is zero, it is presumed that wind energy always can be sold at the spot market. The bidding process is not included in the model. Each day at 12.00, the owner of the distributed resource performs the scheduling of the hourly power exchange P_{sch} for each time step in the scheduling period, which is 24 h. The hourly income from the spot market is:

$$f_{spot}(t) = SP(t) P_{sch}(t) \quad (8)$$

Power flow in the transmission line causes losses, which are bought for spot price:

$$f_{loss}(t) = -SP(t) P_{e,loss}(t) \quad (9)$$

The load income is set equal to the cost for supplying the load with electricity from the external grid, which is paid by spot price:

$$f_{load}(t) = SP(t) \cdot (P_l(t) + c_t P_l(t)^2) \quad (10)$$

This means that the owner of the wind power plant obtains an extra income due to avoided transmission costs. It is assumed that the load is deterministic.

The regulating market is simplified by using average values. The prices for sale and purchase of electricity traded on the regulating market are assumed to be proportional to the spot price:

$$f_{reg}(t) = \begin{cases} (1 - c_{rs}) SP(t) P_{dev}(t) & (P_{dev}(t) \geq 0) \\ (1 + c_{rp}) SP(t) P_{dev}(t) & (P_{dev}(t) < 0) \end{cases} \quad (11)$$

where the deviation between actual and scheduled power exchange, defined as:

$$P_{dev} = P_e - P_{sch} \quad (12)$$

is traded on the regulating market. Fig. 3 illustrates the difference between spot price and regulating price. In the Norwegian regulating market, a discrepancy between the actual and planned production could in fact lead to higher revenue, depending on the overall power balance in the market. This could for instance happen in the cases when the actual power exchange is higher than scheduled at the same time as there is a power deficit in the market. However, it is presumed that in average, deviations from the production plan are disadvantageous, since they increase the uncertainty of the overall power balance.

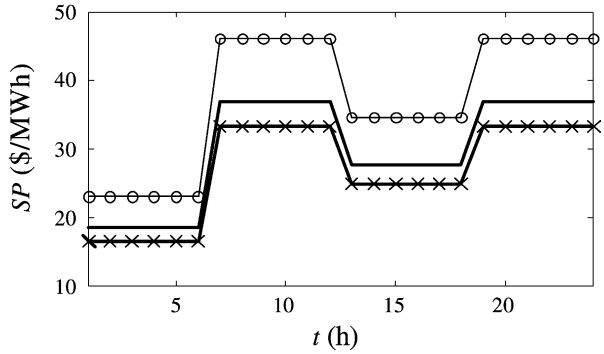

Fig. 3. Simulated time series for spot price (−), price for purchase of electricity in the regulating market (○) and sale of electricity in the regulating market (x).

The annual revenue is given by the following relationship:

$$AR = \sum_{year} (f_{spot} + f_{loss} + f_{load} + f_{reg}) \quad (13)$$

3. Operation strategy

The operation strategy consists of three separate parts: (1) forecasting of wind velocity, (2) scheduling of the power exchange with the market and, (3) on-line operation of the storage. In the present model, the forecasts of load and spot price are assumed to have 100% accuracy. A flowchart of the method is shown in Fig. 4, and the various steps of the algorithm are described below.

3.1. Forecasts

A simple algorithm for computer-generated wind velocity forecasts has been developed. The forecasting is performed once each day before the operation scheduling, and is based on the prediction of mean wind velocity $\bar{v}$ for the whole scheduling period $t = 1 \ldots t_{end}$. It should be noticed that using this method, the forecasted wind velocity will be equal for all hours in the scheduling period. The algorithm includes the following steps:

1. Read wind data $v(t)$ for $t = 1 \ldots t_{end}$ and the coefficient of variation V for mean wind velocity prediction
2. Calculate $\bar{v}$
3. Draw a random number x from the normal distribution with mean $\bar{v}$ and standard deviation $\bar{v} \cdot V$

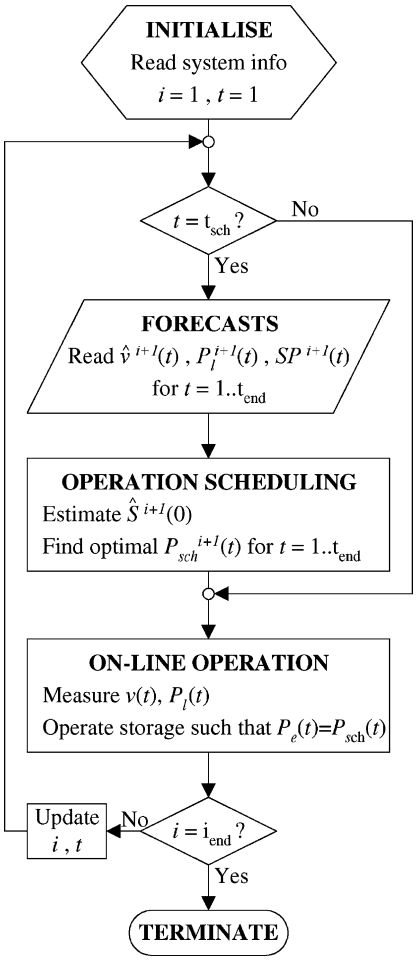

Fig. 4. Flowchart of the operation strategy for a wind power plant with energy storage. The index for day and hour is i and t, respectively.

4. Return the predicted wind velocity $\hat{v}(t) = x$ for $t = 1\ldots t_{\text{end}}$

As an example, for a wind series with mean value 8.6 m/s and standard deviation of 4.4 m/s, the root-mean-squared error (RMSE) of prediction error is found to be 2.5 m/s using the proposed method with $V = 0$.

3.2. Operation scheduling

The operation scheduling of the system is performed at the specified hour t_{sch} each day. The objective is to find the scheduling plan for the next day which maximizes the expected profit. Since the wind velocity forecast is uncertain, and a penalty is given for trading in the regulating market, one should ideally consider the wind velocity as a random variable with a specific distribution in the optimization problem. However, at this stage of the modeling work, the forecasted values are treated as deterministic variables in order to reduce the computational effort to a reasonable size. Trading losses due to deviations between actual and scheduled generation are consequently omitted in the optimization problem.

Given the spot price, load demand and forecast of wind velocity, the optimization task is to determine the hourly trading of electricity in the spot market which maximizes the expected profit over the scheduling period. Mathematically, the scheduling problem can be formulated as:

$$\max\left[F = \sum_{t=1}^{t_{\text{end}}} \text{SP}(t)(P_{\text{sch}}(t) - c_{\text{t}}P_{\text{sch}}(t)^2)\right] \tag{14}$$

subject to the system operating constraints (1)–(7) and the initial storage level. Since there are normally large uncertainties in the prediction of wind velocity, the optimization horizon is chosen to be only 24 h. According to Eq. (14), it is beneficial from an economic point of view to discharge the storage completely at the end of each day. However, if we have good long-term forecasts for the wind velocity, the optimization horizon should be increased. Then it could be favorable to store energy at the end of the next day, for instance if there was a risk for long periods with no wind.

The optimization problem is solved using a dynamic programming algorithm, which requires discretisation of the storage level. The optimization routine returns the optimal path for the next day $\hat{S}^{i+1}(t)$ for $t = 1\ldots t_{\text{end}}$. By using Eqs. (1) and (4), the scheduling of power exchange $P_{\text{sch}}^{i+1}(t)$ for day $i + 1$ can be calculated. The dumpload P_{d} is only used when the storage is completely filled at the same time as the net local production exceeds the transmission line capacity. Alternatively, one or more wind turbines could be shut down or downregulated to avoid overloading the transmission line. The power losses due to downregulation of wind power output will be equal to P_{d}.

The operation scheduling is performed 12 h in advance, which means that the storage level is unknown at the start of the optimization period. If the wind forecasts were 100% correct, the estimated value $\hat{S}^i(t_{\text{end}})$ from the previous optimization should be used. However, because of uncertainties in the wind forecasts, the hourly storage levels will deviate from the estimated values. To get a new estimate of the initial storage level of day $i + 1$, the following equation is employed:

$$\hat{S}^{i+1}(0) = \hat{S}^i(t_{\text{end}}) + \Delta S \tag{15}$$

where ΔS is a storage level correction based on the measured level at the scheduling hour t_{sch} and an improved forecast of the wind velocity for the remaining hours of the day.

3.3. On-line operation

A straightforward operation strategy is used. The energy storage is operated in order to follow the hourly scheduling plan for power exchange with the market. Consequently, it is presumed that the electrical energy produced by the wind

Table 1
The parameter values for the base case

P_e^{max}	4 MW	$\bar{P}_l$	2.6 MW	k_w	2.0
P_w^{max}	10 MW	σ_l	0.52 MW	RMSE	2.6 m/s
P_s^{max}	6 MW	η_s	0.75	$\bar{v}$	8.64 m/s
S^{max}	100 MWh	c_t	0.01 MW^{-1}		

power plant and consumed by the load is continuously measured.

4. System simulation

A case-study is used to test the proposed operation strategy of the distributed resource. The parameters for the base case are listed in Table 1. Time series for wind velocity are computed using a synthesis algorithm described in Ref. [6]. Time series for load demand are computed using the daily load curve in Fig. 5. The mean load for a certain day is obtained from a normal distribution $N(\bar{P}_l, \sigma_l)$, where $\bar{P}_l$ is the daily mean load and σ_l is standard deviation of the daily mean load. The hourly values are obtained by multiplying with the corresponding value of the curve in Fig. 5. The type of energy storage is not specified, but it could for instance be a regenerative fuel cell or a redox flow cell. It should be mentioned that such storage systems are still in the development stage, and the future specific costs are uncertain.

Electricity prices are shown in Fig. 3, and are chosen to be equal for all days. The mean spot price in the base-case is set to 30 $/MWh (270 NOK/MWh). As a comparison, the average spot price in the nordic power market in year 1996 and year 2000 were 254 NOK/MWh and 103 NOK/MWh, respectively [7] (1$ = 9 NOK in November 2001). Moreover, the variations in simulated spot price during the day are chosen to be higher than observed in the market today.

The simulated average price for purchase of electricity in the regulating market is 25% higher than the spot price, and the average price for sales is 10% lower than the spot price. These values are partly based on Ref. [5], assuming a relatively high penetration of wind power in the market.

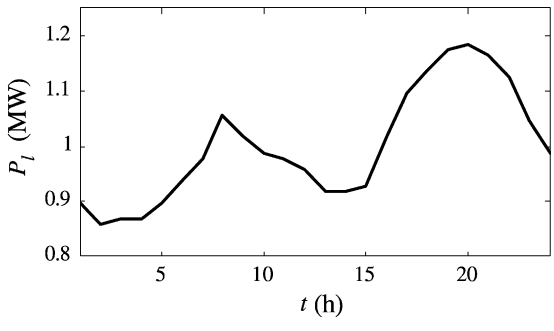

Fig. 5. Typical daily load curve for Norwegian households.

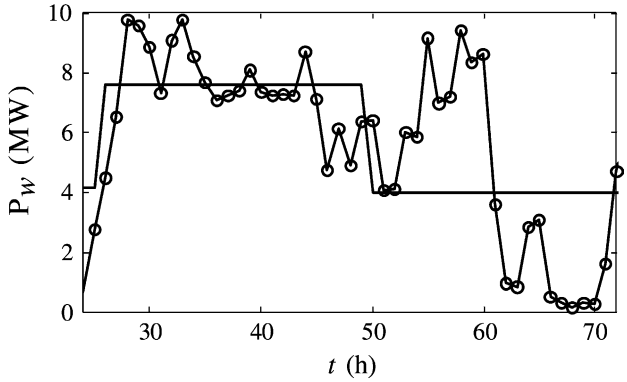

Fig. 6. Actual wind power production P_w (○) and forecasted wind power production $\hat{P}_w$ (−).

4.1. Demonstration of daily operation

The operation strategy will be demonstrated by presenting a 48 h simulation run of the base case. Forecasted and actual values of hourly wind power production are shown in Fig. 6.

Fig. 7 displays the scheduled and actual power exchange with the market. The system manages to follow the production plan most of the time except for some hours at the start and at the end of the simulation period. This discrepancy can be explained from Fig. 8, where the estimated and actual storage levels are plotted. At the start and the end of the period, the actual storage level is empty for a longer period than expected. For those hours, the storage cannot compensate if the wind power production is lower than predicted. This undesirable situation can be avoided by setting the minimum allowable storage level S^{min} larger than zero in the scheduling routine. Moreover, the actual power exchange also deviates from the scheduling plan for $t = 55$. The reason for this discrepancy is that

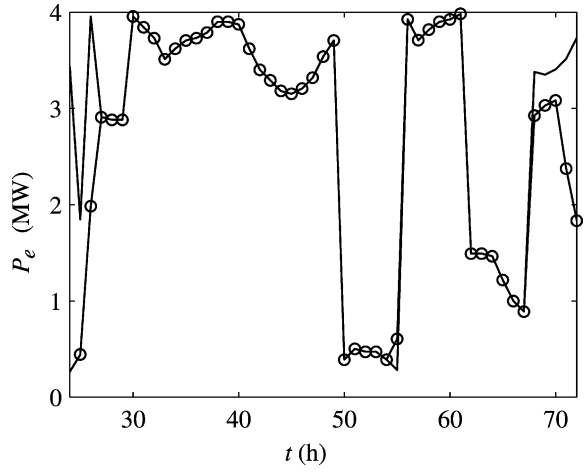

Fig. 7. Actual power exchange P_e (○) and scheduled power exchange P_{sch} (−) with the market.

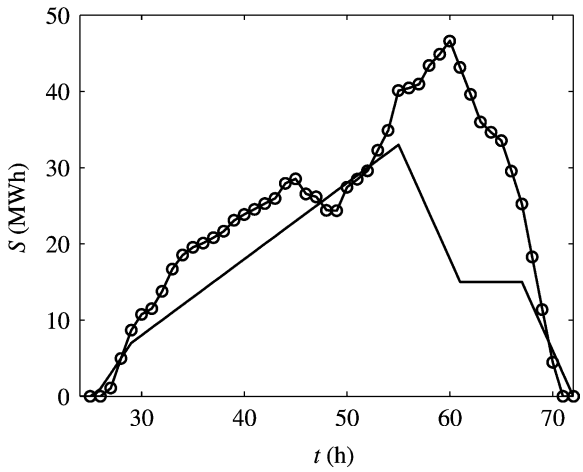

Fig. 8. Actual storage level S (○) and estimated storage level $\hat{S}$ (−) for a storage device with 75% round-trip efficiency.

the power capacity of the storage is too low compared to the wind power production in that hour.

It is important to obtain a good estimate of the initial storage level used in the optimization routine. If the actual storage level is higher than the estimate, the storage can reach its maximum value too early by following the scheduling plan. Likewise, if the storage level is lower than the estimate, the storage can be discharged too early. The latter is observed in Fig. 8, where the estimated storage level at the start of day two ($t = 49$) is higher than the actual value. This causes a full discharge of the storage at the end of the period 1 h earlier than estimated, and the system becomes less flexible.

4.2. Simulation results

A simulation study has been carried out in order to study the impact of storage design and wind forecasting error on the performance and economics of the system. The time step is 1 h, and the length of the time series is 8760 points, i.e. 1 year. The parameter values in Table 1 are used as a base case. It should be noted that the modeling method of wind speed and load described above does not take into account seasonal variations. However, the error caused by this simplification is considered to be small for Norwegian conditions, since there is a close match between the seasonal electricity demand and wind energy in several areas with good wind conditions [8].

Results from simulation runs with different storage parameters P_s^{max} and S^{max} are presented in Table 2. The relative deviation P_{dev}/P_{sch} from scheduled power varies from 3% to 11% for the largest and smallest storage system, respectively. Thus, unpredictable variations in wind power production are smoothed by the storage most of the time. The ratio P_d/P_w is a measure of the energy loss due to transmission constraints, since the dumpload is only used when the net local production exceeds the line capacity.

Table 2
The impact of storage sizing on the performance and economics of the system

Storage sizing				
P_s^{max} (MW)	S^{max} (MWh)	P_{dev}/P_e (%)	P_d/P_w (%)	AR (Mill. $)
4	50	11.2	4.7	1.059
4	100	10.2	1.2	1.090
4	150	10.1	0.4	1.096
6	50	7.6	4.8	1.062
6	100	4.9	1.2	1.097
6	150	4.8	0.4	1.101
8	50	6.6	4.8	1.064
8	100	3.5	1.2	1.099
8	150	3.2	0.4	1.104

The relative usage of the dumpload is low for all storage designs, although there is a clear correlation with S^{max}. A two-fold increase in energy capacity results in a four-fold reduction in the electricity consumed by the dumpload. Moreover, an interesting effect is observed when comparing the different values of P_d/P_w for $S^{max} = 50$ MWh. The usage of the dumpload actually increases slightly for increasing power capacity, although the opposite could be expected, because the ability of the storage to consume excess power also increases. However, with a higher power capacity, it is possible to store more energy during off-peak periods. Consequently, the storage will be completely filled more often. This is undesirable, but can be avoided by adding a limitation on the power capacity used in the scheduling routine.

Furthermore, Table 2 shows that the revenue increases with increasing power and energy capacity of the storage, as expected. On the other hand, the storage device is then likely to be more expensive, which is particularly true for fuel cell systems. Finding an appropriate size of the storage is not only critical for the system operation but is also of great economic importance, due to potential high investment costs. Fig. 9 displays the duration curves of charging, discharging and the energy reserve, which provides information about the utilization of the storage device. It is evident from the charging and discharging curves that an energy storage with separate charging and discharging devices (for instance an electrolyzer and a fuel cell) will have an undesirable low utilization of the total installed capacity. However, the difference between the curves implies that storage designs with different charging and discharging capacities should be investigated further. The usage of the total energy capacity is also relatively low, as can be seen from the duration curve for storage level in Fig. 9. This is beneficial from an operation point of view, since a full storage increases the risk for transmission line overload. In the case of no transmission constraints, the energy capacity could be considerably lower. Moreover, the duration curve also shows that the storage is empty for

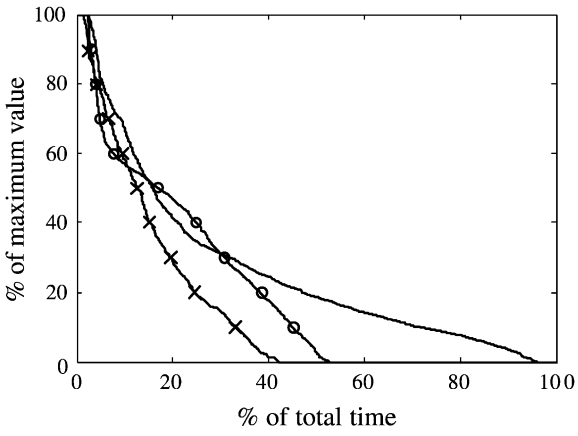

Fig. 9. Duration curves for charge (○), discharge (+) and the storage level (−) of the energy storage device. The base case parameters are used for the simulation.

some times. As this reduces the flexibility of the storage, one should consider to set the minimum allowable storage level in the scheduling routine higher than zero.

An essential parameter in energy storage design is the round-trip efficiency η_s. The ability to take advantage of electricity price variations is in particular dependent on the storage losses. Consequently, if the storage efficiency is low, the storage will only be used to prevent overloading of the line in cases of high wind speeds. This is illustrated in Fig. 10, where the utilization factor of P_s^{max}, defined as:

$$\text{Util.factor} = \sum_{\text{year}} \frac{|P_s(t)|}{P_s^{max}} \tag{16}$$

is plotted against the round-trip efficiency of energy storage. It is clear that the utilization factor decreases significantly for low values of η_s. Fig. 10 also shows the influence on the annual revenue. A sensitivity analysis gives that 10% improvement in the storage efficiency (from 75 to 82.5%)

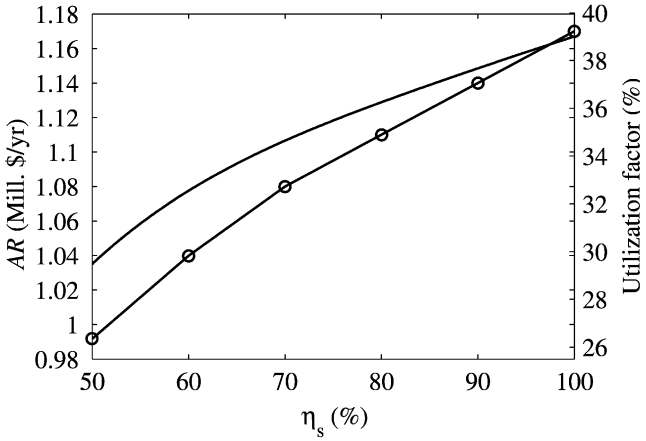

Fig. 10. Annual revenue AR (○) and the utilization of P_s^{max} (−) as a function of electrical energy storage efficiency η_s.

Table 3
The impact of wind forecast error on annual revenue and power exchange with the market

RMSE (m/s)	0.0	2.5	3.0	3.6	5.6
AR (Mill. $)	1.123	1.097	1.064	1.040	0.931
P_{dev}/P_e (%)	0.0	4.9	12.4	16.9	38.4

will lead to about 3.0% increase in the annual revenue, which corresponds to 17000 $/yr.

The economic value of accurate wind forecasts is illustrated in Table 3. As expected, the revenue is highest for perfect forecasting, since in that case all the energy can be traded in the spot market. As the forecasting error increases, it becomes more difficult to follow the scheduled production plan. Hence, more energy must be traded in the regulating market, and the revenue is reduced, according to the price curves in Fig. 3. This is particularly true when employing the persistence method of forecasting, which is simply to use the latest measured wind velocity as a forecast for the whole scheduling period. The persistence method gives a RMSE-value as high as 5.6 m/s for the wind series used here. The benefit of accurate wind forecasts depends strongly on the price difference between spot price and regulating power prices. In this study, the difference is chosen to be relatively large, which means that the effect of forecasting accuracy can be smaller in real markets.

5. Discussion

The simulation results show that with properly sized energy storage, it is possible for owners of wind power plants to take advantage of hourly price variations in the spot market. Furthermore, results obtained from the simulations should ultimately be used as a part of an economic assessment, where also investment costs are considered. It is also interesting to compare energy storage with grid reinforcements in areas where the wind power potential exceeds the capacity of the existing transmission line. The annual revenue for the base case with energy storage is 1.1 Mill.$. For comparison, simulations of the system with a new parallel transmission line instead of energy storage gives a revenue of 1.0 Mill.$.

The investment potential of energy storage as an alternative to grid reinforcements can be calculated by using the following formula:

$$I = \frac{\text{AR(wind + storage)} - \text{AR(wind + line)}}{a} \tag{17}$$

where a is the annuity factor and AR is the annual revenue. By using Eq. (17) with a period of analysis of 20 years and 7% interest rate, energy storage would be the most economic solution if the difference in investment costs between energy storage and the new line is less than

$I = 1.06$ Mill.$. Present cost estimates [4] indicate that electrochemical energy storage systems are likely to be more expensive than grid reinforcements, at least in the near future. On the other hand, for areas where grid expansions lead to unwanted interference with the local environment, energy storage should be considered as a reasonable way to increase the penetration of wind power. Another alternative is to reduce the power output from the wind power plant in periods with high wind and low load by either shutting down units or downregulating the output. For the system studied here, such a strategy without the usage of energy storage would give a yearly revenue of 0.9 Mill.$. The energy loss due to the downregulation is 16%.

The on-line operation strategy of the energy storage described in the paper is simple, namely to follow the specified production plan. Other more sophisticated methods could be employed if wind velocity and the electricity price were represented as stochastic variables, and if forecasts were updated more frequently. The optimal power exchange with the market could for instance be updated each hour, by using principles of stochastic programming. Moreover, in some cases it will be valuable to have an energy reserve in the storage at the end of the day, for instance if high spot prices and low wind speeds are predicted for the next days. This approach is analogous to the so-called water value method used in hydropower planning [9], and will be investigated further.

It should be noticed that the proposed method is not limited to wind power, but could also be useful for the analysis of other intermittent energy resources such as solar, wave and small-scale hydro.

6. Conclusions

A method for the scheduling and operation of a wind power plant with energy storage in a market system has been presented. The method is suitable for any type of electrical energy storage and is also useful for other intermittent energy resources than wind. By implementing the method in a computer simulation model, valuable information about the impact of energy storage sizing on system operation and economics can be obtained. Simulation results of a case study show that with a properly sized energy storage, owners of wind power plants can take advantage of variations in the spot price of electricity, by thus increasing the value of wind power in electricity markets. With available technology and existing price estimates, energy storage devices such as reversible fuel cells are likely to be a more expensive alternative than grid expansions for the siting of wind farms in weak networks, although reducing the environmental impact.

Acknowledgements

This work was funded by Statkraft SF and The Research Council of Norway.

References

[1] Baker JN, Collinson A. Electrical energy storage at the turn of the millennium. Power Engng J 1999;13(3):107–12.
[2] Cruden A, Dudgeon GJW. Opportunities for energy storage operating with renewable energy systems. Proceedings of the EESAT 98, Electric Energy Storage Applications and Technologies; September 2000
[3] Amos WA, Economic assessment of wind energy coupled with a reversible hydrogen fuel cell, National Renewable Energy Laboratory, Golden, CO. Milestone Type P Report; February 2000
[4] Korpaas M, Hildrum R, Holen AT. Hydrogen energy storage for grid-connected wind farms. Proceedings of the 6th IASTED International Conference, Power and Energy Systems; July 2001. p. 590–4
[5] Nielsen LH, Morthorst PE, editors. System integration of wind power on liberalised electricity market conditions. Medium term aspects (in Danish), Risø-R-1055(DA), Risø, Denmark. ; 1998.
[6] Infield D, Scotney A, Lundsager P, Bindner H, Pierik J, Uhlen K, Toftevaag T, Falchetta M, Manninen L, Van Dijk V. Engineering tools for wind diesel systems, vol. 6. EFI Technical Report No. A4330, Trondheim, Norway; September 1995
[7] Homepages of Nordpool—The Nordic Power Exchange, http://www.nordpool.no
[8] Tande JOG, Vogstad K.-O. Operation implications of wind power in a hydro based power system. Proceedings of the European Wind Energy Conference, EWEC99; August 1999. p. 425–8
[9] Fosso OB, Gjelsvik A, Haugstad A, Mo B, Wangensteen I. Generation scheduling in a deregulated system. The Norwegian case. IEEE Trans Power Syst 1999;14(1):75–81.

Optimal Operation of Hydrogen Storage for Energy Sources with Stochastic Input

Magnus Korpaas, Ragne Hildrum, Arne T. Holen, *Member, IEEE*

***Abstract*-- An operation strategy for hydrogen storage in combination with stochastic energy sources is presented. The hydrogen storage can simultaneously be used for power smoothing and provide clean fuel for vehicles. The method is based on optimization of an objective function that takes into account electricity market conditions and penalties for not providing hydrogen and oxygen to the loads. Three case studies where wind is the primary energy source have been analyzed. Simulation results show that the hydrogen storage makes it possible to reduce wind power fluctuations, and at the same time take advantage of hourly variations in the electricity price. In isolated operation mode, utilization of excess heat from the fuel cell leads to a significant reduction of the usage of back-up generator. The results indicate that it is valuable to use optimization techniques for operation of hydrogen storage in connection with stochastic energy sources.**

***Index Terms*—Energy management, Energy storage, Fuel cells, Hydrogen economy, Hydrogen storage, Model predictive control, Linear programming, Operating strategies, Renewable energy, Wind energy**

I. Nomenclature

A. Main symbols

P	power [kW]
V	storage level [Nm^3]
$\dot{V}$	volumetric flow rate [Nm^3/h]
e	electricity cost [NOK/kWh]
η	efficiency
Q	heat [kW]
c	balancing cost parameter
a	transmission losses parameter

B. Subscripts

ely	electrolyzer
fc	fuel cell
sch	scheduled production
dev	deviation from scheduling plan
ex	export
imp	import
w	stochastic generator (wind power)
bg	back-up generator
l	load
ql	electrical heater
d	dump
c	compressor
H	hydrogen
O	oxygen
up	up-regulation of regulating power
dw	down-regulation of regulating power
loss	transmission losses
fcq	heat from fuel cell

II. Introduction

Operation of power systems with high penetration of renewable sources such as wind, solar, wave and small hydro is a challenging task due to the stochastic nature of the energy input. Rapid and flexible control of other generators and loads is required for power smoothing. Alternatively, new electrochemical energy storage systems such as hydrogen systems and redox-flow cells can offer sufficient flexibility for operation in connection with stochastic generators [1]. Such devices can act both as power sinks and sources and they have the advantage of being modular in design. Moreover, good sites for e.g. wind farms are often located in rural areas far away from high-capacity transmission lines [2]. In areas where installation of new capacity is undesirable due to environmental or technical reasons, local energy storage can increase the exploitation of the energy source.

Using hydrogen as a storage medium for intermittent energy sources is a very interesting alternative in the long run, especially because of the possibilities of using hydrogen as a fuel in the transport sector [3]. The hydrogen storage system can in this case simultaneously be used for power smoothing and provide clean fuel for vehicles. As many potential wind farm sites in e.g. Norway is along the coastline, the possibility of utilizing the oxygen from the electrolyzer for fish farms should also be investigated.

In order to optimize the usage of the hydrogen storage system, it is necessary to develop a control strategy that takes into account

- uncertainties in electricity production and consumption
- the interaction with other generators
- the demand for hydrogen and oxygen

In a previous paper, an operation strategy for energy storage in connection with wind farms in a market system was presented [4]. A Dynamic Programming algorithm was used for the daily scheduling. The on-line operation strategy was to control the charging and discharging of the energy storage in

This work was supported by Statkraft SF and the Norwegian Research Council.

M. Korpaas and A. T. Holen are with Department of Electrical Power Engineering, Norwegian University of Science and Technology, 7491 Trondheim, Norway.

Ragne Hildrum is with Statkraft SF, 0216 Oslo, Norway.

order to follow the scheduling plan. In this paper an extension of the method described in [4] is presented. Hydrogen is used as the storage medium, and a hydrogen load is included. In the example considered here, no other sources of hydrogen are present. Thus, the challenge is to find the optimal operation strategy, given that the hydrogen storage system always must be able to supply hydrogen to the load. In addition, an oxygen load is also included. The paper describes a methodology for the on-line operation of such a system, using principles from optimization theory. Examples on the utilization of the method are given both for grid-connected and isolated systems.

III. Approach

A. Description of the concept

The system studied is shown in Fig. 1. A power plant with stochastic input is connected to a local grid, which feeds electricity to one or more consumers. The stochastic generator is the main energy source for electricity and heat, as well as for splitting water into hydrogen and oxygen in the electrolyzer. A fuel cell converts hydrogen to electricity, also producing heat that can be utilized. Several back-up solutions can be considered, depending on the location. In a remote area with no grid-connection, a short-term energy storage device and/or a diesel generator is required. If the electricity consumers are connected to the utility grid, the grid can be used for both power export and import. The value of interacting with the grid is determined by the electricity market conditions. If the installed generation capacity is larger than the grid limit it may sometimes be necessary to dump excess power or decrease the output of the generator.

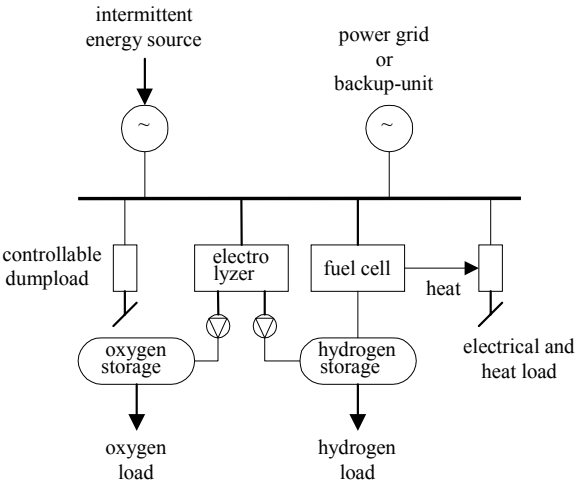

Fig. 1. Schematic figure of a hydrogen storage system connected to a stochastic power generator.

The hydrogen storage system consists of power conversion system, electrolyzer, fuel cell, hydrogen compressor and high-pressure storage tank. Alternatively, the electrolyzer and fuel cell can be combined in a reversible fuel cell. A hydrogen load is included, which can for instance be a hydrogen filling station for fuel cell vehicles or hydrogen tankers. The oxygen produced from electrolysis is a by-product, which is either vented into the air or compressed and stored for later usage.

B. Operation planning methodology

In this section, an operation strategy for the grid-connected mode is first presented. Then, it is described how this strategy can be modified for isolated operation mode.

The power exchanged with the external grid is sold and purchased in an electricity market. A simple market model is employed here. Each day at a specified hour t_{sch}, the owner of the power plant gets access to forecasts of electricity price, loads and his own generation for the next day. Based on this information, a scheduling plan for the next day's power exchange with the market is worked out. Depending on the electricity market conditions, deviations from the scheduling plan can result in a penalty, which reflects the balancing costs of other plants. For each hour in the next day, the scheduling plan, balancing costs, plant measurements and new forecasts of loads and generation are taken into account for finding the optimal usage of the hydrogen storage system. Important plant measurements include storage tank levels, power generation and consumption. The operation strategy is illustrated in Fig. 2.

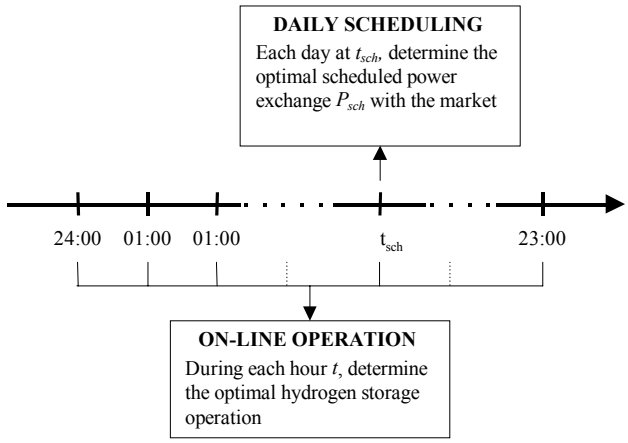

Fig. 2. Illustration of the operation strategy.

C. Mathematical model

In the on-line operation module, the control sequence for a specified time horizon N is computed to minimize operating costs. Only the values for the first time step t in the control sequence are applied, before moving to the next time step. This method of sliding-horizon strategy is known as model predictive control [5]. The variables are divided into state variables $\mathbf{x}(t)$, external inputs $\mathbf{y}(t)$, and time-varying parameters $\mathbf{u}(t)$. Forecasts of external variables are denoted with $\hat{\mathbf{y}}$. The operating costs are minimized by solving the N-horizon optimization problem:

$$\text{Min } F\{\mathbf{x}(t-1), \mathbf{y}(t), \hat{\mathbf{y}}(t+1), .., \hat{\mathbf{y}}(t+N), \mathbf{u}(t), .., \mathbf{u}(t+N)\} \qquad (1)$$

subject to the system constraints

$$
\begin{aligned}
&A\mathbf{x}(t) = B\mathbf{x}(t-1) + C\mathbf{y}(t) \\
&A\mathbf{x}(\tau) = B\mathbf{x}(\tau-1) + C\hat{\mathbf{y}}(\tau)\ ,\ \ \tau = t+1,...,t+N \\
&\mathbf{x}^{\min} \le \mathbf{x} \le \mathbf{x}^{\max}
\end{aligned} \tag{2}
$$

where

- $\mathbf{x}(t\text{-}1)$ contains the state variables, such as storage level, fuel cell power and power export, at the previous time step.
- $\mathbf{y}(t)$ contains the external inputs, such as wind power, electrical load and hydrogen load, for the present time step.
- $\hat{\mathbf{y}}(t+1)$ contains the forecasts of the external inputs for the next time step.
- $\mathbf{u}(t)$ contains the time-varying parameters used in the objective function. These are scheduled power exchange and electricity prices.

The systems constraints (2) consist of power, heat and mass balances for the system shown in Fig. 1. The problem (1) gives the optimum values of **x** for the whole optimization horizon *t*,..,*t*+*N*. Only the values of for the first time step **x**(t) is applied, as the procedure is repeated at each time step.

A variation of the operation method described above can be used for isolated systems. The time series for electricity price is replaced by a cost function of the back-up generator. In cases with several thermal back-up units, the scheduling procedure could be used to determine which generators should be in stand-by mode the next day [6]. However, in the model presented here, power scheduling is omitted in isolated mode. The on-line optimization problem then becomes:

$$\text{Min } F\{\mathbf{x}(t-1), \mathbf{y}(t), \hat{\mathbf{y}}(t+1), ..., \hat{\mathbf{y}}(t+N)\} \tag{3}$$

subject to the system equations (2). There are no time-varying parameters **u** in the operation strategy for isolated operation, since fixed operation costs are used for the back-up generator.

A computer model based on Linear Programming has been developed based on the proposed operation strategy. For the scheduling problem, the objective is to maximize the expected profit from power exchange in the day-ahead market based on forecasts of generation, loads and electricity price:

$$\max F = \sum_{\tau=1}^{M} \begin{bmatrix} e(\tau)\cdot(P_{ex}(\tau) - P_{loss}(\tau)) - \\ c_H \cdot \dot{V}_{Himp}(\tau) - c_{O2} \cdot \dot{V}_{Oimp}(\tau) \end{bmatrix} \tag{4}$$

where

$$P_{loss} = a_{loss} \cdot |P_{ex}| \tag{5}$$

and $\tau = 1 : M$ is the scheduling period, i.e. all 24 hours of the next day. Import costs for hydrogen and oxygen are set high, by thus forcing the electrolyzer to produce sufficient amounts of these gases independent of the electricity market conditions.

During the on-line operation, the mismatch between the actual and scheduled power exchange is traded in the balancing market. In the model, the balancing market is represented by an average penalty cost that reflects the cost of down-regulating and up-regulating conventional power plants. The objective function for on-line operation of grid-connected systems becomes:

$$\max F = \sum_{\tau=t}^{t+N} \begin{bmatrix} e_{dev}(\tau)\cdot\left[P_{ex}(\tau) - P_{sch}(\tau)\right] - e(\tau)\cdot P_{loss}(\tau) - \\ c_H \cdot \dot{V}_{Himp}(\tau) - c_{O2} \cdot \dot{V}_{Oimp}(\tau) \end{bmatrix} \tag{6}$$

where

$$e_{dev} = \begin{cases} (1+c_{up})\cdot e\ , & (P_{ex} - P_{sch}) \le 0 \\ (1-c_{dw})\cdot e\ , & (P_{ex} - P_{sch}) \ge 0 \end{cases} \tag{7}$$

and N is the optimization horizon. If there are no balancing costs, the parameters c_{up} and c_{dw} are set to zero. Consequently, the scheduled power exchange P_{sch} is eliminated in the objective function (6). This is the case for isolated operation, as defined here with one back-up generator. In this case, the objective function is to minimize the usage of the back-up generator, and at the same time avoiding import of hydrogen and oxygen:

$$\min F = \sum_{\tau=t}^{t+N} -e_{bg} \cdot P_{ex}(\tau) + c_H \cdot \dot{V}_{Himp}(\tau) + c_{O2} \cdot \dot{V}_{Oimp}(\tau) \tag{8}$$

where the generation cost e_{bg} is a fixed value, and back-up power is represented by negative power export P_{ex}. Therefore, P_{ex} can only take negative values in isolated operation mode.

The system constraints (2) consist of linear equations for power, heat and fluid balances, which are identical for problem (4), (6) and (8). The power balance is given by the following equations:

$$
\begin{aligned}
&P_{fc} - P_{ely} - P_{ex} - P_{ql} - P_d - P_c = P_l - P_w \\
&P_{fc} = \eta_{fc} \cdot \dot{V}_{Hfc} / \Delta t \\
&P_{ely} = \eta_{ely} \cdot \dot{V}_{Hely} / \Delta t \\
&P_c = (\eta_{Hc} \cdot \dot{V}_{Hely} + \eta_{Oc} \cdot \dot{V}_{Oely}) / \Delta t
\end{aligned} \tag{9}
$$

where η_{fc} is a linear approximation of the electrical efficiency of the fuel cell, taking into account stack losses and power conversion losses. A similar approximation is made for η_{ely}. Compression power P_c is the average electrical work needed to compress the gases from atmospheric pressure to the required pressure level in the storage tanks. Intermediate storage and additional compression for the filling station is not regarded here. Storage balances are formulated as:

$$
\begin{aligned}
&\Delta V_H = \dot{V}_{Hely} - \dot{V}_{Hfc} - \dot{V}_{Hl} + \dot{V}_{Himp} \\
&\Delta V_O = \dot{V}_{Oely} - \dot{V}_{Ol} + \dot{V}_{Oimp}
\end{aligned} \tag{10}
$$

where ΔV is the change in storage level from time step *t*-1 to *t*.

Depending on the type of fuel cell and the operating conditions, it may be possible to utilize heat produced in the fuel cell process. Combined heat and power from low-temperature PEM fuel cells (PEM: Proton Exchange Membrane) has been given increasing attention the last years [7]. Therefore, the possibility of utilizing heat is included in the model:

$$Q_{fc} + \eta_{ql} P_{ql} - Q_d = Q_l$$
$$Q_{fc} = \eta_{fcq} \cdot \dot{V}_{Hfc} / \Delta t \quad (11)$$

where η_{fcq} is the average heat efficiency of the fuel cell and η_{ql} is the efficiency of electrical heating. In present systems, the relationship between heat Q_{fc} and hydrogen flow $\dot{V}_{Hfc}$ is not linear [8]. Nevertheless a simple linear equation will give useful information about the potential advantages of increasing the total fuel cell efficiency, and is therefore assumed to be sufficient at this stage of modeling.

In the linear programming model, upper and lower bound for all state variables **x** must be defined. Special attention is given to the minimum bounds of electrolyzer power and fuel cell power. With present technology, these devices have a minimum operating point ranging from 10 % to 50 % of nominal power, depending on the manufacturer. In periods when hydrogen production is not necessary, the electrolyzer must either be switched completely off or be running at minimum power. The on/off-switching is modeled using binary variables:

$$P_{ely}^{\min}(t) \cdot \gamma_{ely}(t) \le P_{ely}(t) \le P_{ely}^{\max}(t) \cdot \gamma_{ely}(t)$$
$$P_{fc}^{\min}(t) \cdot \gamma_{fc}(t) \le P_{fc}(t) \le P_{fc}^{\max}(t) \cdot \gamma_{fc}(t)$$
$$\gamma_{ely}(t) \in \{0,1\}$$
$$\gamma_{fc}(t) \in \{0,1\} \quad (12)$$

where γ_{ely} and γ_{fc} represents the on/off state of the electrolyzer respective the fuel cell. By the introduction of binary variables, (4), (6) and (8) become mixed integer programming problems, which are computationally far more time consuming than pure linear problems. However, a simple, heuristic approach is assumed to be sufficient for solving the mixed integer program here, keeping the computational effort at a reasonable size. Start-up costs and shutdown costs of the electrolyzer, fuel cell and back-up generator are neglected.

IV. Example

A. Simulation setup

An example system as shown in Fig. 1 has been constructed for testing the operation strategy. The system is a hypothetical, yet realistic wind-hydrogen demonstration plant connected to a fish farm at the coastline. For completeness, a hydrogen filling station for a fuel cell bus is included as a part of the plant. Time series for the other loads, i.e. electrical, heating and oxygen load, are based on values for typical fish farms in Norway. Yearly average load values are given in Table I. All loads are assumed to be deterministic, with no forecasting error.

Three different market conditions for power import and export have been considered. CASE 1 is a grid-connected case with large daily variations in the spot price of electricity. Spot prices for the European Energy Exchange (EEX) from 2002 are used in this example. Each day at 12.00, the plant owner determines the hourly power sales and purchase for the next day, which gives the scheduled power exchange P_{sch}. The balancing cost model is partly based on average balancing prices for Denmark West [9], with constants c_{up}=0.27 and c_{dw}=0.52. CASE 2 is based on Norwegian market conditions, where the spot price variations are small and the balancing costs for wind power are diminutive [10]. Spot prices for the Oslo-area from 2001 have been used, with no balancing costs. In CASE 3, isolated operation of the demonstration plant is simulated, with no possibility for power export. A back-up generator with constant operating costs equal to 0.65 NOK/kWh is used when the wind-hydrogen system is not able to cover the loads. Day-ahead scheduling is omitted in CASE 1 and CASE 2, since the balancing costs are set to zero.

Hourly values and forecasts for wind speed are constructed based on the method described in [4]. The root-mean-squared-error (RMSE) for day-ahead forecasting is 2.6 m/s. In [4] it is shown that the persistence method of forecasting performs unsatisfactory for day-ahead scheduling. On the other hand, the persistence method could be well suited for on-line operation since the wind forecast is updated each time step. Moreover, the persistence method is extremely simple in use, and it shows good performance for predictions a few hours ahead compared to more advanced methods [9]. Therefore, persistence is used for the on-line operation. Table II summarizes the wind characteristics.

It is not the aim of this paper to find the optimal sizing of the system components. The component sizing used in the simulation is based on CASE 3, given that the back-up generator covers about 10 % of the total yearly electricity consumption. It should be emphasized that optimum system sizing is a complex function of both operation costs, investment costs and long-term prediction of the loads, and will not be investigated further here. Table III lists the parameters for the different components.

B. Results from CASE 1

When using the persistence method of forecasting during on-line optimization, it is not given that long forecasting horizon yields good system performance, since the forecasting error increases with the look-ahead time. Therefore, when increasing the horizon, we expect that there is a trade-off between the increasing wind forecast error and the added information about future loads, which are assumed to be deterministic.

TABLE I
AVERAGE VALUES OF THE DIFFERENT LOADS

Electrical load	50 kW
Heat load	50 kW
Hydrogen load	140 Nm^3/day
Oxygen load	3.72 Nm^3/h

TABLE II
MODELING AND PREDICTION OF WIND SPEED

Mean wind speed	8.6 m/s
Root-mean-squared-error (RMSE) of day-ahead prediction	2.6 m/s
Prediction method for on-line operation	persistence

TABLE III

COMPONENT SIZING AND CHARACTERISTICS

Wind power capacity	640 kW
Electrolyzer capacity	530 kW
Fuel cell capacity	100 kW
Minimum electrolyzer power	53 kW
Minimum fuel cell power	10 kW
Electrolyzer efficiency	4.3 kWh/Nm^3
Electrical efficiency of fuel cell	1.75 kWh/Nm^3
Thermal efficiency of fuel cell	1.17 kWh/Nm^3
Hydrogen compression efficiency	0.2 kWh/Nm^3
Oxygen compression efficiency	0.4 kWh/Nm^3
Hydrogen storage capacity	1500 Nm^3
Oxygen storage capacity	1500 Nm^3
Efficiency of electrical heater	1.0

Fig. 4 shows the discrepancy between scheduled and actual power exchange with the market. Deviations from the scheduling plan are settled in the balancing market. According to Fig. 4, heat utilization makes the system less flexible to operate in the power market, except for 0-hour horizon. This indicates that it is difficult to use the fuel cell for combined heat and power and power smoothing at the same time. Fig. 4 also emphasizes that it is sufficient with an optimization horizon of about 15 hours when using the persistence method of forecasting.

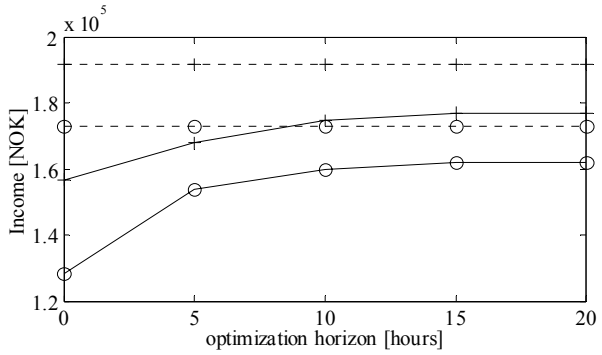

Fig. 3. Yearly income for CASE 1 as a function of optimization horizon with imperfect (-) and perfect (--) wind forecast. Fuel cell with heat utilization is indicated with (+). Fuel cell with no heat utilization is indicated with (o).

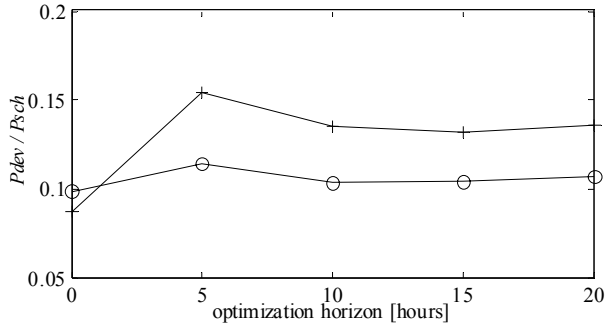

Fig. 4. Schedule deviation as a function of optimization horizon. Fuel cell with heat utilization is indicated with (+). Fuel cell with no heat utilization is indicated with (o)

Table IV summarizes the average usage of the different hydrogen system components and the average power export for CASE 1 with 15-hour optimization horizon. The usage of the hydrogen storage is significantly reduced if the heat from the fuel cell is not utilized. Compared to the installed capacities of the components (Table III) the average usage is especially low for the fuel cell. Moreover, because of the grid connection, it is not necessary to store hydrogen for long periods.

TABLE IV
THE IMPACT OF HEAT UTILIZATION IN THE FUEL CELL AND WIND FORECASTING ERROR ON THE POWER EXPORT AND THE USAGE OF THE HYDROGEN STORAGE SYSTEM

Parameter settings		**Simulation results**			
η_{fcq} [kWh/Nm^3]	RMSE [m/s]	$\overline{P}_{ex}$ [kW]	$\overline{P}_{ely}$ [kW]	$\overline{P}_{fc}$ [kW]	$\overline{V}_H$ [Nm^3]
1.17	2.5	98	82	17	114
1.17	0	104	76	19	71
0	2.5	100	55	7	74
0	0	106	53	10	49

In the model, balancing costs are constant for all hours. In an actual market, the balancing costs will vary between very low and very high, depending on the mismatch between total generation and consumption. In order to show the importance of the balancing costs, simulations with increasing balancing cost parameters c_{up} and c_{dw} has been carried out. Simulation results are presented in Fig. 5. The optimization horizon is set to 15 hours. As expected, the revenue decreases significantly as the balancing costs increase. At the same time, the deviation from the scheduling plan also decreases, since it becomes more important to use the hydrogen storage for balancing purposes. For high balancing costs, the utilization of excess heat from the fuel cell becomes less important. This is in accordance to Fig. 4, which shows that the deviations from the scheduling plan is higher when using the fuel cell for combined heat and power.

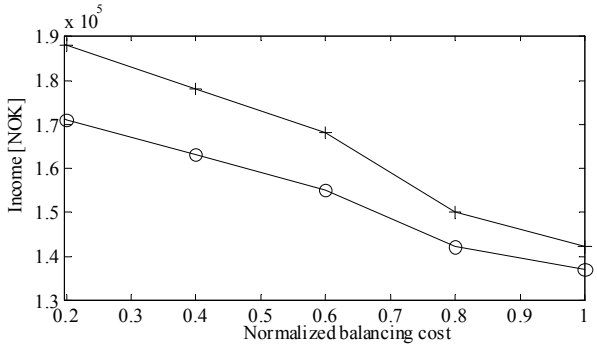

Fig. 5. Yearly income for CASE 1 with increasing balancing cost parameters c_{up} and c_{dw} . Fuel cell with heat utilization is indicated with (+). Fuel cell with no heat utilization is indicated with (o).

C. Results from CASE 2

In CASE 2, there are no balancing costs, and the hourly electricity price variations are smaller than in CASE 1. Simulations with increasing optimization horizon are shown in Fig. 6. Most noticeable is that the added value from improved wind forecasting is relatively small, in contrast to CASE 1. Since there are no balancing costs in this case, the electrolyzer power is practically independent of the wind power

production. The only reason for not importing power from the grid is the costs for grid losses. Therefore, good wind forecasts are not crucial, and the electrolyzer usage is mostly depending on electricity price variations. Furthermore, Fig. 6 shows the importance of using long optimization horizon, which gives advantageous information about future loads and electricity prices.

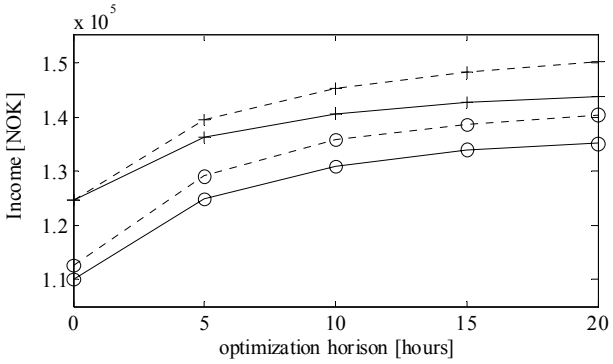

Fig. 6. Yearly income as a function optimization horizon with imperfect (-) and perfect (--) wind forecast. Fuel cell with heat utilization is indicated with (+). Fuel cell with no heat utilization is indicated with (o).

Table V shows that the operation time of the fuel cell is low, even with heat utilization. The reason is that the hourly electricity price variations can not compensate for the losses in the hydrogen storage system. For the market conditions studied in CASE 2, it will be adequate to have a hydrogen storage system without a fuel cell. Hydrogen will then be produced merely for the filling station.

TABLE V
THE IMPACT OF HEAT UTILIZATION IN THE FUEL CELL AND WIND FORECASTING ERROR ON THE POWER EXPORT AND THE USAGE OF THE HYDROGEN STORAGE SYSTEM

Parameter settings		**Simulation results**			
η_{fcq} [kWh/Nm^3]	RMSE [m/s]	$\overline{P}_{ex}$ [kW]	$\overline{P}_{ely}$ [kW]	$\overline{P}_{fc}$ [kW]	$\overline{V}_H$ [Nm^3]
1.17	2.5	116	44	7	93
1.17	0	115	48	8	115
0	2.5	115	39	5	77
0	0	114	40	5	88

D. Results from CASE 3

In this case, isolated operation is examined. The objective is to minimize the usage of the back-up generator, and Fig. 7 shows the relationship between back-up usage and optimization horizon. It is evident that the persistence method of forecasting has an optimum at approximately 5 hours optimization horizon. Beyond this, wrong decisions are made because of the increasing forecasting error. More advanced methods, based on e.g. auto-regressive models will improve the system performance. Fig. 7 also shows that even if perfect forecasts were available, it is sufficient with an optimization horizon of about 15 hours, since the value of increasing the horizon beyond 15 hours is small.

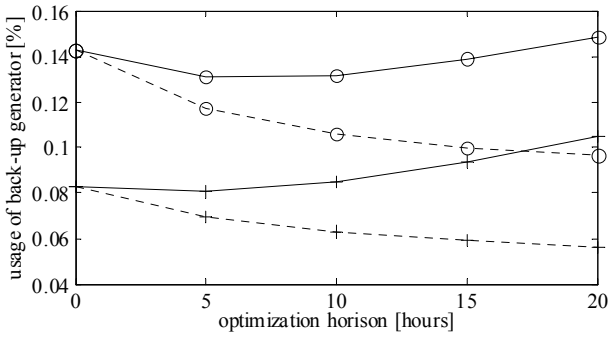

Fig. 7. The usage of back-up generator as a function optimization horizon with imperfect (-) and perfect (--) wind forecast. Fuel cell with heat utilization is indicated with (+). Fuel cell with no heat utilization is indicated with (o).

By utilizing excess heat from the fuel cell, it is possible to reduce the usage of the backup-generator by almost 40 %. This emphasizes the importance of high round-trip efficiency of hydrogen storage. For isolated operation, it is necessary with large electrolyzer and fuel cell for matching the peaks in generation and loads. However, this results in a low utilization factor of the components, as can be seen from Table VI. On the other hand, the average hydrogen content in the storage is relatively high compared to the installed capacity.

TABLE VI
THE IMPACT OF HEAT UTILIZATION IN THE FUEL CELL AND WIND FORECASTING ERROR ON THE POWER EXPORT AND THE USAGE OF THE HYDROGEN STORAGE SYSTEM

Parameter settings		**Simulation results**			
η_{fcq} [kWh/Nm^3]	RMSE [m/s]	$\overline{P}_{ex}$ [kW]	$\overline{P}_{ely}$ [kW]	$\overline{P}_{fc}$ [kW]	$\overline{V}_H$ [Nm^3]
1.17	2.5	10	70	11	974
1.17	0	9	67	12	976
0	2.5	17	77	15	836
0	0	15	75	16	850

V. DISCUSSION

In all three cases, the electrolyzer provided sufficient oxygen to the fish farm. The usage of the oxygen compressor had no significant impact on the system operation, as the electricity consumption was only 0.6 % of the total wind power generation.

The results presented above are based on a model where it is no losses involved in on/off switching of the electrolyzer and fuel cell. However, with present technology, it may be more convenient to run the devices at minimum power level instead of a complete shutdown. This will ensure quick response and to keep the stack temperature on an adequate level. Therefore, simulations of the three case studies where it is not possible to switch off the electrolyzer and the fuel cell have been carried out. The following results were obtained:

- In CASE 1, the reduction of the total power export was 11 %
- In CASE 2, the reduction of the total power export was 15 %

- In CASE 3, the total load covered by the back-up unit increased from 8 % to 11 %

The difference in performance emphasizes that it will be important to develop electrolyzers systems and fuel cells with minimal power consumption in standby-mode.

An interesting question is how the hydrogen load influences the overall economic performance. In order to study the impact of the hydrogen load, simulations of CASE 1-3 have been carried out where the hydrogen load is omitted. In Table VII, these results have been compared to simulations where the hydrogen load is included. The results in Table VII is calculated by applying the following equations:

$$CH = I2 - I1$$
$$ACH = CH / \sum_{year} \dot{V}_{Hl} \quad (13)$$
$$ACE = ACH / (\eta_{ely} + \eta_{Hc})$$

Descriptions of the variables $I1$, $I2$, CH, ACH, and ACE are given in Table VII. As expected, hydrogen production for the filling station will reduce the yearly income. However, by comparing the values for ACE and E in Table VII, it is seen that the additional costs for hydrogen is lower than the average electricity cost in CASE 1 and 2. It should be mentioned that for CASE 2, the hydrogen storage is literally of no use if the hydrogen load is omitted. In CASE 1, on the other hand, the hydrogen storage is continuously used for power smoothing. Furthermore, the hydrogen costs in CASE 3 is significantly lower than the operation costs of the back-up unit, since most of the hydrogen is produced from wind power. For all three cases, using hydrogen as a product of its own will increase the value of hydrogen storage for stochastic generators. However, it is necessary to evaluate the trade-off between investment costs and operational benefits when using hydrogen as a storage medium. Thus, the results from the model should ultimately be combined with an investment analysis in order to determine the actual value of using hydrogen storage. Future work will also include an analysis of using short-term energy storage in connection with the hydrogen storage for isolated operation mode.

TABLE VII
OPERATION COSTS FOR PROVIDING HYDROGEN FUEL TO THE FILLING STATION

	Symbol	**CASE 1**	**CASE 2**	**CASE 3**
Mean electricity price [NOK/kWh]	E	0.200	0.186	0.650
Income, H_2-load included NOK/year]	$I1$	177000	146000	-49660
Income, H_2-load omitted [NOK/year]	$I2$	215000	183000	-16750
Cost of H_2 [NOK/year]	CH	38000	37000	32910
Average cost of H_2 [NOK/Nm^3]	ACH	0.744	0.724	0.644
Average cost of electricity for H_2-load [NOK/kWh]	ACE	0.165	0.161	0.143

VI. CONCLUSIONS

An operation strategy for hydrogen storage in combination with stochastic energy sources has been developed. The mathematical model incorporates principles of linear programming to determine the optimal operation of the system. Results from three case studies, using wind power as an example, have demonstrated that the method is useful for analyzing the performance of the system with respect to component usage and generation uncertainty.

In CASE 1 the wind-hydrogen system is connected to a power network with typical European market conditions. Effective usage of the electrolyzer and the fuel cell makes it possible to reduce wind power fluctuations, and at the same time take advantage of hourly variations in the electricity price. Utilization of excess heat from the fuel cell becomes more important as the balancing costs decreases.

In CASE 2, the wind-hydrogen system is connected to a power network with Norwegian market conditions. In this case, the utilization factor of the fuel cell is very low due to small hourly variations in the electricity price. The electrolyzer is therefore used mainly for providing hydrogen to the filling station. Moreover, the operation of the electrolyzer is more dependent of predictions of loads and electricity price than wind speeds.

In CASE 3, the wind-hydrogen system is operated in isolated mode. It is shown that utilization of excess heat from the fuel cell leads to a significant reduction of the usage of the back-up generator. The option of using excess wind power for production of hydrogen fuel to vehicles makes hydrogen storage especially attractive. Moreover, using wind forecasts for 5-15 hours ahead will improve the operation of the system, compared to a simple load following strategy.

For all three cases, the results show that it is valuable to use optimization techniques for operation of hydrogen storage in connection with stochastic energy sources.

VII. REFERENCES

[1] J. N. Baker and A. Collinson, "Electrical energy storage at the turn of the Millenium," *Power Engineering Journal*, vol. 13, pp. 107-112, Jun. 1999.

[2] J. O. G. Tande, " Exploitation of wind-energy resources in proximity to weak electric grids," *Applied Energy*, vol. 65, pp. 395-401, Apr. 2000.

[3] L. H. Nielsen and K. Jørgensen, "Electric vehicles and renewable energy in the transport sector – energy system consequences," Risø National Laboratory, Roskilde, Denmark, Risø-R-1187(En), Apr. 2000.

[4] M. Korpaas, R. Hildrum, and A. T. Holen, "Operation and sizing of energy storage for wind power plants in a market system," in *Proc.14th Power Systems Computation Conf.*, Session 31, paper 6, pp 1-7.

[5] P.D. Roberts, "A brief overview of model predictive control," *Practical Experiences with Predictive Control* (Ref. No. 2000/023), *IEE Seminar on*, pp.1/1-1/3 .

[6] A. G. Bakirtzis and E. S. Gavanidou, "Optimum operation of a small autonomous system with unconventional energy sources," *Electric Power Systems Research*, vol. 23, pp. 93-102, Mar. 1992.

[7] C. Wallmark and P. Alvfors, "Design of stationary PEFC system configurations to meet heat and power demands," *Journal of Power Sources*, vol. 106, pp. 83-92, Apr. 2002.

[8] J. Hamelin, K. Agbossou, A. Laperrière, F. Laurencelle, and T. K. Bose, "Dynamic behavior of a PEM fuel cell stack for stationary applications," *Int. Journal of Hydrogen Energy*, vol. 26, pp. 625-629, Jun. 2001.

[9] H. Holttinen, T.S. Nielsen, G. Giebel, "Wind energy in the liberalised market – forecast errors in a day-ahead market compared to a more flexible market mechanism," in *Proc. 2nd Int. Symposium on Distributed Generation*, Session 6, pp 1-13.

[10] M. Gustafsson, "Wind power, generation imbalances and regulation cost," presented at the Int. Workshop on Wind Power and the Impacts on Power Systems, Oslo, Norway, 2002.

VIII. BIOGRAPHIES

Magnus Korpaas received his siv.ing (graduate degree in theoretical physics) from Norwegian University of Science and Technology (NTNU), Trondheim, Norway in 1998. He is currently working as a doctoral student at the Department of Electrical Power Engineering, NTNU.

Ragne Hildrum received her siv.ing (graduate degree in electrochemistry) and dr.ing (doctorate in electrochemistry) from The Norwegian Institute of Technology (NTH), Trondheim, Norway in 1988 and 1993 respectively. She is employed at Statkraft SF, Department of R&D.

Arne T. Holen received his siv.ing (graduate degree in electrical engineering) and dr.ing (doctorate in electrical engineering) from The Norwegian Institute of Technology (NTH), Trondheim, Norway in 1963 and 1968 respectively. He is a Professor at Department of Electrical Power Engineering, NTNU. His research interests are power system analysis, including steady state and dynamics, optimization, security and reliability assessment, application of knowledge based systems. He is a member of Power Engineering Society and of The society of Reliability Engineers, Scandinavian Chapter.